frontiers | Research Topics

Women in antimicrobials, resistance and chemotherapy 2023

Edited by
Ana R. Freitas, Cindy Shuan Ju Teh and Krassimira Radoykova Hristova

Published in
Frontiers in Microbiology

ISSN 1664-8714
ISBN 978-2-8325-5326-8
DOI 10.3389/978-2-8325-5326-8

About Frontiers

Frontiers is more than just an open access publisher of scholarly articles: it is a pioneering approach to the world of academia, radically improving the way scholarly research is managed. The grand vision of Frontiers is a world where all people have an equal opportunity to seek, share and generate knowledge. Frontiers provides immediate and permanent online open access to all its publications, but this alone is not enough to realize our grand goals.

Frontiers journal series

The Frontiers journal series is a multi-tier and interdisciplinary set of open-access, online journals, promising a paradigm shift from the current review, selection and dissemination processes in academic publishing. All Frontiers journals are driven by researchers for researchers; therefore, they constitute a service to the scholarly community. At the same time, the *Frontiers journal series* operates on a revolutionary invention, the tiered publishing system, initially addressing specific communities of scholars, and gradually climbing up to broader public understanding, thus serving the interests of the lay society, too.

Dedication to quality

Each Frontiers article is a landmark of the highest quality, thanks to genuinely collaborative interactions between authors and review editors, who include some of the world's best academicians. Research must be certified by peers before entering a stream of knowledge that may eventually reach the public - and shape society; therefore, Frontiers only applies the most rigorous and unbiased reviews. Frontiers revolutionizes research publishing by freely delivering the most outstanding research, evaluated with no bias from both the academic and social point of view. By applying the most advanced information technologies, Frontiers is catapulting scholarly publishing into a new generation.

What are Frontiers Research Topics?

Frontiers Research Topics are very popular trademarks of the *Frontiers journals series*: they are collections of at least ten articles, all centered on a particular subject. With their unique mix of varied contributions from Original Research to Review Articles, Frontiers Research Topics unify the most influential researchers, the latest key findings and historical advances in a hot research area.

Find out more on how to host your own Frontiers Research Topic or contribute to one as an author by contacting the Frontiers editorial office: frontiersin.org/about/contact

Women in antimicrobials, resistance and chemotherapy: 2023

Topic editors

Ana R. Freitas — Cooperativa de Ensino Superior Politécnico e Universitário, Portugal

Cindy Shuan Ju Teh — University of Malaya, Malaysia

Krassimira Radoykova Hristova — Marquette University, United States

Citation

Freitas, A. R., Teh, C. S. J., Hristova, K. R., eds. (2024). *Women in antimicrobials, resistance and chemotherapy: 2023*. Lausanne: Frontiers Media SA.

doi: 10.3389/978-2-8325-5326-8

Table of contents

frontiers | Frontiers in Microbiology

TYPE Editorial
PUBLISHED 06 August 2024
DOI 10.3389/fmicb.2024.1463728

OPEN ACCESS

EDITED AND REVIEWED BY
Jørgen J. Leisner,
University of Copenhagen, Denmark

*CORRESPONDENCE
Ana R. Freitas
✉ ana.freitas@iucs.cespu.pt

RECEIVED 12 July 2024
ACCEPTED 24 July 2024
PUBLISHED 06 August 2024

CITATION
Teh CSJ, Hristova KR and Freitas AR (2024) Editorial: Women in antimicrobials, resistance and chemotherapy: 2023.
Front. Microbiol. 15:1463728.
doi: 10.3389/fmicb.2024.1463728

Editorial: Women in antimicrobials, resistance and chemotherapy: 2023

Cindy Shuan Ju Teh[1], Krassimira R. Hristova[2] and Ana R. Freitas[3,4,5]*

[1]Department of Medical Microbiology, Faculty of Medicine, Universiti Malaya, Kuala Lumpur, Malaysia, [2]Department of Biological Sciences, Marquette University, Milwaukee, WI, United States, [3]UCIBIO, Applied Molecular Biosciences Unit, Laboratory of Microbiology, Department of Biological Sciences, Faculty of Pharmacy, University of Porto, Porto, Portugal, [4]Associate Laboratory i4HB, Institute for Health and Bioeconomy, Faculty of Pharmacy, University of Porto, Porto, Portugal, [5]1H-TOXRUN – One Health Toxicology Research Unit, University Institute of Health Sciences, CESPU, CRL, Gandra, Portugal

KEYWORDS

women's empowerment, antimicrobial resistance, antimicrobial activity, virulence, microbiota, alternative drug therapies

Editorial on the Research Topic
Women in antimicrobials, resistance and chemotherapy: 2023

In honor of International Women's Day 2023, Frontiers in Microbiology launched the second edition of the "*Women in antimicrobials, resistance and chemotherapy*" Research Topic. This dedicated Frontiers Research Topic was entirely curated by women editors, celebrating their remarkable contributions in this field. It's heartening to see such recognition, especially given the historical undervaluation of women's achievements in STEM (science, technology, engineering, and mathematics). Notable women like Ada Lovelace, Rosalind Franklin, Barbara McClintock, and Marie Curie have left indelible marks on scientific progress, yet gender disparities persist (2021).

Gender and antimicrobial resistance (AMR) also intersect. A recent global review by the World Health Organization (WHO) revealed that women might be more susceptible to developing drug-resistant infections compared to men (Wong, 2024). This gender-specific aspect of AMR remains under-recognized, with over 70% of countries failing to acknowledge gender inequalities in their national plans to combat drug-resistant infections. Approximately 20% of these studies focused on Africa, and nearly 15% focused on southeast Asia. In regions with limited access to clean water, women and girls are at greater risk of drug-resistant urinary tract infections due to menstrual-hygiene needs. Additionally, women, who constitute 70% of global health-care workers, are more likely to encounter drug-resistant infections in hospitals and clinics. Higher rates of sexual violence against women also increase their vulnerability to drug-resistant sexually transmitted infections. And if progress on empowering women and girls was already too slow, COVID-19 and the war in Ukraine and Gaza have exacerbated entrenched gender inequalities. In this sense, UN Women's Strategic Plan 2022–2025 centers the activity of women and girls, guiding work across normative spheres, UN coordination, and program implementation, tailored to national contexts and executed with various partners to support women and girls in creating a better future (United Nations, 2021).

The papers published on this Research Topic (8 original Research Articles, one Review, one errata) shed light on the vital work of female researchers addressing antimicrobial resistance—one of the top global health threats of our time.

Thurner and Alatraktchi critically reviewed the role of sub-lethal antibiotics in the evolution of bacterial virulence. Besides the mutations and natural selection, alteration in virulence could also be achieved through enrichment in sub-Minimum Inhibitory Concentration (MIC). To further study how virulence manifests itself under sub-MIC, methodologies for sub-MIC determination and measurement of virulence should be standardized. This will provide useful information for patient management.

Barone et al. investigated the effects of HDAC6 inhibitors, which act on histone deacetylation and bacterial clearance, against *Pseudomonas aeruginosa*. The results showed changes in the production of virulence factors like pyocyanin and rhamnolipids. Selective HDAC6 inhibitors demonstrated potential in reducing inflammation and bacterial load in chronic infection models mimicking the cystic fibrosis (CF) phenotype. However, further research is needed to understand the molecular mechanisms of HDAC6's role in bacterial infections.

Kanafani et al. aimed at exploring the differential activity of ciprofloxacin and levofloxacin on the selection of resistance among 233 clinical isolates of *Pseudomonas aeruginosa*. Levofloxacin required fewer passages than ciprofloxacin to reach breakpoints in some isolates, and induced mutants against both drugs had higher fitness costs compared to parental isolates. Whole genome sequencing revealed alterations in *gyrA, gyrB,* and *parC* genes associated with resistance.

Li et al. described the *in vitro* antibacterial activity of novel β-lactam-β-lactamase inhibitor combinations (BLBLIs) against carbapenem-resistant *Klebsiella pneumoniae* (CRKP) producing metallo- and serine-β-lactamases. Using broth microdilution and time-kill assays, they demonstrated significant bactericidal activity for aztreonam combined with new BLBLIs. However, further studies including more isolates with different carbapenemases are needed for comprehensive susceptibility data.

Xu et al. reported the changes of the gut microbiota in children who received broad-spectrum antibiotics in pediatric intensive care unit (PICU). After the treatment, gene functions of the gut microbiota were altered, mainly in those responsible for metabolism, DNA catabolism, and transmembrane transport. Ninety resistance genes were significantly upregulated in Day 7 compared to Day 1. This study has provided a substantial basis for a better understanding of the structure and function of gut microbiota after the short-term admission to PICU.

Jordão et al. investigated the combination of DNase I enzyme with antimicrobial photodynamic therapy (aPDT) in mice infected with fluconazole-susceptible (CaS) and -resistant (CaR) *Candida albicans* strains. After inoculation, the mice received DNase treatment followed by photosensitizer (PDZ) and light exposure for 5 consecutive days. The combination of DNase with PDZ-aPDT significantly reduced fungal viability in mice tongues, with remission of oral lesions observed after 7 days. This approach holds promise for improving the efficacy of photodynamic treatment.

Ye et al. described a green synthesis method for silver nanoparticles using *Cnidium monnieri* fruit extract, highlighting its simplicity, safety, and environmental friendliness compared to physical and chemical methods. These CM-AgNPs demonstrated antifungal activity against Trichophyton rubrum, *T. mentagrophytes*, and Candida albicans, showing potential for treating fungal infections in humans and animals. Developing new topical antifungal drugs with these green CM-AgNPs could be an effective alternative for managing multidrug-resistant candida and dermatophyte infections.

Kasozi et al. surveyed rural community of livestock farmers to determine whether appropriate practices were used in administration of drugs against animal African trypanosomiasis (AAT) in southwestern Uganda. The survey involved farmers and "professionals" i.e., livestock extension officers and drug shop attendants. On around two-thirds of farms, trypanocidal drugs were being administered by farmers and almost all drugs were obtained from privately-owned drug shops. Farmers were more likely than professionals to use antibiotics as well as trypanocidal drugs to treat AAT, raising concerns as to overuse and misuse of antibiotics. The study also highlights the complexity of issues involved in the fight against AAT using drug treatment, and the importance of best farming practices to reduce the emergence of resistant strains of trypanosomes.

Wiesner-Friedman et al., used the microbial Find, Inform, and Test framework to identify strong associations between sources of antimicrobial resistance (AMR), represented by a panel of 5 ARGs/MGEs. Land application of waste (e.g., dairy manure, biosolids) and dairy concentrated animal feeding operations were indicated as important sources of elevated AMR levels in riverbed sediment and surface water. While the consistency in the types of sources selected is strong, differences in estimated overland influence ranges and database types were noted. Overall, this work indicates offsite migration of wastes and calls for more fine-spatial and temporal studies of AMR in watersheds.

Collectively, these investigations showcase the exceptional quality of research led by diverse women scientists, addressing one of the top ten global public health threats. We hope these articles will inspire readers working in the AMR field to explore and tackle AMR from multifaceted perspectives.

Author contributions

CT: Methodology, Writing – original draft, Writing – review & editing. KH: Methodology, Writing – original draft, Writing – review & editing. AF: Methodology, Writing – original draft, Writing – review & editing, Conceptualization.

Funding

The author(s) declare that no financial support was received for the research, authorship, and/or publication of this article.

Acknowledgments

The Editors are grateful to all authors that participated in this Research Topic and to all (external or editorial board member) reviewers, who have contributed significantly to its success.

Conflict of interest

The authors declare that the research was conducted in the absence of any commercial or financial relationships that could be construed as a potential conflict of interest.

The author(s) declared that they were an editorial board member of Frontiers, at the time of submission. This had no impact on the peer review process and the final decision.

Publisher's note

References

(2021). Editorial: Women must not be obscured in science's history. *Nature*. 591, 501–502. doi: 10.1038/d41586-021-00770-0

United Nations (2021). *UN Women Strategic Plan 2022–2025*. Available at: https://www.unwomen.org/en/digital-library/publications/2021/09/un-women-strategic-plan-2022-2025 (accessed July 8, 2024).

Wong, C. (2024). *Drug-resistant infections more likely to strike women, says WHO*. Nature news. Available at: https://www.nature.com/articles/d41586-024-01476-9 (accessed July 8, 2024).

frontiers | Frontiers in Microbiology

TYPE Original Research
PUBLISHED 05 September 2023
DOI 10.3389/fmicb.2023.1223876

OPEN ACCESS

EDITED BY
Sevcan Aydın,
Istanbul University, Türkiye

REVIEWED BY
Alain Hartmann,
Institut National de recherche pour L'agriculture, L'alimentation et L'environnement (INRAE), France
Ozlem Ates Duru,
Abant Izzet Baysal University, Türkiye

*CORRESPONDENCE
Marc L. Serre
✉ marc_serre@gmail.com

RECEIVED 16 May 2023
ACCEPTED 07 August 2023
PUBLISHED 05 September 2023

CITATION
Wiesner-Friedman C, Beattie RE, Stewart JR, Hristova KR and Serre ML (2023) Identifying sources of antibiotic resistance genes in the environment using the microbial *Find*, *Inform*, and *Test* framework.
Front. Microbiol. 14:1223876.
doi: 10.3389/fmicb.2023.1223876

Identifying sources of antibiotic resistance genes in the environment using the microbial *Find*, *Inform*, and *Test* framework

Corinne Wiesner-Friedman[1], Rachelle E. Beattie[2,3], Jill R. Stewart[4], Krassimira R. Hristova[3] and Marc L. Serre[4]*

[1]Office of Research and Development, U.S. Environmental Protection Agency, Cincinnati, OH, United States, [2]U.S. Geological Survey, Columbia Environmental Research Center, Columbia, MO, United States, [3]Department of Biological Sciences, Marquette University, Milwaukee, WI, United States, [4]Gillings School of Global Public Health, Department of Environmental Sciences and Engineering, University of North Carolina at Chapel Hill, Chapel Hill, NC, United States

Introduction: Antimicrobial resistance (AMR) is an increasing public health concern for humans, animals, and the environment. However, the contributions of spatially distributed sources of AMR in the environment are not well defined.

Methods: To identify the sources of environmental AMR, the novel microbial Find, Inform, and Test (FIT) model was applied to a panel of five antibiotic resistance-associated genes (ARGs), namely, erm(B), tet(W), qnrA, sul1, and intI1, quantified from riverbed sediment and surface water from a mixed-use region.

Results: A one standard deviation increase in the modeled contributions of elevated AMR from bovine sources or land-applied waste sources [land application of biosolids, sludge, and industrial wastewater (i.e., food processing) and domestic (i.e., municipal and septage)] was associated with 34–80% and 33–77% increases in the relative abundances of the ARGs in riverbed sediment and surface water, respectively. Sources influenced environmental AMR at overland distances of up to 13 km.

Discussion: Our study corroborates previous evidence of offsite migration of microbial pollution from bovine sources and newly suggests offsite migration from land-applied waste. With FIT, we estimated the distance-based influence range overland and downstream around sources to model the impact these sources may have on AMR at unsampled sites. This modeling supports targeted monitoring of AMR from sources for future exposure and risk mitigation efforts.

KEYWORDS

microbial FIT, antimicrobial resistance, surface water, sediment, animal feeding operations, land application

1. Introduction

Antimicrobial resistance (AMR) currently exists at higher than natural levels due to antibiotics use and misuse in human and animal medicine and livestock production (Davies and Davies, 2010). Wastes from these origins contain pathogens and associated antibiotic resistance genes (ARGs), which can be dispersed *via* runoff into rivers in the environment (Amarasiri et al., 2019). While putative geographical

sources of pathogens and ARGs have been identified, the extent of their contributions to elevated AMR in the environment remains unknown. Characterizations of AMR spatial sources, their contributions (Nappier et al., 2020), and modeling approaches that suit the conceptual framework of ARG transport, attenuation, and amplification (Singer et al., 2006; Pruden et al., 2012) are needed.

Antibiotic resistance genes and antibiotic-resistant bacteria (ARB) can become elevated intracellularly due to the impacts of human and animal sources by (1) direct dissemination or extracellularly and through horizontal gene transfer (HGT), (2) organic matter enrichment of ARGs, and (3) the dissemination of selective factors (e.g., antibiotics) from sources (Xie et al., 2018). A geospatial study of surface water in the United States supports that land use is a driver of AMR (Keely et al., 2022). Potential sources of elevated AMR in the environment have been identified at locations where human, animal, and industrial waste meet with the environment (Nappier et al., 2020; Zainab et al., 2020; Zheng et al., 2021). Animal feeding operations (AFOs) are likely sources due to frequent antibiotic use for disease treatment and prevention or use in animal feed, often at sub-therapeutic doses (Pruden et al., 2012; Ling et al., 2013; Heaney et al., 2015; Li et al., 2015; Rogers et al., 2018; Lopatto et al., 2019). Other potential sources include wastewater treatment plants (WWTPs) (Bueno et al., 2018; Brown et al., 2019; Pazda et al., 2019; Beattie et al., 2020b) and land application sites of treated (i.e., biosolids and semi-solids) and untreated wastes (i.e., biosolids and wastewater) from agricultural (e.g., manure spreading), industrial, or municipal origins (Munir and Xagoraraki, 2011; Beattie et al., 2018, 2020b; Pepper et al., 2018; Yang et al., 2018; Duarte et al., 2019; Jacobs et al., 2019). Additionally, elevated AMR levels have been detected in groundwater near septic systems (O'Dwyer et al., 2017), and low-intensity developed land cover is a fecal contamination source (Crowther et al., 2003; Alford et al., 2016; Bucci et al., 2017; Hinojosa et al., 2020; McKee et al., 2020; Wiesner-Friedman et al., 2021a). However, ARGs predate manufactured antimicrobials and exist in natural environments (D'Costa et al., 2011; Van Goethem et al., 2018), and different soil types can represent sources (Zhang et al., 2018, 2021; Macedo et al., 2020). Additionally, season (Beattie et al., 2018, 2020a; Zheng et al., 2018; Liu et al., 2020) and precipitation (Ahmed et al., 2018; Keen et al., 2018) are temporal factors to consider.

To model contributions from these sources with known mechanistic approaches (Wang et al., 2019; Costa et al., 2021), knowledge of loadings and decay is needed. While current research shows that first-order decay can represent ARG levels over distance and time and that ARG decay occurs over long time scales (e.g., weeks to months), the decay rate varies depending on the ARG and environmental variables (Mao et al., 2014; Lopatto et al., 2019; Macedo et al., 2020; Barrios et al., 2021; Burch et al., 2021). Furthermore, loadings at sources are not well characterized. Statistical models incorporating first-order decay are helpful to screen potential sources of elevated AMR without requiring mechanistic information (Wang et al., 2019; Costa et al., 2021). Here, we use land-use regression (LUR) to identify the sources of contaminants and quantify their association with environmental responses (Messier et al., 2014). By constructing source terms that characterize contributions through spatial predictor models (SPMs), LUR leverages hyperparameters and databases of spatially distributed sources to describe the decayed range of influence around sources (Wiesner-Friedman et al., 2021b). LUR studies can increase the ecological understanding of how sources influence ARG levels and help develop microbial risk assessments for AMR (Nappier et al., 2020).

To the best of our knowledge, only two studies using LUR or SPMs have characterized source contributions to the AMR levels of rivers and their quantified associations (Pruden et al., 2012; Amos et al., 2015). Pruden et al. (2012) explored different SPMs that account for average upstream capacities and found that WWTPs and AFOs were associated with *sul1* relative abundance in sediment (2012). A recent study (Amos et al., 2015) modeled the decaying contributions [i.e., decaying concentrations of cellular and extracellular *intI1* (i.e., genes related to ARG mobility and pollution) and concentrations of selective pressures (e.g., antibiotics, biocides, microplastics, etc.)] coming from upstream WWTPs, leading to higher levels of *intI1* relative abundance in sediment.

These two LUR studies implemented different SPMs. Pruden et al. (2012) used the inverse distance-weighted (IDW) interpolation of pollution capacities upstream of the sampling location. This SPM is an interpolation of pollution capacities upstream of the sampling point. Therefore, it does not guarantee that pollution decreases away from sources, as would be expected from dilution and degradation processes. Amos et al. (2015) used a sum of exponentially decaying contributions (SEDC) applied to upstream sources. This model is different from the IDW interpolation in that it accounts for the density of sources, and it is such that the predictor value decreases away from sources, which is physically meaningful. Factors including dilution due to flow (Knapp et al., 2012), overland flow, and manure hauling from AFOs to application fields contribute to the dissemination of microbial contamination to rivers (Wiesner-Friedman et al., 2021a,b). Our goal is to expand upon previous modeling with a generalized SPM that incorporates these four components (i.e., density and proximity of upstream sources, overland flow, and dilution) to screen many potential sources of elevated AMR.

By implementing a LUR approach in a new region with a more generalized SPM, we aimed to (1) estimate relative abundance (i.e., ARG/16S rRNA gene) ratios (RARs) that express how AMR levels respond to the influence of different types of upstream sources, (2) characterize the overland range of influence around AMR sources, and (3) predict AMR levels at unsampled river sites. We were further interested in studying source impacts on riverbed sediment and surface water, representing time-integrated effects and transient contamination (Wiesner-Friedman et al., 2021a). To accomplish this, we applied the newly developed microbial *Find, Inform,* and *Test* (FIT) framework (Wiesner-Friedman et al., 2021b), which uses LUR and novel SPMs, and applied FIT to a panel of four ARGs (*ermB*, *tetW*, *qnrA*, and *sul1*) and one resistance-associated gene (*intI1*) (collectively called ARGs throughout) quantified from riverbed sediment and surface water from a mixed-use Great Lakes watershed area. The panel of ARGs in this study were selected for their associations with agricultural resistance [i.e., *tet(W)* and *erm(B)*], clinical significance (i.e., *qnrA*), and as mobile genetic elements (i.e., *intI1* and *sul1*) (Beattie et al., 2018). Three

ARGs have been previously studied using LUR [i.e., *tet(W)*, *sul1*, and *intI1*] but were only measured from sediment (Pruden et al., 2012; Amos et al., 2015), and two [i.e., *erm(B)* and *qnrA*] have not been studied with LUR. Compared to these previous studies, we modeled contributions from new types of spatially distributed sources (e.g., land-applied waste from municipal or industrial origins) and for ARG responses in sediment and surface water.

2. Methods

2.1. Sampling and sample analysis of antibiotic resistance genes

The data used for this study were originally collected and processed by Marquette University researchers (Beattie et al., 2018) based on (1) the number and spatial distribution of samples and (2) the high detection rate of ARGs in riverbed sediment and surface water. The samples were obtained from Kewaunee, Ahnapee, and East Twin Rivers in Kewaunee County, Wisconsin during five sampling events representing four seasons and 20 sampling sites (sampling sites are depicted as circles in Figure 1). Sites were selected based on the impacts of expected variability from the dense livestock agriculture in Kewaunee County and public access to the sites (Beattie et al., 2018). DNA was extracted from samples, and quantitative PCR was used to quantify AMR-associated genes [i.e., *erm(B)*, *qnrA*, *tet(W)*, *sul1*, and *intI1*] and the 16S rRNA gene. Antibiotic resistance gene selection is detailed in a previously published study (Beattie et al., 2018); briefly, genes resistant to antibiotics commonly used in agriculture (tetracycline, macrolides, and sulfonamides; *tet*(W), *erm*(B), and *sul1*), genes found on mobile genetic elements (*intI1* and *sul1*), and genes conferring resistance to clinically important antibiotics (fluoroquinolones; *qnrA*) were chosen to explore the diversity of environmental resistance in the study area. Values measuring below the detection limit (<8% of the data points; see Supplementary Table S1) were set to half the detection limit. Detailed sampling methods, DNA extraction, qPCR protocols, and the full ARG dataset (relative and absolute abundances) can be found in a previously published study (Beattie et al., 2018). River network, precipitation, temperature, and source location data and processing can be found in previously published studies (Wiesner-Friedman et al., 2021a,b).

2.2. Physically meaningful land-use regression model

This study uses a physically meaningful LUR model (i.e., source terms are not allowed to have negative regression coefficients) implemented in FIT without modifiers (i.e., attenuators or amplifiers) to focus on characterizing source contributions to each ARG response, y_i (Wiesner-Friedman et al., 2021b):

$$y_i = \beta_0 + P1_i(\beta_1 + \beta_2 P2_i) + \beta_3 Freezing_i + \left\{\sum_{u=1}^{U} \beta_u s_i^{(u)}\left(\alpha^{(u)}\right)\right\} + \varepsilon_i \quad (1)$$

The ARG response, y_i, represents log10 of the relative abundance z_i, where z_i is the ratio of ARG copies to 16S rRNA gene copies. The first three variables, namely, $P1_i$, $P2_i$, and $Freezing_i$, represent recent precipitation, antecedent precipitation, and a seasonal, Bernoulli-distributed variable representing whether the monthly average temperature was freezing for each i^{th}sample. The first term, β_0, and the last term, ε_i, represent the regression intercept and random error, respectively. β_1, β_2, and β_3 are associated regression coefficients, and $\sum_{u=1}^{U} \beta_u s_i^{(u)}\left(\alpha^{(u)}\right)$ is a sum of contributions from spatially distributed sources. Each source term, $s_i^{(u)}\left(\alpha^{(u)}\right)$, is defined as a function of ground hauling, overland, and downstream decay hyperparameters; $\alpha^{(u)}$, the flow-connected distances (i.e., overland and downstream distances) from the spatial locations of sources of type u (e.g., WWTPs) to the sampling locations of each i^{th}sample; and sample site flow (proxied by Strahler stream order) (Wiesner-Friedman et al., 2021b). The sources can also be weighted by information associated with their scale (e.g., size of the land cover area, gallons of manure, or equally weighted) (Wiesner-Friedman et al., 2021a). Because hyperparameters describe the distance decay of dimensionless quantities that denote the scale of sources, source terms describe dimensionless source contributions to sampling sites. All source terms $s_i^{(u)}$ are SPMs equal to the z-scored Sum of Exponentially Decaying Contributions (SEDC) so that a one standard deviation increase in the u^{th} SEDC represents a β_u increase in the response. An RAR expresses the ratio of relative abundances for a one standard deviation increase in source u. In other words, a one-unit increase in SPM $s_i^{(u)}$ results in a $\left(100(RAR^{(u)} - 1)\right)$ percentage increase in relative abundance z (Wiesner-Friedman et al., 2021b). See Supplementary material S5 for details.

2.3. Data for spatially distributed sources

Multiple spatial databases are available to represent potential sources in Kewaunee County. While many sources of elevated ARGs exist globally, we identified thirteen categories of potential sources that may be important to Kewaunee County ($u = 1,2,\ldots,13$).

The first eight potential sources of the u^{th} categories were spatially related to sampling site locations with SPMs, which are the z-scored overland and river-distance with flow (ORF) SPM: (1) AFOs, (2) manure application fields, (3) septic systems, (4) industrial land application sites, (5) municipal or septage (i.e., domestic-originating) land application sites, (6) WWTPs, (7) low-intensity developed land cover representing rural accumulations on imperviousness, and (8) high-intensity developed land cover representing more urban/residential accumulations on imperviousness. The next three potential sources were soil sources represented by the dominant soil type within a 1-km radius of the sampling location: (9) Type A represents soils with the highest infiltration rate when saturated, likely consisting of sand, sandy loam, loamy sand, or gravel soil types; (10) Type C represents soils with a low infiltration rate when saturated, likely consisting of clay loam, silty clay loam, sandy clay, or silty clay; and (11) Type D represents soils with a very low infiltration or high run-off potential, likely consisting of clay loam, silty clay loam, sandy clay,

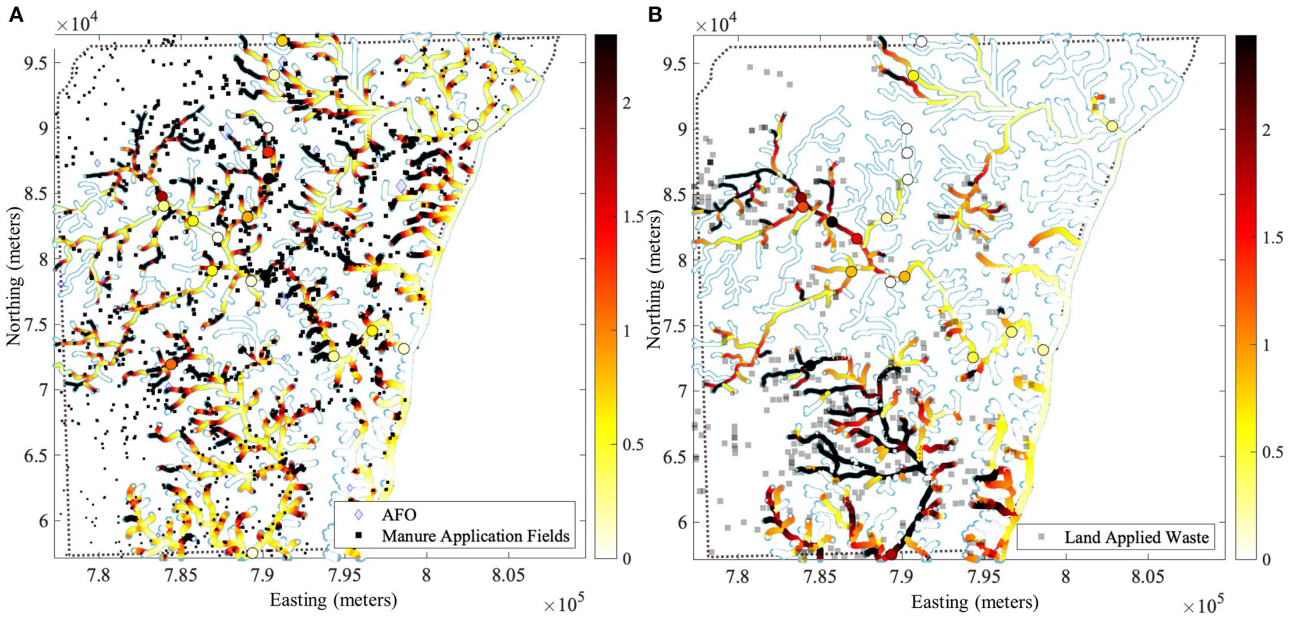

FIGURE 1
Conservative values of the standardized sum of exponentially decaying contribution (SEDC) are shown for two types of spatial prediction models: **(A)** AFOs *via* manure application at agricultural application fields, and **(B)** land application sites with municipal or industrial wastes and septage. These standardized SEDCs are conservative in using the maximum hyperparameter values $\alpha^{(u)}$ (see Equation 1) found across ARG responses. For subpanel a, we used the maximum hyperparameter values $\alpha^{(u)}$ obtained across three relative abundance responses [*erm(B), tet(W),* and *sul1*] in sediment [$max(\alpha^{(u)}) = \{\gamma_G = 14\ km,\ \alpha_O = 13\ km,\ \alpha_R = 2\ km\}$]. For subpanel b, we used the maximum hyperparameter values $\alpha^{(u)}$ obtained across two relative abundance responses [*tet(W)* and *intI1*] in surface water [$max(\alpha^{(u)}) = \{\alpha_O = 10\ km,\ \alpha_R = 10\ km\}$]. An increase of 1 on the color scale corresponds to a one standard deviation increase of the corresponding SEDC. The multiplication of the standardized SEDC shown here with a given regression coefficient β_u from Table 1 gives the increase in the corresponding log10 relative abundance *y*. Circles represent the sampling locations associated with this study and highlight the conservative value of the standardized SEDC at that site. For example, for *erm(B)* in sediment, the β_u for u = AFO *via* manure application fields is $\beta_u = 0.199$, therefore, a one standard deviation increase (shown in orange in the map) in the standardized SEDC for AFO *via* manure application fields increases *y* (the log10 relative abundance) by 0.199, or conversely, the relative abundance *z* increases by a relative abundance ratio (RAR) of $10^{\beta_u} = 1.58$, which corresponds to a 58% increase in relative abundance *z*. Database representations are detailed in Supplementary material S7.

or silty clay. The last two source categories were those related to the sampling site locations using the ground hauling, overland, and river distance with flow (GORF) SPM. Here, the SPM leverages two source locations to capture how land application occurs on land disproportionately closer to the origin of the waste [e.g., manure is hauled from AFOs ($u = 1$) to manure application fields ($u = 2$), and AFOs will minimize hauling distances for cost purposes (Hadrich et al., 2010)]. The sources defined with this SPM are 12) AFOs *via* the ground transport or hauling of manure to fields and 13) domestic-originating land application sites ($u = 5$) with waste that is applied more greatly in proximity to denser residential areas represented by septic system locations ($u = 3$). See previous study for SPM equations and descriptions (Wiesner-Friedman et al., 2021b).

2.4. Application of the FIT framework to ARG responses

The microbial FIT framework is a three-step approach (Wiesner-Friedman et al., 2021b) using the physically meaningful LUR (Equation 1). The three stages of the FIT framework, *Find*, *Inform*, and *Test*, were applied independently to the 10 ARG responses (i.e., sediment and water measurements of five ARGs). This modeling was implemented in MATLAB 2020b (https://scicrunch.org/resolver/RRID:SCR_001622).

In *Find* reliable databases of spatially distributed sources, many candidate databases can be explored for their ability to reproduce source-term relationships for unseen data. Here, for each of the potential ARG source categories ($u = 1,2,\ldots,13$), we explored the candidate options for representing the sources based on (a) available databases [e.g., the Wiscland-2 land cover database, the Wisconsin Pollution Discharge Elimination System (WPDES) database, and county databases available for manure storage and septic systems], (b) coding options, (c) different classes of data, and (d) weighting options (see Supplementary material S2 for details).

The *find* stage obtains a reliability score for each candidate database option. The reliability score is calculated by obtaining hyperparameters for the SPM for a training set of response data. Using training hyperparameters for a test set (see Supplementary material S4), we calculated a reliability score with test-set regression coefficients. The score rewards candidate databases with the most consistently positive test-set regression coefficients [i.e., sign stability score (SSS)], the largest sum of test-set coefficients (M), and the lowest variability of the test-set coefficients (Wiesner-Friedman et al., 2021b). See Supplementary material S2 for the reliability score equation.

In the *inform* stage, source terms are informed with transport-characterizing hyperparameters in ORF and GORF SPMs. In this

TABLE 1 Symbols and abbreviations from Equation 1.

Term	Description
y_i	log10 of the relative abundance z_i, where z_i is the ratio of ARG copies to 16S rRNA gene copies for each i^{th} sample.
$P1_i$	Recent precipitation for each i^{th} sample.
$P2_i$	Antecedent precipitation for each i^{th} sample.
$Freezing_i$	Bernoulli distributed variable representing whether the monthly average temperature was freezing for each i^{th} sample.
$s_i^{(u)}(\alpha^{(u)})$	The impact on each i^{th} sample from the u^{th} source type modeled with the Sum of Exponentially Decaying Contributions (SEDC) Spatial Predictor Models (SPMs) that account for the ground hauling, overland, and river distance flow (Wiesner-Friedman et al., 2021a,b).
β_0	The regression intercept.
β_1	The increase in y_i for a one standard deviation increase in recent precipitation.
β_2	The effect that a one standard deviation increase in antecedent precipitation has on the effect of recent precipitation β_1.
β_3	The effect of freezing temperatures on y_i.
β_u	The increase in y_i for a one standard deviation increase in the source term $s_i^{(u)}(\alpha^{(u)})$.
ε_i	The random error for each i^{th} sample.

stage, hyperparameter values, $\alpha^{(\mathbf{u})}$ (i.e., describing average ground hauling distance γ_G, decay overland α_O, and downstream α_R), were obtained by independently maximizing the RAR ($10^{\beta^{(u)}}$) for every source type. This maximization was subject to a penalty on very low or high values of overland decay and ground hauling hyperparameters, α_O and γ_G, that yielded poor regression qualities (Wiesner-Friedman et al., 2021b). The spatial predictor models leveraging the hyperparameters, $\alpha^{(\mathbf{u})}$, are described in detail in the microbial FIT framework (Wiesner-Friedman et al., 2021b).

The goal of the last stage is to *test* the predictive ability of informed source terms to identify key sources of elevated ARGs in Kewaunee County Rivers and Streams. Before model selection, if the correlation of informed source terms was large ($\rho \geq 0.7$), those yielding the highest univariate R-squared were chosen over correlated options (Dormann et al., 2013). Then, seasonal, precipitation, and source terms were stepwise selected with AIC. The prediction of individual source impacts on unsampled locations was initially assessed through the *find* stage based on the robustness of the source term's consistent contributions and the ARG's log10 relative abundance across training and test sets. Ultimately, the prediction of total source impacts was assessed with the adjusted R^2 resulting from the *test* stage.

2.5. Conducting interviews/surveys with Wisconsin dairy cattle veterinarians

To understand which ARGs are likely to be shed by bovines based on antibiotic usage, we reviewed information from a thorough systematic review outlining and quantifying antibiotic usage on Wisconsin dairy farms (Pol and Ruegg, 2007). Since the publishing of that study, practices may have changed, and a previous ARG study found local knowledge to be beneficial (Rogers et al., 2018). We conducted a small survey with dairy cattle veterinarians and asked Wisconsin dairy cattle veterinarians about the changes they have observed in antibiotic use over their careers. Google Maps was used to search for veterinarians, veterinary services, and "large animal" services. In total, 12 veterinary offices were identified as serving the dairy cattle industry, representing the practices of over 30 veterinarians. Surveys were sent to all 12 offices, and four returned our surveys. See Supplementary material S6.1 for survey questions and veterinarian responses.

3. Results

3.1. The ARGs in this study are biologically linked to antibiotic usage in Wisconsin AFOs

According to the four veterinarians we interviewed, ceftiofur, a beta-lactam (Dowling, 2004), was the most frequently prescribed antibiotic for disease treatment (Dowling, 2004). Other antibiotics that veterinarians prescribe are enrofloxacin, florfenicol, tulathromycin, and oxytetracycline. These interviews (see Supplementary material S4 for interview details and discussion) reflected antibiotic use for disease treatment that was consistent with the findings of the 2007 study on antibiotic usage at AFOs in Wisconsin (Pol and Ruegg, 2007). These antibiotics belong to the broader classes of fluoroquinolones, sulfonamides, macrolides, and tetracyclines, which correspond well with resistance encoded by or co-occurring with the ARGs used for this LUR modeling (Pal et al., 2015; Beattie et al., 2018). Our interviews did indicate that some antibiotics are still used preventatively (e.g., tetracycline flushes) because operations have difficulty monitoring large herds. Preventative antibiotic use is therefore a missing component in understanding the frequency and dose associated with these classes of antibiotics. However, our interviews and the 2007 study provide a biological link between the panel of ARGs from our study and dairy AFOs. Additionally, although *intI1* has been identified as a marker for anthropogenic pollution more broadly, clinical class I integrons can carry ARG cassettes, conferring multidrug resistance with the ability to spread rapidly through horizontal gene transfer (Gillings et al., 2015).

We could not directly obtain information on clinical antibiotic usage in rural Wisconsin. However, one wastewater study (Karthikeyan and Meyer, 2006) indicates a total of six classes of antibiotic compounds found in the influent of municipal wastewater from across Wisconsin. Based on the frequency of the detection of different antibiotic classes, the study indicates that the ARGs for this study may also well represent the anthropogenic impacts of clinical antibiotic use.

3.2. Overland and downstream flow from bovine sources consistently contribute to elevated ARGs

After implementing the FIT framework across five ARGs in sediment and surface water, we found that all five of the ARG responses (see Table 2) are positively associated with bovine sources (i.e., AFOs, AFOs *via* the ground hauling of manure to application fields, or manure application field locations) in at least surface water or sediment. For ARG responses in *sediment*, FIT selected the GORF AFO source term, which represents the contributions from AFOs *via* the ground hauling of manure to application fields. A one standard deviation increase in GORF AFO contributions was associated with RARs of 1.58 and 2.01, representing 58% and 101% increases ($p < 0.10$) in the relative abundance of *erm(B)* and *tet(W)*.

Across ARG responses in *surface water,* FIT selected the GORF AFO source term for *erm(B)*. A one standard deviation increase in these AFO contributions was associated with a 45% ($p < 0.05$) increase in the relative abundance of *erm(B)* in surface water. For *tet(W)* and *qnrA* responses, FIT selected the ORF AFO source term, representing the contributions directly from AFO locations. A one standard deviation increase in AFO contributions was associated with 77% ($p < 0.05$) and 49% ($p < 0.05$) increases in the relative abundance of *tet(W)* and *qnrA*, respectively. For *sul1* and *intI1*, FIT selected the ORF manure application fields representing contributions directly from field locations (i.e., irrespective of AFOs). A one standard deviation increase in manure application field contributions was associated with 41% ($p < 0.10$) and 36% (inclusion lowers AIC) increases in the relative abundance of *sul1* and *intI1,* respectively.

In sediment and surface water, the magnitude of the association between *tet(W)* and AFOs was greatest compared to other ARG responses. A greater association may indicate that more *tet(W)* genes are located at AFOs or may suggest that oxytetracycline is used frequently to prevent diseases at dairy AFOs compared to other antibiotics. Some studies suggest that *tet(W)* and tetracycline resistance may be more specific to dairy feces than other ARGs and antibiotic resistance phenotypes (Srinivasan et al., 2008; Kyselková et al., 2015). The strength of the associations from our study supports that *tet(W)* is correlated with dairy manure.

This is the first study to characterize ARG contributions with GORF or ORF SPMs for bovine sources. Our findings imply that overland and downstream transport and dilution from flow are key processes in disseminating AMR from AFOs and manure fields. This study also suggests that manure hauling to application sites is a factor in elevated ARGs in the environment. Our novel spatial predictors and modeling approach are in agreement with AFO's association with ARGs found by Pruden et al. (2012) using a different SPM and applied to a different geographical region. Pruden et al. (2002) found that the relative abundance of *sul1* in *sediment* was positively correlated ($R^2 = 0.35$, $p < 0.001$) with the average upstream capacities of AFOs. However, these authors found no significant relationship with the relative abundance of *tet(W)* in sediment (Pruden et al., 2012), which could reflect differences in livestock and antibiotic use. Our study quantified seven novel associations between bovine sources and ARG responses. We have quantified the associations between bovine sources and levels of *erm(B)*, *tet(W)*, *qnrA*, *sul1*, and *intI1* in surface water (i.e., five novel associations) and the association between bovine sources and levels of *erm(B)* and *tet(W)* in sediment (i.e., two novel associations), which can inform ecological studies of AMR and microbial risk assessment.

3.3. Flow affects consistent detection of signals from bovine sources

The *find* stage of FIT enables the exploration of many databases of collocated, spatially distributed sources. The result is the set of source locations and associated information that consistently represent sources to the response from a cross-validation approach. Here, we report the *find* stage results for bovine sources because they were the most consistently selected source from the *test* stage of FIT. Across ARG responses in surface water, FIT modeled contributions from AFOs with the county manure storage option and contributions from manure application fields with the crop rotation land cover option.

For ARG responses in *sediment*, FIT modeled contributions from AFOs with WPDES CAFO locations, but differences existed in CAFO weightings. The difference in weighting CAFOs by animal units for *erm(B)* and *tet(W)* and equal weighting for *sul1* may reflect differences in the transport processes resulting in elevated relative abundance, independent of the number of animal units (e.g., some other selective pressure emanating from sources).

One key difference in FIT's database selection was that, to represent AFOs, the WPDES CAFOs option was selected for sediment responses and the county's manure storage option for surface water responses. One explanation for this difference is that sediment sampling was impossible at three sites during one high-flow event (Beattie et al., 2018). These manure storages are known to overflow during high-flow events (Burch et al., 2021), and the additional surface water samples may have better captured transient contamination from manure storages.

3.4. Land application of septage, municipal, and industrial waste is another source of elevated ARGs in the environment

After implementing FIT across 5 ARGs in sediment and surface water, we found that three of the ARG responses (Table 2) are positively associated with land-applied waste sources in sediment (*sul1* and *intI1*) or surface water [*tet(W)* and *intI1*]. ARG responses in *sediment*, *municipal waste*, or *septage* land application characterized land-applied residential waste sources. For *sul1*, FIT selected the ORF land-applied residential waste source term representing land-applied waste from residential origins (i.e., land application of municipal waste or septage consisting of solid or semi-solid residue generated during the treatment of domestic sewage *via* primary, secondary, or advanced wastewater treatment and the wastewater contents of septic or holding tanks, dosing chambers, grease interceptors, seepage beds/pits/trenches, privies, or portable restrooms (Wis. Admin, 2021). A one standard deviation increase in contributions from land-applied waste from

TABLE 2 Regression results for predicting the relative abundance of *erm(B), tet(W), qnrA, sul1, and intI1* (log10 gene copies per 16S-rRNA copies) in riverbed sediment (columns toward the left) and surface water (right-most five columns).

Environmental matrix		Riverbed sediment				Surface water				
ARG (n = sample size)		*erm(B)* ($n = 91$)	*tet(W)* ($n = 91$)	*sul1* ($n = 91$)	*intI1* ($n = 91$)	*erm(B)* ($n = 98$)	*tet(W)* ($n = 98$)	*qnrA* ($n = 98$)	*sul1* ($n = 98$)	*intI1* ($n = 98$)
Recent precip.	Std. Regression Coefficient (β_1)	−0.723**	0.654**	NS	−0.330**	0.415**	0.635**	0.213**	0.637**	0.277**
Recent x antecedent precip.	Std. Regression Coefficient (β_2)	0.561**	0.923**	NS	0.256**	−0.394**	−0.300**	−1.10**	NS	0.637**
Freezing	Regression Coefficient (β_3)	−0.621*	NS	NS	−0.801**	1.94**	NS	NS	NS	NS
Bovine sources	Bovine Source Description	GORF AFO (*via* ground hauling of manure to application fields)	GORF AFO (*via* ground hauling of manure to application fields)	NS	NS	GORF AFO (*via* ground hauling of manure to application fields)	ORF AFO	ORF AFO	ORF Manure app. fields	ORF Manure app. fields
	Std. Regression Coefficient (β_u)	0.199*	0.303*	NS	NS	0.162**	0.247**	0.173**	0.148*	0.134
	RAR ($\mathbf{10}^{\beta_u}$)	1.58*	2.01*	NS	NS	1.45**	1.77**	1.49**	1.41*	1.36
	Influence Range (α_O)	< 13 km				< 10 km				
Land-app. waste sources	Land applied waste Source Description	NS	NS	Land-applied waste- *residential*	Septage ground transport to land app. sludge- *residential*	NS	Land-applied waste- *industrial*	NS	NS	Land-applied waste- *industrial*
	Std. Regression Coefficient (β_u)	NS	NS	0.211**	0.155*	NS	0.134*	NS	NS	0.148*
	RAR ($\mathbf{10}^{\beta_u}$)	NS	NS	1.63**	1.43*	NS	1.36*	NS	NS	1.41*
	Influence Range (α_O)	< 8 km				< 10 km				
Soil sources	Soil Source Description	NS	NS	Type A (Sand, Sandy loam, Loamy sand, and Gravel)	Type A (Sand, Sandy loam, Loamy sand, and Gravel)	Type D (Clay loam, silty clay loam, sandy clay, and silty clay)	NS	NS	NS	NS
	Regression Coefficient (β_u)	NS	NS	0.402**	0.253	0.231	NS	NS	NS	NS
	RAR ($\mathbf{10}^{\beta_u}$)	NS	NS	2.52**	1.79	1.70	NS	NS	NS	NS
	Influence Range (α_{Radius})	1 km								

*p < 0.10, **p < 0.05. NS indicates that no terms were selected for the source category. Other source categories not selected: wastewater treatment plants (WWTPs), septic systems, and developed land cover. No terms were selected for the log10 relative abundance of qnrA in sediment. The sample size is indicated for each of the responses in each column. For each of the climatic and source terms, the standardized regression coefficient, β, is provided resulting from the Test stage of FIT. For each source term, two additional rows result from the Find and Inform stages of the FIT framework. For each source term category (i.e., bovine, land-applied waste, or soil), the source description, the relative abundance ratio ($RAR = 10^{\beta}$), and hyperparameters indicating the influence range around sources, α, are summarized. Precipitation-term associations are shown in blue. The associations with freezing temperatures are shown in white. Bovine source associations are in red. Land-applied waste sources are shown in yellow.

10.3389/fmicb.2023.1223876

residential use was associated with a 63% ($p < 0.05$) increase in the relative abundance of *sul1*. For *intI1,* FIT selected the GORF land-applied waste source term, representing land-applied residential waste weighted by the density of nearby septic systems. A one standard deviation increase in land-applied waste from residential use was associated with a 43% ($p < 0.05$) increase in the relative abundance of *intI1*.

For ARG responses in *surface water*, industrial waste's land application characterized these five ARGs' secondary sources. For *tet(W)*, FIT selected the ORF land-applied industrial waste source term representing by-product solids from the animal product or food processing industry (i.e., remains of butchered animals, paunch manure, cheese production waste, and vegetable waste materials). A one standard deviation increase in land-applied waste from industrial use was associated with a 36% ($p < 0.10$) increase in the relative abundance of *tet(W)*. Then, for *intI1*, FIT selected the ORF land-applied industrial waste source term [i.e., "both the by-product solids from the animal product or food processing and liquid waste such as silage, leachate, whey, whey permeate, whey filtrate, contact cooling water, cooling or boiler water containing water treatment additives, and wash water generated in industrial, commercial, and agricultural operations" (Wis. Admin, 2021)]. A one standard deviation increase in land-applied waste from industrial use was associated with a 41% ($p < 0.10$) increase in the relative abundance of *intI1*.

Our findings are consistent with current knowledge that ARGs are enriched in biosolids from treatment processes (i.e., primary, secondary, or advanced wastewater treatment) (Chen and Zhang, 2013; Burch et al., 2014; Pepper et al., 2018). This is the first study to report an association between modeled contributions from spatially distributed land-applied waste and ARGs recovered from riverbed sediment and surface water. This is also the first study to show that septage and municipal or industrial waste disposal on land pollute and correspond with a quantifiable environmental impact on antibiotic resistance levels in sediment and surface water. The WPDES database lists the facility names associated with the land application sites. After searching on company websites for the products associated with each facility producing industrial wastewater or sludge destined for land application, we found that 88.8% of the industrial land-applied waste sites are associated with dairy and meat products. None (i.e., 0%) of the facilities were associated with pharmaceuticals. This suggests that the disposal of industrial wastes from dairy and meat processing extends the polluting ability of industrial livestock agriculture and that industrially produced, land-applied pharmaceutical waste is not a source of elevated ARGs in this region.

3.5. Sandy soils are associated with sediment ARGs, and clay soils are associated with surface water ARGs

The bottom of Table 2 shows the results from the Inform and Test stages corresponding to the soil as a source. For surface water responses, only soil type D (clay loam, silty clay loam, sandy clay, or silty clay) coverage was associated with a 70% increase in the log10 relative abundance of *erm(B)*. In sediment responses, soil type A (i.e., sand, sandy loam, loamy sand, or gravel) coverage was associated with 152% and 79% increases in *sul1* and *intI1* log10 relative abundances, respectively.

Soil type D contains clay, and we expect ARGs to correlate with clay based on previous research (Mao et al., 2014; Wang et al., 2016). A previous study also suggests that clay microbial communities are more resilient to change from anthropogenic sources compared to other soil types, like sand (Neumann et al., 2013). Therefore, this contribution to *erm(B)* relative abundance of clay soil sources may suggest the long-term impacts of agricultural sources on clay microbial communities. However, we found different results from the surface water results. Overall, soil appears to significantly contribute to the relative abundance of these ARGs, and the differences in soil sources for surface water and sediment in this study have many potential explanations (e.g., adsorption, desorption, and absorption between overland soil, riverbed sediment, and surface water). More observational data and controlled mesocosm-scale experiments are needed to validate these findings and characterize these complex dynamics.

3.6. Regional differences may affect the primary sources of elevated ARGs

WWTPs were expected to show associations with *sul1* and *intI1*, as *sul1* is often conserved in integron-integrase mobile genetic elements (Pruden et al., 2012; Amos et al., 2015), but the FIT model selected neither municipal nor industrial WWTPs associating with any of the five relative abundance responses across surface water or sediment. One explanation is that in this rural area of ~20,000 people (US Census Bureau, 2022), only five of the WWTPs were flow-connected to the 20 sampling sites. Our study area consists of a larger bovine–human ratio (Borchardt et al., 2021; Burch et al., 2021; Wiesner-Friedman et al., 2021a) compared to the study areas of previous ARG research in the South Platte River Basin in Colorado, United States (Pruden et al., 2012), and the Thames Watershed in Oxfordshire, United Kingdom (Amos et al., 2015).

In our study, both *sul1* and *intI1* were associated with land-applied municipal waste and septage. The land-applied municipal waste and septage represent the aggregation of treated septage and wastewater, suggesting that some ARGs may originate from WWTPs, but most likely, the persistent application of biosolids on land represents a more significant source than WWTP effluent or septic systems in this region. Quantitation methods with low detection limits for *intI1,* more flow-connected sampling sites to sources, or a different ARG panel may be needed to detect the impacts of WWTP effluent or septic systems.

3.7. The overland influence range around sources extends up to 13 km

Bovine source terms associated with elevated ARGs in *sediment* had exponential influence ranges of $\alpha_O < 13$ km on the river network, indicating that decayed contributions would still be detected in the river when manure fields were

up to 13 km away from the river network. For all bovine source terms associated with ARG responses in *surface water*, decayed contributions would still be detected when sources were up to 10 km from the river network. For all land-applied waste source terms associated with ARGs, the influence range was up to 8 km for *sediment* and 10 km for *surface water* responses.

These overland, exponential influence ranges, α_O, were determined from the *inform* stage of FIT. In a previous study (Wiesner-Friedman et al., 2021a), we remarked that this hyperparameter captures more than average overland transport. This hyperparameter characterizes the extent to which a microbial response can capture a signal from sources so that longer overland influence ranges may indicate either A) longer transport and B) an increased probability of detection, or both. Previously, we found longer overland influence ranges around sources for host-associated *Bacteroides* in sediment (i.e., $\alpha_O > 1\ km$) vs. surface water (i.e., $\alpha_O < 1\ km$) (Wiesner-Friedman et al., 2021a).

In this study, on average, we found long overland influence ranges [i.e., a mean value of $\hat{\alpha_O} = 7.07$ km (95%CI: 4.22 km, 9.92 km)] for both sediment and surface water. ARGs can exist naturally in soils (D'Costa et al., 2011) and be carried by either aerobic or anaerobic bacteria (Xu et al., 2021); They can be transferred to other bacteria by several genetic mechanisms (Davies and Davies, 2010). These factors may increase the transport of and ability to detect ARGs in surface waters compared to anaerobic *Bacteroides* gene markers. Furthermore, *Bacteroides* persist briefly outside of the gut of their hosts (Ballesté and Blanch, 2010), so shorter overland influence ranges would be expected. One implication of longer influence ranges around bovine sources for ARGs compared to host-associated *Bacteroides* genes is that host-associated markers may underrepresent the risks associated with fecal contamination from bovine sources in surface water. Additionally, this research and previous studies have found an increased probability of detecting microbial genes in sediments compared to surface water (see Supplementary material S2) (Kasich et al., 2012; Wiesner-Friedman et al., 2021a), which suggests that risks associated with particular sources may be underrepresented from sampling transient surface water compared to time-integrated polluted sediment.

The FIT model of ARGs in the environment is the first to characterize overland influence ranges around these sources. A setback distance of 34–67 m from surface water has previously been recommended for manure and slurry land application under experimental conditions (Hall et al., 2020). The exponential influence ranges from our study indicate that sources very close to the river will greatly contribute but that distant sources up to 13 km away from the river network can also impact ARG levels. A factor that may lead to long influence ranges in this region is the karst geology, where fractures, sinkholes, caves, disappearing streams, and springs may provide direct pathways for contaminants, including antibiotics and ARGs, to reach ground and surface waters (Stange and Tiehm, 2020; Xiang et al., 2020). Our findings are consistent with a study in a karst region in Germany, where elevated ARGs and human-specific fecal markers were detected in a spring 9 km away from the suspected source (Stange and Tiehm, 2020).

3.8. The modeling predicts localized impacts to elevated ARGs in sediment and dispersed impacts in surface water

Since this is the first study to report LUR results for *erm(B)* in sediment and *erm(B), tet(W), qnrA, sul1,* and *intI1* in surface water, we identified the databases that most reliably report the spatial location of bovine and land-applied waste sources associated with elevated relative abundance of these ARGs and their corresponding regression coefficients (Table 2), and we have shown the spatial impact of these pollution sources (Figure 1).

Figure 1A shows the geographical distribution of an increase expected in the relative abundances of *erm(B)*, *tet(W)*, and *sul1* in sediment associated with risk-conservative contributions from AFOs *via* the application of manure. This figure, which results from a GORF SPM, suggests that elevated ARGs in riverbed sediment are localized around manure application fields. However, the extent to which those sources (*viz.*, differently sized black squares) qualify as polluters relates to their proximity to AFOs and the scale of the operation (viz. differently sized blue diamonds). This localized pollution may be influenced by ARG soil attachment (Barrios et al., 2021). In previous LUR, AFOs were associated with *sul1* in sediment, but the spatial localization was not reported or depicted (Pruden et al., 2012). Our LUR/FIT modeling showing localized sediment ARG pollution is consistent with the field studies of the enrichment of ARGs in AFO manure application and dissemination into the environment (Fahrenfeld et al., 2014; Wallace et al., 2018).

Figure 1B shows the geographical distribution of an increase expected in the relative abundances of *tet(W)* and *intI1* in surface water associated with risk-conservative contributions from land application sites. This figure, which results from an ORF SPM, suggests that land application sites have a dispersed impact on elevated ARGs in surface water.

These maps indicate locations where additional monitoring may be needed to understand the impacts of different sources on environmental and public (i.e., water users') health. The upper-bound hyperparameter values and database information also serve other regions with similar geography, land use, agricultural practices, and population to preliminarily define monitoring locations for AMR studies.

4. Discussion

This is the first LUR study of ARGs in surface water and the first LUR of more than two ARG responses from sediment samples. Our primary finding is that bovine sources (i.e., AFOs and manure application fields) were consistent sources of elevated ARGs. This continues the large body of work that has detected ARGs in livestock manure and slurry, on soil where the manure or slurry is applied, and downstream of livestock operations (Joy et al., 2013; Fahrenfeld et al., 2014; Peng et al., 2017; Wepking et al., 2017; Guo et al., 2018; Lopatto et al., 2019; Hall et al., 2020; Miller et al., 2020), but it is the first to connect modeled transport from manure land application to elevated AMR.

Previous research has revealed that domestic and industrial wasteland application sites are potential sources of elevated

ARGs (Bondarczuk et al., 2016; Murray et al., 2019). However, our study distinguishes itself as one that found associations with the collective contributions from spatially distributed land-applied waste sites over a large spatial scale and measured ARG levels in the environment. A large body of work has detected microbial contaminants associated with land-applied wastes in soils, groundwater, surface water, and the air near application sites (Brooks et al., 2007; Lapen et al., 2008; Tanner et al., 2008; Edwards et al., 2009; Gottschall et al., 2009; Zerzghi et al., 2010; Esseili et al., 2012; Mohapatra et al., 2016; Pepper et al., 2019). Our research adds to this body of evidence.

While the US Environmental Protection Agency's (EPA's) Part 503 rule (Walker et al., 1994) regulates treatment and land application standards for class A and B biosolids, there are many similarities between pre-treatment class B biosolids and anaerobically treated manure or slurry from dairy CAFOs. Antibiotic-resistant bacteria, endotoxins, prions, pathogenic bacteria, and protozoa have been reported in both (Pepper et al., 2019). Few regulations exist for the treatment of livestock facility waste and its application on land. Regulations of livestock waste have focused on nutrient management, do not require treatment for viruses and pathogens, and only apply to be permitted CAFOs. Class B biosolids must meet minimal treatment and land application requirements. Therefore, one explanation for the increased consistency of association between bovine sources and ARG responses compared to land-applied waste sources is that this land application is more regulated compared to manure and that this additional regulation of treatment and land application locations has resulted in less harm to water quality than bovine manure land application. Another explanation could be that the quantity of bovine manure land application is much greater than other types in this region. However, regulators may want to evaluate current treatment standards, land application restrictions, and environmental monitoring of land application of waste more generally to improve water quality.

The dissemination of fluoroquinolone-associated resistance encoded by both chromosomal and plasmid-derived *qnrA* may increase the risks of quinolone-resistant human pathogens in surface water from plasmid-mediated HGT (Cummings et al., 2011). In the United States, fluoroquinolones are among the most common clinically prescribed classes of antibiotics (Antibiotic Use in the United States, 2017). Our findings that connect AFOs to the levels of *qnrA* in surface water are concerning, and the United States may want to consider broader enforcement of the recent policy limiting the use of antibiotics that are clinically relevant to humans in livestock settings (FDA, 2022).

Aside from the anthropogenic sources, the soil source results in this study support that the processes involving the interaction of anthropogenic sources, nearby soils, sediment, and surface water are too complex for a linear modeling approach to describe. The importance of soil sources in this study shows that characterizing natural processes (i.e., physical, biological, ecological, physicochemical, and chemical dynamics) may help predict ARG levels and mitigate the impacts of anthropogenic sources on AMR. Monitoring the impacts of chronic and acute ARG-associated pollution events (i.e., pollution with antibiotic-resistant bacteria and selective pressures) on adsorption, desorption, and absorption processes for various soil types may provide an additional benefit. More complex modeling calls for refinement in spatial scale and improvement in the prediction of soil characteristics.

A concern for the applicability of this study to other regions may be the availability of spatial databases. However, we found that a strength of this study is that the key ARG sources in this study (i.e., CAFOs, class A and B land application sites, and soil type) are represented by nationally available databases in the United States. Expanding these databases to include industrial livestock land applications and greater detail about application methods and the types of applied waste may be beneficial.

Here, we have focused on spatial relationships. However, we have modeled the impact of freezing temperature and antecedent precipitation (see Table 2 for results and Supplementary material S5 for details). We found that freezing temperature is negatively associated with ARGs in sediment and positively associated with one ARG in surface water, which is consistent with a previous study that found higher ARG abundances during the Wisconsin manure application season (Beattie et al., 2018). In addition, we identified three patterns of association for ARGs with antecedent precipitation (see Supplementary material S5). However, due to the temporal resolution of sampling approximately only once every 3 months, our results can only be interpreted as seasonal effects rather than impacts from recent and antecedent precipitation.

Additionally, due to this temporal resolution, our models may only capture the long-tail decay of ARGs disseminating from sources (Burch et al., 2014; Lopatto et al., 2019; Macedo et al., 2020; Barrios et al., 2021), meaning that peak contamination corresponding to periods directly following manure application is not well-characterized. Sampling at a finer temporal resolution could help to better capture these peaks as well as the impact of different flow events and meteorological variables.

The reproducibility of associations between the three source categories associated with increases in ARGs (i.e., bovine, land-applied waste, and soil) and the ARG responses in sediment and surface water provides evidence that elevated ARGs in the environment are linked to natural occurrence soils and land-applied wastes of bovine, residential, or industrial origins. In our study, we found that a one standard deviation increase in source impacts is associated with increases between 36 and 152%. This is larger than the expected percentage increase (17%) in total relative abundances of ARGs (TARG) in sediment and surface water associated with a total antibiotic selection pressure (TASP) score of 1–2 reported from a meta-analysis (Duarte et al., 2019). The greater association in our study may indicate the combined influence of enrichment from organic matter, antibiotics, and intracellular or extracellular ARGs disseminating from sources (Xie et al., 2018). Our findings call for more robust treatment regulations to remove or reduce ARBs and ARGs from wastes and policies to decrease antimicrobial use in livestock and humans.

Due to measured negative changes to the environment and public health of communities living nearby dense industrial livestock agriculture and land application sites (Greger and Koneswaran, 2010; Lowman et al., 2013; Hooiveld et al., 2016), a collaborative One Health approach (Robinson et al., 2016) may

be beneficial for evaluating the impacts of these sources of mixed contaminants (i.e., pathogens, ARB and ARGs, heavy metals, disinfectants, fire retardants, pharmaceuticals, and polycyclic aromatic hydrocarbons) (Kinney et al., 2006; Ma et al., 2011; Pepper et al., 2018; Murray et al., 2019) on the shared health of humans, animals, and the environment.

Data availability statement

The original contributions presented in the study are included in the article/Supplementary material, further inquiries can be directed to the corresponding author.

Author contributions

All authors listed have made a substantial, direct, and intellectual contribution to the work and approved it for publication.

Funding

This study was supported by a grant from the National Institute of Environmental Health Sciences (NIEHS) T32ES007018. This study was funded in part by the Marquette University Innovation Grant, NSF grant 1316318 as part of the joint NSF-NIH-USDA Ecology and Evolution of Infectious Diseases program, the Engineering Research Centers Program of the National Science Foundation under NSF Cooperative Agreement no. EEC-2133504, and the Department of Army award W9132T2220001 issued by the Office of Army Research.

Conflict of interest

The authors declare that the research was conducted in the absence of any commercial or financial relationships that could be construed as a potential conflict of interest.

Publisher's note

All claims expressed in this article are solely those of the authors and do not necessarily represent those of their affiliated organizations, or those of the publisher, the editors and the reviewers. Any product that may be evaluated in this article, or claim that may be made by its manufacturer, is not guaranteed or endorsed by the publisher.

Author disclaimer

The study presented was not performed or funded by the EPA and was not subject to the EPA's quality system requirements. The views expressed in this article are those of the author(s) and do not necessarily represent the views or policies of the U.S. Environmental Protection Agency. The United States Government has a royalty-free license throughout the world for all copyrightable material contained herein. Any opinions, findings, conclusions, or recommendations expressed in this material are those of the author(s) and do not necessarily reflect the views of the Office of Army Research. Any use of trade, firm, or product names is for descriptive purposes only and does not imply endorsement by the U.S. Government.

Supplementary material

The Supplementary Material for this article can be found online at: https://www.frontiersin.org/articles/10.3389/fmicb.2023.1223876/full#supplementary-material

References

Ahmed, W., Zhang, Q., Lobos, A., Senkbeil, J., Sadowsky, M. J., Harwood, V. J., et al. (2018). Precipitation influences pathogenic bacteria and antibiotic resistance gene abundance in storm drain outfalls in coastal sub-tropical waters. *Environ. Int.* 116, 308–318. doi: 10.1016/j.envint.2018.04.005

Alford, J. B., Debbage, K. G., Mallin, M. A., and Liu, Z-. J. (2016). Surface water quality and landscape gradients in the north carolina cape fear river basin: the key role of fecal coliform. *Southeast Geogr.* 56, 428–453. doi: 10.1353/sgo.2016.0045

Amarasiri, M., Sano, D., and Suzuki, S. (2019). Understanding human health risks caused by antibiotic resistant bacteria (ARB) and antibiotic resistance genes (ARG) in water environments: Current knowledge and questions to be answered. *Crit. Rev. Environ. Sci. Technol.* 2, 1–44. doi: 10.1080/10643389.2019.1692611

Amos, G. C. A., Gozzard, E., Carter, C. E., Mead, A., Bowes, M. J., Hawkey, P. M., et al. (2015). Validated predictive modelling of the environmental resistome. *ISME J.* 9, 1467–1476. doi: 10.1038/ismej.2014.237

Antibiotic Use in the United States (2017). *Progress and Opportunities | Antibiotic Use | CDC.* Available online at: https://www.cdc.gov/antibiotic-use/stewardship-report/2017.html (accessed April 20, 2021).

Balleste, E., and Blanch, A. R. (2010). Persistence of Bacteroides species populations in a river as measured by molecular and culture techniques. *Appl. Environ. Microbiol.* 76, 7608–7616. doi: 10.1128/AEM.00883-10

Barrios, R. E., Bartelt-Hunt, S. L., Li, Y., and Li, X. (2021). Modeling the vertical transport of antibiotic resistance genes in agricultural soils following manure application. *Environ. Pollut.* 285, 117480. doi: 10.1016/j.envpol.2021.117480

Beattie, R. E., Bandla, A., Swarup, S., and Hristova, K. R. (2020a). Freshwater sediment microbial communities are not resilient to disturbance from agricultural land runoff. *Front. Microbiol.* 11, 539921. doi: 10.3389/fmicb.2020.539921

Beattie, R. E., Skwor, T., and Hristova, K. R. (2020b). Survivor microbial populations in post-chlorinated wastewater are strongly associated with untreated hospital sewage and include ceftazidime and meropenem resistant populations. *Sci. Total Environ.* 740, 140186. doi: 10.1016/j.scitotenv.2020.140186

Beattie, R. E., Walsh, M., Cruz, M. C., McAliley, L. R., Dodgen, L., Zheng, W., et al. (2018). Agricultural contamination impacts antibiotic resistance gene abundances in river bed sediment temporally. *FEMS Microbiol. Ecol.* 94, 131. doi: 10.1093/femsec/fiy131

Bondarczuk, K., Markowicz, A., and Piotrowska-Seget, Z. (2016). The urgent need for risk assessment on the antibiotic resistance spread via sewage sludge land application. *Environ. Int.* 87, 49–55. doi: 10.1016/j.envint.2015.11.011

Borchardt, M. A., Stokdyk, J. P., Kieke, B. A., Muldoon, M. A., Spencer, S. K., Firnstahl, A. D., et al. (2021). Sources and risk factors for nitrate and microbial contamination of private household wells in the fractured dolomite aquifer of northeastern wisconsin. *Environ. Health Perspect.* 129, 67004. doi: 10.1289/EHP7813

Brooks, J. P., Maxwell, S. L., Rensing, C., Gerba, C. P., and Pepper, I. L. (2007). Occurrence of antibiotic-resistant bacteria and endotoxin associated with the land application of biosolids. *Can. J. Microbiol.* 53, 616–622. doi: 10.1139/W07-021

Brown, P. C., Borowska, E., Schwartz, T., and Horn, H. (2019). Impact of the particulate matter from wastewater discharge on the abundance of antibiotic resistance genes and facultative pathogenic bacteria in downstream river sediments. *Sci. Total Environ.* 649, 1171–1178. doi: 10.1016/j.scitotenv.2018.08.394

Bucci, J. P., Shattuck, M. D., Aytur, S. A., Carey, R., and McDowell, W. H. (2017). A case study characterizing animal fecal sources in surface water using a mitochondrial DNA marker. *Environ. Monit. Assess.* 189, 406. doi: 10.1007/s10661-017-6107-z

Bueno, I., Williams-Nguyen, J., Hwang, H., Sargeant, J. M., Nault, A. J., Singer, R. S., et al. (2018). Systematic review: impact of point sources on antibiotic-resistant bacteria in the natural environment. *Zoonoses Pub. Health* 65, e162–e184. doi: 10.1111/zph.12426

Burch, T. R., Sadowsky, M. J. and LaPara, T. M. (2014). Fate of antibiotic resistance genes and class 1 integrons in soil microcosms following the application of treated residual municipal wastewater solids. *Environ. Sci. Technol.* 48, 5620–5627. doi: 10.1021/es501098g

Burch, T. R., Stokdyk, J. P., Spencer, S. K., Kieke, B. A., Firnstahl, A. D., Muldoon, M. A., et al. (2021). Quantitative microbial risk assessment for contaminated private wells in the fractured dolomite aquifer of kewaunee county, wisconsin. *Environ. Health Perspect.* 129, 67003. doi: 10.1289/EHP7815

Chen, H., and Zhang, M. (2013). Occurrence and removal of antibiotic resistance genes in municipal wastewater and rural domestic sewage treatment systems in eastern China. *Environ. Int.* 55, 9–14. doi: 10.1016/j.envint.2013.01.019

Costa, C. M. B., Leite, I. R., Almeida, A. K., and de Almeida, I. K. (2021). Choosing an appropriate water quality model-a review. *Environ. Monit. Assess.* 193, 38. doi: 10.1007/s10661-020-08786-1

Crowther, J., Wyer, M. D., Bradford, M., Kay, D., and Francis, C. A. (2003). Modelling faecal indicator concentrations in large rural catchments using land use and topographic data. *J. Appl. Microbiol.* 94, 962–973. doi: 10.1046/j.1365-2672.2003.01877.x

Cummings, D. E., Archer, K. F., Arriola, D. J., Baker, P. A., Faucett, K. G., Laroya, J. B., et al. (2011). Broad dissemination of plasmid-mediated quinolone resistance genes in sediments of two urban coastal wetlands. *Environ. Sci. Technol.* 45, 447–454. doi: 10.1021/es1029206

Davies, J., and Davies, D. (2010). Origins and evolution of antibiotic resistance. *Microbiol. Mol. Biol. Rev.* 74, 417–433. doi: 10.1128/MMBR.00016-10

D'Costa, V. M., King, C. E., Kalan, L., Morar, M., Sung, W. W. L., Schwarz, C., et al. (2011). Antibiotic resistance is ancient. *Nature* 477, 457–461. doi: 10.1038/nature10388

Dormann, C. F., Elith, J., Bacher, S., Buchmann, C., Carl, G., Carré, G., et al. (2013). Collinearity: a review of methods to deal with it and a simulation study evaluating their performance. *Ecography* 36, 27–46. doi: 10.1111/j.1600-0587.2012.07348.x

Dowling, P. M. (2004). Pharmacologic principles. *Eq. Int. Med.* 12, 169–233. doi: 10.1016/B0-72-169777-1/50006-8

Duarte, D. J., Oldenkamp, R., and Ragas, A. M. J. (2019). Modelling environmental antibiotic-resistance gene abundance: a meta-analysis. *Sci. Total Environ.* 659, 335–341. doi: 10.1016/j.scitotenv.2018.12.233

Edwards, M., Topp, E., Metcalfe, C. D., Li, H., Gottschall, N., Bolton, P., et al. (2009). Pharmaceutical and personal care products in tile drainage following surface spreading and injection of dewatered municipal biosolids to an agricultural field. *Sci. Total Environ.* 407, 4220–4230. doi: 10.1016/j.scitotenv.2009.02.028

Esseili, M. A., Kassem, I. I., Sigler, V., Czajkowski, K., and Ames, A. (2012). Genetic evidence for the offsite transport of *E. coli* associated with land application of Class B biosolids on agricultural fields. *Sci. Total Environ.* 433, 273–280. doi: 10.1016/j.scitotenv.2012.06.021

Fahrenfeld, N., Knowlton, K., Krometis, L. A., Hession, W. C., Xia, K., Lipscomb, E., et al. (2014). Effect of manure application on abundance of antibiotic resistance genes and their attenuation rates in soil: field-scale mass balance approach. *Environ. Sci. Technol.* 48, 2643–2650. doi: 10.1021/es404988k

FDA (2022). *CVM Updates FDA Announces Implementation of GFI #213, Outlines Continuing Efforts to Address Antimicrobial Resistance.* Available online at: https://wayback.archive-it.org/7993/20190423131636/; https://www.fda.gov/AnimalVeterinary/NewsEvents/CVMUpdates/ucm535154.htm (accessed January 20, 2022).

Gillings, M. R., Gaze, W. H., Pruden, A., Smalla, K., Tiedje, J. M., Zhu, Y. G., et al. (2015). Using the class 1 integron-integrase gene as a proxy for anthropogenic pollution. *ISME J.* 9, 1269–1279. doi: 10.1038/ismej.2014.226

Gottschall, N., Edwards, M., Topp, E., Bolton, P., Payne, M., Curnoe, W. E., et al. (2009). Nitrogen, phosphorus, and bacteria tile and groundwater quality following direct injection of dewatered municipal biosolids into soil. *J. Environ. Qual.* 38, 1066–1075. doi: 10.2134/jeq2008.0085

Greger, M., and Koneswaran, G. (2010). The public health impacts of concentrated animal feeding operations on local communities. *Fam. Commun. Health* 33, 11–20. doi: 10.1097/FCH.0b013e3181c4e22a

Guo, T., Lou, C., Zhai, W., Tang, X., Hashmi, M. Z., Murtaza, R., et al. (2018). Increased occurrence of heavy metals, antibiotics and resistance genes in surface soil after long-term application of manure. *Sci. Total Environ.* 635, 995–1003. doi: 10.1016/j.scitotenv.2018.04.194

Hadrich, J. C., Harrigan, T. M., and Wolf, C. A. (2010). Economic comparison of liquid manure transport and land application. *Appl. Eng. Agric.* 26, 743–758. doi: 10.13031/2013.34939

Hall, M. C., Mware, N. A., Gilley, J. E., Bartelt-Hunt, S. L., Snow, D. D., Schmidt, A. M., et al. (2020). Influence of setback distance on antibiotics and antibiotic resistance genes in runoff and soil following the land application of swine manure slurry. *Environ. Sci. Technol.* 54, 4800–4809. doi: 10.1021/acs.est.9b04834

Heaney, C. D., Myers, K., Wing, S., Hall, D., Baron, D., Stewart, J. R., et al. (2015). Source tracking swine fecal waste in surface water proximal to swine concentrated animal feeding operations. *Sci. Total Environ.* 511, 676–683. doi: 10.1016/j.scitotenv.2014.12.062

Hinojosa, J., Green, J., Estrada, F., Herrera, J., Mata, T., Phan, D., et al. (2020). Determining the primary sources of fecal pollution using microbial source tracking assays combined with land-use information in the Edwards Aquifer. *Water Res.* 184, 116211. doi: 10.1016/j.watres.2020.116211

Hooiveld, M., Smit, L. A. M., van der Sman-de Beer, F., Wouters, I. M., van Dijk, C. E., Spreeuwenberg, P. (2016). Doctor-diagnosed health problems in a region with a high density of concentrated animal feeding operations: a cross-sectional study. *Environ Health* 15, 24. doi: 10.1186/s12940-016-0123-2

Jacobs, K., Wind, L., Krometis, L. A., Hession, W. C., and Pruden, A. (2019). Fecal indicator bacteria and antibiotic resistance genes in storm runoff from dairy manure and compost-amended vegetable plots. *J. Environ. Qual.* 48, 1038–1046. doi: 10.2134/jeq2018.12.0441

Joy, S. R., Bartelt-Hunt, S. L., Snow, D. D., Gilley, J. E., Woodbury, B. L., Parker, D. B., et al. (2013). Fate and transport of antimicrobials and antimicrobial resistance genes in soil and runoff following land application of swine manure slurry. *Environ. Sci. Technol.* 47, 12081–12088. doi: 10.1021/es4026358

Karthikeyan, K. G., and Meyer, M. T. (2006). Occurrence of antibiotics in wastewater treatment facilities in Wisconsin, USA. *Sci. Total Environ.* 361, 196–207. doi: 10.1016/j.scitotenv.2005.06.030

Kasich, J., Taylor, M., and Nally, S. J. (2012). *Sediment Sampling Guide and Methodologies*. Ohio: Ohio Environmental Protection Agency.

Keely, S. P., Brinkman, N. E., Wheaton, E. A., Jahne, M. A., Siefring, S. D., Varma, M., et al. (2022). Geospatial patterns of antimicrobial resistance genes in the US EPA national rivers and streams assessment survey. *Environ. Sci. Technol.* 56, 14960–14971. doi: 10.1021/acs.est.2c00813

Keen, P. L., Knapp, C. W., Hall, K. J., and Graham, D. W. (2018). Seasonal dynamics of tetracycline resistance gene transport in the Sumas River agricultural watershed of British Columbia, Canada. *Sci. Total Environ. 628–629*, 490–498. doi: 10.1016/j.scitotenv.2018.01.278

Kinney, C. A., Furlong, E. T., Zaugg, S. D., Burkhard, M. R., Werner, S. L., Cahill, J. D., et al. (2006). Survey of organic wastewater contaminants in biosolids destined for land application. *Environ. Sci. Technol.* 40, 7207–7215. doi: 10.1021/es0603406

Knapp, C. W., Lima, L., Olivares-Rieumont, S., Bowen, E., Werner, D., Graham, D. W., et al. (2012). Seasonal variations in antibiotic resistance gene transport in the almendares river, havana, cuba. *Front. Microbiol.* 3, 396. doi: 10.3389/fmicb.2012.00396

Kyselková, M., Jirout, J., Vrchotová, N., Schmitt, H., and Elhottová, D. (2015). Spread of tetracycline resistance genes at a conventional dairy farm. *Front. Microbiol.* 6, 536. doi: 10.3389/fmicb.2015.00536

Lapen, D. R., Topp, E., Metcalfe, C. D., Li, H., Edwards, M., Gottschall, N., et al. (2008). Pharmaceutical and personal care products in tile drainage following land application of municipal biosolids. *Sci. Total Environ.* 399, 50–65. doi: 10.1016/j.scitotenv.2008.02.025

Li, X., Atwill, E. R., Antaki, E., Applegate, O., Bergamaschi, B., Bond, R. F., et al. (2015). Fecal indicator and pathogenic bacteria and their antibiotic resistance in alluvial groundwater of an irrigated agricultural region with dairies. *J Environ Qual* 44, 1435–1447. doi: 10.2134/jeq2015.03.0139

Ling, A. L., Pace, N. R., Hernandez, M. T., and LaPara, T. M. (2013). Tetracycline resistance and Class 1 integron genes associated with indoor and outdoor aerosols. *Environ. Sci. Technol.* 47, 4046–4052. doi: 10.1021/es400238g

Liu, Y., Cheng, D., Xue, J., Weaver, L., Wakelin, S. A., Feng, Y., et al. (2020). Changes in microbial community structure during pig manure composting and its relationship to the fate of antibiotics and antibiotic resistance genes. *J. Hazard. Mater.* 389, 122082. doi: 10.1016/j.jhazmat.2020.122082

Lopatto, E., Choi, J., Colina, A., Ma, L., Howe, A., Hinsa-Leasure, S., et al. (2019). Characterizing the soil microbiome and quantifying antibiotic resistance gene dynamics in agricultural soil following swine CAFO manure application. *PLoS ONE* 14, e0220770. doi: 10.1371/journal.pone.0220770

Lowman, A., McDonald, M. A., Wing, S., and Muhammad, N. (2013). Land application of treated sewage sludge: community health and environmental justice. *Environ. Health Perspect.* 121, 537–542. doi: 10.1289/ehp.1205470

Ma, Y., Wilson, C. A., Novak, J. T., Riffat, R., Aynur, S., Murthy, S., et al. (2011). Effect of various sludge digestion conditions on sulfonamide, macrolide, and tetracycline resistance genes and class I integrons. *Environ. Sci. Technol.* 45, 7855–7861. doi: 10.1021/es200827t

Macedo, G., Hernandez-Leal, L., van der Maas, P., Heederik, D., Mevius, D., Schmitt, H., et al. (2020). The impact of manure and soil texture on antimicrobial resistance gene levels in farmlands and adjacent ditches. *Sci. Total Environ.* 737, 139563. doi: 10.1016/j.scitotenv.2020.139563

Mao, D., Luo, Y., Mathieu, J., Wang, Q., Feng, L., Mu, Q., et al. (2014). Persistence of extracellular DNA in river sediment facilitates antibiotic resistance gene propagation. *Environ. Sci. Technol.* 48, 71–78. doi: 10.1021/es404280v

McKee, B. A., Molina, M., Cyterski, M., and Couch, A. (2020). Microbial source tracking (MST) in Chattahoochee River National Recreation Area: Seasonal and precipitation trends in MST marker concentrations, and associations with *E. coli* levels, pathogenic marker presence, and land use. *Water Res.* 171, 115435. doi: 10.1016/j.watres.2019.115435

Messier, K. P., Kane, E., Bolich, R., and Serre, M. L. (2014). Nitrate variability in groundwater of North Carolina using monitoring and private well data models. *Environ. Sci. Technol.* 48, 10804–10812. doi: 10.1021/es502725f

Miller, D. N., Jurgens, M. E., Durso, L. M., and Schmidt, A. M. (2020). Simulated winter incubation of soil with swine manure differentially affects multiple antimicrobial resistance elements. *Front. Microbiol.* 11, 611912. doi: 10.3389/fmicb.2020.611912

Mohapatra, D. P., Cledón, M., Brar, S. K., and Surampalli, R. Y. (2016). Application of wastewater and biosolids in soil: occurrence and fate of emerging contaminants. *Water. Air. Soil Pollut.* 227, 77. doi: 10.1007/s11270-016-2768-4

Munir, M., and Xagoraraki, I. (2011). Levels of antibiotic resistance genes in manure, biosolids, and fertilized soil. *J. Environ. Q.* 40, 248. doi: 10.2134/jeq2010.0209

Murray, R., Tien, Y. C., Scott, A., and Topp, E. (2019). The impact of municipal sewage sludge stabilization processes on the abundance, field persistence, and transmission of antibiotic resistant bacteria and antibiotic resistance genes to vegetables at harvest. *Sci. Total Environ.* 651, 1680–1687. doi: 10.1016/j.scitotenv.2018.10.030

Nappier, S. P., Liguori, K., Ichida, A. M., Stewart, J. R., and Jones, K. R. (2020). Antibiotic resistance in recreational waters: state of the science. *Int. J. Environ. Res. Public Health* 17. doi: 10.3390/ijerph17218034

Neumann, D., Heuer, A., Hemkemeyer, M., Martens, R., and Tebbe, C. C. (2013). Response of microbial communities to long-term fertilization depends on their microhabitat. *FEMS Microbiol. Ecol.* 86, 71–84. doi: 10.1111/1574-6941.12092

O'Dwyer, J., Hynds, P., Pot, M., Adley, C. C., and Ryan, M. P. (2017). Evaluation of levels of antibiotic resistance in groundwater-derived *E. coli* isolates in the Midwest of Ireland and elucidation of potential predictors of resistance. *Hydrogeol. J.* 25, 939–951. doi: 10.1007/s10040-017-1546-8

Pal, C., Bengtsson-Palme, J., Kristiansson, E., and Larsson, D. G. J. (2015). Co-occurrence of resistance genes to antibiotics, biocides and metals reveals novel insights into their co-selection potential. *BMC Genomics* 16, 964. doi: 10.1186/s12864-015-2153-5

Pazda, M., Kumirska, J., Stepnowski, P., and Mulkiewicz, E. (2019). Antibiotic resistance genes identified in wastewater treatment plant systems - a review. *Sci. Total Environ.* 697, 134023. doi: 10.1016/j.scitotenv.2019.134023

Peng, S., Feng, Y., Wang, Y., Guo, X., Chu, H., Lin, X., et al. (2017). Prevalence of antibiotic resistance genes in soils after continually applied with different manure for 30 years. *J. Hazard. Mater.* 340, 16–25. doi: 10.1016/j.jhazmat.2017.06.059

Pepper, I. L., Brooks, J. P., and Gerba, C. P. (2018). Antibiotic resistant bacteria in municipal wastes: is there reason for concern? *Environ. Sci. Technol.* 52, 3949–3959. doi: 10.1021/acs.est.7b04360

Pepper, I. L., Brooks, J. P., and Gerba, C. P. (2019). Land application of organic residuals: municipal biosolids and animal manures. *Environ. Pollut. Sci.* 13, 419–434. doi: 10.1016/B978-0-12-814719-1.00023-9

Pol, M., and Ruegg, P. L. (2007). Treatment practices and quantification of antimicrobial drug usage in conventional and organic dairy farms in Wisconsin. *J. Dairy Sci.* 90, 249–261. doi: 10.3168/jds.S0022-0302(07)72626-7

Pruden, A., Arabi, M., and Storteboom, H. N. (2012). Correlation between upstream human activities and riverine antibiotic resistance genes. *Environ. Sci. Technol.* 46, 11541–11549. doi: 10.1021/es302657r

Robinson, T. P., Bu, D. P., Carrique-Mas, J., Fèvre, E. M., Gilbert, M., Grace, D., et al. (2016). Antibiotic resistance is the quintessential one health issue. *Trans. R. Soc. Trop. Med. Hyg.* 110, 377–380. doi: 10.1093/trstmh/trw048

Rogers, S. W., Shaffer, C. E., Langen, T. A., Jahne, M., and Welsh, R. (2018). Antibiotic-resistant genes and pathogens shed by wild deer correlate with land application of residuals. *ecohealth* 15, 409–425. doi: 10.1007/s10393-018-1316-7

Singer, R. S., Ward, M. P., and Maldonado, G. (2006). Can landscape ecology untangle the complexity of antibiotic resistance? *Nat. Rev. Microbiol.* 4, 943–952. doi: 10.1038/nrmicro1553

Srinivasan, V., Nam, H-. M., Sawant, A. A., Headrick, S. I., Nguyen, L. T., Oliver, S. P., et al. (2008). Distribution of tetracycline and streptomycin resistance genes and class 1 integrons in Enterobacteriaceae isolated from dairy and nondairy farm soils. *Microb. Ecol.* 55, 184–193. doi: 10.1007/s00248-007-9266-6

Stange, C., and Tiehm, A. (2020). Occurrence of antibiotic resistance genes and microbial source tracking markers in the water of a karst spring in Germany. *Sci. Total Environ.* 742, 140529. doi: 10.1016/j.scitotenv.2020.140529

Tanner, B. D., Brooks, J. P., Gerba, C. P., Haas, C. N., Josephson, K. L., Pepper, I. L., et al. (2008). Estimated occupational risk from bioaerosols generated during land application of class B biosolids. *J. Environ. Qual* 37, 2311–2321. doi: 10.2134/jeq2007.0193

US Census Bureau (2022). *QuickFacts: Kewaunee County, Wisconsin* . Available online at: https://www.census.gov/quickfacts/kewauneecountywisconsin (accessed January 11, 2022).

Van Goethem, M. W., Pierneef, R., Bezuidt, O. K. I., Van De Peer, Y., Cowan, D. A., Makhalanyane, T. P., et al. (2018). A reservoir of "historical" antibiotic resistance genes in remote pristine Antarctic soils. *Microbiome* 6, 40. doi: 10.1186/s40168-018-0424-5

Walker, J., Knight, L., and Stein, L. (1994). *Plain English Guide to the EPA Part 503 Biosolids Rule*. U. S. EPA. Available online at: https://www.epa.gov/biosolids/plain-english-guide-epa-part-503-biosolids-rule (accessed August 24, 2023).

Wallace, J. S., Garner, E., Pruden, A., and Aga, D. S. (2018). Occurrence and transformation of veterinary antibiotics and antibiotic resistance genes in dairy manure treated by advanced anaerobic digestion and conventional treatment methods. *Environ. Pollut.* 236, 764–772. doi: 10.1016/j.envpol.2018.02.024

Wang, F., Stedtfeld, R. D., Kim, O. S., Chai, B., Yang, L., Stedtfeld, T. M., et al. (2016). Influence of soil characteristics and proximity to antarctic research stations on abundance of antibiotic resistance genes in soils. *Environ. Sci. Technol.* 50, 12621–12629. doi: 10.1021/acs.est.6b02863

Wang, Y., Jiang, R., Xie, J., Zhao, Y., Yan, D., Yang, S., et al. (2019). Soil and water assessment tool (SWAT) model: a systemic review. *J. Coastal Res.* 93, 22. doi: 10.2112/SI93-004.1

Wepking, C., Avera, B., Badgley, B., Barrett, J. E., Franklin, J., Knowlton, K. F., et al. (2017). Exposure to dairy manure leads to greater antibiotic resistance and increased mass-specific respiration in soil microbial communities. *Proc. Biol. Sci.* 284. doi: 10.1098/rspb.2016.2233

Wiesner-Friedman, C., Beattie, R. E., Stewart, J. R., Hristova, K. R., and Serre, M. L. (2021a). Characterizing differences in sources and contributions to fecal contamination of sediment and surface water with the microbial FIT framework . *Environ. Sci. Technol.* 56, 4231–4240. doi: 10.1021/acs.est.2c00224

Wiesner-Friedman, C., Beattie, R. E., Stewart, J. R., Hristova, K. R., and Serre, M. L. (2021b). Microbial find, inform, and test model for identifying spatially distributed contamination sources: framework foundation and demonstration of ruminant bacteroides abundance in river sediments. *Environ. Sci. Technol.* 55, 10451–10461. doi: 10.1021/acs.est.1c01602

Wis. Admin (2021). *Code § NR 113*. Available online at: https://docs.legis.wisconsin.gov/code/admin_code/nr/100/113 (accessed June 25, 2023).

Xiang, S., Wang, X., Ma, W., Liu, X., Zhang, B., Huang, F., et al. (2020). Response of microbial communities of karst river water to antibiotics and microbial source tracking for antibiotics. *Sci. Total Environ.* 706, 135730. doi: 10.1016/j.scitotenv.2019.135730

Xie, W. Y., Shen, Q., and Zhao, F. J. (2018). Antibiotics and antibiotic resistance from animal manures to soil: a review. *Eur. J. Soil Sci.* 69, 181–195. doi: 10.1111/ejss.12494

Xu, M., Wang, F., Sheng, H., Stedtfeld, R. D., Li, Z., Hashsham, S. A., et al. (2021). Does anaerobic condition play a more positive role in dissipation of antibiotic resistance genes in soil? *Sci. Total Environ.* 757, 143737. doi: 10.1016/j.scitotenv.2020.143737

Yang, L., Liu, W., Zhu, D., Hou, J., Ma, T., Wu, L., et al. (2018). Application of biosolids drives the diversity of antibiotic resistance genes in soil and lettuce at harvest. *Soil Biol. Biochem.* 122, 131–140. doi: 10.1016/j.soilbio.2018.04.017

Zainab, S. M., Junaid, M., Xu, N., and Malik, R. N. (2020). Antibiotics and antibiotic resistant genes (ARGs) in groundwater: a global review on dissemination, sources, interactions, environmental and human health risks. *Water Res.* 187, 116455. doi: 10.1016/j.watres.2020.116455

Zerzghi, H., Gerba, C. P., Brooks, J. P., and Pepper, I. L. (2010). Long-term effects of land application of class B biosolids on the soil microbial populations, pathogens, and activity. *J. Environ. Qual.* 39, 402–408. doi: 10.2134/jeq2009.0307

Zhang, S., Yang, G., Hou, S., Zhang, T., Li, Z., Liang, F., et al. (2018). Distribution of ARGs and MGEs among glacial soil, permafrost, and sediment using metagenomic analysis. *Environ. Pollut.* 234, 339–346. doi: 10.1016/j.envpol.2017.11.031

Zhang, Y., Cheng, D., Zhang, Y., Xie, J., Xiong, H., Wan, Y., et al. (2021). Soil type shapes the antibiotic resistome profiles of long-term manured soil. *Sci. Total Environ.* 786, 147361. doi: 10.1016/j.scitotenv.2021.147361

Zheng, D., Yin, G., Liu, M., Chen, C., Jiang, Y., Hou, L., et al. (2021). A systematic review of antibiotics and antibiotic resistance genes in estuarine and coastal environments. *Sci. Total Environ.* 777, 146009. doi: 10.1016/j.scitotenv.2021.146009

Zheng, J., Zhou, Z., Wei, Y., Chen, T., Feng, W., Chen, H., et al. (2018). High-throughput profiling of seasonal variations of antibiotic resistance gene transport in a peri-urban river. *Environ. Int.* 114, 87–94. doi: 10.1016/j.envint.2018.02.039

frontiers | Frontiers in Microbiology

TYPE Original Research
PUBLISHED 08 September 2023
DOI 10.3389/fmicb.2023.1209224

OPEN ACCESS

EDITED BY
Bartolome Moya Canellas,
Balearic Islands Health Research Institute (IdISBa), Spain

REVIEWED BY
Theodoros Karampatakis,
Papanikolaou General Hospital of Thessaloniki, Greece
Gabriel Cabot,
Balearic Islands Health Research Institute (IdISBa), Spain

*CORRESPONDENCE
Antoine G. Abou Fayad
✉ aa328@aub.edu.lb

†These authors have contributed equally to this work

RECEIVED 20 April 2023
ACCEPTED 28 August 2023
PUBLISHED 08 September 2023

CITATION
Kanafani ZA, Sleiman A, Frem JA, Doumat G, Gharamti A, El Hafi B, Doumith M, AlGhoribi MF, Kanj SS, Araj GF, Matar GM and Abou Fayad AG (2023) Molecular characterization and differential effects of levofloxacin and ciprofloxacin on the potential for developing quinolone resistance among clinical *Pseudomonas aeruginosa* isolates. *Front. Microbiol.* 14:1209224. doi: 10.3389/fmicb.2023.1209224

Molecular characterization and differential effects of levofloxacin and ciprofloxacin on the potential for developing quinolone resistance among clinical *Pseudomonas aeruginosa* isolates

Zeina A. Kanafani[1,2†], Ahmad Sleiman[2,3,4†], Jim Abi Frem[1], George Doumat[1], Amal Gharamti[1], Bassam El Hafi[2], Michel Doumith[5,6], Majed F. AlGhoribi[5,6], Souha S. Kanj[1,2], George F. Araj[2,7], Ghassan M. Matar[2,3,4] and Antoine G. Abou Fayad[2,3,4*]

[1]Division of Infectious Diseases, Department of Internal Medicine, American University of Beirut Medical Center, Beirut, Lebanon, [2]Center for Infectious Diseases Research, American University of Beirut, Beirut, Lebanon, [3]Faculty of Medicine, Department of Experimental Pathology, Immunology and Microbiology, American University of Beirut, Beirut, Lebanon, [4]World Health Organization Collaborating Center for Reference and Research on Bacterial Pathogens, Beirut, Lebanon, [5]Infectious Diseases Research Department, King Abdullah International Medical Research Center, Riyadh, Saudi Arabia, [6]King Saud bin Abdulaziz University for Health Sciences, Riyadh, Saudi Arabia, [7]Department of Pathology and Laboratory Medicine, American University of Beirut Medical Center, Beirut, Lebanon

Background: Fluoroquinolones are some of the most used antimicrobial agents for the treatment of *Pseudomonas aeruginosa*. This study aimed at exploring the differential activity of ciprofloxacin and levofloxacin on the selection of resistance among *P. aeruginosa* isolates at our medical center.

Methods: 233 *P. aeruginosa* clinical isolates were included in this study. Antimicrobial susceptibility testing (AST) was done using disk diffusion and broth microdilution assays. Random Amplification of Polymorphic DNA (RAPD) was done to determine the genetic relatedness between the isolates. Induction of resistance against ciprofloxacin and levofloxacin was done on 19 isolates. Fitness cost assay was done on the 38 induced mutants and their parental isolates. Finally, whole genome sequencing was done on 16 induced mutants and their 8 parental isolates.

Results: AST results showed that aztreonam had the highest non-susceptibility. RAPD results identified 18 clusters. The 19 *P. aeruginosa* isolates that were induced against ciprofloxacin and levofloxacin yielded MICs ranging between 16 and 256 μg/mL. Levofloxacin required fewer passages in 10 isolates and the same number of passages in 9 isolates as compared to ciprofloxacin to reach their breakpoints. Fitness cost results showed that 12 and 10 induced mutants against ciprofloxacin and levofloxacin, respectively, had higher fitness cost when compared to their parental isolates. Whole genome sequencing results showed that resistance to ciprofloxacin and levofloxacin in sequenced mutants were mainly associated with alterations in *gyrA*, *gyrB* and *parC* genes.

Conclusion: Understanding resistance patterns and risk factors associated with infections is crucial to decrease the emerging threat of antimicrobial resistance.

KEYWORDS

Pseudomonas aeruginosa, hospital-acquired infection, nosocomial infection, antimicrobial resistance, fluoroquinolone resistance, fitness cost

Introduction

Pseudomonas aeruginosa is a gram-negative infectious agent notorious for causing many hospital-acquired infections (Kaier et al., 2019). Infections due to *P. aeruginosa* have been increasing worldwide (Rosenthal et al., 2014; Athanasiou and Kopsini, 2018), and they are particularly challenging to treat owing to the intrinsically resistant nature of this bacteria to several commonly used antimicrobial agents. The bacterium itself possesses a cell wall with low permeability, and it easily acquires resistance to commonly used antimicrobial agents (Dantas et al., 2014; Gupta et al., 2016). This pathogen can cause severe infections, such as bacteraemia, pneumonia, bloodstream infections and intraabdominal infections (Folic et al., 2020). Moreover, *P. aeruginosa* is a leading pathogen in ventilator-associated pneumonias (VAPs) globally (Maraolo et al., 2017). Lately, MDR and XDR (multidrug resistant and extensively drug resistant respectively) *P. aeruginosa* constitutes a major health threat especially in endemic areas (Karampatakis et al., 2018). In Lebanon, a recent study showed that *P. aeruginosa* is the second most common agent isolated in VAP (Kanafani et al., 2019).

Fluoroquinolones are one of the most used antibiotic classes for the treatment of *P. aeruginosa*. Fluoroquinolones, particularly ciprofloxacin and levofloxacin, have some beneficial pharmacokinetic characteristics which render them suitable to use. Furthermore, fluoroquinolones are the only orally administered therapy available to treat *P. aeruginosa* infections. Unfortunately, these factors had favored the widespread use of fluoroquinolones for *P. aeruginosa* infection treatment to the extent that they were rendered inefficient in many cases due to emergence of resistance (Yang et al., 2015). Fluoroquinolones resistance in *P. aeruginosa* is primarily attributed to two mechanisms, mutations in the target genes coding enzymes *GyrA*, *ParC*, and *GyrB*, or an increase in the expression of the efflux pumps MexAB-OprM and MexCD-OprJ through mutations in their regulatory genes *mexR* and *nfxB*, respectively (Higgins et al., 2003).

Furthermore, there is a differential effect on the risk of developing resistance between the different classes of fluroquinolones. The literature shows that the use of levofloxacin is associated with increased resistance as compared to ciprofloxacin. One study on clinical isolates of *P. aeruginosa* showed that the use of levofloxacin, but not ciprofloxacin, is a risk factor for isolating fluoroquinolone-resistant strains (Kaye et al., 2006). Another clinical study on isolates from nosocomial infections showed that treating *P. aeruginosa* with levofloxacin is associated with increased rates of fluoroquinolones resistance. However, the use of ciprofloxacin showed no association with resistance (Lee et al., 2010).

On the other hand, an *in vitro* study comparing the development of resistance when using either ciprofloxacin or levofloxacin, found that ciprofloxacin showed a stronger ability to kill the bacteria while rendering it more susceptible to resistance (Zhao et al., 2020).

Fluoroquinolones-resistant *P. aeruginosa* prevalence in Lebanon is significant, representing 22.7% of nosocomial infections in 2013 (Chamoun et al., 2016). The alarming rate at which resistance to fluoroquinolones is emerging in *P. aeruginosa* emphasizes the need to further characterize this resistance pattern. Therefore, the aim of this study is to explore the molecular characteristics of *P. aeruginosa* infections at the American University of Beirut Medical Center and provide at the molecular level the differential activity of ciprofloxacin and levofloxacin on the selection of resistance among *P. aeruginosa* isolates.

Methodology

Collection and identification of isolates

A total of 233 *P. aeruginosa* clinical isolates, collected between 2017 and 2019, were included in the study. The patient's samples were processed, pathogens isolated and identified [using the Matrix-Assisted Laser Desorption/Ionization Time of Flight (MALDI-TOF) system (Bruker Daltonik, GmbH, Bremen, Germany)] with a score of green flags at the Clinical Microbiology Laboratory of the Department of Pathology and Laboratory Medicine (CML-PLM) at the American University of Beirut Medical Center, Beirut, Lebanon, and referred to our laboratory (Marí-Almirall et al., 2017). The isolates were assigned a sequential number upon reception, with repeat samples from the same patient being given letter designations with their original numbers instead of new numbers.

Disk diffusion

The experiment was performed using the Kirby-Bauer technique. For each isolate, a bacterial suspension equivalent to 0.5 MacFarland was prepared. Then it was subcultured on a round Mueller-Hinton agar plate, in all the directions, to ensure that the bacterial suspension covered all the plate using a sterile swab. The plate was left for around 10 min closed on the bench, followed by the addition of the 8 tested antimicrobials. The plate was then incubated at 37°C for 18–24 h after which the zone of inhibition diameters was measured, and the results were interpreted according to the CLSI M100 guideline (EM100 connect – CLSI M100 ED29, 2019).

Broth microdilution assay

Broth microdilution was performed with ciprofloxacin and levofloxacin on 19 selected *P. aeruginosa* isolates. Serial dilution took place between columns 1 and 11 to have a concentration ranging from 64 μg/mL to 0.0625 μg/mL. The plate was then placed in the incubator at 37°C for 18 h, and the experiments were run in duplicates for each bacterial isolate. The results were interpreted according to the CLSI M100 guideline (EM100 connect – CLSI M100 ED29, 2019).

Random amplification of polymorphic DNA (RAPD)

To further characterize our isolate collection beyond phenotypic testing and to assess their genomic relatedness, RAPD was employed using the illustra™ Ready-To-Go RAPD Analysis Beads (GE Healthcare Life Sciences, Marlborough, MA, United States) with the provided Primer 2 (5′-d[GTTTCGCTCC]-3′). A statistically representative selection of isolates from each group was evaluated by RAPD, and the resulting gels were analyzed using BioNumerics 6.6 (Applied Maths NV, Belgium) to generate Unweighted Pair Group Method with Arithmetic mean (UPGMA) dendrograms.

Induction of resistance

Induction of resistance was done on ciprofloxacin and levofloxacin against 19 selected *P. aeruginosa* clinical isolates. Based on the BMD results of each isolate on ciprofloxacin and levofloxacin, Mueller-Hinton agar plates supplemented with half the MIC of each antibiotic were prepared. Then each isolate was subcultured on agar plates supplemented with its equivalent concentration of each antibiotic separately. The number of passages on each concentration was dependent on the growth rate of the isolate. Once a heavy growth was achieved, an additional passage was done then the isolates were transferred to a 2-fold higher concentration. This was done until each isolate was induced to reach a concentration of 8 and 16 μg/mL of ciprofloxacin and levofloxacin, respectively (Gilbert et al., 2001).

Fitness cost assay

The tested isolates were first subcultured on LB agar and incubated at 37°C for 18–24 h. The next day, a loop full of each bacterial isolate was transferred into 10 mL of sterile cation adjusted Mueller-Hinton broth and incubated at 37°C for 18–24 h. Then, the turbid inoculated broth of each isolate was diluted at a 1:1000 ratio. The latter was then transferred into 4 distinct wells (200 μL each) of a 96 well microtiter plate. The replication rate of each tested isolate was measured using a plate reader (OD 600 nm) for 16 h with reads at 30 min intervals. The results were then averaged, normalized, and plotted on a graph (Mu et al., 2016).

Phe-Arg-β-naphthylamide inhibitor assay

Following the induction of all the 19 isolates against ciprofloxacin and levofloxacin, their MICs were determined for both antimicrobial agents with and without a multi-drug efflux pump inhibitor Phe-Arg-β-naphthylamide (PAβN). Ciprofloxacin or levofloxacin-PAβN inhibitor combinations experiment was performed by adding fixed concentrations of the inhibitors to the experimental wells of a standard antimicrobial broth microdilution assay. We followed CLSI guidelines in this assay. However, minor modifications to broth volumes were made in order to accommodate the presence of the PAβN inhibitor while keeping the concentrations of the ciprofloxacin or levofloxacin and the bacterial suspensions in accordance with CLSI recommendations. For each isolate, PAβN inhibitor was used at a fixed concentration of 25 μg/mL (Schuster et al., 2019). The MICs of the tested isolates were interpreted according to the CLSI M100 guideline (EM100 connect – CLSI M100 ED29, 2019).

Whole genome sequencing (WGS)

Genomic DNA of mutant and parental strains was extracted from their overnight cultures with the QIAamp DNA Mini Kit (Qiagen, Hilden, Germany) and then prepared for sequencing using the Nextera XT DNA library preparation kit (Illumina, Cambridge, United Kingdom) according to the manufacturer's protocols. Sequencing was performed on the Illumina MiSeq instrument using the 2×300 paired-end mode at the microbial genomic facilities in the Infectious Diseases Research Department, King Abdullah International Medical Research Center, Riyadh Saudi Arabia.

Bioinformatics analysis of the isolates

Reads thus generated were first filtered to remove low quality reads with Trimmomatic 0.38 (Bolger et al., 2014)[1] and then assembled using Spades 3.13.0 (Bankevich et al., 2012)[2] with the default options. *In silico* multilocus sequence typing was determined with the mlst 2.18.0 software[3] using the allelic sequences and ST profiles from the *P. aeruginosa* public MLST database.[4] The alterations in genes associated with resistance to ciprofloxacin and levofloxacin were initially identified by BLAST[5] and then confirmed by mapping with Genefinder[6] using the sequence of strain PAO-1 (NC_002516.2) as reference.

Results

Antimicrobial susceptibility testing

The disk diffusion results showed that out of the 233 *P. aeruginosa* isolates, 87 (37%) were non-susceptible to aztreonam, 63 (27%) were non-susceptible to imipenem, 58 (25%) were non-susceptible to Piperacillin-tazobactam, 55 (24%) were non-susceptible to ciprofloxacin, 45 (19%) were non-susceptible to ceftazidime, 32 (14%) were non-susceptible to cefepime, 28 (12%) were non-susceptible to amikacin, and 25 (11%) were non-susceptible to gentamicin (Table 1).

Based on their infection site and susceptibility profiles, the isolates were stratified into different grouping schemes. The first scheme grouped the isolates based on their sampling site into Marí-Almirall et al. (2017), Respiratory (Athanasiou and Kopsini, 2018), Urine (Rosenthal et al., 2014), Bone and Soft Tissue (Gupta et al., 2016), and Blood (Figure 1A). A second separate scheme grouped the isolates

1 http://www.usadellab.org/cms/index.php?page=trimmomatic
2 http://cab.spbu.ru/software/spades
3 Seemann T., mlst Github, https://github.com/tseemann/mlst.
4 https://pubmlst.org/organisms/pseudomonas-aeruginosa
5 https://blast.ncbi.nlm.nih.gov/Blast.cgi
6 Github, https://github.com/ukhsa-collaboration/gene_finder.

10.3389/fmicb.2023.1209224

TABLE 1 Antimicrobial susceptibility testing results of all the 233 *P. aeruginosa* isolates.

Antimicrobial Agents	No. Non-Susceptible (%)
Ceftazidime	45 (19%)
Cefepime	32 (14%)
Imipenem	63 (27%)
Aztreonam	87 (37%)
Ciprofloxacin	55 (24%)
Amikacin	28 (12%)
Gentamicin	25 (11%)
Piperacillin-tazobactam	58 (25%)

based on their antimicrobial susceptibility profiles into Marí-Almirall et al. (2017), Susceptible to all, (Athanasiou and Kopsini, 2018), Non-Susceptible to all (Rosenthal et al., 2014), Non-Susceptible to Fluoroquinolones (Gupta et al., 2016), and Remaining isolates (Figure 1B). Within the second scheme, the isolates did not overlap across different groups.

Molecular epidemiology

Upon assessing the overall genomic relatedness among the analyzed isolates with an 85% genomic similarity cutoff, a total of 18 clusters were identified (Supplementary Figure S1). There were three major clusters with >20 isolates each, four intermediate clusters with 7–18 isolates each, and 11 minor clusters with each containing 2–4 isolates.

According to their sites of infection, when breaking down the isolates into their respective groups, 19 clusters were observed. The respiratory group contained nine clusters (Supplementary Figure S2): 2 major clusters with >20 isolates each, two intermediate clusters with 9 and 17 isolates respectively, and five minor clusters with 2–5 isolates each. The urine group contained 5 clusters (Supplementary Figure S3) with 2–6 isolates each. The bone & soft tissue group contained 4 clusters (Supplementary Figure S4): 2 intermediately sized with 7 and 11 isolates respectively, and two minor clusters with 2 and 5 isolates, respectively. Finally, the blood group only contained one cluster comprised of 5 isolates (Supplementary Figure S5).

On the other hand, when breaking down the overall dendrogram into groups based on the isolates' antimicrobial susceptibility profiles, a total of 18 clusters were observed. Group 1 – "Susceptible to all" contained 6 clusters (Supplementary Figure S6): one major cluster with 20 isolates, three intermediate clusters with 9–15 isolates each, and two minor clusters with 2 and 4 isolates, respectively. Group 2 – "Non-Susceptible to all" did not contain any cluster (Supplementary Figure S7). Group 3 – "Non-Susceptible to Fluoroquinolones" contained seven clusters of 2–8 isolates each (Supplementary Figure S8). Finally, group 4 – "Remaining isolates" contained five clusters (Supplementary Figure S9): 1 cluster with 19 isolates, one cluster with 11 isolates and three clusters with 2–5 isolates each. Furthermore, wgMLST was performed on 8 isolates that represent the major clusters identified (Supplementary Figure S14).

Induction of resistance

Out of the 233 *P. aeruginosa* isolates, 19 were selected for the induction of resistance. The presence of distinct clusters provided guidance in selecting appropriate isolates for downstream applications. Therefore, the selection criteria were based on the susceptibility profiles, site of infection, and the clusters that the isolates belonged to based on the RAPD results. The common criteria between all the selected isolates were their susceptibility to ciprofloxacin and levofloxacin. The antimicrobial susceptibility testing results showed that the acquisition of ciprofloxacin resistance in *P. aeruginosa* led to levofloxacin resistance too and vice versa. All the 19 *P. aeruginosa* isolates that were induced against levofloxacin became non-susceptible to ciprofloxacin (1 intermediate and 18 resistant). Whereas 18 (95%) out of the 19 *P. aeruginosa* isolates that were induced against ciprofloxacin became non-susceptible to levofloxacin. Before the induction of resistance, the range of the minimal inhibitory concentration (MIC) of the 19 *P. aeruginosa* isolates was between <0.0625 μg/mL and 0.25 μg/mL for ciprofloxacin, and between 0.25 μg/mL and 0.5 μg/mL for levofloxacin. However, after the induction of resistance, the 19 *P. aeruginosa* isolates that were induced against ciprofloxacin yielded MICs ranging between 16 μg/mL and 256 μg/mL for ciprofloxacin and between 1 μg/mL and > 512 μg/mL for levofloxacin. Whereas the 19 *P. aeruginosa* isolates that were induced against levofloxacin yielded MICs ranging between 16 μg/mL and 256 μg/mL for levofloxacin and between 1 μg/mL and 32 μg/mL for ciprofloxacin (Table 2). The median MIC when induced against ciprofloxacin increased from 0.125 to 32 (256 folds) for ciprofloxacin and from 0.5 to 64 (128 folds) for levofloxacin. The median MIC when induced with levofloxacin increased from 0.5 to 32 (64 folds) for levofloxacin and 0.125 to 16 (128 folds) for ciprofloxacin.

In addition to that, when broth microdilution was done on the 19 *P. aeruginosa* isolates that were induced against ciprofloxacin with the addition of the multi-drug efflux pump inhibitor PAβN, no difference in MICs was detected in 2 (10%) isolates, two-fold decrease in 11 (58%) isolates, fourfold decrease in 2 (10%) isolates, and eight-fold decrease in 4 (22%) isolates were detected. However, the results of the 19 *P. aeruginosa* isolates that were induced against levofloxacin showed no difference in MICs in 1 (5%) isolate, two-fold decrease in 11 (58%) isolates, fourfold decrease in 4 (22%) isolates, eight-fold decrease in 2 (10%) isolates, and 16-fold in a decrease in 1 (5%) isolate (Supplementary Table S1).

Moreover, throughout the induction of resistance on the 19 selected *P. aeruginosa* isolates, 17 (89%) isolates grew at a higher rate in plates supplemented with ciprofloxacin compared to that with levofloxacin and only 2 (11%) isolates grew at the same rate. Furthermore, the number of passages needed to reach the antibiotic resistance breakpoint was higher for ciprofloxacin in 10 isolates and equal for ciprofloxacin and levofloxacin in 9 isolates.

Fitness cost

This experiment was done to evaluate the cost of acquiring fluoroquinolone resistance on the fitness of *P. aeruginosa*. For each isolate, we compared the induced mutants against ciprofloxacin

10.3389/fmicb.2023.1209224

and levofloxacin separately to the parental isolate prior to induction. For ciprofloxacin, 12 (63%) induced isolates showed a higher fitness cost, lower growth rate, with *p*-values ranging between $p < 0.0001$ and 0.0332 when compared to the parental isolates before induction (Figure 2A; Supplementary Figures S10, S11, S13B–D). However, 7 (37%) induced isolates showed no significant change in fitness cost, same growth rate, when compared to their parental isolates prior to induction with p-values ranging between 0.0827 and 0.9252 (Figure 2B; Supplementary Figures S12, S13A). For levofloxacin, 10 (53%) induced isolates showed a higher fitness cost, lower growth rate, with p-values ranging between $p < 0.0001$ and 0.0391 when compared to the parental isolates before induction (Figure 2A; Supplementary Figures S10, S11, S13A). Whereas 9 (47%) induced isolates showed no significant change in fitness cost, same growth rate, when compared to their parental isolates prior to induction with p-values ranging between 0.0937 and 0.8686 (Figure 2B; Supplementary Figures S12, S13B–D).

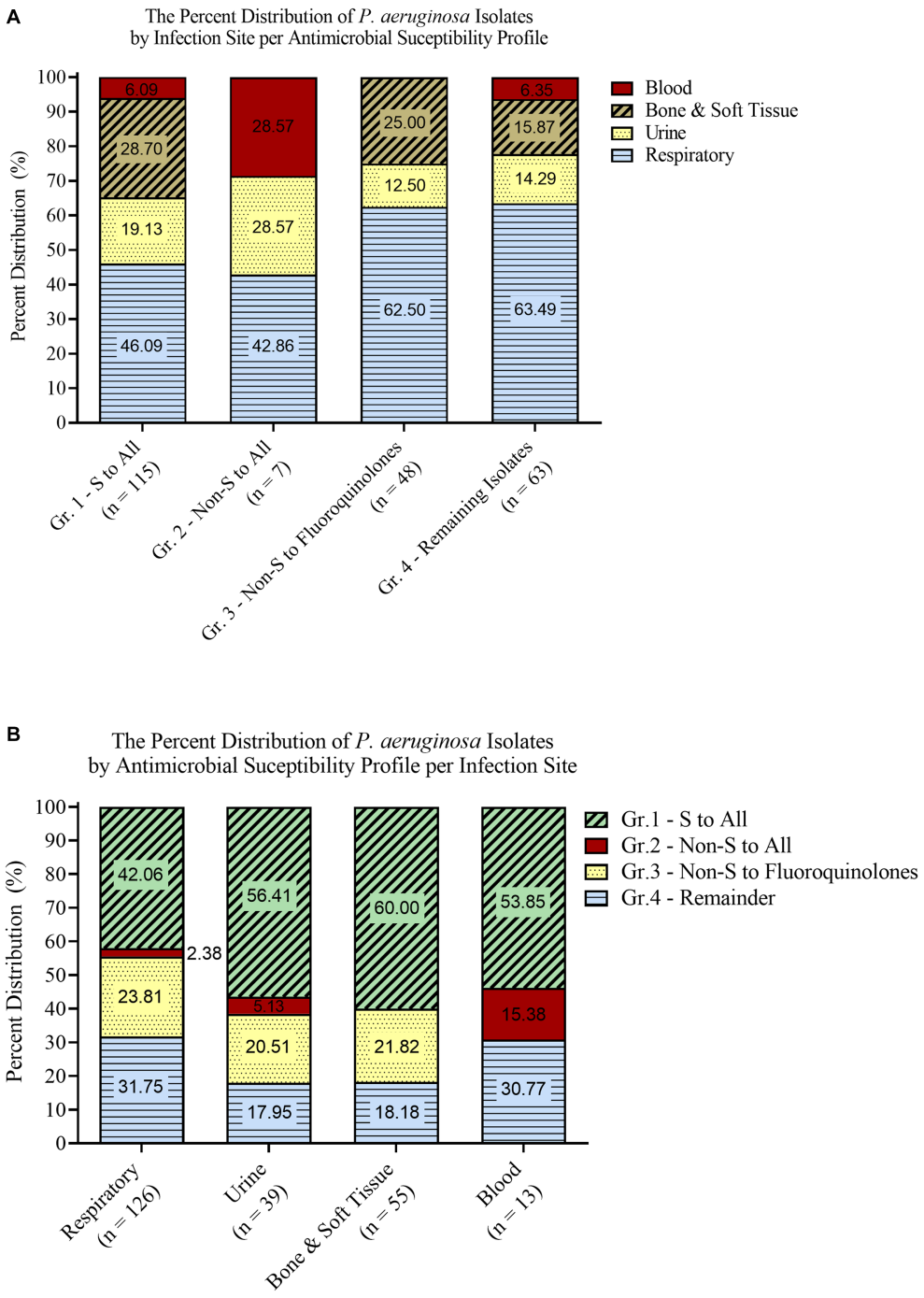

FIGURE 1
Isolate grouping stratified according to infection site **(A)** and antimicrobial susceptibility profiles **(B)**.

10.3389/fmicb.2023.1209224

TABLE 2 Broth microdilution results of the 19 *P. aeruginosa* isolates against ciprofloxacin and levofloxacin before and after induction of resistance.

Isolates codes	Before induction		MIC (μg/mL) After induction		# of passages*
	Antimicrobial IG	MIC (μg/mL)	Ciprofloxacin	Levofloxacin	
PSA-154	Ciprofloxacin	0.125	256	>512	4
	Levofloxacin	0.5	32	256	3
PSA-021	Ciprofloxacin	<0.0625	32	1	5
	Levofloxacin	0.25	16	32	4
PSA-173b	Ciprofloxacin	0.25	64	64	3
	Levofloxacin	0.5	16	64	3
PSA-173a	Ciprofloxacin	0.25	32	64	3
	Levofloxacin	0.5	16	32	3
PSA-115	Ciprofloxacin	0.125	32	64	4
	Levofloxacin	0.5	8	32	3
PSA-276	Ciprofloxacin	0.125	16	16	4
	Levofloxacin	0.5	32	256	3
PSA-242	Ciprofloxacin	0.25	16	16	3
	Levofloxacin	0.5	8	64	3
PSA-025	Ciprofloxacin	0.125	256	512	4
	Levofloxacin	0.5	4	32	3
PSA-026	Ciprofloxacin	0.25	32	64	3
	Levofloxacin	0.5	16	64	3
PSA-186	Ciprofloxacin	0.125	32	128	4
	Levofloxacin	0.5	32	128	3
PSA-118a	Ciprofloxacin	0.25	128	>512	3
	Levofloxacin	0.5	32	128	3
PSA-192	Ciprofloxacin	0.125	16	32	4
	Levofloxacin	0.25	2	32	4
PSA-182	Ciprofloxacin	0.125	16	32	4
	Levofloxacin	0.5	1	16	3
PSA-058	Ciprofloxacin	0.125	32	32	4
	Levofloxacin	0.5	8	32	3
PSA-285b	Ciprofloxacin	0.125	32	64	4
	Levofloxacin	0.5	4	32	3
PSA-113a	Ciprofloxacin	0.25	128	128	3
	Levofloxacin	0.5	16	64	3
PSA-124	Ciprofloxacin	0.25	16	16	3
	Levofloxacin	0.5	16	16	3
PSA-092	Ciprofloxacin	0.125	64	128	4
	Levofloxacin	0.25	8	16	4
PSA-146b	Ciprofloxacin	0.125	32	64	4
	Levofloxacin	0.5	16	32	3

IG, induced against; *, each passage represents a 2-fold increase in the MIC and the numbers indicate the passages required to reach each antibiotic breakpoint.

Whole-genome sequencing

Genome sequence analyses confirmed that parental and isogenic mutant isolates belonged to the same sequence types, and which comprised ST244 ($n = 2$), ST357 ($n = 1$), ST253 ($n = 1$), ST308 ($n = 1$), ST664 ($n = 1$), ST810 ($n = 1$) and ST3137 ($n = 1$). Resistance to ciprofloxacin and levofloxacin in sequenced mutants were mainly associated with alterations in *GyrA*, *GyrB* and *ParC*. Characteristically,

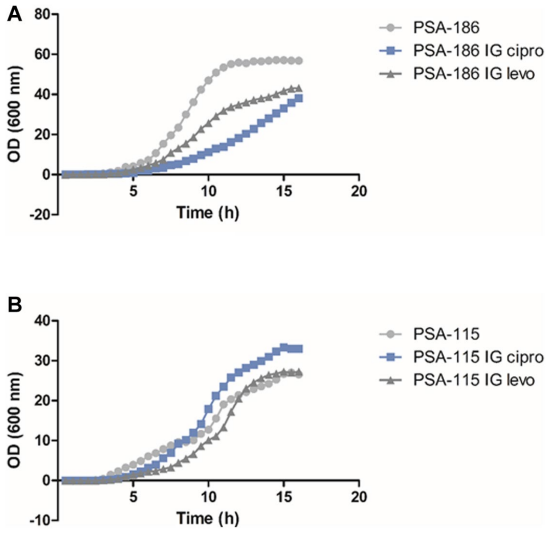

FIGURE 2
Fitness cost assay results of isolates PSA-115 **(B)** and PSA-186 **(A)** compared to their induced mutants. IG cipro, induced against ciprofloxacin; IG levo, induced against levofloxacin.

mutants with a high level of resistance to ciprofloxacin and levofloxacin (i.e., MICs ≥256 μg/mL) had changes in both *GyrA* (Thr83 → Ala/Ile and/or Asp87 → Tyr) and *ParC* (Ser87 → Leu/Trp). Isolate PSA-154 that was induced against ciprofloxacin yielded MICs of 256 μg/mL for ciprofloxacin and > 512 μg/mL for levofloxacin. This high level of resistance was caused by two mutations in the *gyrA* gene (Thr83 → Ala and Asp87 → Tyr) and one in the *parC* gene (Ser87 → Trp). Moreover, another isolates (PSA-025) that was also induced against ciprofloxacin yielded MICs of 256 μg/mL for ciprofloxacin and 512 μg/mL for levofloxacin. Two mutations were detected in these isolates, one in the *gyrA* gene (Thr83 → Ile) and the second was in the *parC* gene (Ser87 → Leu). In comparison, those exhibiting ciprofloxacin MICs between 16 μg/mL and 128 μg/mL or had MIC values ranging between 64 μg/mL and 256 μg/mL for levofloxacin carried only single alterations in *GyrA*. On the other hand, amino acid changes, deletions and/or insertions at positions 466, 467, 468, 476, 477,478, 481, 486, 702, 704, and/or 749 in *GyrB* were detected in mutants with ciprofloxacin and levofloxacin MICs ranging from 4 μg/mL to 32 μg/mL and 32 μg/mL to 64 μg/mL, respectively. A single mutation in the *gyrB* (Ser466 → Phe) of isolate PSA-021 that was induced against ciprofloxacin was detected. Interestingly, this isolate became resistant to ciprofloxacin (MIC: 32 μg/mL) and remained susceptible to levofloxacin (MIC: 1 μg/mL). Only one mutant (PSA-242 IG Cipro) with an MIC of 16 μg/mL against both ciprofloxacin and levofloxacin lacked any modifications in the DNA gyrase or topoisomerase subunits (Table 3).

Genome sequences have also shown that the MexCD,-OprJ efflux regulatory genes *nfxB* and *mexR* were inactivated in 11 (69%) out of the 16 sequenced mutants through various alterations in their respective coding sequences. These alterations ranged from single nucleotide substitutions to deletions or insertions of 1 to 91 nucleotides. Interestingly, the inactivation of *MexR* was identified mainly in mutants induced with levofloxacin, whereas the disruption of NfxR was seen more often in mutants induced with ciprofloxacin (Table 3). However, all the mutants carting these alterations had at most four folds decrease in their respective MICs in the presence of PAβN. Oddly, all mutants generated from strains PSA-154 and PSA-115 that showed the highest MIC shifts in the presence of PAβN (8-to-16-fold decrease) did not show any alterations in these two regulators.

Fitness cost results showed that PSA-154 and PSA-025 that were induced against ciprofloxacin had no significant change in the fitness cost, same growth rate, when compared to their parental isolates. Even though PSA-154-IG ciprofloxacin had 2 mutations in the *gyrA* gene (Thr83 → Ala and Asp87 → Tyr) and one mutation in the *parC* gene (Ser87 → Trp), and PSA-025-IG ciprofloxacin had one mutation in the *gyrA* (Thr83 → Ile) and another one in the *parC* gene (Ser87 → Leu). Moreover, out of the 5 induced mutants that had a single mutation in the *gyrA* gene, 3 (60%) had a higher fitness cost and 2 (40%) had no significant change in the fitness cost when compared to their parental isolates. Furthermore, out of the 9 induced mutants that had alteration in the *gyrB* gene, 6 (66.67%) had a higher fitness cost and 3 (33.33%) had no significant change in the fitness cost when compared to their parental isolates. In addition to that, out of the 11 induced mutants that had the MexCD-OprJ efflux regulatory genes *nfxB* and *mexR* inactivated, 8 (73%) had a higher fitness cost and 3 (27%) had no significant change in the fitness cost when compared to their parental isolates.

Discussion

P. aeruginosa accounts for 10% of all hospital-acquired infections, which makes it the fourth most commonly isolated nosocomial pathogen (Afshari et al., 2012). Yet, the increase in antimicrobial resistance has been an ongoing struggle for a long time, shrinking the repertoire of options to treat these infections. A study assessing *P. aeruginosa* isolates from ICU patients showed that 47.7% of the isolates were drug-resistant, 50% were multidrug resistant, and 2.3% were extensively drug resistant (Gill et al., 2016). Fluoroquinolones are a class of first-line antimicrobials that exhibit anti-pseudomonal activity and are frequently used to treat such infections. In this study, we observe an alarming non-susceptibility of 24% to ciprofloxacin among the *P. aeruginosa* clinical isolates, which is similar to the percentage reported from nosocomial infections in Lebanon (22.7%) (Chamoun et al., 2016). Moreover, a recent study in Lebanon showed that 27% of *P. aeruginosa* isolated from hospitalized patients and 28.6% from ICU patients are resistant to ciprofloxacin (Al-orphaly et al., 2021). This level of resistance is also very close to the percentage reported in a recent national report that investigated the antimicrobial susceptibility profiles of multiple organisms to a number of routinely screened antimicrobial agents across several tertiary care centers (Moghnieh et al., 2019). In fact, all the tested antimicrobials in this study nearly mirrors the national numbers in terms of *P. aeruginosa* susceptibility percentages (Moghnieh et al., 2019) despite the fact that the samples included in this study were exclusively isolated from admitted patients. Therefore, RAPD was utilized to better elucidate the characteristics of the isolate collection and to clarify whether common strains circulate among in-patients or whether they are largely infected by community strains. Following the assessment of the overall genomic relatedness among the analyzed isolates, it appears as though there is not a specific criterium that governed their

TABLE 3 Whole genome sequencing results of the 16 induced mutants and their 8 parental isolates.

Isolates	ST	*gyrA*		*gyrB*		*parC*		*mexR*		*nfxB*	
		nuc	prot	nuc	prot	nuc	prot	nuc	prot	nuc	prot
PSA-154	308										
PSA-154-IG cipro	308	247 A > G 259 G > T	T83 > A D87 > Y			260\ u00B0C > G	S87W				
PSA-154-IG levo	308	259 G > T	D87 > Y								
PSA-021	664										
PSA-021-IG cipro	664			1,397\u00B0C > T	S466 > F			77 ins T	Frame shift		
PSA-021-IG levo	664			2,245\u00B0C > T	P749 > S					271–272 ins C	Frame shift
PSA-115	3,137										
PSA-115-IG cipro	3,137			1,395–1,404 del CTCCCAGGA	S466-E468 del						
PSA-115-IG levo	3,137			1,425–1,436 del CCTGGGCTGTGG	L476 > I C478-G481 del						
PSA-242	810										
PSA-242-IG cipro	810										
PSA-242-IG levo	810			1,395–1,401 del CTCCCA 2108–2010 del TGG	S466-Q467 del L702 del E704 > Q			271–282 del GACCAGCGCAGC	S88-R91del		deletion
PSA-025	253										
PSA-025-IG cipro	253	248\ u00B0C > T	T83 > I			260\ u00B0C > T	S87L			182–216 del TACTGAACCAGATCATCC AGGCCTGCGACCTGGAG	Frame shift
PSA-025-IG levo	253			1,459–1,460 ins ACA	N486 ins			353-end del	E118-end del		
PSA-026	244										
PSA-026-IG cipro	244			2,245\u00B0C > T	P749 > S					544 T > C	S185 > P
PSA-026-IG levo	244	259 G > A	D87 > N					374–388 del TCACCCCGGAGGAAC	Frame shift		
PSA-285b	244										
PSA-285b IG cipro	244	259 G > T	D87 > Y							537–547 del ACGGCGCTTCC	Frame shift
PSA-285b-IG levo	244			1,334–1,335 ins TGT	C477 ins			260–261 ins GCAAC	Frame shift		
PSA-113a	357										
PSA-113a-IG cipro	357	248\ u00B0C > T	T83 > I							514–515 del TA	Frame shift
PSA-113a-IG levo	357	247 A > G	T83 > A	2,246\u00B0C > A	P749 > H			235–244 del AAACCTGGTC	Frame shift		

ST, sequence type; IG, induced against; nuc, nucleotide; prot: protein.

10.3389/fmicb.2023.1209224

distribution across their sites of infection as well as their antimicrobial susceptibility profiles. The majority of detected clusters include samples from different infection sites and susceptibility profiles. However, most isolates from respiratory samples, half of the isolates from urine, and two-third of the isolates from bone and soft tissue, seem to group into distinct clusters which signifies the possibility of hospital spread of isolates circulating between different patients. On the contrary, samples from bloodstream infections are largely independent since there was only 1 cluster with lower overall genomic similarity between the isolates than observed elsewhere. On the other hand, when the samples were analyzed based on their antimicrobial susceptibility grouping, we observed multiple clusters in each group. This shows that common isolates sharing similar antimicrobial susceptibility profiles could be infecting multiple patients at different sites. These findings show that despite our *P. aeruginosa* clinical samples sharing a very similar antimicrobial susceptibility profile with the larger community registry, there is a number of common strains that seem to circulate among in-patients within and at different sites of infection.

The main goal behind the induction of resistance was to mimic the idea of treating patients infected with fluoroquinolone susceptible *P. aeruginosa* with either ciprofloxacin or levofloxacin. Our data showed that exposure to either ciprofloxacin or levofloxacin will lead to resistance against both classes of fluoroquinolones, in contrast to the results from clinical studies (Kaye et al., 2006; Lee et al., 2010; Zhao et al., 2020). One study showed that the risk of isolating a resistant *P. aeruginosa* increased with exposure to levofloxacin, however it did not change with exposure to ciprofloxacin (Kaye et al., 2006). Another study assessing the rate of *P. aeruginosa* resistance among nosocomial infections showed that levofloxacin, administered either orally and parenterally, was positively correlated with developing resistance to either levofloxacin or ciprofloxacin (Lee et al., 2010), whereas treatment with ciprofloxacin was not correlated with resistance to fluoroquinolones (Lee et al., 2010). Nonetheless, an *in vitro* study showed results similar to our study, contrary to the clinical studies. It was shown that ciprofloxacin had a higher ability to kill *P. aeruginosa* but it also showed more susceptibility to resistance (Zhao et al., 2020).

Another important parameter in characterizing resistance is the frequency and speed of developing resistance, reflected by the number of passages needed to reach the resistance breakpoint. Our results showed that levofloxacin required fewer number of passages in a total of 10 tested isolates and an equal number of passages in a total of 9 tested isolates when compared to ciprofloxacin. Thus, resistance against levofloxacin developed faster than ciprofloxacin.

Moreover, the growth rate data showed that fluroquinolone resistance in general reduced the growth rate of the organism, whereby ciprofloxacin resistance impacting the growth rate of the isolates more compared to levofloxacin resistance. A study assessing cost of fitness on quinolone resistance showed that low level mutations showed no cost on fitness in more than half of the organisms. Conversely, organisms with high level mutations showed decreased fitness in all isolates. Interestingly, after serial passage in the laboratory medium, mutant fitness increased again by compensatory mutations (Kugelberg et al., 2005).

To summarize, treatment with ciprofloxacin induces more resistance, while treatment with levofloxacin reaches resistance breakpoint faster and affected the growth rate.

At the molecular level, whole genome sequencing results showed that resistance to ciprofloxacin and levofloxacin in sequenced mutants were mainly associated with alterations in *gyrA*, *gyrB*, and *parC*. Interestingly, the results we got from the induced mutants are similar to the results in studies tackling fluoroquinolone resistance in *P. aeruginosa* clinical isolates. Nouri et al. examined mutations in *gyrA* and *parC* genes in 64 fluoroquinolone resistant *P. aeruginosa* clinical isolates (Nouria et al., 2016). Their results showed that a single *gyrA* substitution (Thr-83 → Ile) was linked with MIC values ranging between 4 and 64 μg/mL for ciprofloxacin and between 4 and 32 μg/mL for levofloxacin. Moreover, isolates with a single *gyrA* substitution (Thr-83 → Ile) and a single *parC* substitution (Ala-88 → Pro or Ser-87 → Leu) had MICs ranging between 8 and 128 or 16 and 256 μg/mL for ciprofloxacin and ranging between 8 and 64 or 8 and 256 μg/mL for levofloxacin. In addition to that, isolates with double *gyrA* substitutions (Thr-83 → Ile and Asp-87 → Asn) and single *parC* substitutions (Ser-87 → Leu) had MICs ranging between 32 and 256 μg/mL for both ciprofloxacin and levofloxacin. Their results showed that three coexisting mutations in *gyrA* and *parC* are associated with higher MIC values for both ciprofloxacin and levofloxacin as compared to two coexisting mutations in *gyrA* and *parC*. Moreover, the latter was associated with higher MIC values for both antimicrobial agents when compared to single mutations in *gyrA* (Nouria et al., 2016). Moreover, Yang et al. work revealed that in 65 ciprofloxacin resistant *P. aeruginosa* clinical isolates a missense mutation in *gyrA* gene (Thr-83 → Ile) was the most detected, followed by missense mutation in *parC* (Ser-87 → Leu), and independent missense mutations in *gyrB* (Ser-467 → Phe and Gln-468 → His). They also showed that *P. aeruginosa* isolates with double mutations (*gyrA* and *gyrB* or *gyrA* and *parC*) had higher MIC values against ciprofloxacin compared to the ones with single *gyrA* mutations (Yang et al., 2015).

The differential effects of ciprofloxacin and levofloxacin on the emerging resistance against *P. aeruginosa* should be taken into consideration when devising a treatment plan. Factors such as the extent of the resistance, speed of resistance, and cost of fitness will affect the clinical decision making when translated into everyday practice.

Understanding the mechanism of action driving the resistance against quinolones can provide insight into developing a new generation of therapeutic drugs that can overcome the resistance.

Further studies assessing the characteristics of resistance in a clinical setting are needed to complete the picture and guide therapy.

Data availability statement

The datasets presented in this study can be found in online repositories. The names of the repository/repositories and accession number(s) can be found in the article/Supplementary material.

Author contributions

ZK, AS, BE, MD, and MA executed the experiments and wrote the manuscript. ZK, SK, JF, GD, and AG performed the clinical analysis. AA, ZK, and GM designed the experiments and planned the study. AA, ZK, SK, and GM proof read and edited the overall

article. All authors contributed to the article and approved the submitted version.

Funding

This work was funded by the Medical Practice Plan (MPP) grant from AUBMC.

Conflict of interest

The authors declare that the research was conducted in the absence of any commercial or financial relationships that could be construed as a potential conflict of interest.

Publisher's note

All claims expressed in this article are solely those of the authors and do not necessarily represent those of their affiliated organizations, or those of the publisher, the editors and the reviewers. Any product that may be evaluated in this article, or claim that may be made by its manufacturer, is not guaranteed or endorsed by the publisher.

Supplementary material

The Supplementary material for this article can be found online at: https://www.frontiersin.org/articles/10.3389/fmicb.2023.1209224/full#supplementary-material

References

Afshari, A., Pagani, L., and Harbarth, S. (2012). Year in review 2011: critical care – infection. *Crit. Care* 16, 242–248. doi: 10.1186/cc11421

Al-orphaly, M., Hadi, H. A., Eltayeb, F. K., Al-hail, H., Samuel, B. G., Sultan, A. A., et al. (2021). Epidemiology of multidrug-resistant *Pseudomonas aeruginosa* in the Middle East and North Africa region. *mSphere* 6, 1–15. doi: 10.1128/mSphere.00202-21

Athanasiou, C. I., and Kopsini, A. (2018). Systematic review of the use of time series data in the study of antimicrobial consumption and *Pseudomonas aeruginosa* resistance. *J Glob Antimicrob Resist* 15, 69–73. doi: 10.1016/j.jgar.2018.06.001

Bankevich, A., Nurk, S., Antipov, D., Gurevich, A. A., Dvorkin, M., Kulikov, A. S., et al. (2012). SPAdes: a new genome assembly algorithm and its applications to single-cell sequencing. *J. Comput. Biol.* 19, 455–477. doi: 10.1089/cmb.2012.0021

Bolger, A. M., Lohse, M., and Usadel, B. (2014). Trimmomatic: a flexible trimmer for Illumina sequence data. *Bioinformatics* 30, 2114–2120. doi: 10.1093/bioinformatics/btu170

Chamoun, K., Farah, M., Araj, G., Daoud, Z., Moghnieh, R., Salameh, P., et al. (2016). Surveillance of antimicrobial resistance in Lebanese hospitals: retrospective nationwide compiled data. *Int. J. Infect. Dis.* 46, 64–70. doi: 10.1016/j.ijid.2016.03.010

Dantas, R. C., Ferreira, M. L., Gontijo-Filho, P. P., and Ribas, R. M. (2014). *Pseudomonas aeruginosa* bacteraemia: independent risk factors for mortality and impact of resistance on outcome. *J. Med. Microbiol.* 63, 1679–1687. doi: 10.1099/jmm.0.073262-0

EM100 connect – CLSI M100 ED29. (2019). Available at: http://em100.edaptivedocs.net/GetDoc.aspx?doc=CLSIM100ED29:2019&xormat=SPDF&src=BB (Accessed April 2, 2020).

Folic, M. M., Djordjevic, Z., Folic, N., Radojevic, M. Z., and Jankovic, S. M. (2020). Epidemiology and risk factors for healthcare-associated infections caused by *Pseudomonas aeruginosa*. *J. Chemother.* 33, 294–301. doi: 10.1080/1120009X.2020.1823679

Gilbert, D. N., Kohlhepp, S. J., Slama, K. A., Grunkemeier, G., Lewis, G., Dworkin, R. J., et al. (2001). Phenotypic resistance of *Staphylococcus aureus*, selected Enterobacteriaceae, and *Pseudomonas aeruginosa* after single and multiple in vitro exposures to ciprofloxacin, levofloxacin, and Trovafloxacin. *Antimicro agents chemother* 45, 883–892. doi: 10.1128/AAC.45.3.883

Gill, J., Arora, S., Khanna, S., and Kumar, K. H. (2016). Prevalence of multidrug-resistant, extensively drug-resistant, and Pandrug-resistant *Pseudomonas aeruginosa* from a tertiary level intensive care unit. *J Glob Infect Dis* 8, 155–159. doi: 10.4103/0974-777X.192962

Gupta, R., Malik, A., Rizvi, M., and Ahmed, S. M. (2016). Incidence of multidrug-resistant Pseudomonas spp. in ICU patients with special reference to ESBL, AMPC, MBL and biofilm production. *J Glob Infect Dis* 8:25. doi: 10.4103/0974-777X.176142

Higgins, P. G., Fluit, A. C., Milato, D., Verhoef, J., and Schmitz, F. (2003). Mutations in GyrA, ParC, MexR and NfxB in clinical isolates of *Pseudomonas aeruginosa*. *Int J Antimicrob Agents* 21, 409–413. doi: 10.1016/S0924-8579(03)00009-8

Kaier, K., Heister, T., Götting, T., Wolkewitz, M., and Mutters, N. T. (2019). Measuring the in-hospital costs of *Pseudomonas aeruginosa* pneumonia: methodology and results from a German teaching hospital. *BMC Infect. Dis.* 19, 1–8. doi: 10.1186/s12879-019-4660-5

Kanafani, Z. A., El Zakhem, A., Zahreddine, N., Ahmadieh, R., and Kanj, S. S. (2019). Ten-year surveillance study of ventilator-associated pneumonia at a tertiary care center in Lebanon. *J. Infect. Public Health* 12, 492–495. doi: 10.1016/j.jiph.2019.01.057

Karampatakis, T., Antachopoulos, C., Tsakris, A., and Roilides, E. (2018). Molecular epidemiology of carbapenem-resistant *Pseudomonas aeruginosa* in an endemic area: comparison with global data. *Eur. J. Clin. Microbiol. Infect. Dis.* 37, 1211–1220. doi: 10.1007/s10096-018-3244-4

Kaye, K. S., Kanafani, Z. A., Dodds, A. E., Engemann, J. J., Weber, S. G., and Carmeli, Y. (2006). Differential effects of levofloxacin and ciprofloxacin on the risk for isolation of quinolone-resistant *Pseudomonas aeruginosa*. *Antimicrob. Agents Chemother.* 50, 2192–2196. doi: 10.1128/AAC.00060-06

Kugelberg, E., Lofmark, S., Wretlind, B., and Andersson, D. I. (2005). Reduction of the fitness burden of quinolone resistance in *Pseudomonas aeruginosa*. *J. Antimicrob. Chemother.* 55, 22–30. doi: 10.1093/jac/dkh505

Lee, Y., Liu, H., Lin, Y., Sun, K., Chun, C., and Hsueh, P. (2010). Fluoroquinolone resistance of *Pseudomonas aeruginosa* isolates causing nosocomial infection is correlated with levofloxacin but not ciprofloxacin use. *Int. J. Antimicrob. Agents* 35, 261–264. doi: 10.1016/j.ijantimicag.2009.11.007

Maraolo, A. E., Cascella, M., Corcione, S., Cuomo, A., Nappa, S., Borgia, G., et al. (2017). Management of multidrug-resistant *Pseudomonas aeruginosa* in the intensive care unit: state of the art. *Expert Rev. Anti-Infect. Ther.* 15, 861–871. doi: 10.1080/14787210.2017.1367666

Marí-Almirall, M., Cosgaya, C., Higgins, P. G., Van Assche, A., Telli, M., Huys, G., et al. (2017). MALDI-TOF/MS identification of species from the *Acinetobacter baumannii* (ab) group revisited: inclusion of the novel a. seifertii and A. dijkshoorniae species. *Clin. Microbiol. Infect.* 23, 210.e1–210.e9. doi: 10.1016/j.cmi.2016.11.020

Moghnieh, R., Araj, G. F., Awad, L., Daoud, Z., Mokhbat, J. E., Jisr, T., et al. (2019). A compilation of antimicrobial susceptibility data from a network of 13 Lebanese hospitals reflecting the national situation during 2015-2016. *Antimicrob. Resist. Infect. Control* 8, 1–17. doi: 10.1186/s13756-019-0487-5

Mu, X., Wang, N., Li, X., Shi, K., Zhou, Z., Yu, Y., et al. (2016). The effect of colistin resistance-associated mutations on the fitness of *Acinetobacter baumannii*. *Front. Microbiol.* 7, 1–8. doi: 10.3389/fmicb.2016.01715

Nouria, R., Rezaeea, M. A., Hasania, A., Aghazadeh, M., and Asgharzadeh, M. (2016). The role of gyrA and parC mutations in fluoroquinolones-resistant *Pseudomonas aeruginosa* isolates from Iran. *Brazilian J Microbiol* 47, 925–930. doi: 10.1016/j.bjm.2016.07.016

Rosenthal, V. D., Maki, D. G., Mehta, Y., Leblebicioglu, H., Memish, Z. A., Al-Mousa, H. H., et al. (2014). International nosocomial infection control Consortiu (INICC) report, data summary of 43 countries for 2007-2012. Device-associated module. *Am. J. Infect. Control* 42, 942–956. doi: 10.1016/j.ajic.2014.05.029

Schuster, S., Bohnert, J. A., Vavra, M., Rossen, J. W., and Kern, W. V. (2019). Proof of an outer membrane target of the efflux inhibitor Phe-Arg-β-Naphthylamide from random mutagenesis. *Molecules* 24, 1–12. doi: 10.3390/molecules24030470

Yang, X., Xing, B., Liang, C., Ye, Z., and Zhang, Y. (2015). Prevalence and fluoroquinolone resistance of *Pseudomonas aeruginosa* in a hospital of South China. *Int. J. Clin. Exp. Med.* 8, 1386–1390.

Zhao, L., Wang, S., Li, X., He, X., and Jian, L. (2020). Development of in vitro resistance to fluoroquinolones in *Pseudomonas aeruginosa*. *Antimicrob. Resist. Infect. Control* 9, 1–8. doi: 10.1186/s13756-020-00793-8

frontiers | Frontiers in Microbiology

TYPE Original Research
PUBLISHED 13 November 2023
DOI 10.3389/fmicb.2023.1237993

OPEN ACCESS

EDITED BY
Ana P. Tedim,
Institute of Health Sciences Studies of Castilla y León (IECSCYL), Spain

REVIEWED BY
Lei Chen,
University of Miami Health System, United States
Rachelle E. Beattie,
United States Geological Survey, United States

*CORRESPONDENCE
Yaya Xu
✉ 616524949@qq.com

RECEIVED 10 June 2023
ACCEPTED 23 October 2023
PUBLISHED 13 November 2023

CITATION
Xu J, Kong X, Li J, Mao H, Zhu Y, Zhu X and Xu Y (2023) Pediatric intensive care unit treatment alters the diversity and composition of the gut microbiota and antimicrobial resistance gene expression in critically ill children.
Front. Microbiol. 14:1237993.
doi: 10.3389/fmicb.2023.1237993

Pediatric intensive care unit treatment alters the diversity and composition of the gut microbiota and antimicrobial resistance gene expression in critically ill children

Jiayue Xu, Xiangmei Kong, Jiru Li, Haoyun Mao, Yueniu Zhu, Xiaodong Zhu and Yaya Xu*

Department of Pediatric Intensive Care Medicine, Xinhua Hospital, Affiliated to the Medical School, Shanghai Jiao Tong University, Shanghai, China

Introduction: Common critical illnesses are a growing economic burden on healthcare worldwide. However, therapies targeting the gut microbiota for critical illnesses have not been developed on a large scale. This study aimed to investigate the changes in the characteristics of the gut microbiota in critically ill children after short-term pediatric intensive care unit (PICU) treatments.

Methods: Anal swab samples were prospectively collected from March 2021 to March 2022 from children admitted to the PICU of Xinhua Hospital who received broad-spectrum antibiotics on days 1 (the D1 group) and 7 (the D7 group) of the PICU treatment. The structural and functional characteristics of the gut microbiota of critically ill children were explored using metagenomic next-generation sequencing (mNGS) technology, and a comparative analysis of samples from D1 and D7 was conducted.

Results: After 7 days of PICU admission, a significant decrease was noted in the richness of the gut microbiota in critically ill children, while the bacterial diversity and the community structure between groups remained stable to some extent. The relative abundance of *Bacilli* and *Lactobacillales* was significantly higher, and that of *Campylobacter hominis* was significantly lower in the D7 group than in the D1 group. The random forest model revealed that *Prevotella coporis* and *Enterobacter cloacae* were bacterial biomarkers between groups. LEfSe revealed that two Gene Ontology entries, GO:0071555 (cell wall organization) and GO:005508 (transmembrane transport), changed significantly after the short-term treatment in the PICU. In addition, 30 KEGG pathways were mainly related to the activity of enzymes and proteins during the processes of metabolism, DNA catabolism and repair, and substance transport. Finally, 31 antimicrobial resistance genes had significantly different levels between the D7 and D1 groups. The top 10 up-regulated genes were Erm(A), ErmX, LptD, eptB, SAT-4, tetO, adeJ, adeF, APH(3')-IIIa, and tetM.

Conclusion: The composition, gene function, and resistance genes of gut microbiota of critically ill children can change significantly after short PICU treatments. Our findings provide a substantial basis for a better understanding of the structure and function of gut microbiota and their role in critical illnesses.

KEYWORDS

gut microbiota, critical illness, children, infection, drug resistance genes

1. Introduction

Common critical illnesses, including sepsis, acute respiratory distress syndrome, and multiorgan failure, are a growing economic burden on healthcare worldwide (Adhikari et al., 2010). Pathophysiological changes that occur in critically ill patients can affect the composition of the intestinal flora. For example, both the hypoperfused and reperfused states of the intestinal wall can lead to intense mucosal inflammation, which further leads to changes in the intestinal environment. Increased nitrate concentrations and altered mucosal oxygen concentrations favor the growth of *Aspergillus phylum* microorganisms, including clinically common gram-negative *Bacilli* such as *Pseudomonas aeruginosa* and *Escherichia coli*. The growth of Firmicutes microorganisms, such as *Staphylococcus aureus* and *Enterococcus*, can also be affected (Dickson, 2016). Disturbances in the intestinal flora are associated with disease progression and clinical prognosis in critically ill patients. Ojima et al. (2022) showed that dysbiosis in the ratio of the *Bacteroides* to the Firmicutes (B/*F* > 8 or B/*F* < 1/8) in critically ill patients within 7 days of admission was associated with increased mortality. Andremont et al. (2020) also showed that carrying rectal or pharyngeal ultra-broad-spectrum β-lactamase-producing *Enterobacteriaceae* was a risk factor for the subsequent development of ventilator-associated pneumonia caused by bacterial infection in critically ill patients. In addition, a strong link exists between the intestinal flora and function of organs such as the brain, lungs, liver, and kidneys. In a study by Dickson et al. (2020) intestine-associated bacteria such as *Trichophytonaceae* and *Enterobacteriaceae* were present in the pulmonary flora of critically ill patients, and an increase in these bacteria predicted the number of days a patient would have without being on a ventilator. The loss of endothelial barrier integrity and dysbiosis of the intestinal flora are major pathophysiological alterations in sepsis that play important roles in sepsis-related acute kidney injury (Xu et al., 2022).

Most bacterial communities in the gut have a symbiotic relationship with the human host; however, many conditionally pathogenic bacteria, such as *Enterobacteriaceae* and *Enterococcaceae*, are also present in the gut and can cause severe infections in immunocompromised patients (Mcinnes et al., 2020). Antibiotic use is a key factor in the induction of drug-resistant genes. In recent years, infections caused by drug-resistant strains of *Escherichia coli*, *Klebsiella pneumoniae*, and *Enterococcus faecalis* have been increasing worldwide (Guzman Prieto et al., 2016; Dunn et al., 2019). In addition, some studies have shown that the expression levels of resistance genes in the gut microbiota increase during antibiotic treatment in children; however, not all resistance genes return to baseline levels after antibiotic discontinuation (Yassour et al., 2016).

Therefore, gut microbiota has gathered increasing attention from clinicians as an important element in the management of critically ill patients. Despite decades of medical and technological advances, therapies targeting the gut flora for critical illnesses have not been developed on a large scale. Metagenomics next generation sequencing (mNGS) is a new method of high-throughput RNA/DNA sequencing that enables the detection of all pathogenic bacteria in a sample without bias (Diao et al., 2022; Gökdemir et al., 2022). This method allows further exploration of the composition, diversity, gene function, and drug resistance genes of the gut microbiota.

This study aimed to describe the changes in the composition, gene function, and drug resistance genes of gut microbiota in critically ill children after receiving short-term PICU treatment and to provide a theoretical basis for the rational use of medication and reduction of the incidence of adverse events in PICU patients.

2. Materials and methods

2.1. Patients and sample collection

This study was approved by the Ethics Committee of Xinhua Hospital, Shanghai Jiao Tong University School of Medicine (approval number: XHEC-D-2022-255). This was a prospective observational study on children admitted to the PICU of Xinhua Hospital, affiliated with Shanghai Jiao Tong University School of Medicine, from March 2021 to March 2022 and who received broad-spectrum antibiotic therapy. The inclusion criteria were as follows: ① age > 28 days and < 18 years and ② receiving broad-spectrum antibiotics within the first 24 h of admission to the PICU. The exclusion criteria were: ① post-rectal surgery; ② presence of infection at the anal site; ③ no follow-up due to death or discharge within 7 days; ④ failure to obtain anal swab samples; and ⑤ refusal to participate in the study by the child's guardian. Anal swabs were collected on days 1 (D1) and 7 (D7) of admission to the PICU from children who met the enrollment criteria. Standardized anal swab samples were collected: the children were placed in the lateral position, and a disposable sterile anal swab was used to enter the anus of the children approximately 3 cm deep, rotated for 2–3 s, and then removed and placed in a DNA preservation solution. The samples were transferred to a −80°C refrigerator for freezing within 24 h after the sampling.

2.2. DNA extraction and library preparation

Fecal DNA was extracted using the TIANamp Magnetic DNA Kit (Tiangen) according to the manufacturer's instructions. The quantity and quality of DNA were assessed using the Qubit (Thermo Fisher Scientific) and NanoDrop (Thermo Fisher Scientific), respectively. DNA libraries were prepared using the Hieff NGS C130P2 OnePot II DNA Library Prep Kit for MGI (Yeasen Biotechnology) according to the manufacturer's protocols. Agilent 2100 (Ronchetti et al., 2022) was used for quality control, and MGISEQ-2000 was used to sequence DNA libraries with single-end 50 bp tags (Lang et al., 2021).

2.3. Metagenomic next-generation sequencing

Before analysis, raw sequencing data were split using bcl2fastq2 (version 2.20), and high-quality sequencing data were generated using Trimmomatic (version 0.36) by removing low-quality reads, adapter contamination, duplicates, and short (length < 36 bp) reads. The human host sequence was subtracted by mapping to the human reference genome (hs37d5) using bowtie2 (version 2.2.6). Reads that could not be mapped to the human genome were retained and aligned with the microorganism genome database for microbial identification by Kraken (version 2.0.7) and estimated for species abundance using Bracken (version 2.5.0). The remaining genomes were compared to those in the microbial genome databases, including the genomes of

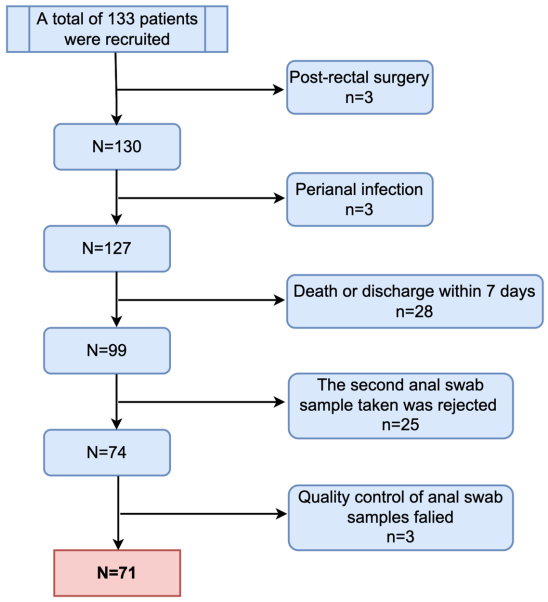

FIGURE 1
Flowchart of patient enrollment.

bacteria, fungi, viruses, and parasites downloaded from GenBank version 238.[1] Gut microbiota data were downloaded from the database of human gut microbiota,[2] and all annotated results (OTUs) were compared with public data. Microorganisms with species detection rates >1% and mean abundances >0.001 were retained. mNGS was performed on an Illumina NovaSeq 6000 (Illumina) using a 150-bp paired-end read protocol.

2.4. Statistical analysis

Statistical analysis of the gut microbiota was performed using R software (version 3.6.0). Alpha diversity was estimated based on the taxonomic profile of each sample, and beta diversity was assessed by the Bray–Curtis and Jaccard–Curtis distances. PERMANOVA was performed using the R package vegan (Hu and Satten, 2022) to analyze Bray–Curtis and Jaccard–Curtis distances between groups, which were subsequently visualized using principal components analysis (PCA) and non-metric multidimensional scaling (NMDS). The relative abundance of microorganisms at different levels between groups was tested by the R package Kruskal Test (Zhang et al., 2021). The genera with mean relative abundances greater than 1% and penetrance greater than 40% among all samples were compared, and false discovery rate correction was adopted to adjust all p values. Accuracy and Gini indices were used to evaluate bacterial biomarkers between groups by the Random Forest predictive algorithm (Hu and Szymczak, 2023). Gene function prediction was performed based on our in-house and Human Project Unified Metabolic Analysis Network 2 (HUMAnN2) (Hu et al., 2022). Gene Ontology (GO) entries between groups were assessed using the linear discriminant analysis (LDA) of effect size (LEfSe) (Erawijantari et al., 2020). Those with an LDA score > 2.0 were considered biomarkers between groups. In addition, STAMP software was used to compare and visualize the different GO entries and KEGG pathways, with both having a corrected p value <0.01. According to the GO database[3] and Kyoto Encyclopedia of Genes and Genomes (KEGG)[4] database, gene functional characteristics were finally described. The comparison of drug resistance genes between groups was performed using DEseq2, and the statistical difference was set at P adjust <0.05 and $|\log2FC| > 1$. These resistance genes were then described with reference to the Comprehensive Antibiotic Research Database (CARD; card.mcmaster.ca). Clinical data analysis was performed using the SPSS (v.25.0) software. The paired t-test or Wilcoxon signed-rank test was used for each continuous variable between the groups.

3. Results

3.1. Patient characteristics

From March 2021 to March 2022, a total of 71 patients were enrolled in the study (Figure 1). Thirty-six of the included children were male (50.7%). Forty-one children were aged over 3 years (57.7%). Most of the enrolled children (71.4%) had underlying diseases, with malignant tumors or leukemia being the most common (19.7%), followed by neurological diseases (12.7%). The site of infection was identified based on the clinical presentation of the children and pathogenic culture results after admission. The respiratory system was the most common site of infection in the enrolled children, followed by the central nervous system, bloodstream infections, urinary system, digestive system, and skin and soft tissues in that order, with approximately one-fifth of the children not having a clear site of infection. Additionally, 25 children had respiratory failure at the time of PICU admission, 10 had shock, 7 had renal insufficiency, 4 had disseminated intravascular coagulation (DIC), and 3 had hepatic insufficiency (Table 1).

3.2. Treatments of patients admitted to the PICU

All the children received intravenous antibiotic therapy upon admission. More than half of the children received two or more classes of antibiotics within 7 days of PICU admission, including antibiotic escalation, antibiotic de-escalation therapy, and antibiotic combinations. Oxazolidinone antibiotics, represented by linezolid, and glycopeptide antibiotics, represented by vancomycin, were the two antibiotics commonly used in the enrolled children, accounting for 78.9 and 74.6% of the total number of patients, respectively. Cefepime, a fourth-generation cephalosporin, was one of the main anti-infective drugs used by the enrolled children, accounting for

1 Download from https://www.ncbi.nlm.nih.gov/.
2 https://gmrepo.humangut.info/home
3 http://www.geneontology.org
4 http://www.genome.jp/kegg/

10.3389/fmicb.2023.1237993

TABLE 1 Patient characteristics.

Characteristic	Number of patients ($n = 71$)	Percentage (%)
Sex M/F	36/35	50.7/49.3
Age		
1 month–3 years	30	42.3
> 3 y	41	57.7
Weight (*Z*-score)		
<−2	11	15.5
−2 to 2	52	73.2
>2	8	11.3
Underlying disease		
None	21	29.6
Malignancy or leukemia	14	19.7
Inherited metabolic diseases	9	12.7
Congenital digestive tract malformation	6	8.5
Neurological diseases	13	18.3
Post-traumatic or surgical	7	9.9
Congenital heart disease	1	1.4
Infection site		
Respiratory	24	33.8
Blood	5	7
Gastrointestinal	2	2.8
Central nervous system	8	11.3
Urinary	4	5.6
Skin	1	1.4
Multi-site infection	12	16.9
Unspecified	15	21.1
Complications		
Shock	10	14.08
Respiratory failure	25	33.8
Acute kidney injury	7	9.86
Hepatic failure	3	4.23
DIC	4	5.63

TABLE 2 Use of antibiotics in critically ill children admitted to the PICU from March 2021 to March 2022.

Antibiotic use	*N*	Percentage (%)
Antibiotic type		
Fourth generation cephalosporins	52	73.2
Glycopeptide antibiotics	53	74.6
Carbapenem antibiotics	25	36.6
Oxazolidinone antibiotics	56	78.9
Combined antibiotics	38	53.5

TABLE 3 Clinical information of critically ill children admitted to the PICU from March 2021 to March 2022.

Clinical characteristics	D1	D7	*p*-value
Clinical indicators			
CRP (mg/L, P50 [P25, P75])	56.00 (4.00, 129.00)	5.00 (1.00, 22.00)	< 0.01
PCT (ng/mL, P50 [P25, P75])	0.69 (0.10, 5.17)	0.27 (0.09, 1.03)	< 0.01
WBC (×10^9/L, P50 [P25, P75])	11.41 (6.43, 15.91)	9.06 (5.77, 13.17)	0.01
Hb (g/L, P50 [P25, P75])	99.00 (84.00, 114.00)	93.00 (83.00, 107.00)	0.12
PLT (×10^9/L, P50 [P25, P75])	264 (142, 398)	310 (183, 425)	0.01
Creatine (μmol/L, P50 [P25, P75])	25.20 (18.2, 34.90)	20.40 (14.80, 30)	< 0.01
Bilirubin (mg/dL, P50 [P25, P75])	10.90 (6.70, 16.90)	9.20 (6.20, 16.90)	0.29
Albumin (g/L, P50 [P25, P75])	36.00 (30.40, 41.20)	37.50 (34.00, 39.70)	0.09
Lactate (mmol/L, P50 [P25, P75])	2.00 (1.50, 3.30)	1.70 (1.20, 2.30)	< 0.01
ICU treatments			
Proton pump inhibitor [*n*, (%)]	16 (22.5)	16 (22.5)	1.00
Vasoactive drugs [*n*, (%)]	12 (16.9)	14 (19.7)	0.66
Mechanical ventilation [*n*, (%)]	22 (31.0)	21 (29.6)	0.86
Parenteral nutrition [*n*, (%)]	26 (36.6)	17 (23.9)	0.10
Probiotic therapy [*n*, (%)]	2 (2.8)	6 (8.5)	0.15
Clinical outcomes			
28-day mortality [*n*, (%)]	7 (9.90)	/	/
PICU length of stay (day, P50 [P25, P75])	9.00 (5.00, 17.00)	/	/
Length of hospital stay (day, P50 [P25, P75])	26.00 (13.00, 45.00)	/	/

Data are presented as median (P50), 25th percentile (P25), and 75th percentile (P75) or number (*n*) and percentage (%). CRP, C-reactive protein; PCT, procalcitonin; WBC, white blood cell count; PLT, platelet count; PICU, pediatric intensive care unit.

73.2% of the total number of users. More than one-third of the children received carbapenem-based antibiotics (Table 2).

Additionally, 22.5% of the children received proton pump inhibitors on day 1 of admission, 12% received vasoactive drugs, 22% were treated with invasive mechanical ventilation, 36.6% were treated with parenteral nutrition, and only a minority (2%) received probiotics. Although the proportion of children receiving supportive treatment changed on day 7 of admission, there was no statistically significant difference (Table 3).

Seven days after PICU treatment, a significant decrease as observed in the levels of C-reactive protein ($p < 0.01$), procalcitonin ($p < 0.01$), creatinine ($p < 0.01$), and lactate ($p = 0.02$) as well as white

blood cell count ($p = 0.01$). A significant increase in platelet count ($p = 0.01$) was noted, compared with the admission levels. No significant changes were observed in the indicators, such as hemoglobin and liver function (total bilirubin and albumin). In terms of clinical outcomes, 7 children died during the 28-day follow-up period. The mean ± standard deviation of the length of stay in the PICU and the total length of hospital stay were 16.39 ± 28.06 and 36.55 ± 38.67 days, respectively (Table 3).

3.3. Changes in gut microbiome in critically ill children after short-term PICU treatment

3.3.1. Short-term PICU treatment alters the richness of the gut microbiome but not the diversity and the community structure

Based on the Wayne diagram of operational taxonomic units (OTU) (Figure 2A) at the species level, children had 749 OTUs on day 1 of PICU admission and 608 OTUs on day 7, of which, 484 OTUs were common to both groups. The species composition of the gut microbiota of critically ill children changed to some extent after a short treatment in the PICU.

Alpha diversity analysis was based on Shannon, Simpson, Chao1, and ACE indicators. As shown in Table 4, Shannon and Simpson indices in the D1 and D7 groups, which represent bacterial diversity, were 1.51 ± 0.80 vs. 1.38 ± 0.70 and 0.60 ± 0.28 vs. 0.57 ± 0.26 (both $p > 0.05$), respectively. The ACE and Chao1 indices in the D1 and D7 groups were 60.22 ± 68.10 vs. 40.62 ± 41.89 and 59.62 ± 67.50 vs. 40.62 ± 41.87 (both $p < 0.01$), indicating that the bacterial richness was significantly decreased in the D7 group (more detailed information can be found in Supplementary Table S1). These results showed that compared with that in the D1 group, the bacterial richness decreased significantly but not the evenness in the D7 group. The PCA and NMDS based on the Bray–Curtis and Jaccard-Curtis distances showed that the beta diversity of the gut microbiota did not differ significantly between the two groups ($p > 0.05$) (Figures 2B–E; Supplementary Table S2). Our results suggested that the community structure of the gut microbiome of the children remained somewhat stable even under the influence of antibiotics and other treatments they received.

3.3.2. Changes in the relative abundance of gut microbiota community

To provide a comprehensive understanding of the gut microbiota of critically ill children, we analyzed the composition at each taxonomic level of colonization. At the phylum taxonomic level, *Bacteroidetes*, *Firmicutes*, *Proteobacteria*, and *Actinobacteria* were the main phyla in critically ill children before and after PICU

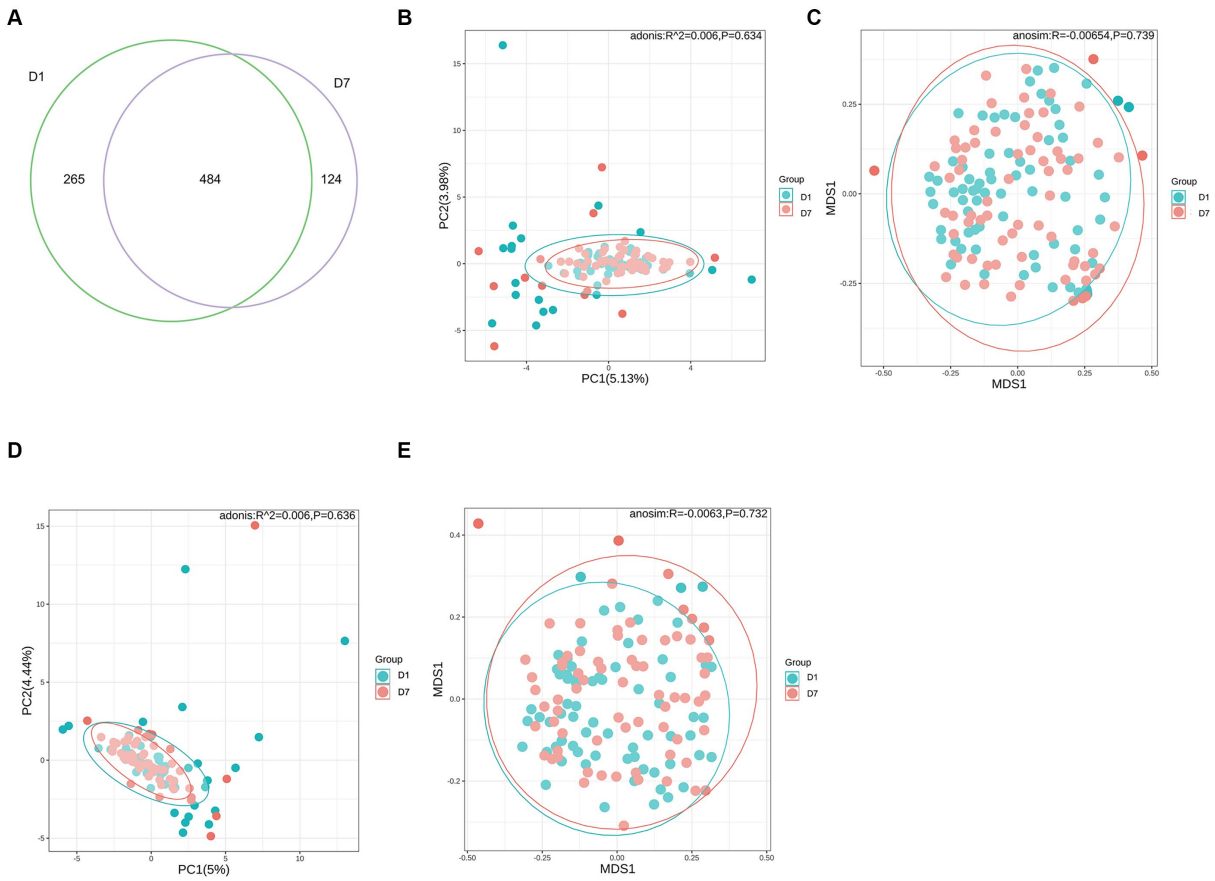

FIGURE 2
OTUs and β-diversity analysis of the microbiota in the D1 and D7 groups. **(A)** Venn diagram of the number of OTUs in the gut microbiota of children in groups D1 and D7. **(B–E)** PCA and NMDS analyses of β-diversity.

treatment, with *Bacteroidetes* and *Firmicutes* dominating (Figures 3A,B). In a controlled analysis of two stool samples from all children, the relative abundances of both *Bacteroidetes* and *Actinobacteria* decreased, compared with those at PICU admission, while the relative abundances of *Firmicutes* and *Proteobacteria* increased; however, none of these changes were statistically different. Notably, the composition of the gut microbiota of critically ill children varied greatly between individuals and that the proportion of individual microbiota changed considerably after a short period of PICU treatment. For example, in the first child (S1), the sum of the relative abundances of *Bacteroidetes* in the anal swab sample on day 1 of PICU admission exceeded 92%, while the relative abundance of *Proteobacteria* on day 7 of admission was approximately 35%, and the relative abundance of *Bacteroidetes* was approximately zero (Figures 3A,B).

Further controlled analyses of the gut microbiota of the children at the other levels were performed. The results showed that median and quartiles of both relative abundance (%) of *Bacilli* (15.79 [0.34, 19.42] vs. 70.03 [10.73, 59.56], $p = 0.03$) and *Lactobacillales* (1.25 [0.14, 19.41] vs. 6.29 [0.20, 58.41], $p = 0.04$) were significantly higher after a short period of PICU treatment in critically ill children. Whereas the mean ± standard deviation of relative abundance (%) of *Campylobacter hominis* was significantly lower (2.10 ± 0.85 vs. 0.63 ± 0.37, $p = 0.02$) (Figure 4; Supplementary Table S3).

A random forest analysis was also performed to analyze the possibility of using the gut microbiota as a novel biological marker for assessing

TABLE 4 Comparison of α diversity between the D1 and D7 groups presented as median (P50), 25th percentile (P25), and 75th percentile (P75).

	D1 Group	D7 Group	*p*-value
Shannon index, P50 (P25, P75)	1.62 (0.88, 2.18)	1.46 (0.81, 1.91)	0.16
Simpson index, P50 (P25, P75)	0.72 (0.45, 0.82)	0.65 (0.43, 0.79)	0.2
ACE index, P50 (P25, P75)	32.00 (20.00, 54.00)	24.00 (20.00, 40.50)	<0.01
Chao1 index, P50 (P25, P75)	32.00 (20.00, 54.00)	24.00 (20.00, 40.50)	<0.01

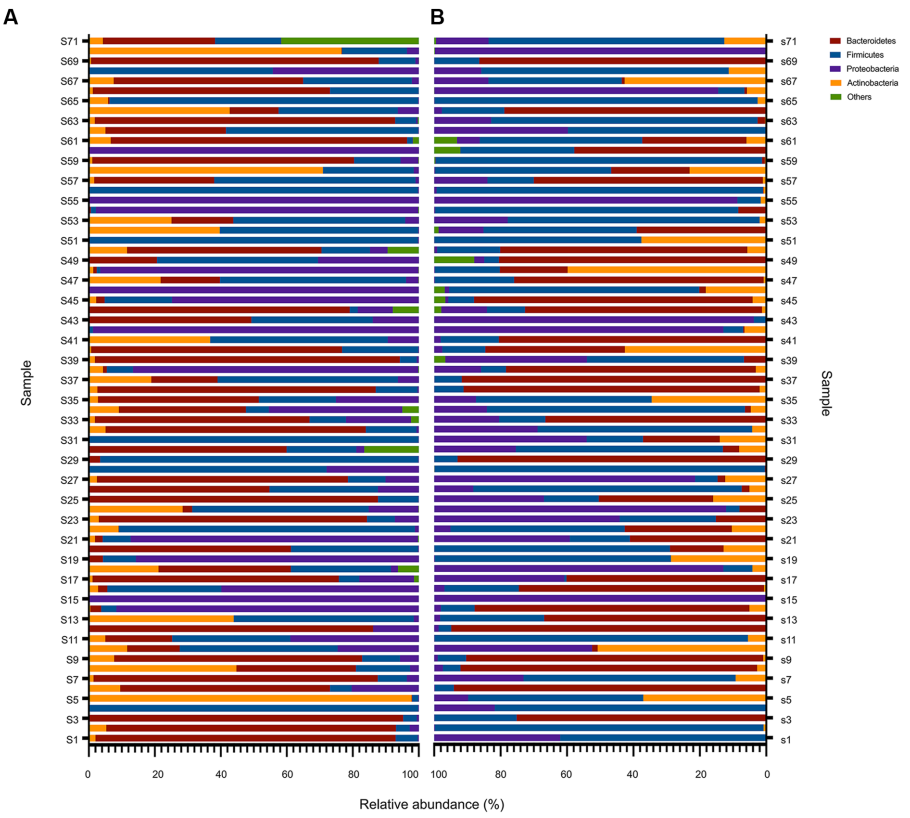

FIGURE 3
Overall composition of the bacteria at the phylum level before and after PICU treatments in critically ill children. Changes in the relative abundance of bacteria at the phylum level in the gut microbiota of critically ill children in the D1 **(A)** and D7 **(B)** groups. Based on the metagenomic sequencing results, the top four microbiota communities at the phylum taxonomic level in groups D1 and D7 were selected, and the remaining were categorized as "others." The results are presented as a relative abundance histogram. The vertical coordinate represents the sequence number of the anal swab sample (sample name), and the horizontal coordinate represents the relative abundance of the community.

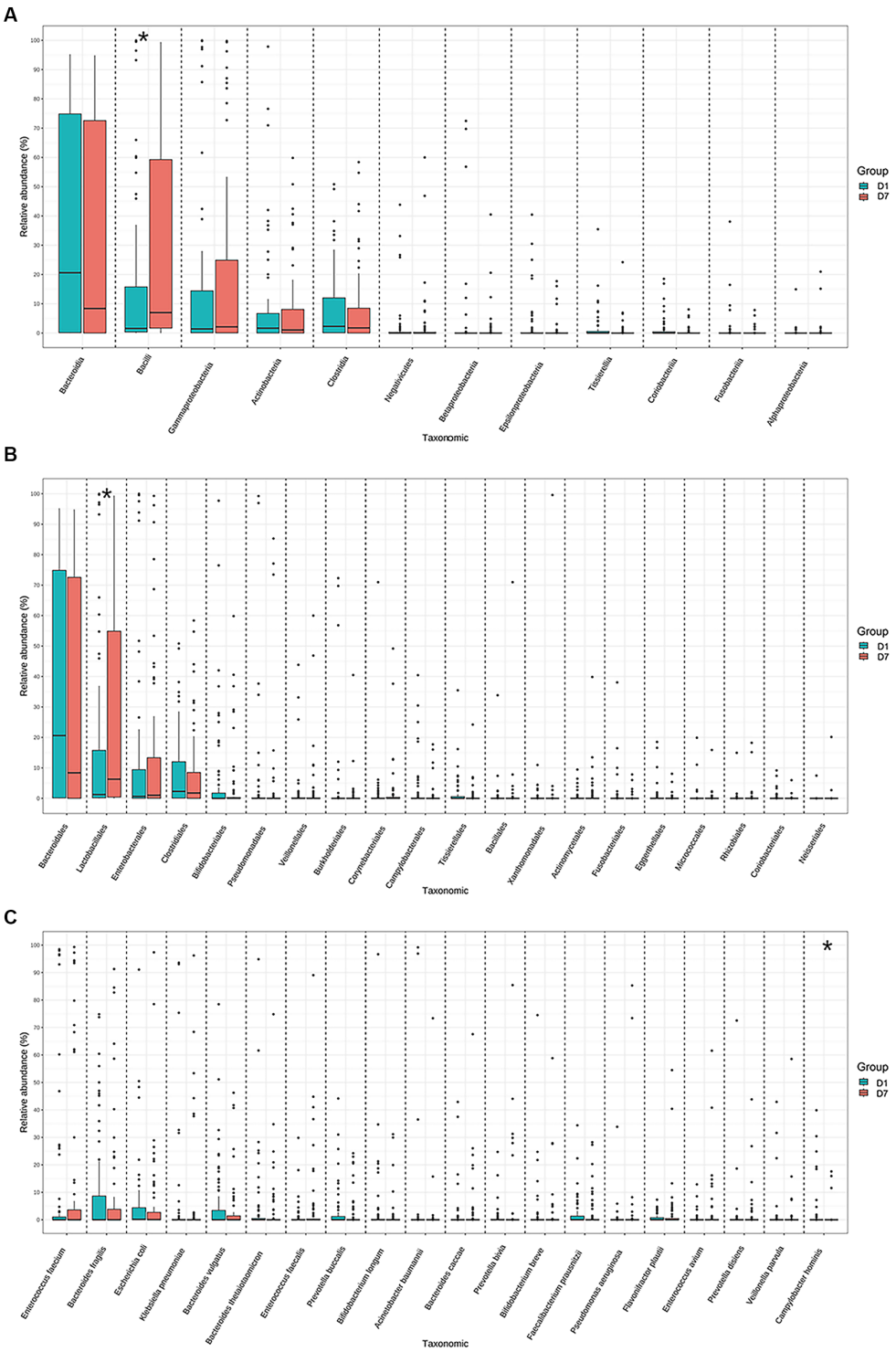

FIGURE 4
Relative abundances of the top 20 bacteria at the class, order, and species levels in the D1 and D7 groups. Distribution of the top 20 bacterial communities at the **(A)** class, **(B)** order, and **(C)** species levels. *$p < 0.05$.

changes in the condition of critically ill children at the species level. The assessment of Accuracy and Gini indices revealed that *Prevotella coporis* and *Enterobacter cloacae* played major roles in grouping as biological markers to distinguish the two groups (Figures 5A,B).

3.3.3. Functional analysis of gene expression in the gut microbiome

The Venn diagram in Figure 6A shows that 960,000 genes were detected in the gut microbiota of the D1 group and 805,009 ARG in

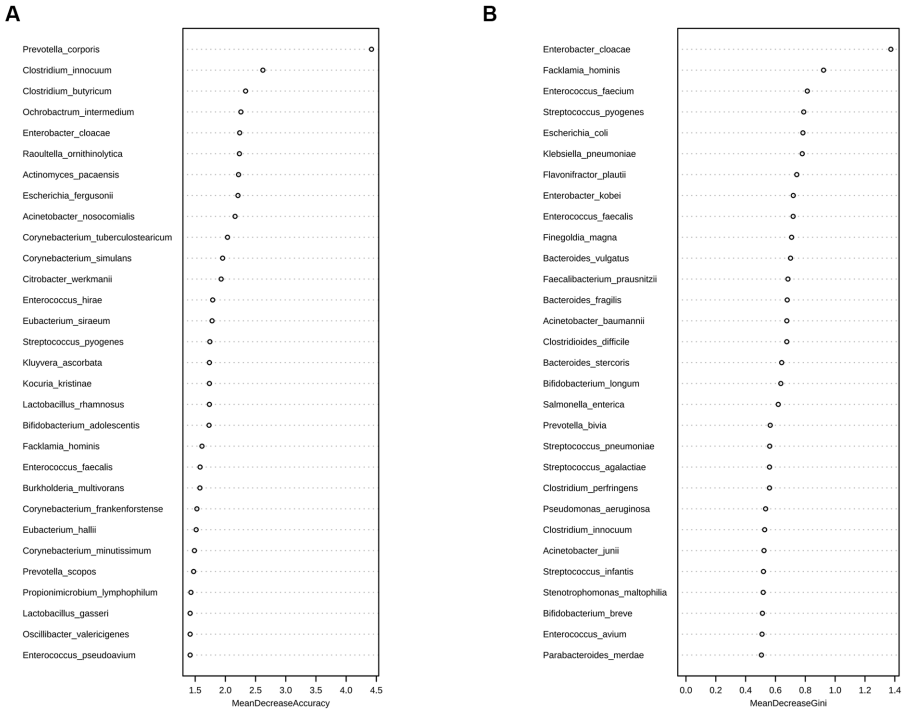

FIGURE 5
Random forest analysis of the D1 and D7 groups at the species level. Random forest analysis is a machine-learning algorithm that can effectively classify and predict grouped samples. The Accuracy **(A)** and Gini **(B)** indices are common evaluation metrics, with higher values indicating greater importance of the variable. The horizontal coordinates represent the values of Accuracy and Gini indices, and the vertical coordinates represent the strain names. The figure shows the strains that played major roles in the D1 and D7 groups, with *Prevotella coporis* and *Enterobacter cloacae* having the most significant classification effects.

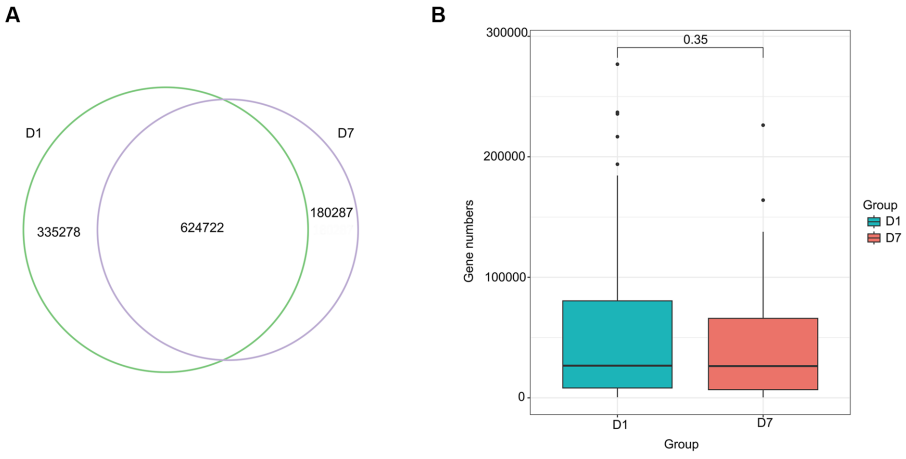

FIGURE 6
Venn diagram and Box diagram of the number of genes detected in the D1 and D7 groups. **(A)** Venn diagram of the number of unique or shared genes detected in the gut microbiota of the D1 and D7 groups. **(B)** Box plot of the number of genes detected in the gut microbiota of the D1 and D7 groups.

the D7 group, of which, 624,722 genes were common to both groups. Although the number of genes decreased after 7 days of PICU treatment, compared with that at the time of admission to the PICU, this change was not statistically significant ($p > 0.05$) (Figure 6B).

As shown in Figure 7, the gut microbiota gene function in children changed significantly after a short-term PICU treatment. A total of 30 significantly altered KEGG pathways were obtained using *P* corrected <0.01 as the screening criterion, and the expression of these 30 pathways was suppressed. They mainly included changes in enzyme and transcription factor activities during metabolism, represented by phosphoribosylglycinamide formyltransferase 1, and alterations in enzyme and protein activities during DNA catabolism and repair, represented by DNA repair proteins RadA/Sms and exodeoxyribonuclease I. In addition, changes were observed in the biopolymer transport protein

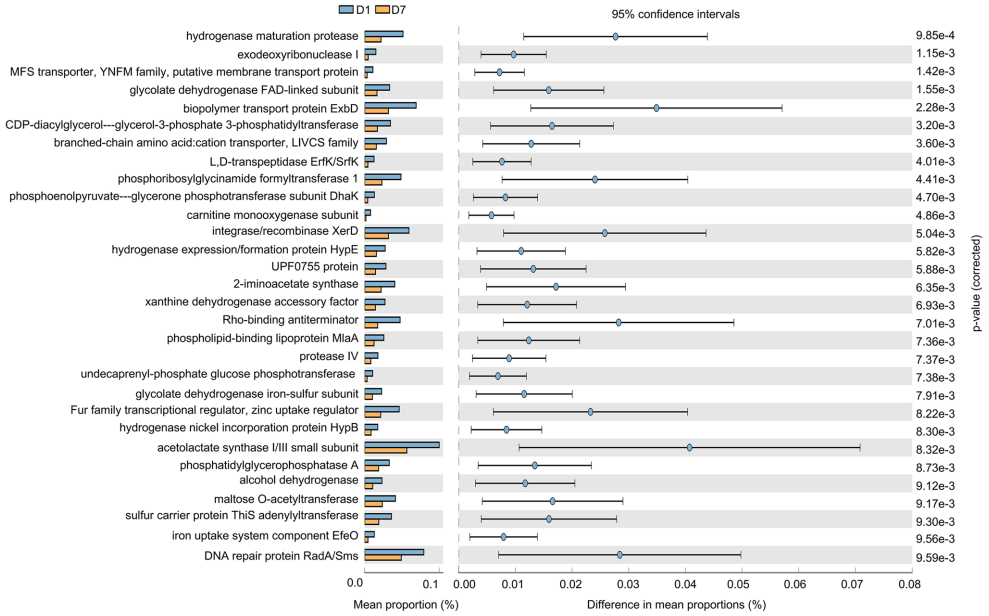

FIGURE 7
Gene function prediction of KEGG pathways. The histograms on the left represent the names of KEGG pathways and their relative abundances, and the dot plots on the right represent the corrected *p*-values. Corrected $p < 0.05$ was considered significant and retained.

ExbD as a representative of substance transport protein activity. This suggests that the imbalance in intestinal microorganisms was accompanied by changes in the processes of material metabolism, material transport, and genetic material breakdown and repair.

Similarly, we comparatively analyzed the expression of GO entries by *P* corrected <0.01 (Figure 8A) and found that 24 GO entries underwent significant down-regulation after short-term PICU treatment. The main biological processes (BPs) involved included DNA-templated transcription termination, DNA catabolic process, and transcription antitermination; of them, the DNA catabolic process was similar to that found in the KEGG analysis of the exodeoxyribonuclease I activity. This was consistent with the changes in exodeoxyribonuclease I activity found in the KEGG analysis. Furthermore, LEfSe (Figure 8B) showed that two GO entries, GO:0071555 (cell wall organization) and GO:005508 (transmembrane transport), changed significantly after short-term PICU treatment. The involved BP of transmembrane transport was consistent with the changes in transporter protein activity in the KEGG analysis.

3.3.4. Differential analysis of the expression of antimicrobial resistance genes in the gut microbiome

Overall, 31 antibiotic resistance genes (ARGs) with significant differences were detected in the D7 group compared with the D1 group, including 19 resistance genes with upregulated expression. The top 10 differentially up-regulated resistance genes, in order, were: Erm(A), ErmX, LptD, eptB, SAT-4, tetO, adeJ, adeF, APH(3′)-IIIa, and tetM (Figure 9; Supplementary Table S4). The Comprehensive Antibiotic Resistance Database (CARD) showed that tetM, LptD, and eptB can be found in resistant *Klebsiella pneumoniae*, and LptD can cause resistance to carbapenem antibiotics. Besides, adeJ, adeF, and tetM can be found in resistant *Acinetobacter baumannii*, and adej can cause resistance to carbapenem antibiotics.

4. Discussion

The human gastrointestinal tract stores a large number of microorganisms, and close communication occurs between them and their hosts. Disturbances in the structure and function of gut microbiota are associated with numerous pathological processes in the human body, including inflammatory bowel disease, type II diabetes, and colorectal cancer (Manor et al., 2020). In recent years, with increasing research, more studies have demonstrated that the gut is a key factor in the initiation and development of critical illnesses and that intestinal failure is associated with poor prognosis (Szychowiak et al., 2022). Therefore, understanding the structure and function of gut microbiota and their role in critical illnesses is crucial.

In the present study, children received broad-spectrum antibiotics intravenously after enrollment, and different proportions of children received proton pump inhibitors, vasoactive drugs, invasive mechanical ventilation, parenteral nutritional support, and probiotics, in addition to exhibiting varying conditions such as underlying disease, site of infection, pathogenic bacteria, and immune status. The microbial environment in the gut of critically ill patients, often influenced by genetics, diseases, and therapeutic factors, is often disturbed (Wozniak et al., 2022), characterized by reduced abundance and diversity and an increase in conditionally pathogenic bacteria (e.g., *Clostridium difficile*, multi-drug-resistant bacteria) (Szychowiak et al., 2022). For example, intestinal emptying can be reduced in critically ill patients with decreased bacterial excretion, leading to excessive growth of pathogenic bacteria in the intestine (Dickson, 2016; Ladopoulos et al., 2018). Antibiotic use has been associated with decreased gut microbiota diversity (Ramirez et al., 2020). In addition, a study in adults showed that the combination of meropenem, gentamicin, and vancomycin led to an increase in *Enterobacter* and other pathogenic bacteria in the intestine, whereas *Bifidobacteria* and butyrate-producing flora were reduced (Palleja et al., 2018). Drugs

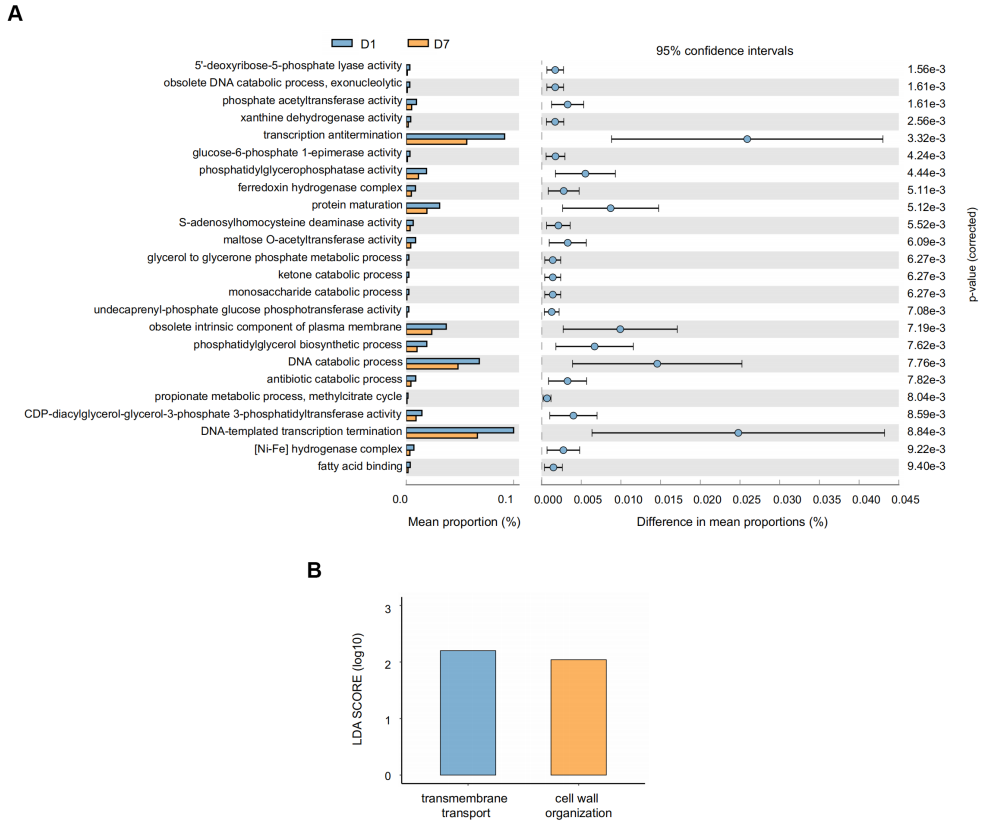

FIGURE 8
Gene function prediction and LEfSe analysis of GO entries. **(A)** The histograms on the left represent the names of GO entries and their relative abundances, and the dot plots on the right represent the corrected *p*-values. A corrected $p < 0.05$ was considered significant and retained. **(B)** The specific changed GO entries identified by linear discriminant analysis (LDA) and effect size (LEfSe) analysis were presented, and LDA scores >2.0 were considered significant.

such as non-steroidal anti-inflammatory drugs, proton pump inhibitors, and β-blockers can affect bacterial growth by altering the pH of the intestine (Wozniak et al., 2022), and continuous parenteral nutrition has been associated with significant disturbances in the flora (Dahlgren et al., 2019).

In this study, the diversity of the gut microbiota was investigated. The ACE and Chao1 indices of the children in the D7 group were significantly lower than those in the D1 group. The ACE and Chao1 indices are two indicators that describe the richness of the gut microbiota (Szychowiak et al., 2022), which implies that a significant decrease in the number of bacterial species in the gut microbiota occurred after 7 days of treatment in the PICU. While the Shannon and Simpson indices, describing both richness and evenness (Szychowiak et al., 2022), did not change significantly in our study.

Studies performed on the gut flora of critically ill children, using follow-up data, remain insufficient. Rogers et al. found that the Shannon diversity index of the gut flora was decreased significantly compared with healthy children, and it was significantly negatively correlated with the time spent in the PICU (Rogers et al., 2016). This differed from our results, which showed that the Shannon index did not change significantly after short-term PICU treatment. One of the reasons for this discrepancy might be that we followed-up with the patients for different periods of time. Our study further investigated changes in the composition of the gut microbiota in critically ill children after short-term PICU treatment, while Rogers et al. followed-up with patients for 30 days. The results showed that on both days 1 and 7 of PICU admission, the composition of the children's gut microbiota at the phylum level was dominated by the *Firmicutes*, *Bacteroides*, *Aspergillus*, and *Actinomycetes*, and a majority of patients had a predominant proportion of the *Firmicutes* and *Bacteroides*. In 2005, Eckburg et al. found that the sum of the relative abundances of *Firmicutes* and *Bacteroidetes* exceeded 90% in the human gut microbiota (Eckburg et al., 2005). We further compared changes in flora at the phylum level, where the relative abundance of *Bacillus* decreased. β-hexosaminidase in the *Methanobacterium* has been shown to be a driver of lymphocyte-specific differentiation and that β-hexosaminidase-specific lymphocytes are protective against intestinal inflammation in a mouse model of colitis (Bousbaine et al., 2022). A study conducted on 115 critically ill patients revealed similar results, with patients leaving the ICU showing a significant decrease in the relative abundance of the *Firmicutes* and *Bacteroidetes* of the gut microbiota, a significant increase in the *Proteobacteria*, and an increase in pathogenic colonization with *Enterobacter* spp. and *Staphylococcus* spp., compared with those at the time of admission to the ICU (Mcdonald et al., 2016).

Notably, there were differences in the composition of the flora among individual patients after ICU treatment (Figure 3). Ojima et al. (2016) conducted a longitudinal observational study of the gut

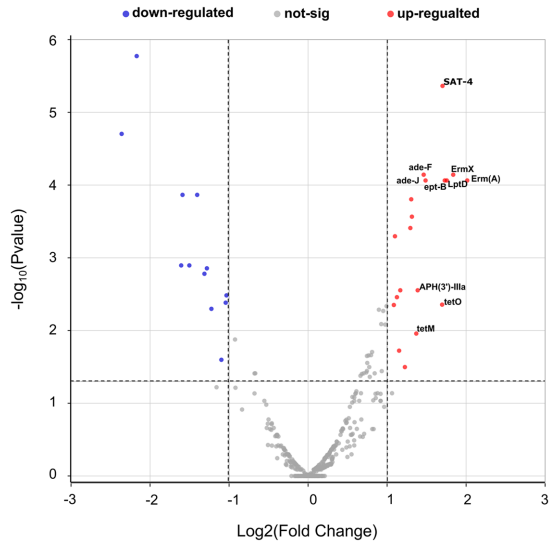

FIGURE 9
Volcano plots of antimicrobial resistance gene expression in the D1 and D7 groups. The horizontal coordinates in the graph represent the $\log_2$ fold change, and the vertical coordinates represent the-log10 (p-value). The horizontal dashed line in the figure represents the p-value threshold (0.05), and the two vertical dashed lines represent $\log_2FC = 1/-1$. The red dots represent $p < 0.05$ and $\log_2$ fold change ≥ 1, which means that the expression of resistance genes is significantly upregulated. The blue dots represent $p < 0.05$ and $\log_2$ fold change ≤ -1, which means that the expression of resistance genes is significantly down-regulated. While the gray dots mean that there is no significant change. The top ten up-regulated resistance genes are labeled in the figure.

microbiota of 12 mechanically ventilated patients in a large tertiary care hospital; they found that the percentages of the *Bacteroidetes* and *Firmicutes* changed significantly during the follow-up period and that an extreme imbalance of flora might be associated with poor patient prognosis. Disturbances in the flora have been shown to be associated with increased susceptibility to nosocomial infections, sepsis, organ failure, and severe COVID-19 (Lynch and Pedersen, 2016; Ojima et al., 2016; Yeoh et al., 2021). In the present study, children treated in the PICU showed significant changes in C-reactive protein, calcitonin, white blood cells, platelets, creatinine, and lactate levels. In addition, the relative abundance of colonies such as *Bacilli*, *Lactobacillales*, and *Campylobacter hominis* changed significantly. Chao1 and ACE indices also decreased significantly, and the random forest analysis revealed that the species levels of *Prevotella corporis* and *Enterbacter cloacae* were specific markers before and after PICU treatment in critically ill children. This suggests that future studies should correlate changes in the gut microbiota of patients with changes in clinical indicators to provide novel reference indicators for assisting in the assessment of changes in patient conditions.

Our study found that after a short period of PICU treatment, the gene function of the gut microbiota of critically ill children can undergo significant changes, mainly including the processes of metabolism, DNA degradation, and transmembrane transport. However, it should be noted that our results are derived from computerized predictions, and their exact roles in human physiological activities remain unclear. Nevertheless, several studies have confirmed the involvement of metabolites of the gut microbiota in the regulation of vital organ functions. Hayakawa et al. (2011) found that changes in the composition of the flora, including increases in *Enterococcus faecalis* and *Pseudomonas aeruginosa*, accompanied by decreases in the three major short-chain fatty acids, butyric acid, propionic acid, and acetate, could occur within 6 h of the onset of critical illness. Short-chain fatty acids are products of the glycolytic process of dietary fibers by intestinal microorganisms, including acetate and butyrate; they are involved in regulating human immune functions, including promoting the differentiation and expansion of T cells, forming a complete mucosal immune system, and influencing the phagocytosis of macrophages (Furusawa et al., 2013). Butyrate also plays a role in regulating the transcription factor HIF-1, which is involved in maintaining the stable function of the intestinal barrier by decreasing the oxygen concentration in tissues (Lopez-Siles et al., 2017). Fatty acids may also be involved in the physiological functions of the brain, lungs, and cardiovascular system by activating the vagus nerve, reducing lung inflammation, and affecting renin secretion (Wozniak et al., 2022). Short-chain fatty acid levels have been shown to be negatively correlated with the severity of portal hypertension and systemic inflammation, emphasizing the role of gut microbiota in enterohepatic interactions and the progression of liver pathologies such as cirrhosis (Juanola et al., 2019). Short-chain fatty acids also play a role in acute kidney injury (AKI) by modulating the inflammatory response, and thus improving AKI outcomes (Andrade-Oliveira et al., 2015). Therefore, gut microbiota disorders can cause a decrease in beneficial metabolites, further causing adverse outcomes such as immune and organ dysfunction and increasing susceptibility to disease. Moreover, GO analysis in our study revealed that bacterial cell wall synthesis and the transmembrane transport of macromolecules were affected in the gut microbiota of critically ill children after a short period of ICU treatment. We hypothesized that this may be related to patients receiving antibiotics, proton pump inhibitors, and inadequate organ perfusion, causing a disturbance of the intestinal microenvironment and further affecting the physiological activity of the flora.

The intestine is a major site of drug-resistant bacteria. A healthy gut microbiota is a stable and diverse community that protects the host from invasion by pathogenic bacteria. Antibiotics can disrupt the stable ecosystem of the gut, providing conditions for colonization by drug-resistant bacteria, increasing resistance gene load, and further spreading resistant bacteria to other sites, causing infection (Anthony et al., 2021). Norgaard et al. found that the use of broad-spectrum β-lactam antibiotics was most significantly associated with increased microbial destruction and resistance characteristics in patients treated with hematopoietic stem cell transplantation (Nørgaard et al., 2023). The increasing prevalence of carbapenem-resistant *Enterobacteriaceae* poses a major global health threat (Jean et al., 2022). Studies have shown that the risk of infection with carbapenem-resistant *Acinetobacter baumannii* can increase by four-fold with exposure to carbapenems, and a new meta-analysis confirmed an association between carbapenem-resistant *P. aeruginosa* and increased mortality (Brink, 2019).

Our study has some limitations. First, while the purpose of this study was to describe the composition and function of the flora of critically ill children after PICU treatment, the degree of influence of factors was not evaluated. Second, owing to the observational nature of our study, it was not possible to control for the variables that might

have affected the intestinal flora. Third, this study was a single-center study, and there was a certain selection bias.

5. Conclusion

After short-term treatment in the PICU, the richness of the gut microbiota in critically ill children was significantly decreased, while the bacterial diversity and the community structure between groups remained stable to some extent. The composition of some colonies was also altered significantly, with a significant increase in the relative abundances of *Bacilli* and *Lactobacillales* and a significant decrease in the relative abundance of *C. hominis*. GO and KEGG analyses showed that gene functions of the gut microbiota were also altered, mainly in genes responsible for metabolism, DNA catabolism, and transmembrane transport. In addition, the expression of resistance genes in critically ill children was changed significantly after short-term treatment in the PICU. The top 10 up-regulated genes were *Erm(A)*, *ErmX*, *LptD*, *eptB*, *SAT-4*, *tetO*, *adeJ*, *adeF*, *APH(3′)-IIIa*, and *tetM*.

Data availability statement

The data presented in this study are deposited in the NCBI SRA repository, accession number PRJNA1033539 (http://www.ncbi.nlm.nih.gov/bioproject/1033539).

Ethics statement

The studies involving humans were approved by Ethics Committee of Xinhua Hospital, Shanghai Jiao Tong University School of Medicine. The studies were conducted in accordance with the local legislation and institutional requirements. Written informed consent for participation in this study was provided by the participants' legal guardians/next of kin.

Author contributions

JX and YZ: study design. HM and YZ: data collection. JX and XK: statistical analysis. YX: data interpretation. JX, YX, and YZ: manuscript preparation. JL and JX: literature search. All authors contributed to the article and approved the submitted version.

Acknowledgments

We sincerely thank Dinfectome Inc., Nanjing, China, for providing help in mNGS sequencing.

Conflict of interest

The authors declare that the research was conducted in the absence of any commercial or financial relationships that could be construed as a potential conflict of interest.

Publisher's note

Supplementary material

The Supplementary material for this article can be found online at: https://www.frontiersin.org/articles/10.3389/fmicb.2023.1237993/full#supplementary-material

References

Adhikari, N. K., Fowler, R. A., Bhagwanjee, S., and Rubenfeld, G. D. (2010). Critical care and the global burden of critical illness in adults. *Lancet* 376, 1339–1346. doi: 10.1016/S0140-6736(10)60446-1

Andrade-Oliveira, V., Amano, M. T., Correa-Costa, M., Castoldi, A., Felizardo, R. J., de Almeida, D. C., et al. (2015). Gut bacteria products prevent AKI induced by ischemia-reperfusion. *J. Am. Soc. Nephrol.* 26, 1877–1888. doi: 10.1681/ASN.2014030288

Andremont, O., Armand-Lefevre, L., Dupuis, C., de Montmollin, E., Ruckly, S., Lucet, J. C., et al. (2020). Semi-quantitative cultures of throat and rectal swabs are efficient tests to predict ESBL-Enterobacterales ventilator-associated pneumonia in mechanically ventilated ESBL carriers. *Intensive Care Med.* 46, 1232–1242. doi: 10.1007/s00134-020-06029-y

Anthony, W. E., Burnham, C. D., Dantas, G., and Kwon, J. H. (2021). The gut microbiome as a reservoir for antimicrobial resistance. *J. Infect. Dis.* 223, S209–S213. doi: 10.1093/infdis/jiaa497

Bousbaine, D., Fisch, L. I., London, M., Bhagchandani, P., Rezende de Castro, T. B., Mimee, M., et al. (2022). A conserved Bacteroidetes antigen induces anti-inflammatory intestinal T lymphocytes. *Science* 377, 660–666. doi: 10.1126/science.abg5645

Brink, A. J. (2019). Epidemiology of carbapenem-resistant gram-negative infections globally. *Curr. Opin. Infect. Dis.* 32, 609–616. doi: 10.1097/QCO.0000000000000608

Dahlgren, A. F., Pan, A., Lam, V., Gouthro, K. C., Simpson, P. M., Salzman, N. H., et al. (2019). Longitudinal changes in the gut microbiome of infants on Total parenteral nutrition. *Pediatr. Res.* 86, 107–114. doi: 10.1038/s41390-019-0391-y

Diao, Z., Han, D., Zhang, R., and Li, J. (2022). Metagenomics next-generation sequencing tests take the stage in the diagnosis of lower respiratory tract infections. *J. Adv. Res.* 38, 201–212. doi: 10.1016/j.jare.2021.09.012

Dickson, R. P. (2016). The microbiome and critical illness. *Lancet Respir. Med.* 4, 59–72. doi: 10.1016/S2213-2600(15)00427-0

Dickson, R. P., Schultz, M. J., van der Poll, T., Schouten, L. R., Falkowski, N. R., Luth, J. E., et al. (2020). Lung microbiota predict clinical outcomes in critically ill patients. *Am. J. Respir. Crit. Care Med.* 201, 555–563. doi: 10.1164/rccm.201907-1487OC

Dunn, S. J., Connor, C., and McNally, A. (2019). The evolution and transmission of multi-drug resistant Escherichia coli and *Klebsiella pneumoniae*: the complexity of clones and plasmids. *Curr. Opin. Microbiol.* 51, 51–56. doi: 10.1016/j.mib.2019.06.004

Eckburg, P. B., Bik, E. M., Bernstein, C. N., Purdom, E., Dethlefsen, L., Sargent, M., et al. (2005). Diversity of the human intestinal microbial flora. *Science* 308, 1635–1638. doi: 10.1126/science.1110591

Erawijantari, P. P., Mizutani, S., Shiroma, H., Shiba, S., Nakajima, T., Sakamoto, T., et al. (2020). Influence of gastrectomy for gastric cancer treatment on faecal microbiome and metabolome profiles. *Gut* 69, 1404–1415. doi: 10.1136/gutjnl-2019-319188

Furusawa, Y., Obata, Y., Fukuda, S., Endo, T. A., Nakato, G., Takahashi, D., et al. (2013). Commensal microbe-derived butyrate induces the differentiation of colonic regulatory T cells. *Nature* 504, 446–450. doi: 10.1038/nature12721

Gökdemir, F. Ş., İşeri, Ö. D., Sharma, A., Achar, P. N., and Eyidoğan, F. (2022). Metagenomics next generation sequencing (mNGS): an exciting tool for early and accurate diagnostic of fungal pathogens in plants. *J. Fungi* 8:1195. doi: 10.3390/jof8111195

Guzman Prieto, A. M., van Schaik, W., Rogers, M. R., Coque, T. M., Baquero, F., Corander, J., et al. (2016). Global emergence and dissemination of enterococci as nosocomial pathogens: attack of the clones? *Front. Microbiol.* 7:788. doi: 10.3389/fmicb.2016.00788

Hayakawa, M., Asahara, T., Henzan, N., Murakami, H., Yamamoto, H., Mukai, N., et al. (2011). Dramatic changes of the gut flora immediately after severe and sudden insults. *Dig. Dis. Sci.* 56, 2361–2365. doi: 10.1007/s10620-011-1649-3

Hu, W., Chen, Z. M., Li, X. X., Lu, L., Yang, G. H., Lei, Z. X., et al. (2022). Faecal microbiome and metabolic signatures in rectal neuroendocrine tumors. *Theranostics* 12, 2015–2027. doi: 10.7150/thno.66464

Hu, Y. J., and Satten, G. A. (2022). A rarefaction-without-resampling extension of PERMANOVA for testing presence-absence associations in the microbiome. *Bioinformatics* 38, 3689–3697. doi: 10.1093/bioinformatics/btac399

Hu, J., and Szymczak, S. (2023). A review on longitudinal data analysis with random forest. *Brief. Bioinform.* 24:bbad002. doi: 10.1093/bib/bbad002

Jean, S. S., Harnod, D., and Hsueh, P. R. (2022). Global threat of carbapenem-resistant gram-negative bacteria. *Front. Cell. Infect. Microbiol.* 12:823684. doi: 10.3389/fcimb.2022.823684

Juanola, O., Ferrusquía-Acosta, J., García-Villalba, R., Zapater, P., Magaz, M., Marín, A., et al. (2019). Circulating levels of butyrate are inversely related to portal hypertension, endotoxemia, and systemic inflammation in patients with cirrhosis. *FASEB J.* 33, 11595–11605. doi: 10.1096/fj.201901327R

Ladopoulos, T., Giannaki, M., Alexopoulou, C., Proklou, A., Pediaditis, E., and Kondili, E. (2018). Gastrointestinal dysmotility in critically ill patients. *Ann. Gastroenterol.* 31, 273–281. doi: 10.20524/aog.2018.0250

Lang, J., Zhu, R., Sun, X., Zhu, S., Li, T., Shi, X., et al. (2021). Evaluation of the MGISEQ-2000 sequencing platform for Illumina target capture sequencing libraries. *Front. Genet.* 12:730519. doi: 10.3389/fgene.2021.730519

Lopez-Siles, M., Duncan, S. H., Garcia-Gil, L. J., and Martinez-Medina, M. (2017). *Faecalibacterium prausnitzii*: from microbiology to diagnostics and prognostics. *ISME J.* 11, 841–852. doi: 10.1038/ismej.2016.176

Lynch, S. V., and Pedersen, O. (2016). The human intestinal microbiome in health and disease. *N. Engl. J. Med.* 375, 2369–2379. doi: 10.1056/NEJMra1600266

Manor, O., Dai, C. L., Kornilov, S. A., Smith, B., Price, N. D., Lovejoy, J. C., et al. (2020). Health and disease markers correlate with gut microbiome composition across thousands of people. *Nat. Commun.* 11:5206. doi: 10.1038/s41467-020-18871-1

McDonald, D., Ackermann, G., Khailova, L., Baird, C., Heyland, D., Kozar, R., et al. (2016). Extreme dysbiosis of the microbiome in critical illness. *mSphere* 1, e00199–e00116. doi: 10.1128/mSphere.00199-16

McInnes, R. S., McCallum, G. E., Lamberte, L. E., and van Schaik, W. (2020). Horizontal transfer of antibiotic resistance genes in the human gut microbiome. *Curr. Opin. Microbiol.* 53, 35–43. doi: 10.1016/j.mib.2020.02.002

Nørgaard, J. C., Jørgensen, M., Moestrup, K. S., Ilett, E. E., Zucco, A. G., Marandi, R. Z., et al. (2023). Impact of antibiotic treatment on the gut microbiome and its resistome in hematopoietic stem cell transplant recipients. *J. Infect. Dis.* 228, 28–36. doi: 10.1093/infdis/jiad033

Ojima, M., Motooka, D., Shimizu, K., Gotoh, K., Shintani, A., Yoshiya, K., et al. (2016). Metagenomic analysis reveals dynamic changes of whole gut microbiota in the acute phase of intensive care unit patients. *Dig. Dis. Sci.* 61, 1628–1634. doi: 10.1007/s10620-015-4011-3

Ojima, M., Shimizu, K., Motooka, D., Ishihara, T., Nakamura, S., Shintani, A., et al. (2022). Gut dysbiosis associated with antibiotics and disease severity and its relation to mortality in critically ill patients. *Dig. Dis. Sci.* 67, 2420–2432. doi: 10.1007/s10620-021-07000-7

Palleja, A., Mikkelsen, K. H., Forslund, S. K., Kashani, A., Allin, K. H., Nielsen, T., et al. (2018). Recovery of gut microbiota of healthy adults following antibiotic exposure. *Nat. Microbiol.* 3, 1255–1265. doi: 10.1038/s41564-018-0257-9

Ramirez, J., Guarner, F., Bustos Fernandez, L., Maruy, A., Sdepanian, V. L., and Cohen, H. (2020). Antibiotics as major disruptors of gut microbiota. *Front. Cell. Infect. Microbiol.* 10:572912. doi: 10.3389/fcimb.2020.572912

Rogers, M. B., Firek, B., Shi, M., Yeh, A., Brower-Sinning, R., Aveson, V., et al. (2016). Disruption of the microbiota across multiple body sites in critically ill children. *Microbiome* 4:66. doi: 10.1186/s40168-016-0211-0

Ronchetti, L., Terrenato, I., Ferretti, M., Corrado, G., Goeman, F., Donzelli, S., et al. (2022). Circulating cell free DNA and citrullinated histone H3 as useful biomarkers of NETosis in endometrial cancer. *J. Exp. Clin. Cancer Res.* 41:151. doi: 10.1186/s13046-022-02359-5

Szychowiak, P., Villageois-Tran, K., Patrier, J., Timsit, J. F., and Ruppé, É. (2022). The role of the microbiota in the management of intensive care patients. *Ann. Intensive Care* 12:3. doi: 10.1186/s13613-021-00976-5

Wozniak, H., Beckmann, T. S., Fröhlich, L., Soccorsi, T., Le Terrier, C., de Watteville, A., et al. (2022). The central and biodynamic role of gut microbiota in critically ill patients. *Crit. Care* 26:250. doi: 10.1186/s13054-022-04127-5

Xu, Y., Kong, X., Zhu, Y., Xu, J., Mao, H., Li, J., et al. (2022). Contribution of gut microbiota toward renal function in sepsis. *Front. Microbiol.* 13:985283. doi: 10.3389/fmicb.2022.985283

Yassour, M., Vatanen, T., Siljander, H., Hämäläinen, A. M., Härkönen, T., Ryhänen, S. J., et al. (2016). Natural history of the infant gut microbiome and impact of antibiotic treatment on bacterial strain diversity and stability. *Sci. Transl. Med.* 8:343ra81–343ra81. doi: 10.1126/scitranslmed.aad0917

Yeoh, Y. K., Zuo, T., Lui, G. C., Zhang, F., Liu, Q., Li, A. Y., et al. (2021). Gut microbiota composition reflects disease severity and dysfunctional immune responses in patients with COVID-19. *Gut* 70, 698–706. doi: 10.1136/gutjnl-2020-323020

Zhang, L., Li, Y., Zhou, J., Li, J., Tong, C., Cai, J., et al. (2021). Comparison of the community-acquired pneumonia and COVID-19 at the early stage: findings from two cohort studies. *Ann. Palliat. Med.* 10, 9572–9582. doi: 10.21037/apm-21-2006

frontiers | Frontiers in Microbiology

TYPE Original Research
PUBLISHED 20 November 2023
DOI 10.3389/fmicb.2023.1291030

OPEN ACCESS

EDITED BY
Krassimira Radoykova Hristova,
Marquette University, United States

REVIEWED BY
Kandasamy Selvam,
Periyar University, India
Rajivgandhi Govindan,
University of Chile, Chile

*CORRESPONDENCE
Aiwen Huang
✉ hawen83@sina.com
Bin Qiu
✉ summer328cn@163.com

RECEIVED 08 September 2023
ACCEPTED 03 November 2023
PUBLISHED 20 November 2023

CITATION
Ye M, Yang W, Zhang M, Huang H, Huang A and Qiu B (2023) Biosynthesis, characterization, and antifungal activity of plant-mediated silver nanoparticles using *Cnidium monnieri* fruit extract.
Front. Microbiol. 14:1291030.
doi: 10.3389/fmicb.2023.1291030

Biosynthesis, characterization, and antifungal activity of plant-mediated silver nanoparticles using *Cnidium monnieri* fruit extract

Mingqi Ye[1], Wenwen Yang[1], Minxin Zhang[2], Huili Huang[2], Aiwen Huang[1,2]* and Bin Qiu[3]*

[1]Fujian University of Traditional Chinese Medicine Fuzong Teaching Hospital (900TH Hospital), Fuzhou, China, [2]Department of Clinical Pharmacy, 900TH Hospital of Joint Logistics Support Force of PLA, Fuzhou, China, [3]College of Chemistry, Fuzhou University, Fuzhou, China

The present study describes a novel method for green synthesis of silver nanoparticles using *Cnidium monnieri* (CM-AgNPs). *Cnidium monnieri* fruit is an excellent anti tinea drug that can be used externally to treat superficial fungal infections in the human body. The aqueous ethanolic extract of *Cnidium monnieri* fruit was prepared and employed in the synthesis of stable silver nanoparticles via biological reduction method. The synthesis conditions of CM-AgNPs was systematically optimized using Box–Behnken design. CM-AgNPs were well characterized by UV-spectroscopy and X-ray powder diffraction (XRD), and it was confirmed that the synthesized particles were AgNPs. The possible functional groups required for the reduction and stabilization of CM-AgNPs in the extract were identified through FTIR spectrum. The size of CM-AgNPs structure was confirmed to be approximately 44.6 nm in polydisperse spherical shape through scanning electron microscopy (SEM), transmission electron microscopy (TEM), and laser dynamic light scattering (DLS). Further, the minimum inhibitory concentration 90% (MIC_{90}) ratios values of Cm-AgNPs against *Trichophyton rubrum* (7 d), *T. mentagrophytes* (7 d) and *Candida albicans* (24 h) were 3.125, 3.125, and 0.78125 μg/mL, respectively, determined by the broth micro dilution method. Finally, the result was concluded that the synthesized AgNPs could be further evaluated in large scale as a potential human topical antifungal agent.

KEYWORDS

AgNPs, *Cnidium monnieri*, green synthesis, characterization, antifungal

1 Introduction

In recent years, nanoparticles (NPs) have been widely used in biological, pharmaceutical, electronic, chemical and energy industries (Yoon et al., 2020; Jin Nam et al., 2021; Mobini et al., 2021; Targhi et al., 2021; Zhao et al., 2021; Wei et al., 2022). Due to the need to reduce or eliminate the use or generation of toxic and harmful substances in compounds, reduce pollution to the environment and develop more sustainable methods, biosynthesis of nanoparticles (NPs) using natural product extracts has been proposed as a harmless, rapid and efficient alternative synthesis route. As a safe and non-toxic method, biosynthetic silver nanoparticles (AgNPs) was used to produce biocompatible nanoparticles by using bioactive molecules with functions of

reduction, capping and stabilization, which were suitable for many medical applications, such as antibacterial, anticancer, antioxidant, anti-diabetic, antiviral, and anti-inflammatory (Chinnasamy et al., 2019; Mehmood et al., 2020; Tian et al., 2020; Jang et al., 2022). Different parts of plants could be used to synthesize silver nanoparticles (Ma et al., 2021; Moorthy et al., 2021; Mirzaie et al., 2022; Abdel-Aty et al., 2023). Using plant extracts biosynthetic silver nanoparticles, AgNPs were covered with active ingredients from plants, which can not only stabilize AgNPs, but also enhance their antifungal activity (Robles-Martinez et al., 2019). Biosynthesized AgNPs can treat infections caused by *Trichophyton rubrum* in animals' models, and after 14 days of treatment, the structure of the animal's epidermis and dermis can be restored well, and the synthesized AgNPs have no risk of antimicrobial resistance or systemic side effects of other drugs (Abdallah et al., 2023).

Superficial infections, including cutaneous and mucocutaneous infections, are a common public health problem and can be caused by dermatophytes, candida, and Malassezia (Noites et al., 2023). Superficial fungal infections usually cause chronic and non-inflammatory lesions, long treatment course, easy relapse, pain, unattractive and other problems affecting the quality of life of patients (Abd-Elsalam and Abouelatta, 2023). A number of comorbidities such as diabetes, cancer, immune deficiency or peripheral artery disease may increase susceptibility to superficial fungi. Filamentous fungi *T. rubrum* and *T. mentagrophytes* were one of the most important pathogens causing dermatomycosis in the UK, Poland and Sweden, accounting for about 90% of cases (Nenoff et al., 2014). Although *Candida albicans* is a common fungal symbiont in the human microbiota, it may cause superficial skin, nails, and mucous membrane infections (Glazier, 2022). Long-term use of azoles, allylamines, and terbinafine in the treatment of dermatophytes may develop drug resistance and toxicity, leading to treatment failure (Sardana et al., 2023). The need to slow down and prevent the development of drug resistance and reduce side effects has prompted researchers to develop new alternative treatment drugs for superficial infections.

Cnidium monnieri (L.) Cuss, an annual plant in the umbelliferous family, is widely used as a traditional herb in China, Japan and Vietnam to treat various diseases. It has a wide range of pharmacological activities, the main component being osthole, which has an allergy-inhibiting (antipruritic) effect on the skin, as well as bacterial, fungal and viral inhibition (Munir et al., 2022). According to modern research, the mechanism of treating *T. rubrum* is that the water extract from *C. monnieri* can destroy the mycelial morphology and internal structure of *T. rubrum* and inhibit its growth (Yanyun et al., 2021). The extract of *C. monnieri* fruit contains various reducing components, including flavonoids, coumarins, phenolic acids, and lignans, which contribute to the reduction of silver nitrate (Wu et al., 2019; Ni et al., 2020). The complex components contained in the extract of *C. monnieri* fruit are coated on silver nanoparticles to prevent aggregation and facilitate the stability of silver nanoparticles. *C. monnieri* are widely distributed and have low prices, making it low-cost to synthesize AgNPs using them.

In this report, we innovatively prepared AgNPs using the extract of dried and mature fruit of the anti ringworm drug *C. monnieri*, using a simple biosynthesis method, and studied their activity against *T. rubrum*, *T. mentagrophytes*, and *C. albicans*. Compared with physical and chemical synthesis methods, the process of green synthesis of AgNPs using *C. monnieri* fruit extract is simple, does not use toxic reagents, and the process of preparation is relatively safe and environmental friendly. The synthesized CM-AgNPs are expected to be used in various dosage forms for superficial fungal infections in humans and animals, but further research is to be demonstated their efficacy.

2 Materials and methods

2.1 Materials

Silver nitrate purchased from Yida Technology (Quanzhou) Co. Ltd., concentration 0.1001 mol/L, diluted for use in the experiment. *C. monnieri* fruit was provided by the pharmacy of the No.900 Hospital of Joint Logistics Support Force of PLA. Deionized water was used to synthesize, extract and purify the nanoparticles. All chemicals used were analytical grade. *T. rubrum* (BNCC340195) and *T. mentagrophytes* (BNCC340405) were purchased as standard strains from Beijing BeNa Culture Collection. *C. albicans* was a clinically isolated strain, which was provided by the laboratory department of the No.900 Hospital of Joint Logistics Support Force of PLA. RPMI 1640 culture medium was purchased from Wuhan Boster Biological Technology Co. Ltd. Potato dextrose agar (PDA) was purchased from Wenzhou Kangtai Biotechnology Co. Ltd. Sabouraud dextrose agar (SDA) was purchased from Zhengzhou Antu Bioengineering Co. Ltd. Fluconazole and terbinafine were purchased from China National Institutes for Food and Drug Control.

2.2 Preparation of plant extracts

50 g of *C. monnieri* fruit was weighed and soaked in 500 mL of 75% ethanol for 0.5 h, then heated and refluxed extraction twice for 2 h each time. The extracted solution was combined and concentrated under reduced pressure until there was no alcohol taste. Pure water was added to dilute to 250 mL and filtered by 0.22 μm microporous membrane to obtain *C. monnieri* fruit extract, which was stored at −40°C.

2.3 Synthesis of CM-AgNPs

CM-AgNPs were synthesized with different concentrations of *C. monnieri* fruit extract (65, 132.5, 200 mg/mL). NaOH solution (0.1 M) was used to adjust the pH of *C. monnieri* fruit extract (8, 10, 12). 6 mL of pH-adjusted *C. monnieri* fruit extract was slowly dripped into 20 mL of silver nitrate at different concentrations (5, 12.5, 20 mM), and stirred continuously for 30 min at 700 rpm with the help of magnetic stirrers (Srećković et al., 2023). The resulting CM-AgNPs solution was centrifuged at 13,000 rpm for 20 min at 20°C. The supernatant was removed and the precipitate was redispersed in deionized water and centrifuged again at 13,000 rpm for 20 min. This process was repeated three times. Finally, the centrifugal precipitate was freeze-dried, weighed and redissolved with deionized water.

2.4 Systematic optimization of synthesis of CM-AgNPs

System optimization of CM-AgNPs was performed using a Box–Behnken design (BBD) with the help of Design Expert® ver. 13.0 software (Stat-Ease Inc., Minneapolis, USA). The three most influential factors, $AgNO_3$ concentration, *C. monnieri* fruit extract concentration and pH value, were used as independent variables and tested at three different levels, as shown in Table 1. A total of 17 tests were recommended for the selected design. The particle size (nm) and polydispersity index (PDI) of the synthesized silver nanoparticles (CM-AgNPs) were analyzed in response. After putting the data into BBD, mathematical modeling was carried out to analyze the results. The optimum conditions for the synthesis of CM-AgNPs were determined by means of numerical desirable function and graphic optimization techniques.

2.5 Chemical synthesis of bare AgNPs

Reference The preparation method of bare AgNPs and make appropriate modifications (Bharti et al., 2021; Fu et al., 2021; Jassim et al., 2022; Velgosova et al., 2022). 9.45 mg of $NaBH_4$ Was weighed and added To 25 mL of NaOH solution (0. L Mol/L) To prepare a reducing agent. The 20 mL of $AgNO_3$ solution and sodium citrate solution (As dispersant) with a concentration of 0.01 Mol/L each were added into The conical flask and stirred evenly, then 1 mL of The reducing agent solution Was added drop By drop, and The solution turned brownish black at room temperature for 5 Min. The resulting bare AgNPs solution Was centrifuged at 13,000 rpm for 20 Min at 20°C, and The precipitate Was rinsed three times with deionized water

2.6 Characterization of AgNPs

CM-AgNPs synthesized under optimal conditions and chemically synthesized bare AgNPs were scanned using a microplate reader (Infinite E Plex, Tecan Austria Gmbh, Austria) in the wavelength range of 200–800 nm. Fourier transform infrared (FTIR, Nicolet 6,700, Thermo Fisher, United States) spectra of CM-AgNPs and *C. monnieri* fruit extract were recorded using KBr particles. X-ray diffractometer (XRD, D8 Advance, Bruker, Germany) was used to analyze CM-AgNPs under diffraction conditions of copper target, Cu Kα radiation, measuring angle $2\theta = 5–90°$. SEM was used to observe the morphology of Cm-AgNPs and energy dispersive X-ray spectroscopy (EDX) results were obtained (Mira Lms, Tescan, Czech Republic). The shape and dimensions of CM-AgNPs were determined at 100 kV by TEM (Tecnai, Thermo Scientific FEI, United States). Particle size, PDI and zeta potential values of CM-AgNPs and bare AgNPs were recorded by dynamic light scattering (DLS) using a laser particle size analyzer (ZSU3100, Malvern Panalytical, Worcestershire, UK).

2.7 Antifungal assays

2.7.1 MIC determination of *Trichophyton rubrum* and *Trichophyton Mentagrophytes*

The strains of *T. rubrum* and *T. mentagrophytes* were inoculated on PDA medium and cultured at 28°C for 7–14 days. The number of spores was determined by cell counting plate (177-112C, Watson, Japan), and the concentration was adjusted to 7.1×10^4–1.1×10^5 CFU/mL by RPMI 1640 medium dilution. MIC was determined according to CLSI-M38 document (Alexander et al., 2017a), RPMI 1640 culture medium was added to the 96-well plates and the sample was diluted

TABLE 1 Response surface experiment design and results.

Runs	Concentration of $AgNO_3$ (mM)	Concentration of *Cnidium monnieri* fruit extraxt (mg/mL)	pH	Particle size (nm)	PDI
1	12.5	132.5	10	74.87	0.2857
2	5	132.5	8	113.23	0.2412
3	12.5	200	12	83.18	0.2576
4	12.5	132.5	10	80.98	0.2916
5	12.5	132.5	10	83.36	0.3019
6	12.5	200	8	97.05	0.2734
7	20	65	10	139.43	0.4307
8	12.5	65	12	73.06	0.3765
9	5	200	10	130.7	0.2725
10	12.5	132.5	10	81.09	0.2816
11	20	132.5	12	87.84	0.2848
12	20	200	10	82.43	0.2978
13	12.5	132.5	10	89.27	0.3647
14	20	132.5	8	112.67	0.4023
15	12.5	65	8	103.33	0.2918
16	5	65	10	88.71	0.3443
17	5	132.5	12	129.9	0.2191

to different concentrations using broth microdilution method (terbinafine was dissolved with DMSO, other drugs were dissolved with deionized water, DMSO content was 0.5%). In columns 1–9 of the 96-well plates, concentration of bare AgNPs lyophilized powder in nutritional broth was 250–0.98 μg/mL, concentration of *C. monnieri* fruit extract lyophilized powder was 15,000–58.59 μg/mL, concentration of CM-AgNPs lyophilized powder was 250–0.098 μg/mL, concentration of terbinafine was 0.25–0.00098 μg/mL, and concentration of fluconazole was 64–0.25 μg/mL. Meanwhile, the growth control group (column 10) with only fungal solution added, the control group containing 0.5%DMSO solvent (column 11) and the blank control group (column 12) were set up. Culture at 28°C for 7 d.

2.7.2 MIC determination of *Candida albicans*

C. albicans was inoculated on SDA medium and cultured at 35°C for 24 h. The number of spores was determined by cell counting plate, and the concentration was adjusted to 5.9×10^4 CFU/mL by RPMI 1640 medium dilution. MIC was determined according to CLSI-M27 document (Alexander et al., 2017b), the samples were diluted to different concentrations by adding RPMI 1640 culture medium into the 96-well plate (terbinafine was dissolved with DMSO, other drugs were dissolved with deionized water, DMSO content was 1%). In columns 1–9 of the 96-well plates, concentration of *C. monnieri* fruit extract lyophilized powder was 12,500–48.83 μg/mL, concentration of CM-AgNPs lyophilized powder was 25–0.098 μg/mL, concentration of bare AgNPs lyophilized powder was 500–1.95 μg/mL, concentration of fluconazole was 64–0.25 μg/mL, and concentration of terbinafine was 0.5–0.001953 μg/mL. Meanwhile, the growth control group (column 10) with only fungal solution added, the control group containing 1%DMSO solvent (column 11) and the blank control group (column 12) were set up. Culture at 35°C for 24 h.

2.7.3 Result interpretation

Absorption values of 96-well plates at 630 nm were determined using a microplate reader (Infinite E Plex, Tecan Austria Gmbh, Austria), and MIC_{90} of *C. monnieri* fruit extract, bare AgNPs and CM-AgNPs against *T. rubrum*, *T. mentagrophytes* and *C. albicans* were determined by combining visual and microplate detection of percentage inhibition and make a comparison. During the experiment, quality control compounds terbinafine and fluconazole were used as controls, and the MIC fluctuation range was no more than one drug gradient concentration, and the MIC was within the MIC standard range of quality control strains published by CLSI-M38 and CLSI-M27 (Alexander et al., 2017a, 2017b), which was considered reliable experimental data. The experiment was repeated three times and the percentage inhibition was calculated using the following equation:

$$\%\ \text{inhibition} = (A_{\text{Growth control}} - A_{\text{Sample}}) / A_{\text{Growth control}} \times 100\%.$$

3 Results and discussion

3.1 Analysis of response surface results

The synthesized CM-AgNPs were systematically optimized using Box–Behnken design of Design Expert® ver.13.0 software to find the optimal conditions. Concentration of $AgNO_3$, Concentration of *C. monnieri* fruit extract and pH were selected as three independent variables at different levels, and the particle size (nm) and PDI of silver nanoparticles were optimized as responses. A total of 17 tests were recommended for the selected design (Table 1). The obtained data were fitted with the quadratic polynomial model, and various statistical parameters were used for fitting analysis. Equations (1) and (2) were polynomial equations generated after modelling as data, indicating that the two response variables analyzed (particle size and PDI) have both interaction and curvature effects. The 3D response diagram (Figure 1) illustrates the good fit of the data in the selected model, where A is concentration of $AgNO_3$ (mM), B is concentration of *C. monnieri* fruit extraxt (mg/mL), C is pH value of *C. monnieri* fruit extract.

$$\text{Particle size} = 81.91 - 5.02A - 1.40B - 6.54C - 24.75AB - 10.38AC + 4.10BC + 25.08A^2 + 3.32B^2 + 3.92C^2 \quad (1)$$

$$\text{Polydispersity index} = 0.3069 + 0.0423A - 0.0427B - 0.0088C \quad (2)$$

For particle size response, ANOVA results show that the model is extremely significant, $p < 0.01$, where AB and A^2 were important model items. $R^2 = 0.9182$, the *F* value of the missing item was 5.71, and the missing item was not significant. For PDI response, ANOVA results showed that the model was significant ($p < 0.05$), where A and B were important model items. $R^2 = 0.5587$, the F value of missing item was 1.78, the missing item was not significant, the smaller R^2 may be due to the fact that PDI results were close to each other in the test range, as they are mostly in the acceptable range below 0.300.

The optimal conditions for CM-AgNPs synthesis were suggested by numerical optimization. The goal of each response variable was to minimize to the smallest possible value. The best conditions were found to be concentration of $AgNO_3$ was 18.38 mM, concentration of *C. monnieri* fruit extraxt was 196.77 mg/mL and adjusted to 200 mg/mL, and the pH value of *C. monnieri* fruit extraxt was 11.75. The predicted results showed particle size of 70.1779 nm and PDI of 0.202.

3.2 Characterization of optimized silver nanoparticles

3.2.1 UV–vis analysis

In this study, AgNPs were synthesized under optimized conditions using *C. monnierii* fruit extract. The plant extract serves as a reducing agent to convert silver ions (Ag^+) into silver nanoparticles (Ag^0), termed CM-AgNPs. The synthesis of AgNPS was confirmed through UV–Vis analysis (Figure 2A), with CM-AgNPs exhibiting surface plasmon resonance peak at 420 nm and bare AgNPs exhibiting SPR peak at 406 nm. The position and shape of the displayed SPR peak depend on the particle size and shape of the AgNPs (Rajivgandhi et al., 2019). This experiment synthesized AgNPs by adjusting the pH value, which can accelerate the synthesis and reduce the particle size. Studies have shown that pH value has a certain impact on the synthesis of AgNPs; under alkaline conditions, the hydroxyl groups in plant extracts were more likely to lose H^+, causing the whole molecule to be negatively charged; these negatively charged phytochemicals not only easier to interact with Ag^+, but also easier to lose electrons for reduction reaction (Luo et al., 2018). The schematic diagram (Figure 2B) describes the possible mechanism of plant synthesis of AgNPs. Silver ions (Ag^+) were reduced to form silver atoms (Ag^0),

10.3389/fmicb.2023.1291030

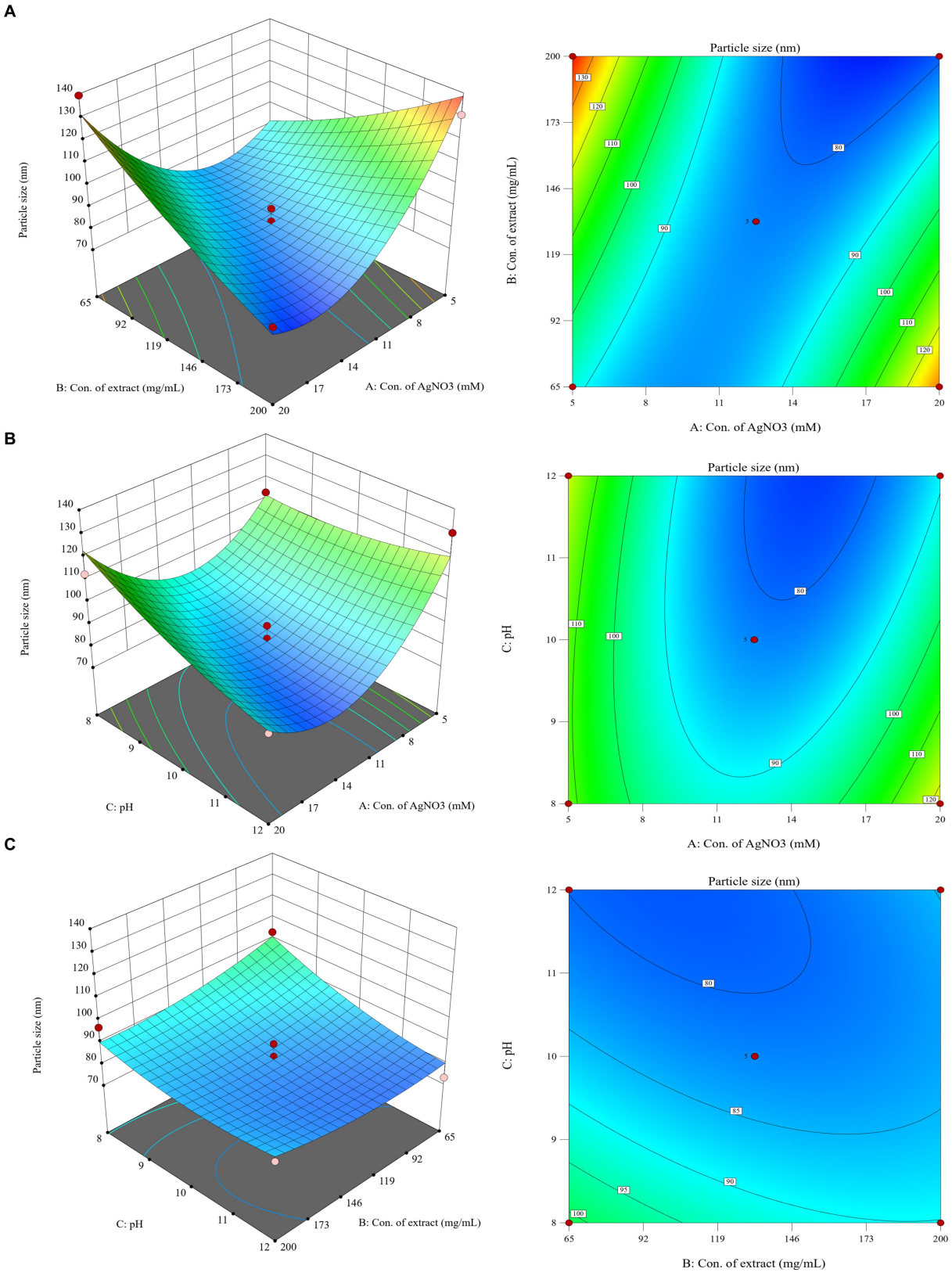

FIGURE 1
3D response surface plots and 2D contour plots showing the influence of interaction between **(A)**: concentration of $AgNO_3$, **(B)**: concentration of *C. monnierii* fruit extract and **(C)**: pH on the particle size of silver nanoparticles.

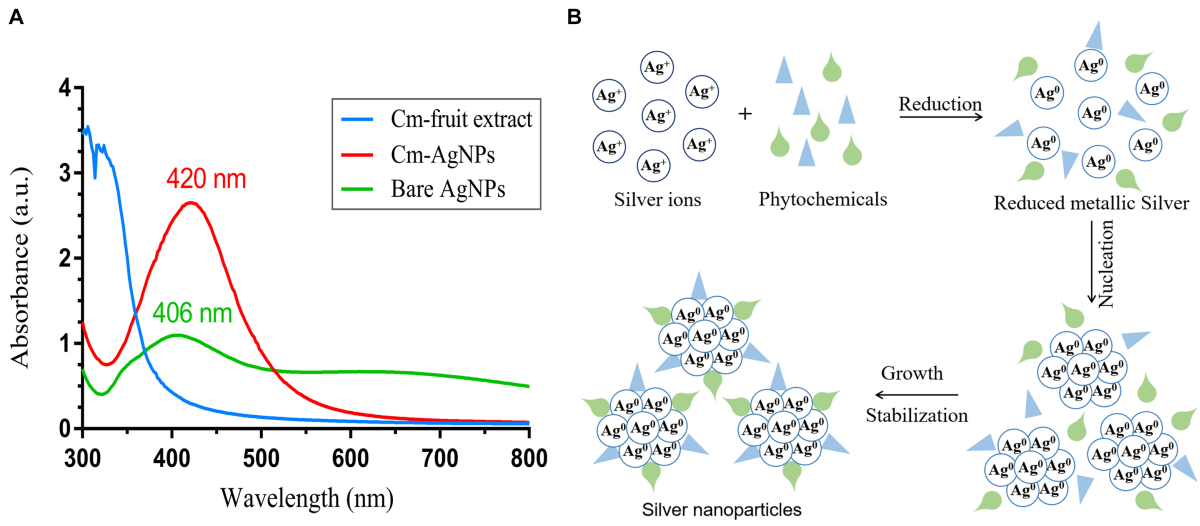

FIGURE 2
(A) UV–Vis spectrum of Cm-fruit extract, CM-AgNPs and bare AgNPs; **(B)** possible mechanism miagram of plant-mediated synthesis of AgNPs.

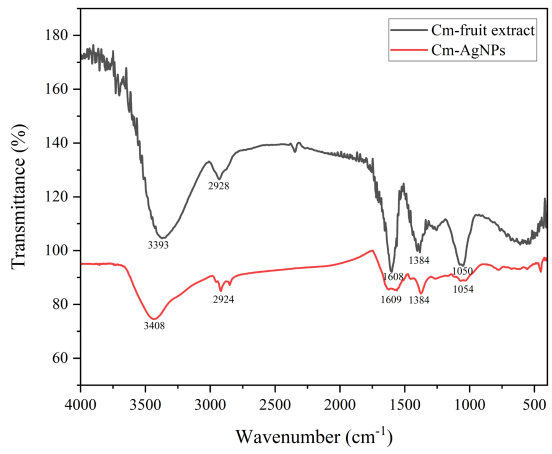

FIGURE 3
FTIR spectra of Cm-fruit extract and CM-AgNPs.

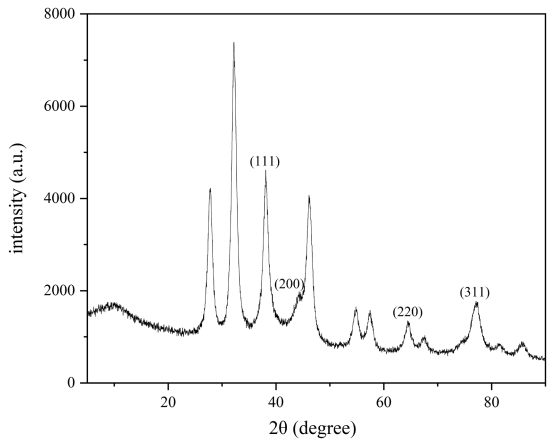

FIGURE 4
XRD patterns of CM-AgNPs.

which slowly aggregated into small silver nanoparticles. During this process, AgNP was restricted by phytochemicals so that the silver could not grow close to each other at the nanoscale and thus form small silver nanoparticles.

3.2.2 FTIR analysis

FTIR analysis was performed to determine the major phytochemicals involved in plant synthesis and sealing of CM-AgNPs. As shown in Figure 3, IR spectra confirmed the binding of silver ions with the extract of *C. monnierii* fruit. CM-AgNPs show the corresponding FTIR signal, O-H (3,408 cm^{-1}), C-H (2,924 cm^{-1}), benzene ring skeleton (1,609 cm^{-1}), -CH_3 (1,384 cm^{-1}) and -C-O (1,054 cm^{-1}). These signals matched corresponding peaks in the FTIR spectra of the *C. monnierii* fruit extract. This indicates that many organic functional groups in *C. monnierii* fruit extract actually remained on the surface of CM-AgNPs.

3.2.3 XRD analysis

The structure of CM-AgNPs was analyzed through XRD measurement (Figure 4). It can be seen that the main diffraction peaks were located at 38.08, 44.24, 64.46, and 77.46 °, pointing to (111), (200), (220), and (311) diffraction planes, respectively. CM-AgNPs showed the diffraction peak characteristics of the metal face-centered cube (JCPDS File No. 4–0783), indicating that the silver nanoparticles formed in this synthesis were essentially crystalline (Zhang et al., 2020; Rajivgandhi et al., 2020b). From the peak intensity ratio of (111) to other diffraction peaks, it can be concluded that the (111) plane was the main orientation in the silver crystal structure of CM-AgNPs.

3.2.4 SEM, EDX, and TEM analysis

As shown in Figure 5A, the SEM analysis of CM-AgNPs detected agglomeration, which may be caused by drying the AgNPs solution during detection (Rajivgandhi et al., 2020a). The

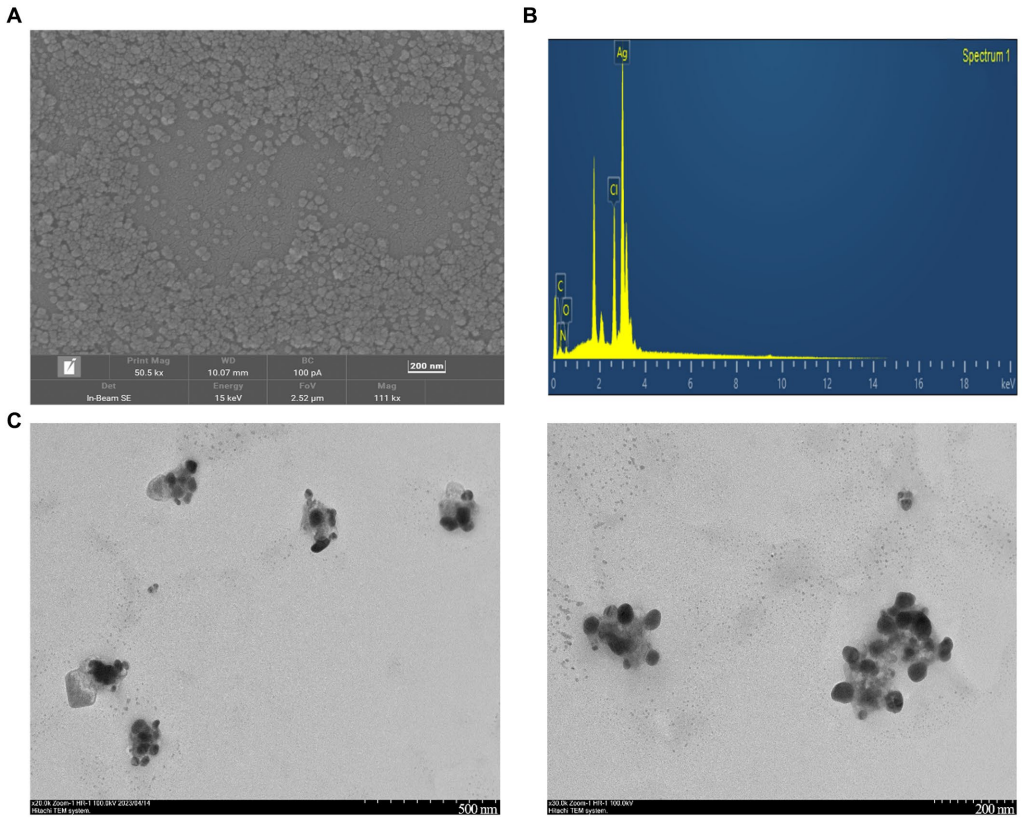

FIGURE 5
(A) SEM images of CM-AgNPs (200 nm); **(B)** EDX spectra of CM-AgNPs; **(C)** TEM images of CM-AgNPs (500, 200 nm).

EDX results indicate that the sample contains silver, which confirms the formation of elemental silver (Figure 5B). The shape and size of the optimized CM-AgNPs can be directly observed by TEM (Figure 5C). It can be seen that the diameter of the synthesized AgNPs was about 44.6 nm and the distribution was uniform. The active ingredients in the extract were attached to the surface of the AgNPs to prevent the aggregation of particles, and the synthesized AgNP was spherical.

3.2.5 DLS and stability analysis

Dynamic light scattering (Figure 6A) shows that the optimized average particle size of CM-AgNPs was 56.31 nm, PDI was 0.2375, and zeta potential was −44.95 mV (mean value of three measurements). DLS (Figure 6B) shows that the average particle size of chemically synthesized bare AgNPs was 91.57 nm, PDI was 0.4340, and zeta potential was −50.55 mV (mean value of three measurements). AgNPs were negatively charged on the surface and dispersed in the medium. Electrostatic repulsion between negatively charged nanoparticles may prevent AgNPs from aggregating, which may be responsible for AgNPs stability. This property involved the surface interaction of AgNPs and their effect on cells. DLS used fluid mechanics to detect particle size, so there are some differences between the particle size results and TEM particle size observation results.

After four weeks of synthesis of optimized CM-AgNPs, the detected average particle size was 51.00 nm and PDI was 0.2634. Compared to four weeks ago, the changes were relatively small, indicating good stability of CM-AgNPs.

3.3 Analysis of antifungal activity

After culturing the fungi for 7 days or 24 h, the 96-well plates were removed from the constant temperature incubator and photographed (Figure 7). After the lyophilized powder of *C. monnieri* fruit extract and bare AgNPs were added to the 96-well plate, the dark color affected the detection results of the microplate reader, and the calculated percentage inhibition was not accurate, so two people were used to visually observe the results (Table 2). The minimum inhibitory concentration of CM-AgNPs, terbinafine, and fluconazole with the percentage inhibition greater than 90% calculated by scanning the OD value at 630 nm using microplate reader was MIC_{90} (Table 2). Based on all the results, it can be concluded that the order of efficacy for *T. rubrum* and *T. mentagrophytes* was as follows: terbinafine > CM-AgNPs > fluconazole > bare AgNPs > lyophilized powder of *C. monnieri* fruit extract. Terbinafine has good efficacy against *T. rubrum* and *T. mentagrophytes*, but there are patients with dermatophyte infection who have no clinical response to terbinafine treatment (Bortoluzzi et al., 2023). Therefore, the research and development of alternative therapeutic drugs is significant. For *C. albicans*, the order of efficacy was fluconazole > CM-AgNPs > bare AgNPs > lyophilized powder of *C. monnieri* fruit extract. CM-AgNPs

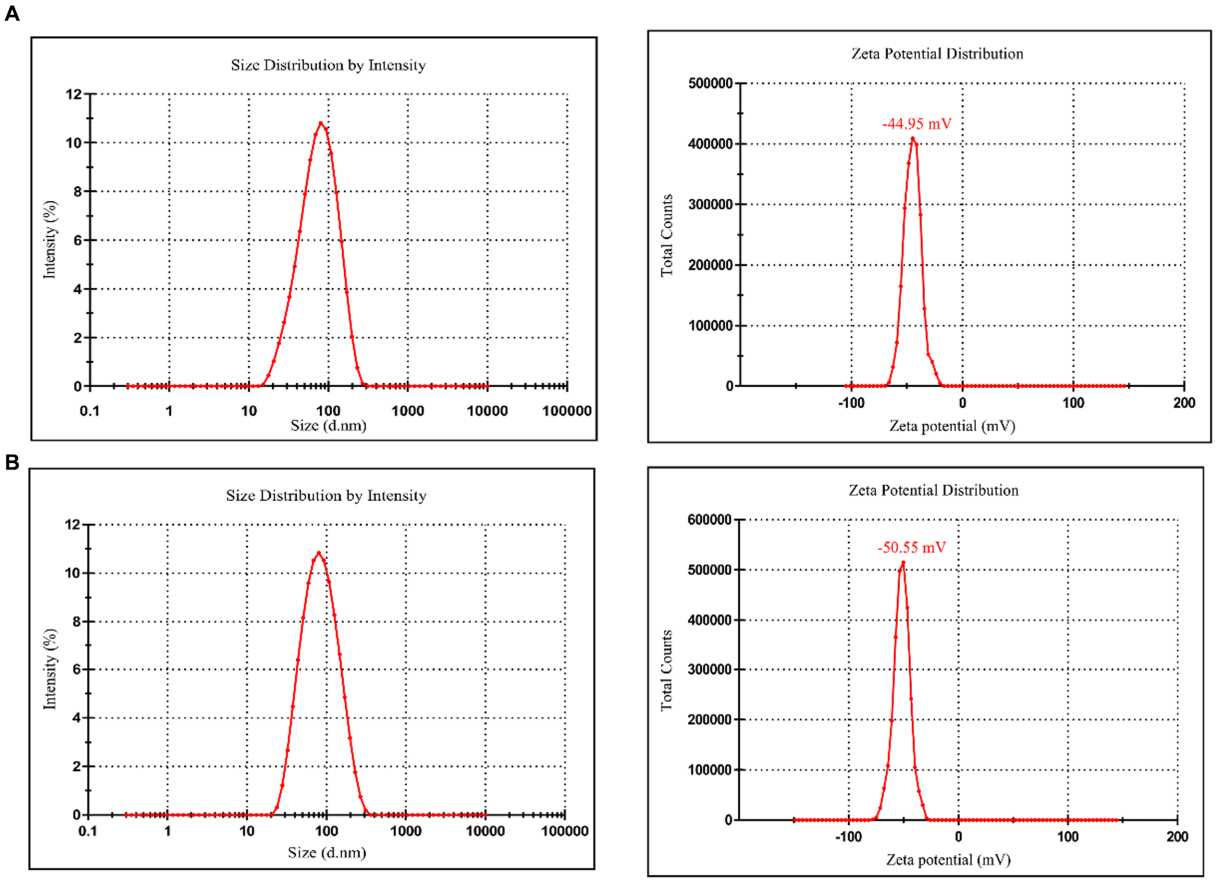

FIGURE 6
(A) Particle size and zeta potential distribution of CM-AgNPs; **(B)** Particle size and zeta potential distribution of bare AgNPs.

TABLE 2 MIC_{90} results of various drugs against *Trichophyton rubrum* (7 d), *Trichophyton Mentagrophytes* (7 d), and *Candida albicans* (24 h).

Medicaments	MIC_{90} (μg/mL)		
	Trichophyton rubrum	*Trichophyton Mentagrophytes*	*Candida albicans*
Bare AgNPs	125	125	31.25
C. monnieri fruit extract	1875	7,500	12,500
CM-AgNPs	3.125	3.125	0.78125
Terbinafine	0.0156	0.0625	–
Fluconazole	8	64	0.5

has similar efficacy to fluconazole and is expected to be a potential treatment for *C. albicans*. The MIC of AgNPs synthesized by *Scabiosa atropurpurea* fruit extract against *T. rubrum* and *C. albicans* were 7.81 and 3.9 μg/mL, respectively (Essghaier et al., 2022). Compared with them, the MIC of CM-AgNPs were smaller, which may be due to the better inhibitory effect of *C. monnieri* fruit on ringworm fungi, enhancing the antifungal activity of CM-AgNPs. Studies have shown that AgNPs inhibit fungal growth by affecting fungal morphology, causing membrane infiltration, and producing reactive oxygen species (ROS) to disturb osmotic balance, making cells unstable (Elbahnasawy et al., 2021). AgNPs can also release high affinity silver ions (Ag^+), inactivating the thiol groups in fungal cell wall, forming insoluble compounds,and then damaging enzymes and lipids bound to the membrane, eventually leading to cell lysis (Astuti et al., 2019).

4 Conclusion

In this paper, AgNPs were synthesized from *C. monnieri* fruit, a common Chinese medicine for the treatment of tinea disease. The synthesis method is simple, with small particle size, good stability and low MIC, demonstrating strong medicinal potential for anti dermatophytes. XRD results indicated that CM-AgNPs were face centered cubic (FCC) crystals. TEM showed that the

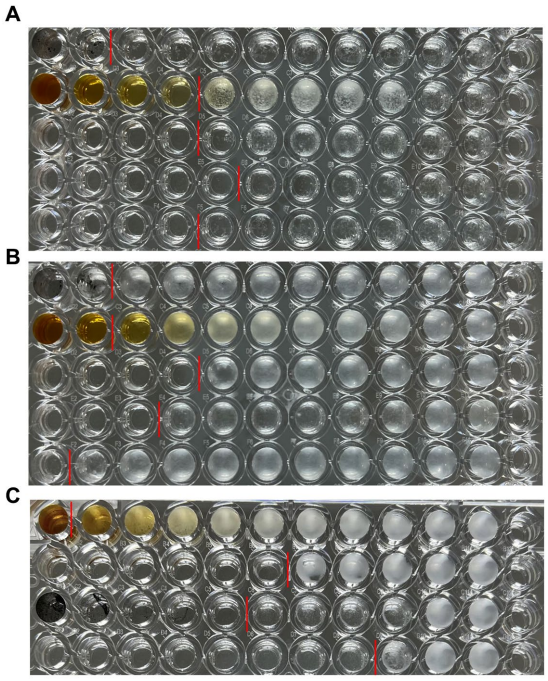

FIGURE 7
Results of antifungal 96-well plates, **(A)** *T. rubrum*, **(B)** *T. mentagrophytes*, **(C)** *C. albicans*; **(A)** and **(B)** from top to bottom are bare AgNPs freeze-dried powder, *C. monnieri* fruit extract freeze-dried powder, CM-AgNPs freeze-dried powder, terbinafine, and fluconazole; **(C)** From top to bottom, there are *C. monnieri* fruit extract freeze-dried powder, CM-AgNPs freeze-dried powder, bare AgNPs freeze-dried powder, and fluconazole.

generated nanoparticles were spherical, and the extract of *C. monnieri* fruit was coated on AgNPs, stabilizing the AgNPs, and reducing their aggregation. It was known through FTIR and EDX detection that chemical components such as flavonoids and coumarins in the extract of *C. monnieri* fruit may be involved in the synthesis of CM-AgNPs. For the tested fungi, the anti fungal efficacy of AgNPs synthesized through green synthesis of *C. monnieri* fruit extract was superior to that of chemically synthesized AgNPs, indicating that the extract of *C. monnieri* fruit actually enhanced the antifungal effect of AgNPs. For *C. albicans*, the MIC_{90} of CM-AgNPs was similar to fluconazole. For *T. rubrum* and *T. mentagrophytes*, the antifungal activity of CM-AgNPs was better than that of fluconazole, although weaker than terbinafine. In view of the increased resistance to antifungal agents in clinical candida and dermatophyte infections and the emergence of multiple drug-resistant strains with difficult treatment, the results are of great significance for the development of new topical antifungal drugs, and can be applied in the biomedical field. Cm-AgNPs can be further developed into various topical formulations for the treatment of patients with superficial fungal infections. As a potential alternative treatment strategy, it may help patients cure fungal infections.

Data availability statement

The original contributions presented in the study are included in the article/supplementary material, further inquiries can be directed to the corresponding authors.

Author contributions

M-QY: Investigation, Methodology, Writing – original draft. W-WY: Software, Writing – original draft. M-XZ: Formal analysis, Writing – review & editing. H-LH: Resources, Writing – review & editing. A-WH: Conceptualization, Investigation, Validation, Writing – review & editing. BQ: Conceptualization, Writing – review & editing.

Funding

The author(s) declare financial support was received for the research, authorship, and/or publication of this article. Natural Science Foundation of Fujian Province (2021 J011274).

Conflict of interest

The authors declare that the research was conducted in the absence of any commercial or financial relationships that could be construed as a potential conflict of interest.

Publisher's note

References

Abdallah, B. M., Rajendran, P., and Ali, E. M. (2023). Potential treatment of dermatophyte trichophyton rubrum in rat model using topical green biosynthesized silver nanoparticles with achillea santolina extract. *Molecules* 28:1536. doi: 10.3390/molecules28041536

Abdel-Aty, A. M., Barakat, A. Z., Bassuiny, R. I., and Mohamed, S. A. (2023). Statistical optimization, characterization, antioxidant and antibacterial properties of silver nanoparticle biosynthesized by saw palmetto seed phenolic extract. *Sci. Rep.* 13:15605. doi: 10.1038/s41598-023-42675-0

Abd-Elsalam, W. H., and Abouelatta, S. M. (2023). Contemporary techniques and potential transungual drug delivery nanosystems for the treatment of onychomycosis. *AAPS PharmSciTech* 24:150. doi: 10.1208/s12249-023-02603-x

Alexander, B. D., Procop, G. W., Dufresne, P., Espinel-Ingroff, A., Fuller, J., Ghannoum, M. A., et al. (2017a). *Reference method for broth dilution antifungal susceptibility testing of filamentous fungi; approved standard, Clsi document m38.* Clinical and Laboratory Standards Institute.

Alexander, B. D., Procop, G. W., Dufresne, P., Fuller, J., Ghannoum, M. A., Hanson, K. E., et al. (2017b). *Reference method for broth dilution antifungal susceptibility testing of yeasts; approved standard, Clsi document m27.*

Astuti, S. D., Puspita, P. S., Putra, A. P., Zaidan, A. H., Fahmi, M. Z., Syahrom, A., et al. (2019). The antifungal agent of silver nanoparticles activated by diode laser as light source to reduce c. Albicans biofilms: an in vitro study. *Lasers Med. Sci.* 34, 929–937. doi: 10.1007/s10103-018-2677-4

Bharti, S., Mukherji, S., and Mukherji, S. (2021). Antiviral application of colloidal and immobilized silver nanoparticles. *Nanotechnology* 32:205102. doi: 10.1088/1361-6528/abe489

Bortoluzzi, P., Prigitano, A., Sechi, A., Boneschi, V., Germiniasi, F., Esposto, M. C., et al. (2023). Report of terbinafine resistant trichophyton spp. in Italy: clinical presentations, molecular identification, antifungal susceptibility testing and mutations in the squalene epoxidase gene. *Mycoses* 66, 680–687. doi: 10.1111/myc.13597

Chinnasamy, G., Chandrasekharan, S., and Bhatnagar, S. (2019). Biosynthesis of silver nanoparticles from *melia azedarach*: enhancement of antibacterial, wound healing, antidiabetic and antioxidant activities. *Int. J. Nanomedicine* 14, 9823–9836. doi: 10.2147/IJN.S231340

Elbahnasawy, M. A., Shehabeldine, A. M., Khattab, A. M., Amin, B. H., and Hashem, A. H. (2021). Green biosynthesis of silver nanoparticles using novel endophytic rothia endophytica: characterization and anticandidal activity. *J. Drug Deliv. Sci. Technol.* 62:102401. doi: 10.1016/j.jddst.2021.102401

Essghaier, B., Toukabri, N., Dridi, R., Hannachi, H., Limam, I., Mottola, F., et al. (2022). First report of the biosynthesis and characterization of silver nanoparticles using *scabiosa atropurpurea* subsp. Maritima fruit extracts and their antioxidant, antimicrobial and cytotoxic properties. *Nanomaterials (Basel, Switzerland)* 12:1585. doi: 10.3390/nano12091585

Fu, L., Hsu, J., Shih, M., Hsieh, C., Ju, W., Chen, Y., et al. (2021). Process optimization of silver nanoparticle synthesis and its application in mercury detection. *Micromachines.* 12:1123. doi: 10.3390/mi12091123

Glazier, V. E. (2022). Efg1, everyone's favorite gene in *candida albicans*: a comprehensive literature review. *Front. Cell. Infect. Microbiol.* 12, 1–12. doi: 10.3389/fcimb.2022.855229

Jang, Y., Zhang, X., Zhu, R., Li, S., Sun, S., Li, W., et al. (2022). Viola betonicifolia-mediated biosynthesis of silver nanoparticles for improved biomedical applications. *Front. Microbiol.* 13:891144. doi: 10.3389/fmicb.2022.891144

Jassim, A. Y., Wang, J., Chung, K. W., Loosli, F., Chanda, A., Scott, G. I., et al. (2022). Comparative assessment of the fate and toxicity of chemically and biologically synthesized silver nanoparticles to juvenile clams. *Colloids Surf. B: Biointerfaces* 209:112173. doi: 10.1016/j.colsurfb.2021.112173

Jin Nam, H., Sun Kim, Y., Jin Kim, Y., Nam, S., and Choa, S. (2021). Enhanced conductivity in highly stretchable silver and polymer nanocomposite conductors. *J. Nanosci. Nanotechnol.* 21, 3218–3226. doi: 10.1166/jnn.2021.19309

Luo, Q., Su, W., Li, H., Xiong, J., Wang, W., Yang, W., et al. (2018). Antibacterial activity and catalytic activity of biosynthesised silver nanoparticles by flavonoids from petals of lilium casa blanca. *Micro Nano Lett.* 13, 824–828. doi: 10.1049/mnl.2018.0055

Ma, D., Kanisha Chelliah, C., Alharbi, N. S., Kadaikunna, S., Khaled, J. M., Alanzi, K. F., et al. (2021). *Chrysanthemum morifolium* extract mediated ag nps improved the cytotoxicity effect in a549 lung cancer cells. *Journal of King Saud University-Science.* 33:101269. doi: 10.1016/j.jksus.2020.101269

Mehmood, Y., Farooq, U., Yousaf, H., Riaz, H., Mahmood, R. K., Nawaz, A., et al. (2020). Antiviral activity of green silver nanoparticles produced using aqueous buds extract of *syzygium aromaticum*. *Pak. J. Pharm. Sci.* 33, 839–845. doi: 10.36721/PJPS.2020.33.2.SUP.839-845.1

Mirzaie, A., Badmasti, F., Dibah, H., Hajrasouliha, S., Yousefi, F., Andalibi, R., et al. (2022). Phyto-fabrication of silver nanoparticles using typha azerbaijanensis aerial part and root extracts. *Iran. J. Public Health* 51, 1097–1106. doi: 10.18502/ijph.v51i5.9425

Mobini, S., Rezaei, M., and Meshkani, F. (2021). One-pot hard template synthesis of mesoporous spinel nanoparticles as efficient catalysts for low temperature co oxidation. *Environ. Sci. Pollut. Res.* 28, 547–563. doi: 10.1007/s11356-020-10398-8

Moorthy, K., Chang, K., Wu, W., Hsu, J., Yu, P., and Chiang, C. (2021). Systematic evaluation of antioxidant efficiency and antibacterial mechanism of bitter gourd extract stabilized silver nanoparticles. *Nano* 11:2278. doi: 10.3390/nano11092278

Munir, N., Mehmood, Z., Shahid, M., Aslam, S., Abbas, M., Mehboob, H., et al. (2022). Phytochemical constituents and in vitro pharmacological response of *cnidium monnieri*. *A natural ancient medicinal herb. Dose-Response.* 20:500437421. doi: 10.1177/15593258221115543

Nenoff, P., Krüger, C., Ginter-Hanselmayer, G., and Tietz, H. (2014). Mycology – an update. Part 1: dermatomycoses: causative agents, epidemiology and pathogenesis. *Jddg: Journal Der Deutschen Dermatologischen Gesellschaft.* 12, 188–210. doi: 10.1111/ddg.12245

Ni, J., Ren, Q., Luo, J., Chen, Z., Xu, X., Guo, J., et al. (2020). Ultrasound-assisted extraction extracts from stemona japonica (blume) miq. And *cnidium monnieri* (l.) cuss. Could be used as potential *rhipicephalus sanguineus* control agents. *Exp. Parasitol.* 217:107955. doi: 10.1016/j.exppara.2020.107955

Noites, A., Borges, I., Araújo, B., Da Silva, J. C. G. E., de Oliveira, N. M., Machado, J., et al. (2023). Antimicrobial activity of some medicinal herbs to the treatment of cutaneous and mucocutaneous infections: preliminary research. *Microorganisms.* 11:272. doi: 10.3390/microorganisms11020272

Rajivgandhi, G. N., Maruthupandy, M., Li, J., Dong, L., Alharbi, N. S., Kadaikunnan, S., et al. (2020a). Photocatalytic reduction and anti-bacterial activity of biosynthesized silver nanoparticles against multi drug resistant *staphylococcus saprophyticus* bdums 5 (mn310601). *Mater. Sci. Eng. C* 114:111024. doi: 10.1016/j.msec.2020.111024

Rajivgandhi, G., Maruthupandy, M., Muneeswaran, T., Anand, M., Quero, F., Manoharan, N., et al. (2019). Biosynthesized silver nanoparticles for inhibition of antibacterial resistance and biofilm formation of methicillin-resistant coagulase negative staphylococci. *Bioorg. Chem.* 89:103008. doi: 10.1016/j.bioorg.2019.103008

Rajivgandhi, G. N., Ramachandran, G., Maruthupandy, M., Manoharan, N., Alharbi, N. S., Kadaikunnan, S., et al. (2020b). Anti-oxidant, anti-bacterial and anti-biofilm activity of biosynthesized silver nanoparticles using gracilaria corticata against biofilm producing k. *Pneumoniae. Colloids and Surfaces a: Physicochemical and Engineering Aspects.* 600:124830. doi: 10.1016/j.colsurfa.2020.124830

Robles-Martinez, M., Gonzalez, J., Perez-Vazquez, F. J., Montejano-Carrizales, J. M., Perez, E., and Patino-Herrera, R. (2019). Antimycotic activity potentiation of *allium sativum* extract and silver nanoparticles against trichophyton rubrum. *Chem. Biodivers.* 16:e1800525. doi: 10.1002/cbdv.201800525

Sardana, K., Sharath, S., Khurana, A., and Ghosh, S. (2023). An update on the myriad antifungal resistance mechanisms in dermatophytes and the place of experimental and existential therapeutic agents for trichophyton complex implicated in tinea corporis and cruris. *Expert Rev. Anti-Infect. Ther.* 21, 977–991. doi: 10.1080/14787210.2023.2250555

Srećković, N. Z., Nedić, Z. P., Monti, D. M., and Elia, D, L., Dimitrijević, S. B., and Mihailović, N. R., et al. (2023). Biosynthesis of silver nanoparticles using *salvia pratensis* l. aerial part and root extracts: bioactivity, biocompatibility, and catalytic potential. *Molecules* 28,:1387. doi:10.3390/molecules28031387

Targhi, A. A., Moammeri, A., Jamshidifar, E., Abbaspour, K., Sadeghi, S., Lamakani, L., et al. (2021). Synergistic effect of curcumin-cu and curcumin-ag nanoparticle loaded niosome: enhanced antibacterial and anti-biofilm activities. *Bioorg. Chem.* 115:105116. doi: 10.1016/j.bioorg.2021.105116

Tian, S., Saravanan, K., Mothana, R. A., Ramachandran, G., Rajivgandhi, G., and Manoharan, N. (2020). Anti-cancer activity of biosynthesized silver nanoparticles using *avicennia marina* against a549 lung cancer cells through ros/mitochondrial damages. *Saudi J. Biol. Sci.* 27, 3018–3024. doi: 10.1016/j.sjbs.2020.08.029

Velgosova, O., Macák, L., Cižmárová, E., and Mára, V. (2022). Influence of reagents on the synthesis process and shape of silver nanoparticles. *Materials.* 15:6829. doi: 10.3390/ma15196829

Wei, Z., Xu, S., Jia, H., and Zhang, H. (2022). Green synthesis of silver nanoparticles from mahonia fortunei extracts and characterization of its inhibitory effect on chinese cabbage soft rot pathogen. *Front. Microbiol.* 13:1030261. doi: 10.3389/fmicb.2022.1030261

Wu, X., Gao, X., Zhu, X., Zhang, S., Liu, X., Yang, H., et al. (2019). Fingerprint analysis of *cnidium monnieri* (l.) Cusson by high-speed counter-current chromatography. *Molecules* 24:4496. doi: 10.3390/molecules24244496

Yanyun, C., Ying, T., Wei, K., Hua, F., Haijun, Z., Ping, Z., et al. (2021). Preliminary study on antifungal mechanism of aqueous extract of *cnidium monnieri* against trichophyton rubrum. *Front. Microbiol.* 12:707174. doi: 10.3389/fmicb.2021.707174

Yoon, J., Shin, M., Lim, J., Kim, D. Y., Lee, T., and Choi, J. W. (2020). Nanobiohybrid material-based bioelectronic devices. *Biotechnol. J.* 15:e1900347. doi: 10.1002/biot.201900347

Zhang, D., Ramachandran, G., Mothana, R. A., Siddiqui, N. A., Ullah, R., Almarfadi, O. M., et al. (2020). Biosynthesized silver nanoparticles using *caulerpa taxifolia* against a549 lung cancer cell line through cytotoxicity effect/morphological damage. *Saudi J. Biol. Sci.* 27, 3421–3427. doi: 10.1016/j.sjbs.2020.09.017

Zhao, X., Li, C., Wang, Y., Han, W., and Yang, Y. (2021). Hybridized nanogenerators for effectively scavenging mechanical and solar energies. *Iscience.* 24:102415. doi: 10.1016/j.isci.2021.102415

frontiers | Frontiers in Microbiology

TYPE Correction
PUBLISHED 19 January 2024
DOI 10.3389/fmicb.2024.1351990

OPEN ACCESS

APPROVED BY
Frontiers Editorial Office,
Frontiers Media SA, Switzerland

*CORRESPONDENCE
Aiwen Huang
✉ hawen83@sina.com
Bin Qiu
✉ summer328cn@163.com

RECEIVED 10 January 2024
ACCEPTED 10 January 2024
PUBLISHED 19 January 2024

CITATION
Ye M, Yang W, Zhang M, Huang H, Huang A and Qiu B (2024) Corrigendum: Biosynthesis, characterization, and antifungal activity of plant-mediated silver nanoparticles using *Cnidium monnieri* fruit extract. *Front. Microbiol.* 15:1351990. doi: 10.3389/fmicb.2024.1351990

Corrigendum: Biosynthesis, characterization, and antifungal activity of plant-mediated silver nanoparticles using *Cnidium monnieri* fruit extract

Mingqi Ye[1], Wenwen Yang[1], Minxin Zhang[2], Huili Huang[2], Aiwen Huang[1,2]* and Bin Qiu[3]*

[1]Fujian University of Traditional Chinese Medicine Fuzong Teaching Hospital (900TH Hospital), Fuzhou, China, [2]Department of Clinical Pharmacy, 900TH Hospital of Joint Logistics Support Force of PLA, Fuzhou, China, [3]College of Chemistry, Fuzhou University, Fuzhou, China

KEYWORDS

AgNPs, *Cnidium monnieri*, green synthesis, characterization, antifungal

A corrigendum on
Biosynthesis, characterization, and antifungal activity of plant-mediated silver nanoparticles using *Cnidium monnieri* fruit extract

by Ye, M., Yang, W., Zhang, M., Huang, H., Huang, A., and Qiu, B. (2023). *Front. Microbiol.* 14:1291030. doi: 10.3389/fmicb.2023.1291030

In the published article, there was an error in affiliation 1. Instead of "College of Pharmacy, Fujian University of Traditional Chinese Medicine, Fuzhou, China," it should be "Fujian University of Traditional Chinese Medicine Fuzong Teaching Hospital (900TH Hospital), Fuzhou, China."

The authors apologize for this error and state that this does not change the scientific conclusions of the article in any way. The original article has been updated.

Publisher's note

All claims expressed in this article are solely those of the authors and do not necessarily represent those of their affiliated organizations, or those of the publisher, the editors and the reviewers. Any product that may be evaluated in this article, or claim that may be made by its manufacturer, is not guaranteed or endorsed by the publisher.

frontiers | Frontiers in Microbiology

TYPE Original Research
PUBLISHED 13 December 2023
DOI 10.3389/fmicb.2023.1296522

OPEN ACCESS

EDITED BY
Krassimira Radoykova Hristova,
Marquette University, United States

REVIEWED BY
Justice Opare Odoi,
Council for Scientific and Industrial Research (CSIR), Ghana
Stefan Magez,
Vrije University Brussels, Belgium

*CORRESPONDENCE
Keneth Iceland Kasozi
✉ keneth.kasozi@ed.ac.uk
Susan Christina Welburn
✉ sue.welburn@ed.ac.uk

RECEIVED 18 September 2023
ACCEPTED 16 November 2023
PUBLISHED 13 December 2023

CITATION
Kasozi KI, MacLeod ET, Sones KR and Welburn SC (2023) Trypanocide usage in the cattle belt of southwestern Uganda. *Front. Microbiol.* 14:1296522. doi: 10.3389/fmicb.2023.1296522

Trypanocide usage in the cattle belt of southwestern Uganda

Keneth Iceland Kasozi[1,2]*, Ewan Thomas MacLeod[1], Keith Robert Sones[1,3] and Susan Christina Welburn[1,4]*

[1]Infection Medicine, College of Medicine and Veterinary Medicine, Biomedical Sciences: Edinburgh Medical School, College of Medicine and Veterinary Medicine, The University of Edinburgh, Edinburgh, Scotland, United Kingdom, [2]School of Medicine, Kabale University, Kabale, Uganda, [3]Keith Sones Associates, Warkworth House, Warkworth, Banbury, United Kingdom, [4]Zhejiang University - University of Edinburgh Institute, Zhejiang University School of Medicine, Haining, China

Background: Systematic infrastructure and regulatory weaknesses over many decades, in communities struggling with animal African trypanosomiasis (AAT) would be expected to create an environment that would promote drug misuse and risk development of drug resistance. Here, we explore rural community practices of livestock keepers, livestock extension officers and drug shop attendants to determine whether appropriate practice was being followed in administration of trypanocides and other drugs.

Methods: A questionnaire-based survey was undertaken in southwestern Uganda in 2022 involving 451 farmers who kept cattle, sheep or goats and 79 "professionals" who were either livestock extension officers or drug shop attendants.

Results: Respondents reported using one or more type of trypanocidal drug on 80.1% of the 451 farms in the last 30 days. Diminazene aceturate was used on around three-quarters of farms, while isometamidium chloride was used on around one-fifth. Homidium bromide was used on less than 1% of farms. Cattle were significantly more likely to be treated with trypanocides than sheep or goats. On around two-thirds of farms, trypanocides were prepared and injected by farmers, with extension officers administering these drugs on most of the other third, especially on cattle farms. Almost all drugs were obtained from privately-owned drug shops. For treatment of AAT with trypanocides, prescription-only medicines were routinely used by farmers without professional supervision and in the absence of a definitive diagnosis. While a far greater proportion of professionals had a better education and had received training on the use of trypanocides than farmers, there was relatively little difference in their ability to use these drugs correctly. Farmers were more likely than professionals to use only DA to treat trypanosomiasis and were more likely to use antibiotics as well as trypanocidal drugs to treat the animal. Furthermore, they estimated, on average, that twice the recommended dose of either diminazene aceturate or isometamidium chloride was needed to treat a hypothetical 400 kg bovine. A minority of both farmers and professionals reported that they observed the recommended withdrawal times following injection of trypanocidal drugs and very few of either group knew the recommended withdrawal times for milk or meat. Only one in six farmers reported using the sanative pair (alternating use of diminazene aceturate and isometamidium chloride), to reduce the risk of drug resistant trypanosome strains emerging, while this approach was more widely used by professionals. Farmers reported using antibiotics more commonly than the professionals, especially in sheep and goats, raising concerns as to overuse and misuse of this critical class of drugs. In addition to using trypanocides, most farmers also reported using a topical veterinary pesticide for the control of ticks and tsetse. On average, farmers spent 12.2% of their income from livestock sales on trypanocides.

Conclusion: This study highlights the complexity of issues involved in the fight against AAT using drug treatment. A multistakeholder campaign to increase awareness among farmers, drug shop attendants, and extension workers of the importance of adherence to recommended drug dosing, using the sanative pair and following recommended drug withdrawal guidance would promote best practice, reduce the risk of emergence of resistant strains of trypanosomes, and support enhanced food safety.

KEYWORDS

neglected tropical diseases, zoonoses, trypanocides, animal African trypanosomiasis, antimicrobial resistance (AMR), veterinary drug shops, pharmacovigilance, Stamp Out Sleeping Sickness

1 Introduction

Antimicrobial resistance (AMR) is considered by the World Health Organization (WHO) to be one of the top 10 global public health threats facing humanity (WHO, 2015, 2021). Best practice to minimize the risk of AMR is generally considered to include only using antimicrobials under the supervision of a fully qualified health professional on an individual patient or animal basis after a definitive diagnosis. Other features of best practice include using the right active ingredient at the right dose, administered in the correct way, respecting recommended withdrawal times, and not relying solely on a single active ingredient for prolonged periods of time. For vector-borne diseases, such as trypanosomiasis, integrated control which combines actions against the vector (tsetse) and pathogen (trypanosomes) is also recommended (FAO, 1998).

In the context of animal health on remote farms in low- and middle-income countries (LMICs), such as the cattle belt of southwestern Uganda where the current study was conducted, these ideals are especially hard to attain. Fully trained private veterinary professionals are often not present and even if they are, their services are not affordable for most livestock keepers. While government-employed district veterinary officers and livestock extension officers are usually present in these areas, they tend to be limited in their reach due to shortage of resources, especially inadequate transport, and are too few to reach all who could benefit from their services (Perry et al., 2005).

In such areas, alternative systems have emerged in which farmers have to be largely self-reliant and obtain their animal health products, advice and, in some cases, services almost entirely from privately-owned drug shops where they encounter staff ranging from untrained, through certificate and diploma holders to degree-educated professionals. Drug shop staff often have local knowledge, are community members (easy to access), cost effective and can balance their lack of technical training with understanding of cultural and traditional practices (Caudell et al., 2020).

While liberalization of animal health services has some associated benefits, such as increased access to medicines and potential economic growth, it has also generated enormous challenges including unregulated markets, misuse and overuse of veterinary products, regulatory weakness, and AMR, especially in countries where drug regulatory and distribution systems are weak (Jaime et al., 2022).

Trypanocide resistance in both humans (Kasozi et al., 2022) and animals (Wangwe et al., 2019; Kasozi et al., 2023) raises major public health risks following expression of cross-species resistance genes (Kasozi et al., 2022; Okello et al., 2022). Animal African trypanocide resistance has previously been associated with poor farming practices, farmer treatments, underdosing and untrained personnel (Ngumbi and Silayo, 2017; Kasozi et al., 2022).

In this study, we assessed farmer trypanocide (and other drug) usage practices in southwestern Uganda where antimicrobial drugs are heavily used.

2 Methods

This study comprised of a questionnaire-based survey (Supplementary File 1) conducted in the cattle belt of southwestern Uganda between July and October 2022. The objective was to determine how trypanocidal drugs were being used in this area to control animal African trypanosomiasis in cattle, sheep, and goats. Focused on the districts of Ibanda, Isingiro, Kazo, Kiruura, Mbarara, Rwampara, and Sheema (Figure 1), the study team worked with district veterinary officers to identify livestock keeping communities in areas where trypanocide resistance was suspected. The study was approved by the Edinburgh Medical School Research Ethics Committee (22-EMREC-022) and in Uganda, it was approved by the Ethics Committee at the College of Veterinary Medicine of Makerere University (SVAR-IACUC/114/2022). After acquiring local consent from the respective chief administrative officers, 557 participants were purposefully recruited: 478 from farms and 79 who were district extension officers or drug shop attendants. Extension officers were persons working for the local government legally employed by the government, while drug shop attendants included assistants and technicians. Assistants are often relatives including wives, partners, and husbands of the owner of the drug shop by the National Drug Authority (NDA) standards. Technicians were individuals who held a veterinary certificate or diploma from one of the vocational institutions in Uganda and licensed to operate veterinary drug shops. The study protocol was registered with BMC ISRCTN (Supplementary File 2). The pre-tested questionnaire was written in English but administered in the appropriate local language by trained enumerators. Each questionnaire took around 30–45 min to complete. Responses to the questions in the questionnaire were

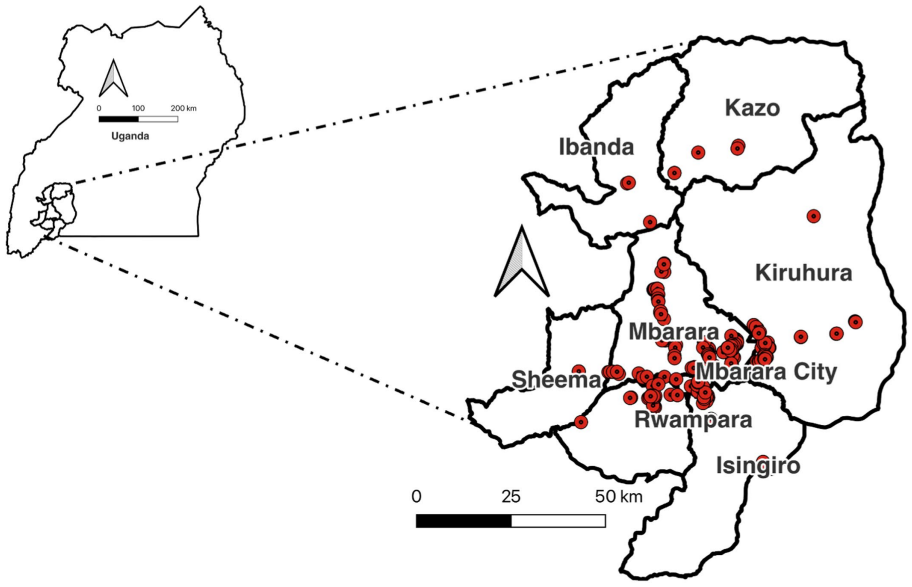

FIGURE 1
Survey villages in the seven districts and one city of southwestern Uganda along the cattle belt.

recorded in English and entered directly into a tablet connected to the internet where possible; in areas without stable internet connection, responses were captured as hard copy and entered on a tablet as soon as possible. Respondents' locations were recorded using a Global Positioning System (GPS), but these locations were anonymized and used only to illustrate their geographical distribution within the study site.

On farms, the respondents were whoever was available at the time of the visit and included members of the farming family as well as paid employees. District extension officers with responsibility for livestock who were included in the study were interviewed either at their official government offices or their private drug shops. In drug shops, respondents included both unqualified assistants and diploma-level technicians, who could be employees or owners (these two groups are referred to as "drug shop attendants" throughout this paper) as well as extension officers.

2.1 Statistical analysis

Survey responses were entered into Microsoft Office Forms which presented the data in MS Excel spreadsheets. This was exported into the open-source software R version 4.3.1 using the pacman, party, rio, and tidyverse packages which, in addition to MS Excel, were used to generate descriptive statistics. Odds ratios were calculated using the epiR package version 2.0.63; for observations with zero fields the odd ratios were generated using MedCalc® at 95% confidence interval. One sample tests were computed using the rstatix package and significance reported when $p < 0.05$. Since the focus of the study was use of trypanocidal drugs, which are primarily used in cattle, sheep, and goats, only farms that kept ruminants were included in the analyses (Supplementary File 3).

3 Results

3.1 Demographic information

The survey was administered to 478 farmers and 79 additional respondents who were drug shop attendants or extension officers (hereafter referred to as professionals). Twenty-seven farm respondents who reported that they did not keep ruminants were not included in the analyses making the farm sample size 451 (Table 1). These farmers were listed on a livestock keeping registry but did not hold any ruminant stock when they were visited.

The category "farmer" included farming heads of households, their spouses and other family members. The category "farm employee" were paid workers. On each farm only one person was interviewed so the 451 farmers represented 451 different farms. Around three-quarters (77.4%) of the farm respondents were farming family members and a little under a quarter (22.6%) were employees. Close to three-quarters (75.4%) of the farm respondents were male. Drug shop attendants and extension workers were more evenly split between men (54.4%) and women (45.6%). The age of farmers ranged from 14 to 82 years; just under 90% were in the range 18–61 years and the mean age was 38.8 (median = 37.0) years. Drug shop attendants and extension officers were all in the age range 18–61 years and their mean age was 35.2 (median = 35.0) years. A little over half of all respondents were the head or second-in-command of the farm or drug shop/extension office. Among farmers, most (94.0%) had received either no formal education or only basic education while among drug shop attendants and extension officers three-quarters (74.7%) had received tertiary education (Table 1).

Cattle were kept on 307 of the 451 farms (68.1%), with or without small ruminants. Both cattle and sheep/goats were kept on 191 farms (42.3%), cattle only on 110 (24.4%) and sheep/goats only on 150 (33.3%). More than half of respondents who kept cattle (51.0%)

TABLE 1 Number and percentages on demographic information for respondents.

Parameter	Variables	Farmers ($n = 451$)	Professionals ($n = 79$)
Sex	Female	111 (24.6)	36 (45.6)
	Male	340 (75.4)	43 (54.4)
Primary role	Farmer	306 (67.8)	
	Farm employee	145 (32.2)	
	Drug shop assistant		35 (44.3)
	Drug shop technician		28 (35.4)
	Extension worker		16 (20.3)
Education	No formal	200 (44.3)	2 (2.5)
	Basic	224 (49.7)	18 (22.8)
	Tertiary	27 (6.0)	59 (74.7)
Authority	Head	208 (46.1)	35 (44.3)
	Second-in-command	45 (10.0)	8 (10.1)
	Other family member	96 (21.3)	2 (2.5)
	Employee	102 (22.6)	34 (43.0)
Age (years)*	Children (14–17)	12 (2.7)	
	Young adults (18–25)	101 (22.5)	11 (13.9)
	Adults (26–35)	94 (20.9)	35 (44.3)
	Mature (36–45)	102 (22.7)	27 (34.2)
	Elderly (46–61)	105 (23.4)	6 (7.6)
	Most elderly (62–82)	35 (7.8)	
	Median (IQR)	37.0 (22.0)	35.0 (12.0)

*$n = 449$ for farmers as two participants withdrew consent.

reported keeping crossbreeds, with the remainder relatively evenly split between exotic breeds (26.8%) and local breeds, most likely Ankole (22.1%). More than three-quarters of respondents (75.7%) who reported keeping small ruminants kept local breeds. Mean reported herd size for cattle was 104, although this covered a wide range from 1 to 20,000, with a median cattle herd size of 24. The mean flock size for small ruminants was 34, again with a wide range from 1 to 1,000 with a corresponding median flock size of 16. Respondents were often reluctant to report the exact number of animals they kept so these values should be treated with caution. On a little over half of farms (52.6%), other livestock species and/or domestic animals (dogs, cats, pigs, and chickens) were kept in addition to ruminants. Around two-thirds of respondents considered their farms to be semi-commercial with the remaining third classifying them as subsistence (Table 2).

3.2 Knowledge on trypanosomiasis

Among farmers, around a fifth (22.0%) knew that tsetse were involved in trypanosome transmission compared to more than half (53.2%) among professionals (Table 3). There was no statistically significant difference ($p < 0.05$) between the proportions of the two groups who were able to correctly identify either the best approach (i.e., trypanocide use against antibiotics, bush burning, ethnomedicine, and acaricide mono options) for the control of trypanosomiasis (64.3% of farmers compared to 68.3% of professionals selected "use of trypanocides" from a list of alternative but ineffective methods) or the season when the burden of the disease is highest (78.9% of farmers vs. 87.3% of professionals correctly selected "wet season"). While less than a quarter (23.9%) of farmers reported that they had received training on the correct use of trypanocides, more than four-fifths (87.3%) of professionals reported receiving such training (Table 3).

3.3 Drug usage practices

Almost two-thirds (66.1%) of farmers reported that they prepared and injected trypanocidal drugs on their farms, with extension officers administering the drugs on 21.7% of farms and drug shop attendants administering trypanocides on 12.2% of farms. Drug shop attendants were significantly less likely to treat animals on farms that only kept cattle (7.3% of cattle only farms vs. 22.5% of sheep/goat only farms, $p < 0.05$). When asked about extension officers, 59.0% of farmers considered that they were accessible in their communities and 42.6% considered they were reliable with treatments (Table 4). Most respondents considered that private

10.3389/fmicb.2023.1296522

outlets were the cheapest source of trypanocidal drugs and nearly all drugs (97.3% of farm respondents) were reported to have been purchased from private drug shops.

Most of the farmers (96.9%) and professionals (98.7%) injected trypanocides using the recommended intramuscular route. Irrespective of who administered the trypanocidal drug, in all cases the water used to prepare the solution for injection came from a tap, bore hole, stream, or other non-sterile source; no respondents reported using commercially prepared water for injection (Table 4). Farmers on cattle only farms were almost three-times more likely to use bottled drinking water as farmers on sheep/goat only farms (19.1 vs. 6.7%, $p < 0.05$).

TABLE 2 Livestock kept on respondents' farms.

Types of livestock		Number (%) farms (n = 451)
Ruminant groups	Cattle only farms	110 (24.4)
	Sheep/goats only farms	150 (33.3)
	Both (ruminants)	191 (42.3)
	Cattle with/without sheep/goats	307 (68.1)
	Sheep/goats with/without cattle	348 (77.2)
Farm species	Ruminants only	214 (47.4)
	Ruminants + dogs/cats	92 (20.4)
	Ruminants + dogs/ cats + pigs + chickens	82 (18.2)
	Ruminants + pigs + chickens	63 (14.0)
Ruminant breeds	Cattle crosses	152 (50.0)
	Exotic cattle	80 (26.1)
	Local (Ankole)	66 (21.0)
	Do not know (cattle)	9 (2.9)
	Median cattle herd size (IQR)	24 (39)
	Mean cattle herd size (range)	104 (1–20,000)
	Sheep/goat crosses	60 (17.2)
	Exotic sheep/goats	23 (6.7)
	Local sheep/goats	259 (75.4)
	Do not know (sheep/goats)	6 (1.7)
	Median sheep/goat herd size (IQR)	16 (26)
	Mean sheep/goat herd size (range)	34 (1–1,000)
Nature of farming	Semi-commercial	297 (65.9)
	Subsistence	154 (34.1)

3.4 Trypanocide combination patterns used on farms

Drugs reported to have been used during the past 30 days on farms or, for professionals, that they had administered during the past 30 days are shown in Table 5. In Table 6, these results were used to calculate the number and proportion of farms on which the different drugs were used, or the number and proportion of professionals who reported using these drugs during the past 30 days.

More than four-fifths of farmers (81.8%) reported that one or more type of trypanocidal drug had been used on their farm during the past 30 days (Table 6). All but two (97.5%) professionals reported that they had administered one or more type of trypanocidal drug during the same period; this could have been either to their own livestock (all professionals reported that they also kept ruminant livestock) or as a fee-paying service to animals owned by others. In comparison, around one-third of farmers (35.0%) reported that antibiotics had been used on their farms during this period but just one drug shop attendant or extension officers (1.3%) reported having used an antibiotic during the past 30 days (Table 6).

Diminazene aceturate (DA) was by far the most used trypanocide: 77.2% of farmers reported that DA had been used on their farms in the last 30 days while 21.7% reported the use of isometamidium chloride (ISM), just three (0.7%) reported that homidium bromide (HB) had been used and 5.1% reported no drugs had been used. Among professionals, 96.2% reported that they had used DA, 45.6% reported using ISM and just one reported using HB during the past 30 days (Table 6).

Seventeen percent of farmers and 44.3% of professionals reported that they had used both DA and ISM in the past 30 days. Twenty-two percent of farmers but just one professional reported that they had used both a trypanocide and an antibiotic during the past 30 days (Table 6).

Drug usage varied markedly between farms where cattle were kept and farms where just sheep and goats were kept: 92.8% of farms where cattle were kept reported that a trypanocide had been administered during the past 30 days compared to 62.0% of farms that just kept sheep and goats (Table 6). Diminazene aceturate was the most used drug on both types of farms; 84.7% of farms with cattle reporting using this drug compared to 61.3% of farms with just sheep and goats. Isometamidium chloride usage was much less common on farms with just sheep and goats: 30.3% of farms with cattle used ISM compared to just 4.7% of farms with just sheep and goats. Similarly, far more farms with cattle used both DA and ISM: 23.5% of farms with cattle reported doing so compared to 4.0% of farms with just sheep and goats. All these differences in proportions between farms with/without cattle are statistically significant at $p < 0.05$. Antibiotic usage was slightly higher on farms with just sheep and goats: 36.4% of farms with

TABLE 3 Determinants of knowledge on trypanosomiasis based on extension meeting trainings, disease epidemiology and control in the study population.

Topic	Number (%) of correct farmer responses (N = 451)	Number (%) of correct professional responses (N = 79)	Odds ratio (95% CI)	Chi-square p values
Extension meetings trainings	217 (46.1)	66 (83.5)	5.5 (2.9–10.2)	<0.001
Trypanocides for disease control	290 (64.3)	54 (68.3)	1.2 (0.7–2.0)	0.57
Tsetse major vector	99 (22.0)	42 (53.2)	4.0 (2.4–6.6)	<0.0001
Disease in rainy season	356 (78.9)	69 (87.3)	1.8 (0.9–3.9)	0.08

TABLE 4 Major practice patterns in the study population.

Trypanocide practices		Farms with both cattle and sheep/goats (*N* = 191)	Sheep/goats only on farms (*N* = 150)	Farms with cattle but no sheep/goats (*N* = 110)	Farmers (*N* = 451)	Professionals (*N* = 79)	Farmers for sheep/goats vs. cattle		Farmers vs. Professionals	
							OR (95% CI)	X^2-*p* value	OR (95% CI)	X^2-*p* value
Administer treatments	Drug shop attendants	13 (6.8)	34 (22.7)	8 (7.3)	55 (12.2)	11 (13.9)	0.3 (0.1–0.6)	0.001	1.2 (0.6–2.3)	0.67
	Extension officer	44 (23.0)	25 (16.7)	29 (26.4)	98 (21.7)	16 (20.3)	1.8 (1.0–3.3)	0.06	0.9 (0.5–1.6)	0.77
	Farmers	134 (70.2)	91 (60.7)	73 (66.4)	298 (66.1)	52 (65.8)	1.3 (0.8–2.1)	0.35	1.0 (0.6–1.6)	0.96
Correct route	Avoid Intravenous	188 (98.4)	149 (99.3)	106 (96.4)	443 (98.2)	78 (98.7)	0.2 (0.0–1.4)	0.17*	1.4 (0.2–11.4)	1.00*
	Intramuscular	188 (98.4)	143 (95.3)	106 (96.4)	437 (96.9)	78 (98.7)	0.2 (0.0–1.5)	0.17*	2.5 (0.3–19.3)	0.71*
Lowest priced trypanocides	Private outlets	141 (73.8)	103 (68.7)	85 (77.3)	329 (72.9)	61 (77.2)	1.5 (0.8–2.7)	0.13	1.2 (0.7–2.2)	0.43
	Informal market	2 (1.0)	0 (0)	0 (0)	2 (0.4)	0 (0)	1.4 (0.0–69.2)	0.00*	1.1 (0.1–23.8)	1.00*
	Government	1 (0.5)	1 (0.7)	2 (1.8)	4 (0.9)	3 (3.8)	2.6 (0.2–81.9)	0.57	4.4 (0.8–21.7)	0.07*
	Uniform price	37 (19.4)	13 (8.7)	12 (10.9)	62 (13.7)	14 (17.7)	1.3 (0.6–3.0)	0.55	1.4 (0.7–2.6)	0.29
	Do not know	10 (5.2)	33 (22.0)	11 (10.0)	54 (12.0)	1 (1.3)	0.4 (0.2–0.8)	0.01	0.1 (0.0–0.5)	0.002*
Source of trypanocides	Private outlet	187 (97.9)	145 (96.7)	107 (97.3)	439 (97.3)	79 (100)	1.2 (0.3–6.4)	1.00*	4.5 (0.3–77.2)	0.23*
	Government	1 (0.5)	1 (0.7)	3 (2.7)	5 (1.1)	0 (0)	2.7 (0.3–80.6)	0.62*	0.5 (0.0–9.3)	1.00*
	Do not know	3 (1.6)	4 (2.7)	0 (0)	7 (1.6)	0 (0)	0.15 (0.0–2.8)	0.14*	0.4 (0.0–6.6)	0.60*
Water source	Borehole	15 (7.9)	5 (3.3)	8 (7.3)	28 (6.2)	4 (5.1)	2.2 (0.7–7.8)	0.17	0.8 (0.2–2.2)	1.00*
	Bottled	36 (18.8)	10 (6.7)	21 (19.1)	67 (14.9)	10 (12.7)	3.3 (1.5–7.6)	0.003	0.8 (0.4–1.6)	0.63
	Tap	53 (27.7)	61 (40.7)	45 (40.9)	159 (35.3)	34 (43.0)	1.0 (0.6–1.7)	0.97	1.4 (0.8–2.3)	0.19
	Stream	2 (1.0)	0 (0)	1 (0.9)	3 (0.7)	0 (0)	4.1 (0.2–102.1)	0.42*	0.8 (0.0–15.7)	1.00*
	Well	85 (44.5)	70 (46.7)	35 (31.8)	190 (42.1)	9 (11.4)	0.6 (0.3–0.9)	0.02	0.2 (0.1–0.4)	<0.0001
	Do not know	0 (0)	4 (2.7)	0 (0)	4 (0.9)	22 (27.8)	0.15 (0.0–2.8)	0.14*	41.3 (15.0–149.5)	<0.0001
Extension officer	Accessibility	116 (60.7)	78 (52.0)	72 (65.4)	266 (59.0)	71 (89.9)	0.6 (0.3–0.9)	0.03	6.2 (2.9–13.1)	<0.001
	Reliability	77 (40.3)	68 (45.3)	47 (42.7)	192 (42.6)	70 (88.6)	1.1 (0.7–1.8)	0.68	10.3 (5.3–22.7)	<0.0001

OR, Odds ratio. 95% CI, 95% confidence intervals with lower and upper limits reported. Superscript (*) indicates Fisher's exact *p* value being reported.

10.3389/fmicb.2023.1296522

10.3389/fmicb.2023.1296522

TABLE 5 Drugs administered during the past 30 days (number of cases).

Drugs administered in past 30 days	All farms with ruminants	Farms with both cattle and sheep/goats	Farms with cattle with/without sheep/goats	Farms with sheep/goats but no cattle	Farms with cattle but no sheep/goats	Drug shop attendants and extension officers
DA only	204 (45.2)	90 (47.1)	136 (44.3)	71 (47.3)	43 (39.1)	41 (51.9)
DA + Ab	67 (14.9)	25 (13.1)	52 (16.9)	15 (10.0)	27 (24.5)	0 (0.0)
DA + ISM	46 (10.2)	31 (16.2)	44 (14.3)	2 (1.3)	13 (11.8)	33 (41.8)
DA + ISM + Ab	28 (6.2)	19 (9.9)	27 (8.8)	2 (1.3)	7 (6.4)	1 (1.3)
DA + ISM + HB	0 (0.0)	0 (0.0)	0 (0.0)	0 (0.0)	0 (0.0)	1 (1.3)
DA + ISM + HB + Ab	3 (0.7)	1 (0.5)	1 (0.3)	2 (1.3)	0 (0.0)	0 (0.0)
ISM only	20 (4.4)	8 (4.2)	20 (6.5)	1 (0.7)	11 (10.0)	1 (1.3)
ISM + Ab	1 (0.2)	1 (0.5)	1 (0.3)	0 (0.0)	0 (0.0)	0 (0.0)
Ab only	59 (13.1)	12 (6.3)	19 (6.2)	41 (27.3)	6 (5.5)	0 (0.0)
None	23 (5.1)	4 (2.1)	7 (2.3)	16 (10.7)	3 (2.7)	2 (2.5)
Totals	451 (100)	191 (100)	307 (100)	150 (100)	110 (100)	79 (100)

DA, Diminazene aceturate; ISM, Isometamidium chloride; HB, Homidium bromide; Ab, Antibiotic. Percentages in brackets.

TABLE 6 Total number of cases administering the different types of drug.

Drugs administered in past 30 days	All farms with ruminants	Farms with both cattle and sheep/goats	Farms with cattle with/without sheep/goats	Farms with sheep/goats but no cattle	Farms with cattle but no sheep/goats	Drug shop attendants and extension officers
DA or ISM or HB	369 (81.8)	175 (91.6)	281 (91.5)	93 (62.0)	101 (92.8)	77 (97.5)
DA	348 (77.2)	166 (86.9)	260 (84.7)	92 (61.3)	90 (81.8)	76 (96.2)
ISM	98 (21.7)	60 (31.4)	93 (30.3)	7 (4.7)	31 (28.2)	36 (45.6)
HB	3 (0.7)	1 (0.5)	1 (0.3)	2 (1.3)	0 (0.0)	1 (1.3)
DA + ISM	77 (17.0)	51 (26.7)	72 (23.5)	6 (4.0)	20 (18.2)	35 (44.3)
DA or ISM or HB + Ab	99 (22.0)	46 (24.1)	81 (26.4)	19 (12.7)	34 (30.9)	1 (1.3)
Ab	158 (35.0)	58 (30.4)	100 (32.6)	60 (40.0)	40 (36.4)	1 (1.3)
None	23 (5.1)	4 (2.1)	7 (2.3)	16 (10.7)	3 (2.7)	2 (2.5)
Total cases	451 (100)	191 (100)	307 (100)	150 (100)	110 (100)	79 (100)

Percentages in brackets.

cattle reported using antibiotics compared to 40.0% of farms with just sheep and goats.

Farmers reported that trypanocidal drugs were administered to animals in their herds or flocks between one and five times a month; on three-quarters of farms this was done once a month. Since the most used trypanocide is DA, which has curative but not prophylactic activity, it is assumed this means on an individual animal basis based on perceived need.

3.5 Observance of drug withdrawal periods following treatment

Only 35.9% of farmers and even fewer, 13.8%, of professionals, reported that they observed the recommended withdrawal times following administration of trypanocidal drugs (Table 7). Farmers who kept just cattle were more likely to observe withdrawal times than farmers who just kept sheep/goats (38.2 vs. 24.0%; $p < 0.05$). For professionals, this likely means that they did not personally follow up on the animals once they had been treated. However, less than 5% of all respondents, whether farmers or professionals, knew the recommended withdrawal times for either meat or milk for the most commonly used trypanocide, DA. Drug shop attendants and extension officers demonstrated better theoretical knowledge than farmers on the correct dosage of trypanocidal drug: overall around twice as many of the former knew the correct dose (for DA, 62.0% of professionals compared to 31.0% of farmers; for ISM, 60.8% compared to 33.5%).

3.6 Trypanocide dosage and prophylactic practices

On average, the professionals identified close to the correct number of sachets or tablets of DA, ISM or HB needed to treat a hypothetical 400 kg bovine at the recommended dose while farmers suggested around double the recommended dose of DA or ISM was needed (Table 8). The choice of hypothetical 400 kg was based on information on cattle live weights in the study area provided by professional

TABLE 7 Trypanocide withdrawal practices and dosing.

Trypanocide practices	Farms with both cattle and sheep/goats (*N* = 191)	Farms with sheep/goats but no cattle (*N* = 150)	Farms with cattle but no sheep/goats (*N* = 110)	Farmers (*N* = 451)	Professionals (*N* = 79)	Farms with sheep/goats and cattle only		Farmers vs. Professionals	
						OR (95% CI)	*p* values	OR (95% CI)	*p* values
Trypanocide withdrawals done	84 (44.0)	36 (24.0)	42 (38.2)	162 (35.9)	11 (13.9)	1.9 (1.1–3.3)	0.01	0.3 (0.2–0.6)	<0.001
Correct milk withdrawal period on DA[a]	7 (3.7)	3 (2.0)	4 (3.6)	14 (3.1)	2 (2.5)	1.8 (0.4–10.1)	0.45	0.8 (0.2–3.6)	1.00
Correct meat withdrawal period on DA[b]	13 (6.8)	3 (2.0)	4 (3.6)	20 (4.4)	1 (1.3)	1.8 (0.4–10.1)	0.45	0.3 (0.0–2.1)	0.34
Correct dose to treat an adult cow: DA	24 (12.6)	102 (68.0)	14 (12.7)	140 (31.0)	49 (62.0)	0.1 (0.0–0.1)	<0.0001	3.6 (2.2–6.0)	<0.001
Correct dose to treat an adult cow: ISM	31 (16.2)	101 (67.3)	19 (17.3)	151 (33.5)	48 (60.8)	0.1 (0.1–0.2)	<0.0001	3.1 (1.9–5.0)	<0.001
Correct dose to treat an adult cow: HB	92 (48.2)	114 (76.0)	73 (66.4)	279 (61.9)	56 (70.9)	0.6 (0.3–1.1)	0.09	1.5 (0.9–2.5)	0.13

DA, Diminazene aceturate; ISM, Isometamidium chloride; HB, Homidium bromide. DA withdrawal period for milk a = 3 days, b = 20 days for meat.

TABLE 8 Estimates of number of sachets/tablets of trypanocides needed to treat a 400 kg bovine.

Trypanocide	Recommended dose rate (mg/kg/bodyweight)	Number of sachets/tablets per 400 kg bovine for recommended dose	Farms with both cattle and sheep/goats	Farms with sheep/goats but no cattle	Farms with cattle but no sheep/goats	Farmers	Professionals
			Mean (Median, IQR)				
Diminazene aceturate	3.5 mg/kg	1.3 sachets[1]	3.6 (4.0, 3)[c]	1.8 (1.0, 1)[b]	3.9 (5.0, 2)[c]	3.1 (3.0, 4)[c]	1.6 (1.0, 1)[a]
Isometamidium chloride	0.5 mg/kg	1.6 sachets[2]	3.7 (4.0, 3)[c]	1.9 (1.0,2)[a]	3.8 (4.0, 2)[c]	3.1 (4.0, 4)[c]	1.6 (1.0, 1)[#]
Homidium bromide	1 mg/kg	1.6 tablets[3]	2.0 (2.0, 2)[b]	1.5 (1.0, 0)[#]	1.7 (1.0, 1)[#]	1.8 (1.0, 1)[a]	1.5 (1.0, 1)[#]

One sample *t*-test statistic. [a]*p* value < 0.05, [b]*p* < 0.001, and [c]*p* < 0.0001. [#]*p* > 0.05. [1]Standard sachet contain 1.05 g active ingredient. [2]Standard sachet contains 125 mg active ingredient. [3]Tablet contains 250 mg active ingredient.

10.3389/fmicb.2023.1296522

informants during the prequestionnaire trial. When farmers who kept only cattle were compared with those who only kept sheep/goats, the former suggested on average three-times the recommended dose of DA and more than twice the recommended dose of ISM, while the latter suggested close to the recommended dose in each case.

In addition to using trypanocides, 69.8% (315/451) of farmers also reported using a topical veterinary pesticide for the control of ticks and tsetse, despite only one in five reporting that they were aware that tsetse flies were involved in the transmission of AAT.

Farmers reported spending a median expenditure of USD 103 (mean USD 213.6) each month on trypanocides (range USD 2.2–USD 6504) on their farms, although the range was very large, depending on the farm size (USD 2.2–USD 6504). As a proportion of the monthly income from livestock sales, farmers reported a median expenditure of 6.9% (mean = 12.2%) on trypanocidal drugs on their farms (range from 0 to close to 100%). Both the proportion of income and expenditure were higher on farms that kept cattle than those that did not.

4 Discussion

The current study found that on around two-thirds of farms, trypanocidal drugs were being administered by farmers and that almost all drugs were obtained from privately-owned drug shops. Best practice for controlling trypanosomiasis in cattle, sheep, and goats, was not being followed since prescription-only medicines were being routinely administered by farmers without professional supervision and in the absence of a definitive diagnosis.

The most used trypanocide in cattle, sheep, and goats was diminazene aceturate (DA). This drug is cheaper and more widely available than isometamidium chloride (ISM) in the study area (personal observation), and less likely to cause a local reaction at the site of injection (Giordani et al., 2016).

In this study, the way in which farmers administered trypanocidal drugs was compared to the way drug shop attendants (unqualified assistants and diploma-holding technicians) and extension officers administered these products. While most drug shop attendants and all extension officers were better educated than farmers, and a far greater proportion had received specific training on use of trypanocidal drugs, there was surprisingly, relatively little difference in their ability to use these drugs appropriately and according to the manufacturer's instructions.

There was no evidence that knowledge of trypanosomiasis epidemiology influenced the use of therapeutics since farmers lack access to routine laboratory analysis for pathogen speciation. Compared to drug shop attendants and extension workers, farmers were more likely to use only DA to treat trypanosomiasis; more likely to use antibiotics as well as trypanocides; and they estimated, on average, that twice the recommended dose of DA and ISM was needed to treat a hypothetical 400 kg bovine. There are several possible reasons for this. Firstly, cattle weights can be problematic to assess correctly (Machila et al., 2008), in this study we used a hypothetical weight of 400 kg bovine, Ankole crosses generally have a mean weight of 476 kg (Manzi et al., 2018) while Zebu cattle from central and western Uganda range from 150 to 340 kg (Kagoro-Rugunda et al., 2018) due to genetic, dietary, husbandry practices and geographical location differences. Cattle weight estimations have been found to be difficult not only for farmers but also for clinicians in Kenya demonstrating the need to interpret perceived animal weight estimates presented here with caution (Machila et al., 2008). The differences between dead weight (killing out and slaughterhouse deductions) and liveweight (purchase weight) and resulting price differentials at the market can also result in confusion.

Secondly, during the widely publicized, large-scale Stamp Out Sleeping Sickness Campaign (SOS), to eliminate zoonotic *Trypanosoma brucei rhodesiense,* the causative agent of Human African Trypanosomiasis (HAT) from the cattle zoonotic reservoir in Uganda, a dose of 7 mg of DA per kg bodyweight, was used (Roderick et al., 2000). This is double the dose recommended to treat the most pathogenic AAT species of trypanosome in cattle (*Trypanosoma congolense* and *Trypanosoma vivax*) as a higher dose is needed to eliminate *Trypanosoma brucei* s.l. as recommended by the manufacturer.[1] Although the current study area was not in the target area for SOS it appears that messages about the benefits of this approach may have spread beyond the SOS area (Welburn and Coleman, 2015; Hamill et al., 2017; Wangoola et al., 2019).

Finally, emergence of trypanocidal drug resistance is commonly ascribed to under-dosing and it is noteworthy that the current study suggests that farmers in this study tended to use more than the recommended dosages of DA and ISM, not less. A similar finding was reported by Roderick et al. (2000) (Wangoola et al., 2019), where Masai pastoralists administered DA and HB to their cattle and tended to give more than the recommended dose. Sub-standard trypanocides with less than the stated amount of active ingredient as well as counterfeit products with no active ingredient have been reported in many African countries (Perry et al., 2005; Bengaly et al., 2018; Tekle et al., 2018) and it is possible that increased dosing may be as a response to either perceived or actual poor quality drugs in the marketplace.

Traditionally, one of the main ways recommended to reduce the risk of trypanocide resistance emerging is the use of the "sanative pair" concept. Diminazene aceturate and ISM are chemically distinct and periodically switching between the two active ingredients is widely considered to be an effective way to prevent drug resistant strains of trypanosomes emerging (Watson, 2013). The current study indicates that only one in every six farmers were using the sanative pair approach (slightly more, around one in five, for those who were cattle keepers), although this practice appeared to be more widely used by drug shop attendants or extension officers. This may be an underestimate, as respondents were only asked about their trypanocide usage during the past 30 days, and it is possible that they switched drugs beyond this timeframe.

The finding that farmers reported using antibiotics much more commonly than drug shop attendants and extension officers does raise concerns about overuse and misuse of this critical class of drugs (Ndaki et al., 2021). From the farmers' perspective, however, use of both trypanocidal drugs and antibiotics is perhaps a rational response in an environment where tick-borne diseases (Kasozi et al., 2019), many of which can be treated with antibiotics, and trypanosomiasis are both prevalent and definitive diagnosis is not normally available. The very low usage of antibiotics reported by drug shop attendants and extension officers is a surprising finding that warrants further investigation.

1 https://www.ceva-africa.com/en/Products/Product-list/VERIBEN-Rrecommended

The observation that most respondent farmers reported that they used a topical veterinary pesticide to control ticks and tsetse on their animals is encouraging. This approach to controlling tsetse, as part of an integrated approach to controlling trypanosomiasis (Bardosh et al., 2013; Muhanguzi et al., 2014), that is cost effective (Okello et al., 2021) for farmers has been actively promoted in northern Uganda since 2006 by the Stamp-Out Sleeping Sickness (SOS) campaign began (Welburn and Coleman, 2015). That campaign, which also involved field training of veterinary undergraduate students from Makerere University, may have had longer lasting impacts when they took their learning into professional practice in Uganda.

5 Conclusion

It is likely that for the foreseeable future, livestock keepers in the cattle belt of southwestern Uganda will continue to treat their own animals using drugs obtained from private drug shops and without the benefit of expert supervision or definitive diagnosis. The reported overdosing with trypanocides and observation that farmers were using a topical veterinary pesticide to control ticks and tsetse on their animals was unexpected outside of the SOS districts. Although the current study area is not within the target area for SOS it appears that messages about the benefits of double dosing of trypanocides for *T. brucei* s.l., and application of topical veterinary pesticides for prevention of re-infection by trypanosomes and, treatment of tick-borne-diseases, may have spread beyond the SOS area (Waiswa et al., 2020) and warrants further investigation.

Some aspects of trypanocidal drug use by farmers would benefit from greater emphasis, support, and training, particularly as regard live weight estimations and drug dosing. A study exploring drug quality in the region would be helpful in gaining a deeper understanding how farmers and practitioners are making decisions on dosing. It is in the best interests of farmers, animal health professionals, drug shops owners, veterinary pharmaceutical companies, state extension services, and the wider local and global community to promote best practice for the use of antimicrobials, and a multi-stakeholder campaign to increase awareness of the sanative pair concept and the importance of following drug withdrawal periods could be a useful way forward. Such approaches could reduce the risk of drug resistant strains of trypanosomes emerging, enhance food safety and support safe use of antimicrobials.

Data availability statement

The raw data supporting the conclusions of this article will be made available by the authors, without undue reservation.

Ethics statement

The studies involving humans were approved by Edinburgh Medical School Research Ethics Committee (22-EMREC-022). The studies were conducted in accordance with the local legislation and institutional requirements. Written informed consent for participation in this study was provided by the participants' legal guardians/next of kin. The animal studies were approved by Ethics Committee at the College of Veterinary Medicine of Makerere University (SVAR-IACUC/114/2022). Written informed consent was obtained from the owners for the participation of their animals in this study.

Author contributions

KIK: Conceptualization, Data curation, Formal analysis, Investigation, Methodology, Validation, Writing – original draft, Writing – review & editing. ETM: Conceptualization, Data curation, Formal Analysis, Funding acquisition, Investigation, Methodology, Project administration, Resources, Software, Supervision, Validation, Writing – review & editing. KRS: Data curation, Formal Analysis, Methodology, Project administration, Resources, Supervision, Validation, Visualization, Writing – review & editing. SCW: Conceptualization, Data curation, Formal Analysis, Funding acquisition, Investigation, Methodology, Project administration, Resources, Software, Supervision, Validation, Visualization, Writing – review & editing.

Funding

The author(s) declare financial support was received for the research, authorship, and/or publication of this article. This research was supported by the National Institute for Health Research (16/136/33) using United Kingdom aid from the United Kingdom Government (SCW). This work was also supported by Zhejiang University Research Fund (SCW) and funded by the Commonwealth Scholarship Commission (UGSC–2021–447) in the United Kingdom and the Small Grants Programme of the Royal Society of Tropical Medicine and Hygiene (2021) in partnership with the National Institute for Health Research (NIHR) (KIK).

Conflict of interest

Author KRS is an honorary fellow in Biomedical Sciences: Edinburgh Medical School, College of Medicine and Veterinary Medicine, The University of Edinburgh, in which capacity this work was undertaken. KRS is also employed by and affiliated to Keith Sones Associates.

The remaining authors declare that the research was conducted in the absence of any commercial or financial relationships that could be construed as a potential conflict of interest.

Publisher's note

Author disclaimer

The views expressed in this publication are those of the author(s) and not necessarily those of the NIHR or the Department of Health and Social Care.

Supplementary material

The Supplementary material for this article can be found online at: https://www.frontiersin.org/articles/10.3389/fmicb.2023.1296522/full#supplementary-material

References

Bardosh, K., Waiswa, C., and Welburn, S. C. (2013). Conflict of interest: use of pyrethroids and amidines against tsetse and ticks in zoonotic sleeping sickness endemic areas of Uganda. *Parasit. Vectors* 6:204. doi: 10.1186/1756-3305-6-204

Bengaly, Z., Vitouley, S. H., Somda, M. B., Zongo, A., Têko-Agbo, A., Cecchi, G., et al. (2018). Drug quality analysis of isometamidium chloride hydrochloride and diminazene diaceturate used for the treatment of African animal trypanosomosis in West Africa. *BMC Vet. Res.* 14:361. doi: 10.1186/s12917-018-1633-7

Caudell, M. A., Dorado-Garcia, A., Eckford, S., Creese, C., Byarugaba, D. K., Afakye, K., et al. (2020). Towards a bottom-up understanding of antimicrobial use and resistance on the farm: a knowledge, attitudes, and practices survey across livestock systems in five African countries. *PLoS One* 15:e0220274. doi: 10.1371/journal.pone.0220274

FAO (1998). Drug management and parasite resistance in bovine trypanosomiasis in Africa. FAO. p. 38. Available at: https://www.fao.org/3/W9791E/w9791e01.htm#P0_0 (Accessed August 29, 2023).

Giordani, F, Morrison, LJ, and Rowan, TIMG (2016). The animal trypanosomiases and their chemotherapy: a review (October).

Hamill, L., Picozzi, K., Fyfe, J., von Wisseman, B., Wastling, S., Wardrop, N., et al. (2017). Evaluating the impact of targeting livestock for the prevention of human and animal trypanosomiasis, at village level, in districts newly affected with *T. b. Rhodesiense* in Uganda. *Infect. Dis. Poverty* 6:16. doi: 10.1186/s40249-016-0224-8

Jaime, G., Hobeika, A., and Figuié, M. (2022). Access to veterinary drugs in sub-Saharan Africa: roadblocks and current solutions. *Front. Vet. Sci.* 8:558973. doi: 10.3389/fvets.2021.558973

Kagoro-Rugunda, J., Lejju, G. B., Andama, J. B., Matofari, M. W., and Nalwanga, J. W. (2018). A pilot study on roles and operations of actors in the beef value chain in central and Western Uganda. *Int. J. Dev. Sustain.* 7, 2063–2079.

Kasozi, K. I., MacLeod, E. T., Ntulume, I., and Welburn, S. C. (2022). An update on African Trypanocide pharmaceutics and resistance. *Front. Vet. Sci.* 9:82811. doi: 10.3389/fvets.2022.828111

Kasozi, K. I., MacLeod, E. T., Waiswa, C., Mahero, M., Ntulume, I., and Welburn, S. C. (2022). Systematic review and meta-analysis on knowledge attitude and practices on African animal Trypanocide resistance. *Trop. Med. Infect. Dis.* 7:205. doi: 10.3390/tropicalmed7090205

Kasozi, K. I., MacLeod, E. T., and Welburn, S. C. (2022). Systematic review and meta-analysis on human African Trypanocide resistance. *Pathogens* 11:1100. doi: 10.3390/pathogens11101100

Kasozi, K. I., MacLeod, E. T., and Welburn, S. C. (2023). African animal trypanocide resistance: a systematic review and meta-analysis. *Front. Vet. Sci.* 9:950248. doi: 10.3389/fvets.2022.950248/full

Kasozi, K. I., Namayanja, M., Gaithuma, A. K., Mahero, M., Matovu, E., Yamagishi, J., et al. (2019). Prevalence of hemoprotozoan parasites in small ruminants along a human-livestock-wildlife interface in western Uganda. *Vet. Parasitol. Reg. Stud. Rep.* 17, 100309–100311. doi: 10.1016/j.vprsr.2019.100309

Machila, N., Fevre, E. M., Maudlin, I., and Eisler, M. C. (2008). Farmer estimation of live bodyweight of cattle: implications for veterinary drug dosing in East Africa. *Prev. Vet. Med.* 87, 394–403. doi: 10.1016/j.prevetmed.2008.06.001

Manzi, M., Rydhmer, L., Ntawubizi, M., Karege, C., and Strandberg, E. (2018). Growth traits of crossbreds of Ankole with Brown Swiss, Holstein Friesian, Jersey, and Sahiwal cattle in Rwanda. *Trop. Anim. Health Prod.* 50, 825–830. doi: 10.1007/s11250-017-1501-7

Muhanguzi, D., Picozzi, K., Hattendorf, J., Thrusfield, M., Welburn, S. C., Kabasa, J. D., et al. (2014). Improvements on restricted insecticide application protocol for control of human and animal African trypanosomiasis in eastern Uganda. *PLoS Negl. Trop. Dis.* 8:e3284. doi: 10.1371/journal.pntd.0003284

Ndaki, P. M., Mushi, M. F., Mwanga, J. R., Konje, E. T., Ntinginya, N. E., Mmbaga, B. T., et al. (2021). Dispensing antibiotics without prescription at community pharmacies and accredited drug dispensing outlets in Tanzania: a cross-sectional study. *Antibiotics* 10:1025. doi: 10.3390/antibiotics10081025

Ngumbi, A. F., and Silayo, R. S. (2017). A cross-sectional study on the use and misuse of trypanocides in selected pastoral and agropastoral areas of eastern and northeastern Tanzania. *Parasit. Vectors* 10:607. doi: 10.1186/s13071-017-2544-3

Okello, W. O., MacLeod, E. T., Muhanguz, D., Waiswa, C., and Welburn, S. C. (2021). Controlling tsetse flies and ticks using insecticide-treated cattle in Tororo district Uganda: cost benefit analysis. *Front. Vet. Sci. Vet. Epidemiol. Econom.* 8:616865. doi: 10.3389/fvets.2021.616865

Okello, I., Mafie, E., Eastwood, G., Nzalawahe, J., and Mboera, L. E. G. (2022). African animal trypanosomiasis: a systematic review on prevalence, risk factors and drug resistance in sub-Saharan Africa. *J. Med. Entomol.* 59, 1099–1143. doi: 10.1093/jme/tjac018

Perry, B., Pratt, A. N., Sones, K., and Stevens, C. (2005). An appropriate level of risk: balancing the need for safe livestock products with fair market access for the poor. *Int. Livest. Res. Inst.* 23:82.

Roderick, S., Stevenson, P., Mwendia, C., and Okech, G. (2000). The use of trypanocides and antibiotics by Maasai pastoralists. *Trop. Anim. Health Prod.* 32, 361–374. doi: 10.1023/A:1005277518352

Tekle, T., Terefe, G., Cherenet, T., Ashenafi, H., Akoda, K. G., Teko-Agbo, A., et al. (2018). Aberrant use and poor quality of trypanocides: a risk for drug resistance in south western Ethiopia. *BMC Vet. Res.* 14:4. doi: 10.1186/s12917-017-1327-6

Waiswa, C., Azuba, R., Makeba, J., Waiswa, I. C., and Wangoola, R. M. (2020). Experiences of the one-health approach by the Uganda trypanosomiasis control council and its secretariat in the control of zoonotic sleeping sickness in Uganda. *Parasit. Epidemiol. Control* 11:e00185. doi: 10.1016/j.parepi.2020.e00185

Wangoola, E. M., Bardosh, K., Among Acup, C., and Welburn, S. C. (2019). Waiswa C & Bugeza J factors associated with persistence of African animal trypanosomiasis in Lango subregion, northern Uganda. *Trop. Anim. Health Prod.* 51, 2011–2018. doi: 10.1007/s11250-019-01900-7

Wangwe, I. I., Wamwenje, S. A., Mirieri, C., Masila, N. M., Wambua, L., and Kulohoma, B. W. (2019). Modelling appropriate use of trypanocides to restrict wide-spread multi-drug resistance during chemotherapy of animal African trypanosomiasis. *Parasitol. Int.* 146, 774–780. doi: 10.1017/S0031182018002093

Watson, M. J. (2013). What drives population-level effects of parasites? Meta-analysis meets life-history. *Int. J. Parasitol. Parasit. Wildl.* 2, 190–196. doi: 10.1016/j.ijppaw.2013.05.001

Welburn, S. C., and Coleman, P. (2015). "Human and animal African trypanosomiasis" in *One Health: The Theory and Practice of Integrated Health Approaches*. eds. Z. Jakob, M. Tanner, E. Schelling and M. Whittaker.

WHO (2015). Global action plan on antimicrobial resistance. World Heal Organ. 1–28. Available at: https://www.who.int/publications/i/item/9789241509763

WHO (2021). Antimicrobial resistance. WHO News. Available at: https://www.who.int/news-room/fact-sheets/detail/antimicrobial-resistance (Accessed August 29, 2023).

frontiers | Frontiers in Microbiology

TYPE Review
PUBLISHED 21 December 2023
DOI 10.3389/fmicb.2023.1299321

OPEN ACCESS

EDITED BY
Cindy Shuan Ju Teh,
University of Malaya, Malaysia

REVIEWED BY
Gianmarco Mangiaterra,
University of Urbino, Italy
Fernando Baquero,
Ramón y Cajal Institute for Health Research, Spain

*CORRESPONDENCE
Fatima AlZahra'a Alatraktchi
✉ alzahraa@ruc.dk

RECEIVED 27 September 2023
ACCEPTED 27 November 2023
PUBLISHED 21 December 2023

CITATION
Thurner F and Alatraktchi FA (2023) Need for standardization in sub-lethal antibiotics research.
Front. Microbiol. 14:1299321.
doi: 10.3389/fmicb.2023.1299321

Need for standardization in sub-lethal antibiotics research

Fabian Thurner and Fatima AlZahra'a Alatraktchi*

Department of Science and Environment, Roskilde University, Roskilde, Denmark

While monitoring and managing resistant and persistent microbes is of utmost importance and should not be glossed over, one must also focus on mitigating the microbe's ability to cause harm. Exploring the concept of lowering or even suppressing the microbe's virulence with sub-Minimum Inhibitory Concentration (MIC) antibiotics holds promise and warrants further investigation. At present, such antibiotic concentrations have mostly been studied to cover the side-effects of gradient exposure, overlooking the possibility of utilizing them to influence not only bacterial virulence, but also colonization, fitness and collateral sensitivities. This review focuses on conflicting findings of studies demonstrating both increased and decreased virulence in microbes under sub-MIC antibiotic exposure. It identifies lack of standardization in this field of research as one of the main culprits for discordant results across numerous studies on virulence. It critically discusses important terminology related to bacterial traits and existing methods to determine MIC and sub-MIC ranges. Lastly, possible directions toward standardized sub-MIC profiling and thereby tailored treatment options in the future are explored.

KEYWORDS

sub-lethal antibiotics, MIC, sub-MIC, MSC, MIPC, virulence, standardization

1 Introduction

Antibiotics represent a curse and blessing at the same time. While their positive effects on global welfare are undeniable, the emergence of antimicrobial resistance (AMR) undoubtably poses severe challenges for the health care sector. Especially multidrug resistant (MDR) pathogens such as methicillin-resistant *Staphylococcus aureus* (MRSA) cause havoc in hospital environments around the globe (Turner et al., 2019). Moreover, persistent bacteria contribute to long term, recurrent infections that are tough to treat (Madhusoodanan, 2022). Combined efforts are being made to mitigate AMR and therefore lower the clinical burden on a global scale.

At present, to elucidate the dynamics of resistance evolution, sub-lethal antibiotic concentrations have largely been studied in the context of gradient exposure (Lagator et al., 2021). Thus, the possibility of harnessing sub-lethal doses of antibiotics to impact virulence, colonization, fitness and collateral sensitivities has not received sufficient attention. In particular the possibility to lower or even suppress bacterial virulence is not yet a well-recognized path, although ultimately, it is not the resistance but the virulence which causes disease (Laxminarayan et al., 2013). Evidence is increasing that pathogenic transcripts can be affected by low antibiotic concentrations below the Minimum Inhibitory Concentration (MIC) (Chen et al., 2021; Nolan and Behrends, 2021). Our own research demonstrated that toxin production in environmental *Pseudomonas aeruginosa* isolates changes when exposed to sub-inhibitory antibiotic concentrations (Mojsoska et al., 2021).

Current research on the effect of sub-MIC antibiotics on virulence points in many directions, making it tough to draw comparative and informed conclusions. In this review,

we propose the term Virulence Inhibiting Concentration (VIC) as the potential sub-MIC antibiotic concentration inhibiting virulence of a given pathogen. We believe that standardization of MIC and sub-MIC zone methodologies would contribute to the determination of the VIC of various pathogens (Figure 1). To prove this claim, this paper highlights how different methods for MIC profiling can lead to contradictory results across virulence studies using the same reference strains. However, we also acknowledge that other contributing factors such as strain-specific features like mutations in regulatory systems or specific environmental adaptation mechanisms that impact virulence regulation cannot be ruled out in other studies that use different strains. Thus, lack of standardization in MIC and sub-MIC determination is solely one piece of the puzzle and future efforts need to be directed toward fully understanding the impact of sub-lethal antibiotics on virulence. Lastly, we aim to give an overview of what needs to be taken into consideration when taking on the challenge to standardize sub-MIC research.

2 Characterizations of bacterial resistance, tolerance, and persistence

AMR is a global public health "ticking bomb." Predictions estimate that by 2050, the annual global gross domestic product (GDP) will see a decline of 1.1–3.8% relative to a base-case scenario assuming no AMR effects. This shortfall is projected to reach costs of USD 1 trillion to USD 3.8 trillion per year after 2030 (OECD, 2018). Among natural reasons such as genetic mutation and acquisition of resistance conferring genes via horizontal gene transfer (HGT), rise in AMR can primarily be attributed to the overuse of antibiotics in medicine and agriculture and the spread of resistant microorganisms in the environment, particularly in low-income countries with poor sanitation, allowing for food and drinking water contamination (Blair et al., 2015; Von Wintersdorff et al., 2016; Bastaraud et al., 2020; Uddin et al., 2021; Urban-Chmiel et al., 2022). Diseases caused by resistant pathogens are notoriously hard to treat and the amount of novel antibiotics able to eradicate them is near zero: The World Health Organization (WHO) reports that in the 2021 clinical pipeline of 45 novel antibiotics only two are active against at least one MDR bacterium from the "critical" category (World Health Organization, 2021). Next to AMR, the emergence of drug-tolerant subpopulations of microbes exacerbates the situation by causing recurrent infections in the host (Madhusoodanan, 2022).

It was as early as 2000 that the concept of a "selective window" at which selection of resistance conferring genes is strongest had been formally proposed (Negri et al., 2000). There, the first experimental evidence of selection of low-level antibiotic resistant genetic variants is presented. Later in 2011, pioneering studies introduced the terminology Minimal Selective Concentration (MSC) and specified a sub-MIC window where the fitness cost of the resistance is balanced by the antibiotic-conferred selection for the resistant mutant (Figure 2) (Gullberg et al., 2011; Liu et al., 2011). Subsequently, key-literature exploring selection dynamics at sub-MIC antibiotic levels has been published (Hughes and Andersson, 2012; Andersson and Hughes, 2014; Gullberg et al., 2014; Lundström et al., 2016; Khan et al., 2017; Kraupner et al., 2018; Wistrand-Yuen et al., 2018). It was not before 2020 that a sub-MSC window selective for persisters, termed the minimal increased persistence concentration has been proposed (MIPC, Figure 2) (Stanton et al., 2020). Since MSC and MIPC have been delineated based on microbial traits such as resistance and persistence, we believe it imperative to have a fundamental understanding of these terms in order to fully comprehend the sub-MIC zones.

MIC represents the lowest concentration of a given antibiotic that inhibits microbial growth. Since an increase in resistance is reflected in an increase in MIC, it can be used to give insight into a pathogen's resistance. MIC values are dependent on many factors such as microbial strain, type of antibiotic and method of MIC determination and are widely used in clinical settings to quickly assess resistance in bacterial isolates. Here, it is important to mention the concept of heteroresistance, a phenomenon describing a bacterial isolate that contains sub-populations of cells displaying a significantly higher MIC (Andersson et al., 2019; Balaban et al., 2019). An excellent paper by Andersson et al. further goes into detail and outlines the factors to consider when studying heteroresistance, while focusing on mechanistic details and clinical relevance of the transient phenomenon (Andersson et al., 2019).

Tolerant cells can survive but not grow under antibiotic exposure many times the MIC (Kester and Fortune, 2014). Notably, due to the inherent nature of bacteriostatic antibiotics to inhibit growth, the definition of tolerance can only be applied in the context of bactericidal antibiotics. The special phenomenon when subpopulations with different tolerance levels coexist within the same clonal population is

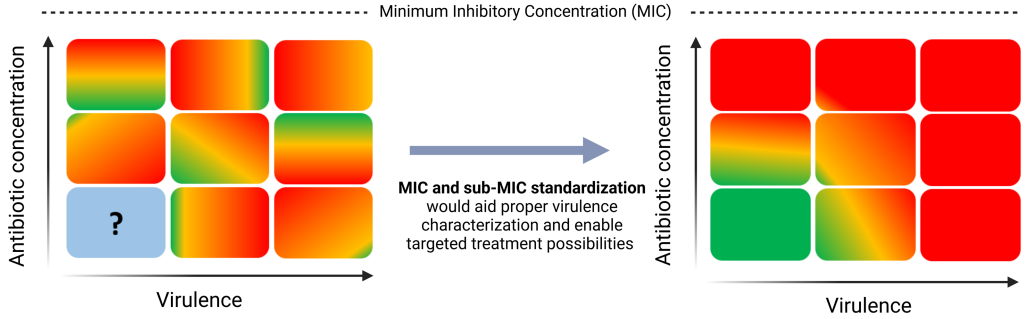

FIGURE 1
Need for standardization in sub-MIC research to aid virulence characterization in pathogenic bacteria.

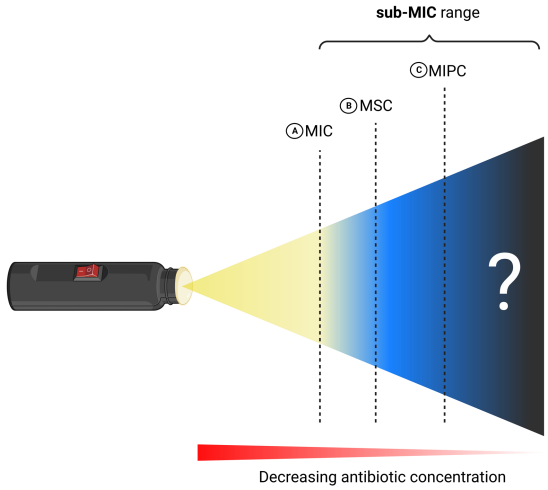

FIGURE 2
Schematic illustration of MIC and sub-MIC zones. **(A)** Minimum Inhibitory Concentration (MIC). **(B)** Minimum Selective Concentration (MSC) and **(C)** Minimum Increased Persistence Concentration (MIPC). Created with BioRender.com.

called persistence, a term coined by Joseph Bigger in 1944 (Bigger, 1944; Kester and Fortune, 2014; Brauner et al., 2017; Balaban et al., 2019). Mainly attributed to epigenetics, persistent pathogens manage to increase their survival in the presence of antibiotics without resistance-conferring genes (Riber and Hansen, 2021). This phenomenon arises from reprogramming the transcriptional landscape and allows for establishment of dormant cell states. When in dormancy, such cells downregulate their metabolism and do not divide and are therefore not vulnerable to antibiotics affecting cell division (Riber and Hansen, 2021).

The standard staring point to evaluate tolerance/persistence is through performance of time-kill assays and generation of characteristic biphasic killing curves. However, these do not always reflect persistence, since a similar curve can arise from resistant mutants in the sample population. To rule this out, the surviving bacteria should be regrown under the same antibiotic conditions. If resistance was the major driver of the biphasic curve observed, a much higher proportion of the population will show reduced killing in the second assay. If persistence caused the biphasic killing curve in the first place, no change in killing should be observed (Balaban et al., 2019). Moreover, since persistence can easily be mistaken for transient phenomena such as heteroresistance, it is advised to perform the assays at substantially high concentrations of antibiotics. In persisters, only a weak dependence of antibiotic concentration on killing is expected, whereas strong correlation hints at resistance mechanisms in play (Balaban et al., 2019). However, as time-kill curves rarely follow strict exponentiality it is impossible to quantify tolerance and persistence and the killing rate cannot be compared across different strains and growth conditions. Moreover, time-kill assays are labor intensive and thus rarely utilized in the health care sector (Brauner et al., 2017). Therefore, Brauner et al. developed a novel method to quantify tolerance without the need to perform time-kill assays. They propose clinical implementation of a simple timescale parameter: The "minimum duration for killing 99% of the population" (MDK_{99}) (Brauner et al., 2017). The MDK can be easily determined by exposing populations of bacteria to different antibiotic concentrations for varied time periods, subsequently evaluating the presence or lack of survivors (Brauner et al., 2017).

3 Impact of sub-lethal antibiotic concentrations on virulence are yet to be explored

Virulence represents the ability of a pathogen to cause harm in the infected host. Virulence factors can lead to improved adhesion, evasion of the hosts' immune system or production of toxins, all of which aid harmful microbes to colonize the host at a cellular level (Sharma et al., 2017). One notorious example of a pathogen that uses toxins as virulence factors is *Bacillus anthracis* which establishes systemic infection by using two lethal toxins termed "lethal factor" and "edema factor" (Sharma et al., 2017). Pyocyanin is another example of a toxin that has been proven to have great implications in the chronic nature of pseudomonal infections (Hall et al., 2016; Alatraktchi et al., 2020).

Another determinant of virulence is biofilm formation in pathogens such as *Staphylococcus aureus* and *Pseudomonas aeruginosa.* It acts as a physical barrier against the host defense systems (Sharma et al., 2023). Furthermore, the virulence factor alginate has been shown to play an essential role in thick biofilm formation as well as protection of the pathogen against the hosts by shielding against antibiotics, neutralizing reactive oxygen species and counteracting macrophagic uptake (Simpson et al., 1988; Yu et al., 1995; Skariyachan et al., 2018). Lastly, biofilm formation has major clinical implications in chronic infections and has been shown to be mechanically linked to emergence of persisters (Pan et al., 2023).

Sub-lethal antibiotic exposure evidently alters bacterial virulence and the underlying mechanisms by which the antibiotic concentrations modify various virulence traits are multifaceted and complex. In a paper from 2006, Linares et al. illuminates this area of research by pointing out that sub-MIC antibiotics can also act as signaling agents instead of weapons (Linares et al., 2006). By using a combination of genomic and functional assays they demonstrate that sub-lethal levels of Tobramycin, Tetracycline and Norfloxacin influences virulence in *Pseudomonas aeruginosa.* Low doses of these antibiotics increased the bacterium's ability to colonize potential hosts by enhancing biofilm formation and motility. Moreover, sub-MIC Tetracycline was shown to trigger the type III section system, leading to enhanced cytotoxicity of the bacterium (Linares et al., 2006). Another example of how sub-MIC antibiotics can act as signals can be found in a study by Shang et al., who revealed that some β-lactam antibiotics promote expression of a cluster of lipoprotein-like genes that consequently enhance virulence of MRSA (Shang et al., 2019; Chen et al., 2021). Lastly, the antibiotic Fosfomycin was shown to bind to Lys154 and Asp108 of the α-toxin of *Staphylococcus aureus,* thereby inhibiting its activity (An et al., 2019).

Researchers have investigated the effect of different sub-MIC concentrations of various antibiotics on selected virulence traits of a variety of bacterial species and associated strains. In an excellent review, the results of such studies focusing on virulence in *Pseudomonas aeruginosa* have been consolidated (Nolan and Behrends, 2021). They identified a common trend that most sub-MIC antibiotics reduce the *in vitro* virulence of *Pseudomonas aeruginosa*

(Nolan and Behrends, 2021). Furthermore, they conclude that that so far, the virulence of planktonic *Pseudomonas aeruginosa* has been assessed mostly over a short time (<24 h antibiotic exposure). They stress the point that results obtained in such regulated, short-term single strain assays are not necessarily translatable to the pathogens' *in vivo* virulence (Nolan and Behrends, 2021). Another exhaustive review summarizes the impact of sub-MIC antibiotic exposure on virulence in *Staphylococcus aureus* (Chen et al., 2021). They state that manifestations of effects on virulence of sub-MIC antibiotics points into different directions, dependent on the virulence profile, growth stage and culture conditions of *Staphylococcus aureus* at the time of antibiotic administration (Chen et al., 2021).

A study from 2021 by Davarzani et al. investigated the effect of sub-MIC concentrations of the antibiotic Gentamicin on alginate and biofilm production in *Pseudomonas aeruginosa*. They found that alginate and biofilm production under exposure of 1/2 MIC and 1/4 MIC was either significantly up- or downregulated to various degrees depending on the clinical isolate. The MIC values of Gentamicin for the clinical isolates P1, P2, P3 and for the two reference strains 8821 M and PAO1 have been calculated to be 0.25, 0.25, 1, 2 and 0.5 μg/mL, respectively (Davarzani et al., 2021).

An excellent study investigated the effects of sub-inhibitory concentrations of quinolones, aminoglycosides, β-lactams and macrolides on alginate production in *Pseudomonas aeruginosa* (Majtán and Hybenová, 1996). Some antibiotics such as Enoxacin or Nalidixic acid followed a discernible pattern of decreasing alginate production with increasing sub-MIC concentration. Others, such as Ciprofloxacin showed significant upregulation of alginate at low concentrations 1/16 MIC (50 μg/mL) but downregulation at 1/4 MIC (190 μg/mL) (Majtán and Hybenová, 1996).

A sub-MIC study from Molinari et al. concludes that production of pseudomonal virulence factors like pyocyanin, various exotoxins such as elastases and proteases and pathogenic behavior like motility is highly strain-, antibiotic- and concentration-dependent (Molinari et al., 1993). Notably, they were able to achieve unambiguous results for Azithromycin which inhibited pyocyanin production in all 10 strains tested.

Furthermore, Mojsoska et al. investigated the effect of sub-MIC concentrations of Ciprofloxacin, Tobramycin and Meropenem on pyocyanin production in environmental *Pseudomonas* strains (Mojsoska et al., 2021). Their results point out that virulence in *Pseudomonas* is both dependent on the strain and the antibiotic used: Tobramycin significantly downregulated levels of pyocyanin in the Pae112 strain whereas in PAO1 levels remained unchanged. On the other hand, Ciprofloxacin caused upregulation of virulence across all strains tested (Mojsoska et al., 2021).

While it is clear that sub-lethal antibiotics have great impact on bacterial virulence, the extent and general direction of it remains mostly unclear. We acknowledge that many factors such as the genetic background of the strains can contribute to the ambiguous results. Nonetheless, we claim that with standardization in MIC determination and consequently more accurate determination of sub-lethal antibiotic concentrations, bacterial virulence can generally be better understood, and the proposed VIC could be better determined. The following section aims to give examples of how initial MIC determination across studies using the same reference strains differs and how this makes it impossible to properly compare sub-MIC concentrations and their impact on bacterial traits such as virulence.

3.1 Variability in MIC determination contributes to inconsistent sub-MIC calculations across studies

To detect antibiotic resistances in bacterial isolates as well as to find the right drug to treat infections, antibiotic susceptibility testing has become an integral part of the health care and research sector (Jorgensen and Ferraro, 2009). The metric to quantify resistance is termed Minimum Inhibitory Concentration (MIC). The European Committee for Antimicrobial Susceptibility Testing (EUCAST) defines it as the lowest concentration "that, under defined *in vitro* conditions, prevents the growth of bacteria within a defined period of time"(EUCAST, 2000). Next to the EUCAST framework, CLSI represents another established organization describing MIC determination in standardized ways (CLSI, 2023). Various phenotypical-, molecular- and mass spectrometry-based methods for MIC determination have been described (Gajic et al., 2022). As investigating the entirety of methods would be outside the scope of this review paper, it will instead focus on three more frequently used and accessible methods in routine clinical microbiology: "Microbroth dilution," "disk-diffusion" and "gradient test" (Figure 3).

To precisely calculate various sub-MIC concentrations, it is imperative to properly determine the MIC of the antibiotics of interest in the first place. Since standardized frameworks are available this might seem like a simple task to achieve. However, this review identified various discrepancies in MIC determination across numerous studies, ultimately contributing to different MIC values and consequently, incomparable results. For antimicrobial susceptibility testing of rapidly growing aerobic bacteria, EUCAST and CLSI recommend the broth microdilution (EUCAST, 2022; CLSI, 2023). To cultivate microorganisms, un-supplemented cation-adjusted Mueller-Hinton (MH) broth or agar is used for non-fastidious organisms. For fastidious organisms EUCAST stipulates the use of cation-adjusted MH broth or agar supplemented with 5% lysed horse blood and 20 mg/L B-NAD (EUCAST, 2022). In the broth microdilution method, a defined number of bacteria is inoculated in increasing concentrations of an antibiotic of choice. According to established organizations, the growth should be assessed visually by the unaided eye: Microbial growth can manifest both as turbidity of the media or as a visible deposit of cells at the bottom of the well. The absence of both cloudiness and cell deposits indicates lack of growth and determines the MIC value (EUCAST, 2022) (Figure 3A).

Although most published studies investigating the impact of sub-MIC antibiotics perform the broth microdilution for the initial MIC determination, changes in parameters such as media used for the dilution drastically alter the outcome of MIC levels. A striking example of this are three papers investigating sub-MIC effects of Gentamicin on virulence in *Pseudomonas aeruginosa,* each using different media. Davarzani et al. determined the MIC of Gentamicin for the reference strain PAO1 as 0.5 μg/mL, Khan et al. reported it to be 8 μg/mL and Marr et al. calculated a value between 1 and 2 μg/mL (Marr et al., 2007; Khan et al., 2020; Davarzani et al., 2021). Those three independent studies used MHB, Tryptic Soy Broth (TSB) and Lysogeny Broth (LB), respectively. Sometimes, the change in calculated MIC can be minor: Comparing the calculated MIC of Ciprofloxacin in two studies by Mojsoska et al. and Gupta et al., who used LB and MHB as a media, respectively, only a small difference is observed: 0.125 μg/mL vs. 0.25 μg/mL (Gupta et al., 2016; Mojsoska

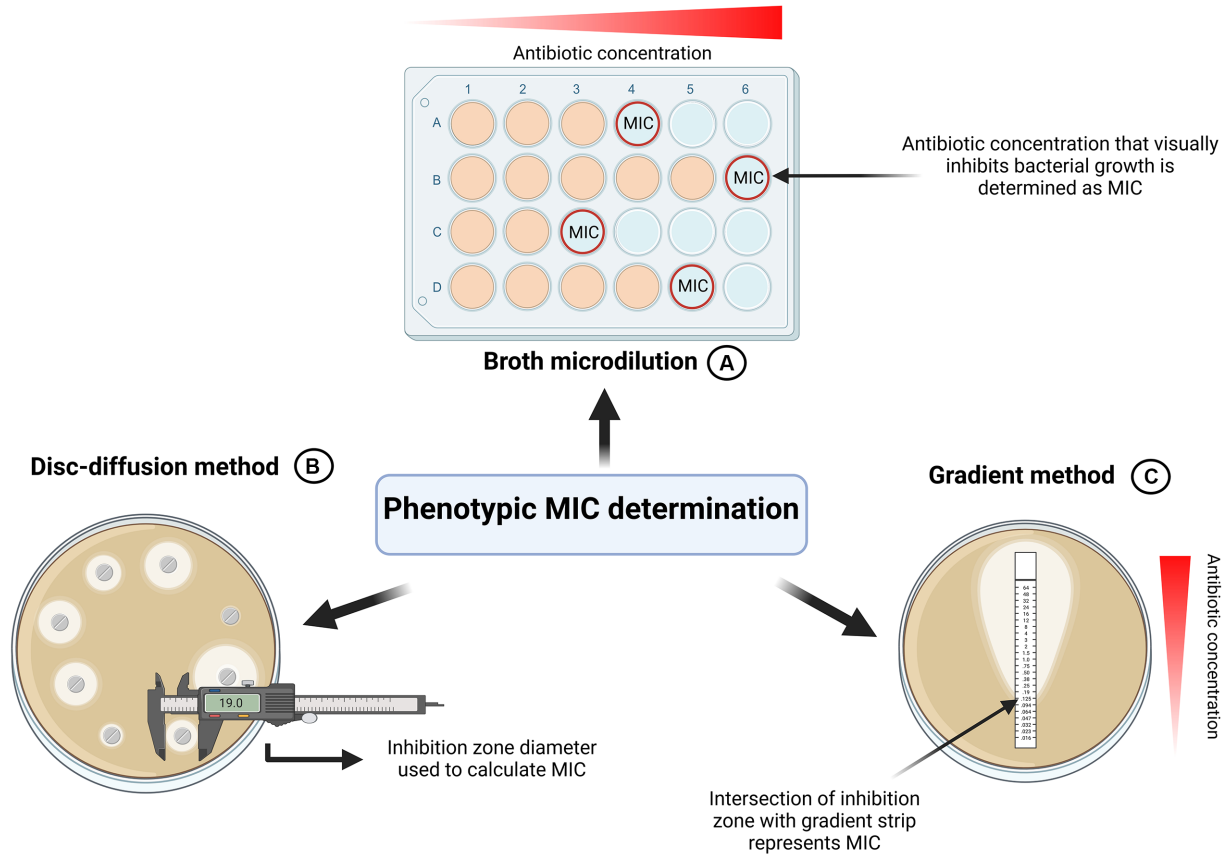

FIGURE 3
Graphical summary of phenotypic MIC determination. **(A)** Broth Microdilution. Standardized by EUCAST and CLSI (EUCAST, 2022; CLSI, 2023). Most commonly used method for MIC determination. **(B)** Disk-diffusion method (EUCAST, 2023). MIC is determined based on inhibition zone parameter. **(C)** Gradient method. Concentration at which the inhibition zone intercepts the strip represents MIC. Created with BioRender.com.

et al., 2021). However, in some cases such as MIC determination of Azithromycin, alterations in media can lead to drastic differences: Shen et al. used LB media and reported a MIC of 6.25 μg/mL for PAO1, whereas Bahari et al. used MHB and reported 256 μg/mL (Shen et al., 2008; Bahari et al., 2017). The examples above show that a minute change in protocol such as using different media for MIC determination impacts the outcome significantly. Consequently, the effects of sub-MIC on virulence cannot be directly compared between such studies. This observation is in line with a study from Imani Rad et al., who determined MIC of the antimicrobial agent allicin using 6 culture media including TSB, MHB, and LB. They concluded that the type of culture media significantly impacts MIC for various standard strains and that it directly influences stability of allicin (Imani Rad et al., 2017). Furthermore, it has been shown that β-lactam antibiotics can undergo rapid degradation in growth media. This highlights the need for caution when interpreting MIC values, as the actual concentration might decrease during the experiment (Brouwers et al., 2020).

Although the broth microdilution is most used to determine MIC in studies investigating sub-MICs, alternative methods exist: The disk diffusion method and the gradient method (Figures 3B,C).

Some sub-MIC studies employ the gradient method as an auxiliary method to the broth microdilution, but it is rarely seen as the only method for MIC determination (Kraupner et al., 2018). It centers on plastic strips impregnated with a predefined antibiotic concentration gradient on the underside (Jorgensen and Ferraro, 2009; Gajic et al., 2022). These strips are placed face down on an agar plate inoculated with the bacterium of interest. Following incubation, with the help of concentration markings on the top side of the strip, the MIC can be determined by the point where the growth inhibition zone intersects with the test strip (Jorgensen and Ferraro, 2009; Gajic et al., 2022) (Figure 3C). Generally, studies showed that the MIC values gathered from the antimicrobial gradient method are in good agreement with MIC values determined using the standardized microbroth dilution method (Baker et al., 1991; Citron et al., 1991; Huang et al., 1992; Jorgensen and Ferraro, 2009).

Development of the disk-diffusion method dates to the early 1940s and still represents a widely used method for accurate MIC determination today (Abraham et al., 1941; Heatley, 1944; Gajic et al., 2022; EUCAST, 2023). However, we found that the disk diffusion method is not widely used for MIC determination in sub-MIC studies. We argue that this could be because it does not yield quantitative MIC information but rather classifies pathogens into resistant, intermediate and susceptible phenotypes. While in sub-MIC studies the broth microdilution and gradient method is preferred, disk diffusion is more suitable for testing in routine clinical laboratories.

Standardized frameworks for MIC determination are in place, however, not all studies adhere to them. As demonstrated in section 3, different parameters for MIC determination inevitably contribute to contrasting results across multiple studies investigating the effect of

sub-MIC antibiotics on virulence and therefore hinders the exploration of a potential VIC.

4 Zones below MIC have been explored and specified

Almost 50 years ago, Lorian discussed that antibiotic concentrations far below the MIC value led to morphological changes in bacteria (Lorian, 1975). In 1990, Baquero surmised that a dangerous window for emergence of microbial resistance exists (Baquero, 1990). In 2003, Drlica built on that assumption and developed an *in vitro* framework with the goal to identify microbe-antibiotic relationships that could most likely lead to emergence of resistance (Drlica, 2003; Drlica and Zhao, 2007). The pharmacodynamic model explained that selection of resistant bacteria can occur at concentrations between the MIC of the fully susceptible strain (lower limit, MIC_{sus}) and the MIC of the fully resistant strain [upper limit, MIC_{res}, also called mutant prevention concentration (MPC)]. The range between those established boundaries was termed the "Mutant Selection Window" (Drlica, 2003; Drlica and Zhao, 2007).

4.1 Minimum selective concentration

Excellent reviews thoroughly discuss that selection for resistance is happening far below MIC at sub-lethal antibiotic levels (Andersson and Hughes, 2012, 2014; Hughes and Andersson, 2012). They rightfully argue that experimental data is needed to unravel the intricacies of sub-lethal antibiotic concentration on selective pressure for resistance. To push this notion forward, they pioneered this field of research, contributing vital insights by conducting multiple keystone studies (Gullberg et al., 2011, 2014; Wistrand-Yuen et al., 2018). One of these excellent papers showed that *Salmonella enterica* evolved high-level resistance under sub-MIC selection pressure (Wistrand-Yuen et al., 2018). Most interestingly, it was demonstrated that spectra of resistance mutations differed between bacteria exposed to antibiotic levels above or below MIC (Wistrand-Yuen et al., 2018).

Using competition experiments between isogenic pairs of resistant mutants and susceptible strains of *Escherichia coli* and *Salmonella enterica,* Gullberg et al. showed that selection of resistance occurs far sub-MIC (Gullberg et al., 2011). Fluorescent-activated cell sorting (FACs) has been used to keep track of and quantify the amount of resistant and susceptible cells over time during competition for 80 generations in various antibiotic concentrations. They calculated the selection coefficient and plotted it against antibiotic concentrations. The point at which the resistant mutant outgrew the susceptible was determined as the Minimum Selective Concentration (MSC). They found that the MSC for Streptomycin was 1/4 MIC_{sus}, for Tetracycline 1/100 MIC_{sus} and for Ciprofloxacin it varied between 1/10 and 1/230 MIC_{sus} (depending on the resistance mutation) (Gullberg et al., 2011). Most interestingly, they could also show *de novo* resistant mutants can be selected for at sub-MIC concentrations (Gullberg et al., 2011). A graphical summary of the method used to determine MSC in isolated competition models can be seen in Figure 4. In contrast to this quantitative assay, a qualitative study arrived at similar conclusions using not FACs, but an elegant chromogenic culture assay to assess selection for resistance over time (Liu et al., 2011). They showed that in *Escherichia coli* 1/5 MIC of Ciprofloxacin and 1/20 MIC of Tetracycline select for outgrowth of resistant cells in competition experiments (Liu et al., 2011). Another study demonstrated that multidrug resistance plasmids are selected at antibiotic concentrations far below the MIC (Gullberg et al., 2014).

All of the above studies provide compelling data that selection for resistance is happening at sub lethal antibiotic levels. However, one might argue that while isolated competition experiments provide valuable insight into MSC, extrapolation of the findings to entire communities is non-trivial. Hence, efforts have also been made to determine MSC not in a single species setting but in complex communities that closely represent ecosystems. These studies commonly perform high-cost metabolomic studies to define which genes increase in abundance during antibiotic exposure-response experiments. This aids experiments especially when investigating resistances that are dependent on many genes (e.g.: β-lactams) (Lundström et al., 2016). Those genes are then quantified by qPCR over time under antibiotic exposure. Next to genotypic MSC determinations, most of these studies additionally employ phenotypic methods such as counting CFUs on resistance plates or taxonomic endpoints. Figure 5 depicts a schematic overview of the existing generalized workflow to measure MSC in complex microbial environmental samples.

One of such studies used elaborate biofilm flow-through systems to assess if Tetracycline in aquatic bacterial biofilms promotes emergence of resistance by measuring phenotypic and genotypic endpoints (Lundström et al., 2016). With the help of an exploratory metabolomic assay, they identified *tetA* and *tetG* to be most significantly upregulated when stimulated with Tetracycline. By quantifying abundance of *tetG* and *tetA* with qPCR and counting CFUs they report that selection for resistance occurs at low concentration levels below MIC (≤1 μg/L), which agree with native Tetracycline concentrations in aquatic environments.

Another study followed a similar approach to calculated LOEC (lowest observed effect of concentration) and NOEC (no observed effect of concentration) of Ciprofloxacin in complex aquatic communities (Kraupner et al., 2018). They found that the most sensitive endpoints were taxonomic diversity and the gene *qnrD*, stating the NOEC in the flow through system to be 0.1 μg/L, which is identical to MSC determined by Gullberg et al. in a simplified competition experiment (Gullberg et al., 2011). The LOEC for Ciprofloxacin selection was determined to be 1 μg/L. In this study, the use of NOEC as a reasonable exposure limit for Ciprofloxacin in the environment to prevent selection for resistance is proposed (Kraupner et al., 2018).

Lastly, a study from 2018 quantified positive selection for the antibiotic Cefotaxime resistance in complex wastewater ecosystems with qPCR (Murray et al., 2018). Based on previous studies, the MSC has been profiled with qPCR and calculated by the intercepting point of selection coefficient plot with the x-axis (Gullberg et al., 2011). In line with other experiments, they proved strong positive selection of resistance genes at low, environmentally relevant concentrations (Murray et al., 2018). They could also identify a gap in MSC determination: Quantification of the antibiotic during MSC determination experiments is necessary, since in their case the antibiotic was rapidly degraded by the bacterial community (Murray et al., 2018). This means that the MSC of cefotaxime (0.4 μg/L) is likely to be even lower.

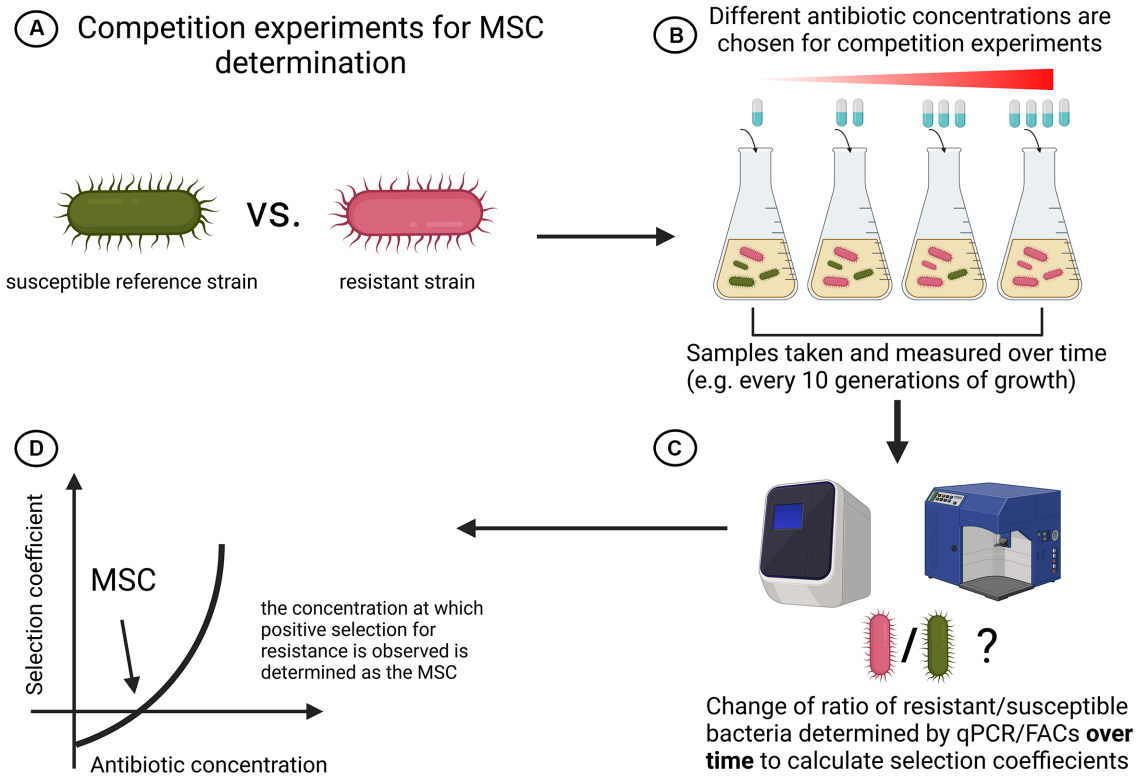

FIGURE 4
Schematic overview of simple strain competition experiments for MSC determination. **(A)** A susceptible reference strain competes with a resistant strain. To isolate effects of antibiotics seen, isogenic strains are recommended. **(B)** Both strains are cocultured and each setup is treated with a different antibiotic concentration. Samples are taken with equal spacing. **(C)** Ratio of resistant over susceptible bacteria is regularly determined with either qPCR or FACs. **(D)** The selection coefficient is plotted against the antibiotic concentration and MSC is determined as the point where the graph intersects with the x-axis (Gullberg et al., 2011). Created with BioRender.com.

To conclude, multiple studies investigating the interplay between low levels of antibiotics and selective pressures for resistance have been conducted (Gullberg et al., 2011, 2014; Liu et al., 2011; Wistrand-Yuen et al., 2018). A handful of studies explored selection dynamics of resistance in complex microbial communities by determining genotypic, phenotypic and taxonomic endpoints (Lundström et al., 2016; Kraupner et al., 2018; Murray et al., 2018; Stanton et al., 2020). While all those studies provide essential contributions to advance research, a standardized way to determine MSC in simple and complex samples needs to be found.

4.2 Minimum increased persistence concentration—a zone below MSC?

Even less so than the MSC window, MIPC is a newly emerging framework that has, to the best of our knowledge, only been thematized recently (Stanton et al., 2020). They add to existing literature and proposes that a selective window below the MSC exists: The Minimum Increased Persistence Concentration (MIPC) (Stanton et al., 2020). They incubated *Enterobacteriaceae* for 7 days in Tetracycline Hydrochloride and quantified the change in gene expression of the resistance conferring gene *tetG*. In line with Lundström et al., they could see an increase in *tetG* prevalence compared to the control (Lundström et al., 2016; Stanton et al., 2020). However, when comparing the starting prevalence of *tetG* with day 7 prevalence of *tetG*, a reduction of the resistance gene could be observed. They suggest that this negative selection could be attributed to increased persistence (reduced rate of negative selection) in the pathogens (Stanton et al., 2020). They also argue that what Lundström et al. described in their paper could have been caused by increased persistence, and not as suggested by enrichment of resistance (Lundström et al., 2016; Stanton et al., 2020). Thus, they define the MIPC as a "concentration above which a significant increase in persistence is observed" and warn that it might lie below MSC (Stanton et al., 2020). The MIPC might represent an important threshold above which antibiotic concentrations lead to diminished disappearing of resistant bacteria. On one hand, this microbial enrichment would increase human exposure and overall mutation risk compared to antibiotic-free environments. On the other hand, increased persistence would lead to negative selection for resistance genes between MIPC and MSC (Stanton et al., 2020). Due to MIPC being below MSC, Stanton et al. argue that MIPC could be considered over MSC when setting antibiotic limits in the environment.

As evident in Section 4, zones below MIC have been specified and explored. When reading experimental articles about sub-MIC antibiotic treatment and its impact on virulence, a question naturally comes to mind: In which sub-MIC zone does the tested antibiotic

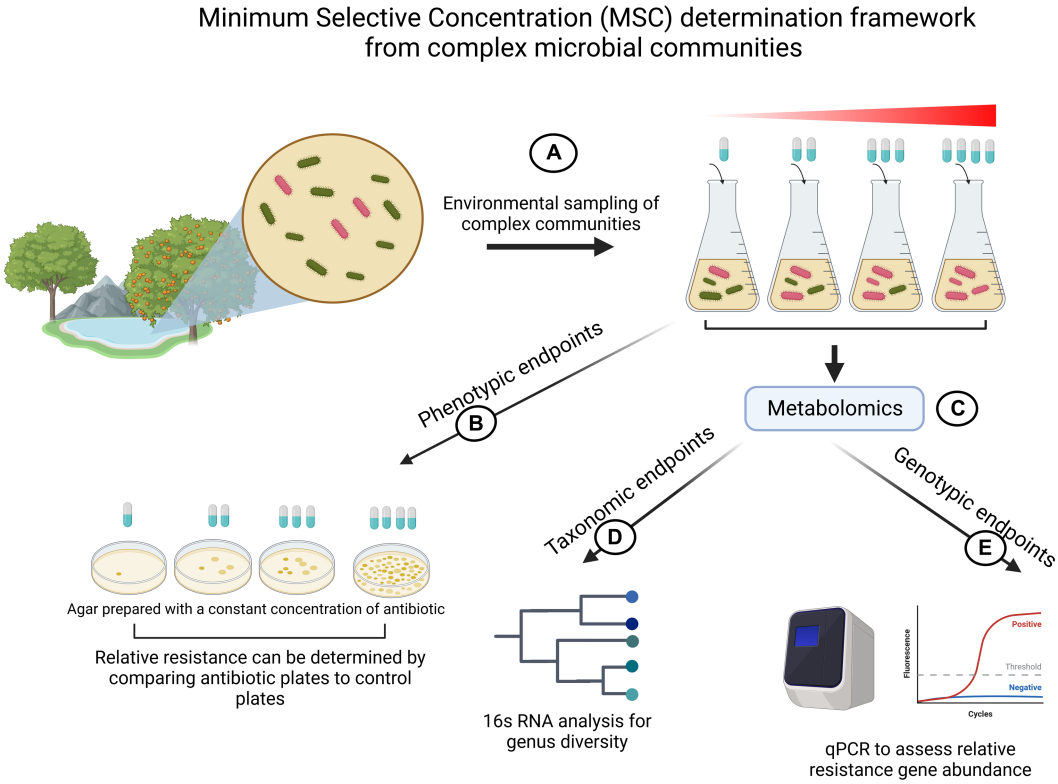

FIGURE 5
Illustration of MSC determination experimental flow for complex microbial communities. **(A)** Complex environmental samples of microbial communities are sampled and cultivated in the presence of different antibiotic concentrations. **(B)** Phenotypic profiling of resistance by counting colony forming units (CFUs) on plates prepared with a fixed amount of antibiotics. **(C)** Metabolomic exploratory assays to gain 16 s RNA data and to profile which genes respond to antibiotics. **(D)** 16 s RNA is used to explore taxonomical diversity in response to identify an antibiotic concentration which exerts selective pressure on the community. **(E)** Tracking relative abundance of resistance genes to gain insight about MSC. Created with BioRender.com.

concentration fall? All we see are concentration levels represented as fractions of MIC (e.g.: 1/2 or 1/16) but it is often unclear precisely where within the sub-MIC range a particular experiment falls. A standardized categorization of sub-MIC ranges would help to link an observed effect on virulence to a certain sub-MIC zone. This would make it easier to classify impact on bacterial virulence and thus pave the way toward targeted treatment.

5 What to do now?—toward a standardized framework to combat virulence

The central claim of this critical review is that the reason for ambiguous results across sub-MIC studies on virulence can in part be attributed to the absence of standardized MIC and sub-MIC methodology. To begin with, we explained the importance of having clear definitions for terms such as "persistence" and "tolerance" in sub-MIC research. Later we highlight that the lack of sub-MIC understanding already starts at the stage of MIC determination. Various examples for studies that use different MIC determination methods and therefore calculate different values for similar strains and antibiotics are given. We identified this as one of the main issues for incomparable results. Lastly, studies investigating the sub-MIC area (MSC and MIPC) are presented. Across them, consensus exists that selection for bacterial fitness traits such as persistence and resistance happens far below the MIC. While this is invaluable insight for environmental agencies to pose limitations, the connection between those findings and medical treatment possibilities needs to be made: If we gain profound understanding of sub-MIC ranges, we could characterize virulence within different ranges, opening up endless possibilities for tailored treatment opportunities.

5.1 Starting at the beginning—standardizing MIC determination

Perhaps not surprising, successful sub-MIC profiling calls for rigid MIC determination. Well defined frameworks such as EUCAST and CLSI are already in place, nevertheless, studies commonly deviate from those protocols when calculating MIC. EUCAST and CLSI generally recommend the broth microdilution, which agrees with the approach chosen in numerous studies. Other methods such as the disk diffusion and the gradient test are viable options, however we recommend the broth microdilution as the main method of choice for MIC determination (EUCAST, 2022; CLSI, 2023).

When performing the broth microdilution, various discrepancies can arise, with the most frequent being the use of different media (LB,

MHB, TSB) between studies. This review points out the major impact the choice of growth media had on numerous study outcomes and further underlines the importance of the standardized MHB media. However, this holds only true in the case of experimental settings performed on rich, unmodified media. Experiments requiring minimal or depleted media require MIC determination in the same growth conditions. These altered growth conditions could affect the bacterial physiology, and therefore greatly modify the bacterial metabolism and antibiotic susceptibility. According to EUCAST and CLSI, the assessment of growth after antibiotic exposure should be conducted visually by the unaided eye. However, some studies used a photo-spectrometric readout. While it is difficult to infer the impact of this deviation on the outcome of various studies, it is nonetheless a step in the protocol that should be conducted according to already standardized frameworks. Moreover, it is vital to adhere to other parameters imposed by EUCAST, such as the purity of culture and the correct density of inoculum (5×10^5 CFU/mL) (EUCAST, 2022). Lastly, other culture conditions such as time and temperature of incubation present yet another aspect of MIC determination in need of standardization.

Increasing efforts need to be focused on assessing antibiotic stability over the course of the MIC determination. While MIC tests generally presume antibiotics to be stable in growth media, degradation for antibiotics including β-lactams have been reported (Brouwers et al., 2020). One study that investigated the effect of typically used media (such as LB, MHB, TSB) found that the type of culture media influenced the stability and subsequently the MIC of the antibacterial agent allicin (Imani Rad et al., 2017). Efforts should be directed on further understanding dynamics of antibiotics in various media to avoid possible MIC determination biases and, subsequently, inaccurate sub-MIC investigation. When MIC has been calculated according to the standardized broth microdilution, sub-MIC studies usually employ double dilutions to calculate sub-MICs (e.g.: 1/2, 1/4, 1/8…). Since virulence is impacted by minute changes in antibiotic concentration, it would me more insightful to do arithmetic dilutions for more reliable and granular results. Should diffusion tests be used, measuring colony size by imagine-scanning techniques could prove useful to measure sub-inhibitory effects.

5.2 How to standardize sub-MIC zones?

Recently, zones below MIC such as MSC and MIPC have been described (Gullberg et al., 2011, 2014; Liu et al., 2011; Andersson and Hughes, 2012, 2014; Hughes and Andersson, 2012; Stanton et al., 2020). In contrast to MIC determination, no agreed guidelines and methodologies to profile sub-MIC for a given organism exist.

Recent endeavors to develop methods for determination of MSCs of antibiotics present an excellent start and efforts toward understanding selective pressures on microbial traits have been made in recent years. Although the body of research in this area is limited, intriguing similarities, but also limitations of experimental intricacies can be observed.

MSC determination experiments can be conducted based on Gullberg et al. in simplified two strain competition experiments: There, general consensus is to track the ration of tagged (e.g.: fluorescent) susceptible and resistant isogenic strains in a co-culture (Gullberg et al., 2011). The antibiotic concentration at which the resistant mutant outgrows the susceptible one is termed MSC (Figure 4). Such systems could readily be standardized in many ways: First, it is of utmost importance that for every pathogen a susceptible reference strain against which the pathogen of interest is competing, needs to be found. Second, as in MIC determination, the media in which the experiment takes place must be standardized and investigated for potential antibiotic degradation to rule out biases. Third, guidelines for parameters of the competition like number of serial passages, overall duration of the experiment and time of sampling must be standardized. Lastly, a common readout method to track the ratio of the competing cells must be found (FACs, qPCR). The implementation of standardized guidelines to test for MSC with strain competition experiments in clinical settings is an important step that needs to be taken. However, the method also comes with some limitations that need to be addressed: The competing strains used by past studies are isogenic with the only exception being the fluorescent tags by which their abundance can be tracked. This presents an issue, since clinical isolates are most probably not isogenic, making it hard to attribute the effect we see solely to the antibiotic. Nonetheless, we argue that it would still give an estimate of the area in which selection for resistance might occur.

Simple strain competitions are vital and should be readily standardized in clinical contexts. However, it also becomes clear that findings might not be translatable to bigger microbial communities and, ultimately, with the aim of treatment, to *in vivo* environments. A limited number of studies investigating MSC of microbial communities have been conducted (Lundström et al., 2016; Kraupner et al., 2018; Murray et al., 2018; Stanton et al., 2020). However, thus far, the focus of MSC research has primarily been on exploring its application in determining environmental regulation thresholds. Analysis of such studies for this review revealed a consensual workflow that could potentially be translated to sub-MIC virulence profiling and treatment opportunities (Figure 5). Most studies measure MSC for various types of endpoints, all of which should follow agreed guidelines: Phenotypic endpoints to assess MSC in environmental communities presents invaluable information in case not all genes that contribute to resistance are known. CFU counts could present a method that could easily be standardized in terms of media used and number of bacteria plated.

Furthermore, most studies investigating selective properties of antibiotics in environmental communities utilize genotypic endpoints. Before measuring the endpoints, metabolomic assays such as shotgun-sequencing are employed to find genes that are impacted by antibiotic exposure. Subsequently, the relative abundance of these genes is then quantified using the gold-standard qPCR assay. Due to the high cost of large-scale metabolomics, we propose the following: In order to standardize this workflow, exploratory metabolomic data should be available for everyone, preferably in a large database that shows up and downregulated genes across multiple species of communities under exposure of antibiotics. That way the assay does not need to be done every time and a core list of crucial genes can readily be analyzed with qPCR. As argued by Stanton et al., it is also necessary to assess the starting prevalence of genes. This would help assess if the genes are under positive or negative selection and one could therefore differentiate between resistance and persistence mechanisms (Stanton et al., 2020). When establishing general protocols for genotypic endpoint measurements, this is something that needs to be considered.

However, Kraupner et al. warn that changes in gene abundance should not always be taken at face value since they could also be consequences of taxonomic shifts (Kraupner et al., 2018). Taxonomic analysis represents another intriguing way that has been used to study MSC and should be considered when profiling a microbial community. For this, a diversity analysis to identify an antibiotic concentration which exerts selective pressure on the community could be employed.

For a successful MSC profiling of complex communities, investigation of phenotypic, genotypic and, possibly taxonomic endpoints are essential. A rigid guide exploring phenotypic and genotypic MSC determination should readily be standardized for rapid profiling of complex communities. Taxonomic analysis presents a new way to look at the whole picture but due to its steep costs and need of specific equipment it does not need to be prioritized when outlining standardized protocols.

The newly emerging concept of a sub-MSC zone, the MIPC zone presents another thought-provoking concept. To the best of our knowledge, only one study came up with this term and investigated the matter (Stanton et al., 2020). Between the MSC and the MIPC, they explain that the number of resistant bacteria could be higher than if there was no antibiotic present (Stanton et al., 2020). They highlight that selection happens below the MSC level and that we need to look even deeper to fully profile pathogens. Future work needs to be focused on fully characterizing persistent phenotypes and understanding the underlying epigenetic mechanisms. qPCR endpoints for generalized pathogen- specific set of genes accountable for persistence then need to be analyzed for reduced rate of negative selection under antibiotic exposure.

5.3 Transition to *ex vivo* microbial community studies could open the door for targeted therapies

As discussed earlier, isogenic strain experiments could present an integral part of clinical diagnostics and profiling of single strain pathogens against a reference strain. But as the step toward clinical profiling of larger microbial communities needs to be made, community assays discussed in this review present a solid base to build upon. They already have a good framework in place and could be used to successfully profile complex human communities from phenotypic, genotypic and possible taxonomic angles. For this, standard media best representing the *in vivo* environment needs to be established.

With a proper sub-MIC profiling in place, the impact of antibiotics on virulence could be systematically unraveled and a VIC of a specific antibiotic could potentially be determined more accurately for a given pathogen. This brings up the last issue briefly discussed in this review: How should virulence be measured? Virulence presents a complex topic and is highly strain specific. Every pathogen has different ways of causing harm to the host, and many ways to measure it exist. However, going over the methodology to assess virulence in main pathogens lies outside the scope of this paper. Nonetheless, we propose that when characterizing a number of clinical isolates, it is crucial to profile specific virulence molecules for a virulence signature against a reference strain.

The overarching claim of this review was that the challenge of investigating impact of sub-MIC antibiotics on virulence lies in part in the absence of uniform MIC and sub-MIC profiling. This review highlights topics that need to be regulated and gives suggestions on how to build a framework for successful profiling. It identifies MIC determination as one of the main culprits in need for standardization. It explains that experimental frameworks for competition experiments and environmental community analysis should be built upon to extend their applicability to clinical settings. Consensus in virulence measurements combined with a full sub-MIC profiling would pave the way for potential targeted treatment and would allow us to better understand how virulence manifests itself in the sub-MIC world.

Author contributions

FT: Data curation, Formal analysis, Investigation, Visualization, Writing – original draft, Writing – review & editing. FA: Conceptualization, Funding acquisition, Investigation, Project administration, Resources, Supervision, Visualization, Writing – review & editing.

Funding

The author(s) declare financial support was received for the research, authorship, and/or publication of this article. This work was supported by L'Oréal-UNESCO for Women in Science.

Conflict of interest

The authors declare that the research was conducted in the absence of any commercial or financial relationships that could be construed as a potential conflict of interest.

Publisher's note

References

Abraham, E. P., Chain, E., Fletcher, C. M., Florey, H. W., Gardner, A. D., Heatley, N. G., et al. (1941). Further observations on penicillin. *Lancet* 238, 177–189. doi: 10.1016/S0140-6736(00)72122-2

Alatraktchi, F. A., Svendsen, W. E., and Molin, S. (2020). Electrochemical detection of Pyocyanin as a biomarker for *Pseudomonas aeruginosa*: a focused review. *Sensors (Basel)* 20:5218. doi: 10.3390/S20185218

An, Y., Wang, Y., Zhan, J., Tang, X., Shen, K., Shen, F., et al. (2019). Fosfomycin protects mice from *Staphylococcus aureus* pneumonia caused by α-Hemolysin in extracellular vesicles by inhibiting MAPK-regulated NLRP3 Inflammasomes. *Front. Cell. Infect. Microbiol.* 9:253. doi: 10.3389/fcimb.2019.00253

Andersson, D. I., and Hughes, D. (2012). Evolution of antibiotic resistance at non-lethal drug concentrations. *Drug Resist. Updat.* 15, 162–172. doi: 10.1016/J.DRUP.2012.03.005

Andersson, D. I., and Hughes, D. (2014). Microbiological effects of sublethal levels of antibiotics. *Nat. Rev. Microbiol.* 12, 465–478. doi: 10.1038/NRMICRO3270

Andersson, D. I., Nicoloff, H., and Hjort, K. (2019). Mechanisms and clinical relevance of bacterial heteroresistance. *Nat. Rev. Microbiol.* 17, 479–496. doi: 10.1038/s41579-019-0218-1

Bahari, S., Zeighami, H., Mirshahabi, H., Roudashti, S., and Haghi, F. (2017). Inhibition of *Pseudomonas aeruginosa* quorum sensing by subinhibitory concentrations of curcumin with gentamicin and azithromycin. *J. Glob. Antimicrob. Resist.* 10, 21–28. doi: 10.1016/j.jgar.2017.03.006

Baker, C. N., Stocker, S. A., Culver, D. H., and Thornsberry, C. (1991). Comparison of the E test to agar dilution, broth microdilution, and agar diffusion susceptibility testing techniques by using a special challenge set of bacteria. *J. Clin. Microbiol.* 29, 533–538. doi: 10.1128/JCM.29.3.533-538.1991

Balaban, N. Q., Helaine, S., Lewis, K., Ackermann, M., Aldridge, B., Andersson, D. I., et al. (2019). Definitions and guidelines for research on antibiotic persistence. *Nat. Rev. Microbiol.* 17, 441–448. doi: 10.1038/s41579-019-0196-3

Baquero, F. (1990). Resistance to quinolones in gram-negative microorganisms: mechanisms and prevention. *Eur. Urol.* 17, 3–12. doi: 10.1159/000464084

Bastaraud, A., Cecchi, P., Handschumacher, P., Altmann, M., and Jambou, R. (2020). Urbanization and waterborne pathogen emergence in low-income countries: where and how to conduct surveys? *Int. J. Environ. Res. Public Health* 17:480. doi: 10.3390/ijerph17020480

Bigger, J. W. (1944). The bactericidal action of penicillin on staphylococcus pyogenes. *Irish J. Med. Sci.* 19, 553–568. doi: 10.1007/BF02948386

Blair, J. M. A., Webber, M. A., Baylay, A. J., Ogbolu, D. O., and Piddock, L. J. V. (2015). Molecular mechanisms of antibiotic resistance. *Nat. Rev. Microbiol.* 13, 42–51. doi: 10.1038/nrmicro3380

Brauner, A., Shoresh, N., Fridman, O., and Balaban, N. Q. (2017). An experimental framework for quantifying bacterial tolerance. *Biophys. J.* 112, 2664–2671. doi: 10.1016/J.BPJ.2017.05.014

Brouwers, R., Vass, H., Dawson, A., Squires, T., Tavaddod, S., and Allen, R. J. (2020). Stability of β-lactam antibiotics in bacterial growth media. *PLoS One* 15:e0236198. doi: 10.1371/journal.pone.0236198

Chen, J., Zhou, H., Huang, J., Zhang, R., and Rao, X. (2021). Virulence alterations in *staphylococcus aureus* upon treatment with the sub-inhibitory concentrations of antibiotics. *J. Adv. Res.* 31, 165–175. doi: 10.1016/J.JARE.2021.01.008

Citron, D. M., Ostovari, M. I., Karlsson, A., and Goldstein, E. J. (1991). Evaluation of the E test for susceptibility testing of anaerobic bacteria. *J. Clin. Microbiol.* 29, 2197–2203. doi: 10.1128/jcm.29.10.2197-2203.1991

CLSI (2023). Performance standards for antimicrobial susceptibility testing. Available at: https://clsi.org/standards/products/microbiology/documents/m100/ (Accessed September 7, 2023).

Davarzani, F., Yousefpour, Z., Saidi, N., and Owlia, P. (2021). Different effects of sub-minimum inhibitory concentrations of gentamicin on the expression of genes involved in alginate production and biofilm formation of *Pseudomonas aeruginosa*. *Iran. J. Microbiol.* 13, 808–816. doi: 10.18502/IJM.V13I6.8085

Drlica, K. (2003). The mutant selection window and antimicrobial resistance. *J. Antimicrob. Chemother.* 52, 11–17. doi: 10.1093/jac/dkg269

Drlica, K., and Zhao, X. (2007). Mutant selection window hypothesis updated. *Clin. Infect. Dis.* 44, 681–688. doi: 10.1086/511642

EUCAST (2000). Terminology relating to methods for the determination of susceptibility of bacteria to antimicrobial agents. *Clin. Microbiol. Infect.* 6, 503–508. doi: 10.1046/j.1469-0691.2000.00149.x

EUCAST (2022). EUCAST reading guide for broth microdilution. Available at: https://www.eucast.org/fileadmin/src/media/PDFs/EUCAST_files/Disk_test_documents/2022_manuals/Reading_guide_BMD_v_4.0_2022.pdf (Accessed September 7, 2023).

EUCAST (2023). EUCAST disk diffusion method for antimicrobial susceptibility testing. Available at: https://www.eucast.org/fileadmin/src/media/PDFs/EUCAST_files/Disk_test_documents/2023_manuals/Manual_v_11.0_EUCAST_Disk_Test_2023.pdf (Accessed June 1, 2023).

Gajic, I., Kabic, J., Kekic, D., Jovicevic, M., Milenkovic, M., Mitic Culafic, D., et al. (2022). Antimicrobial susceptibility testing: a comprehensive review of currently used methods. *Antibiotics (Basel)* 11:427. doi: 10.3390/ANTIBIOTICS11040427

Gullberg, E., Albrecht, L. M., Karlsson, C., Sandegren, L., and Andersson, D. I. (2014). Selection of a multidrug resistance plasmid by sublethal levels of antibiotics and heavy metals. *MBio.* 5:e01918-14. doi: 10.1128/MBIO.01918-14

Gullberg, E., Cao, S., Berg, O. G., Ilbäck, C., Sandegren, L., Hughes, D., et al. (2011). Selection of resistant bacteria at very low antibiotic concentrations. *PLoS Pathog.* 7:e1002158. doi: 10.1371/JOURNAL.PPAT.1002158

Gupta, P., Chhibber, S., and Harjai, K. (2016). Subinhibitory concentration of ciprofloxacin targets quorum sensing system of *pseudomonas aeruginosa* causing inhibition of biofilm formation & reduction of virulence. *Indian J. Med. Res.* 143, 643–651. doi: 10.4103/0971-5916.187114

Hall, S., McDermott, C., Anoopkumar-Dukie, S., McFarland, A. J., Forbes, A., Perkins, A. V., et al. (2016). Cellular effects of pyocyanin, a secreted virulence factor of *Pseudomonas aeruginosa*. *Toxins (Basel)* 8:236. doi: 10.3390/toxins8080236

Heatley, N. G. (1944). A method for the assay of penicillin. *Biochem. J.* 38, 61–65. doi: 10.1042/BJ0380061

Huang, M. B., Baker, C. N., Banerjee, S., and Tenover, F. C. (1992). Accuracy of the E test for determining antimicrobial susceptibilities of staphylococci, enterococci, campylobacter jejuni, and gram-negative bacteria resistant to antimicrobial agents. *J. Clin. Microbiol.* 30, 3243–3248. doi: 10.1128/JCM.30.12.3243-3248.1992

Hughes, D., and Andersson, D. I. (2012). Selection of resistance at lethal and non-lethal antibiotic concentrations. *Curr. Opin. Microbiol.* 15, 555–560. doi: 10.1016/J.MIB.2012.07.005

Imani Rad, H., Arzanlou, M., Mahsa, R. O., Ravaji, S., and Peeri Doghaheh, H. (2017). Effect of culture media on chemical stability and antibacterial activity of allicin. *J. Funct. Foods* 28, 321–325. doi: 10.1016/j.jff.2016.10.027

Jorgensen, J. H., and Ferraro, M. J. (2009). Antimicrobial susceptibility testing: a review of general principles and contemporary practices. *Clin. Infect. Dis.* 49, 1749–1755. doi: 10.1086/647952

Kester, J. C., and Fortune, S. M. (2014). Persisters and beyond: mechanisms of phenotypic drug resistance and drug tolerance in bacteria. *Crit. Rev. Biochem. Mol. Biol.* 49, 91–101. doi: 10.3109/10409238.2013.869543

Khan, S., Beattie, T. K., and Knapp, C. W. (2017). The use of minimum selectable concentrations (MSCs) for determining the selection of antimicrobial resistant bacteria. *Ecotoxicology* 26, 283–292. doi: 10.1007/S10646-017-1762-Y

Khan, F., Lee, J. W., Javaid, A., Park, S. K., and Kim, Y. M. (2020). Inhibition of biofilm and virulence properties of *Pseudomonas aeruginosa* by sub-inhibitory concentrations of aminoglycosides. *Microb. Pathog.* 146:104249. doi: 10.1016/j.micpath.2020.104249

Kraupner, N., Ebmeyer, S., Bengtsson-Palme, J., Fick, J., Kristiansson, E., Flach, C.-F., et al. (2018). Selective concentration for ciprofloxacin resistance in *Escherichia coli* grown in complex aquatic bacterial biofilms. *Environ. Int.* 116, 255–268. doi: 10.1016/J.ENVINT.2018.04.029

Lagator, M., Uecker, H., and Neve, P. (2021). Adaptation at different points along antibiotic concentration gradients. *Biol. Lett.* 17:20200913. doi: 10.1098/RSBL.2020.0913

Laxminarayan, R., Duse, A., Wattal, C., Zaidi, A. K. M., Wertheim, H. F. L., Sumpradit, N., et al. (2013). Antibiotic resistance-the need for global solutions. *Lancet Infect. Dis.* 13, 1057–1098. doi: 10.1016/S1473-3099(13)70318-9

Linares, J. F., Gustafsson, I., Baquero, F., and Martinez, J. L. (2006). Antibiotics as intermicrobial signaling agents instead of weapons. *Proc. Natl. Acad. Sci. U. S. A.* 103, 19484–19489. doi: 10.1073/pnas.0608949103

Liu, A., Fong, A., Becket, E., Yuan, J., Tamae, C., Medrano, L., et al. (2011). Selective advantage of resistant strains at trace levels of antibiotics: a simple and ultrasensitive color test for detection of antibiotics and genotoxic agents. *Antimicrob. Agents Chemother.* 55, 1204–1210. doi: 10.1128/AAC.01182-10

Lorian, V. (1975). Some effects of subinhibitory concentrations of antibiotics on bacteria. *Bull. N. Y. Acad. Med.* 51, 1046–1055.

Lundström, S. V., Östman, M., Bengtsson-Palme, J., Rutgersson, C., Thoudal, M., Sircar, T., et al. (2016). Minimal selective concentrations of tetracycline in complex aquatic bacterial biofilms. *Sci. Total Environ.* 553, 587–595. doi: 10.1016/J.SCITOTENV.2016.02.103

Madhusoodanan, J. (2022). How persister bacteria evade antibiotics, prolong infections. *Proc. Natl. Acad. Sci. U. S. A.* 119:e2215617119. doi: 10.1073/pnas.2215617119

Majtán, V., and Hybenová, D. (1996). Inhibition of *Pseudomonas aeruginosa* alginate expression by subinhibitory concentrations of antibiotics. *Folia Microbiol. (Praha)* 41, 61–64. doi: 10.1007/BF02816342

Marr, A. K., Overhage, J., Bains, M., and Hancock, R. E. W. (2007). The Lon protease of *Pseudomonas aeruginosa* is induced by aminoglycosides and is involved in biofilm formation and motility. *Microbiology (Reading)* 153, 474–482. doi: 10.1099/mic.0.2006/002519-0

Mojsoska, B., Ghoul, M., Perron, G. G., Jenssen, H., and Alatraktchi, F. A. Z. (2021). Changes in toxin production of environmental *Pseudomonas aeruginosa* isolates exposed to sub-inhibitory concentrations of three common antibiotics. *PLoS One* 16:e0248014. doi: 10.1371/journal.pone.0248014

Molinari, G., Guzmán, C. A., Pesce, A., and Schito, G. C. (1993). Inhibition of *Pseudomonas aeruginosa* virulence factors by subinhibitory concentrations of azithromycin and other macrolide antibiotics. *J. Antimicrob. Chemother.* 31, 681–688. doi: 10.1093/JAC/31.5.681

Murray, A. K., Zhang, L., Yin, X., Zhang, T., Buckling, A., Snape, J., et al. (2018). Novel insights into selection for antibiotic resistance in complex microbial communities. *MBio.* 9:e00969-18. doi: 10.1128/MBIO.00969-18

Negri, M.-C., Lipsitch, M., Blázquez, J., Levin, B. R., and Baquero, F. (2000). Concentration-dependent selection of small phenotypic differences in TEM-lactamase-

mediated antibiotic resistance. *Antimicrob. Agents Chemother.* 44, 2485–2491. doi: 10.1128/AAC.44.9.2485-2491.2000

Nolan, C., and Behrends, V. (2021). Sub-inhibitory antibiotic exposure and virulence in *pseudomonas aeruginosa*. *Antibiotics (Basel)* 10:1393. doi: 10.3390/antibiotics10111393

OECD (2018). *Stemming the superbug tide*. OECD Available at: https://www.oecd-ilibrary.org/social-issues-migration-health/stemming-the-superbug-tide_9789264307599-en (Accessed September 7, 2023).

Pan, X., Liu, W., Du, Q., Zhang, H., and Han, D. (2023). Recent advances in bacterial persistence mechanisms. *Int. J. Mol. Sci.* 24:14311. doi: 10.3390/ijms241814311

Riber, L., and Hansen, L. H. (2021). Epigenetic memories: the hidden drivers of bacterial persistence? *Trends Microbiol.* 29, 190–194. doi: 10.1016/j.tim.2020.12.005

Shang, W., Rao, Y., Zheng, Y., Yang, Y., Hu, Q., Hu, Z., et al. (2019). β-Lactam antibiotics enhance the pathogenicity of methicillin-resistant *Staphylococcus aureus* via SarA-controlled lipoprotein-like cluster expression. *MBio* 10:e00880-19. doi: 10.1128/mBio.00880-19

Sharma, A. K., Dhasmana, N., Dubey, N., Kumar, N., Gangwal, A., Gupta, M., et al. (2017). Bacterial virulence factors: secreted for survival. *Indian J. Microbiol.* 57, 1–10. doi: 10.1007/S12088-016-0625-1

Sharma, S., Mohler, J., Mahajan, S. D., Schwartz, S. A., Bruggemann, L., and Aalinkeel, R. (2023). Microbial biofilm: a review on formation, infection, antibiotic resistance, control measures, and innovative treatment. *Microorganisms* 11:1614. doi: 10.3390/microorganisms11061614

Shen, L., Shi, Y., Zhang, D., Wei, J., Surette, M. G., and Duan, K. (2008). Modulation of secreted virulence factor genes by subinhibitory concentrations of antibiotics in *Pseudomonas aeruginosa*. *J. Microbiol.* 46, 441–447. doi: 10.1007/s12275-008-0054-x

Simpson, J. A., Smith, S. E., and Dean, R. T. (1988). Alginate inhibition of the uptake of *Pseudomonas aeruginosa* by macrophages. *J. Gen. Microbiol.* 134, 29–36. doi: 10.1099/00221287-134-1-29

Skariyachan, S., Sridhar, V. S., Packirisamy, S., Kumargowda, S. T., and Challapilli, S. B. (2018). Recent perspectives on the molecular basis of biofilm formation by Pseudomonas aeruginosa and approaches for treatment and biofilm dispersal. *Folia Microbiol. (Praha)* 63, 413–432. doi: 10.1007/S12223-018-0585-4

Stanton, I. C., Murray, A. K., Zhang, L., Snape, J., and Gaze, W. H. (2020). Evolution of antibiotic resistance at low antibiotic concentrations including selection below the minimal selective concentration. *Commun. Biol.* 3:467. doi: 10.1038/s42003-020-01176-w

Turner, N. A., Sharma-Kuinkel, B. K., Maskarinec, S. A., Eichenberger, E. M., Shah, P. P., Carugati, M., et al. (2019). Methicillin-resistant *Staphylococcus aureus*: an overview of basic and clinical research. *Nat. Rev. Microbiol.* 17, 203–218. doi: 10.1038/s41579-018-0147-4

Uddin, T. M., Chakraborty, A. J., Khusro, A., Zidan, B. R. M., Mitra, S., Emran, T. B., et al. (2021). Antibiotic resistance in microbes: history, mechanisms, therapeutic strategies and future prospects. *J. Infect. Public Health* 14, 1750–1766. doi: 10.1016/J.JIPH.2021.10.020

Urban-Chmiel, R., Marek, A., Stępień-Pyśniak, D., Wieczorek, K., Dec, M., Nowaczek, A., et al. (2022). Antibiotic resistance in Bacteria—a review. *Antibiotics (Basel)* 11:1079. doi: 10.3390/antibiotics11081079

Von Wintersdorff, C. J. H., Penders, J., Van Niekerk, J. M., Mills, N. D., Majumder, S., Van Alphen, L. B., et al. (2016). Dissemination of antimicrobial resistance in microbial ecosystems through horizontal gene transfer. *Front. Microbiol.* 7:173. doi: 10.3389/FMICB.2016.00173/BIBTEX

Wistrand-Yuen, E., Knopp, M., Hjort, K., Koskiniemi, S., Berg, O. G., and Andersson, D. I. (2018). Evolution of high-level resistance during low-level antibiotic exposure. *Nat. Commun.* 9:1599. doi: 10.1038/S41467-018-04059-1

World Health Organization (2021). 2021 antibacterial agents in clinical and preclinical development: an overview and analysis. Available at: https://www.who.int/publications/i/item/9789240047655 (Accessed September 7, 2023).

Yu, H., Schurr, M. J., and Deretic, V. (1995). Functional equivalence of *Escherichia coli* sigma E and *Pseudomonas aeruginosa* AlgU: *E. coli* rpoE restores mucoidy and reduces sensitivity to reactive oxygen intermediates in algU mutants of *P. aeruginosa*. *J. Bacteriol.* 177, 3259–3268. doi: 10.1128/JB.177.11.3259-3268.1995

frontiers | Frontiers in Microbiology

TYPE Original Research
PUBLISHED 22 December 2023
DOI 10.3389/fmicb.2023.1274201

OPEN ACCESS

EDITED BY
Ana R. Freitas,
Cooperativa de Ensino Superior Politécnico e Universitário, Portugal

REVIEWED BY
Shakir Khan,
Harvard Medical School, United States
Celia Fortuna R.,
Cooperativa de Ensino Superior Politécnico e Universitário, Portugal

*CORRESPONDENCE
Ana Claudia Pavarina
ana.pavarina@unesp.br

RECEIVED 14 August 2023
ACCEPTED 01 December 2023
PUBLISHED 22 December 2023

CITATION
Jordão CC, Klein MI, Barbugli PA, Mima EGO, de Sousa TV, Ferrisse TM and Pavarina AC (2023) DNase improves the efficacy of antimicrobial photodynamic therapy in the treatment of candidiasis induced with *Candida albicans*. *Front. Microbiol.* 14:1274201. doi: 10.3389/fmicb.2023.1274201

DNase improves the efficacy of antimicrobial photodynamic therapy in the treatment of candidiasis induced with *Candida albicans*

Cláudia Carolina Jordão[1], Marlise Inêz Klein[2], Paula Aboud Barbugli[1], Ewerton Garcia de Oliveira Mima[1], Tábata Viana de Sousa[1], Túlio Morandin Ferrisse[1] and Ana Claudia Pavarina[1]*

[1]Laboratory of Applied Microbiology, Department of Dental Materials and Prosthodontics, School of Dentistry, São Paulo State University (UNESP), Araraquara, Brazil, [2]Department of Oral Diagnosis, Piracicaba Dental School, State University of Campinas (UNICAMP), Piracicaba, Brazil

The study evaluated the association of DNase I enzyme with antimicrobial photodynamic therapy (aPDT) in the treatment of oral candidiasis in mice infected with fluconazole-susceptible (CaS) and -resistant (CaR) *Candida albicans* strains. Mice were inoculated with *C. albicans*, and after the infection had been established, the tongues were exposed to DNase for 5 min, followed by photosensitizer [Photodithazine®(PDZ)] and light (LED), either singly or combined. The treatments were performed for 5 consecutive days. Treatment efficacy was evaluated by assessing the tongues via fungal viable population, clinical evaluation, histopathological and fluorescence microscopy methods immediately after finishing treatments, and 7 days of follow-up. The combination of DNase with PDZ-aPDT reduced the fungal viability in mice tongues immediately after the treatments by around 4.26 and 2.89 $\log_{10}$ for CaS and CaR, respectively (versus animals only inoculated). In the fluorescence microscopy, the polysaccharides produced by *C. albicans* and fungal cells were less labeled in animals treated with the combination of DNase with PDZ-aPDT, similar to the healthy animals. After 7 days of the treatment, DNase associated with PDZ-aPDT maintained a lower count, but not as pronounced as immediately after the intervention. For both strains, mice treated with the combination of DNase with PDZ-aPDT showed remission of oral lesions and mild inflammatory infiltrate in both periods assessed, while animals treated only with PDZ-aPDT presented partial remission of oral lesions. DNase I enzyme improved the efficacy of photodynamic treatment.

KEYWORDS

photochemotherapy, *Candida albicans*, antifungal drug resistance, fungi, enzyme

1 Introduction

Oropharyngeal candidiasis (OPC) is the most prevalent infection caused by *Candida* spp. (Akpan and Morgan, 2002; Eggimman et al., 2003). Infections caused by *Candida* spp. are associated with biofilm formation, a complex microstructure of cells adhered to a surface and enveloped by an extracellular matrix (ECM) (Flemming et al., 2007). ECM contributes to

preserving biofilms and conserving stable interactions between cells, surfaces (substrate), and the environment (Flemming et al., 2007). In addition, ECM reduces the susceptibility of microorganisms against therapies classically used (Flemming et al., 2007; Seneviratne et al., 2008). Biochemical analyses show that the production of polysaccharides (β-1-3-glucan, β-1-6-glucan, β-1-6-mannan and chitin, for example), nucleic acids (extracellular DNA—eDNA) and lipids protect the biofilm' cells and keep stable interactions between ECM components (Eggimman et al., 2003; Nett et al., 2007; Martins et al., 2010). The antifungal resistance of *Candida albicans* biofilms is multifactorial, including the stimulation of drug efflux pumps, the physiological state of the cells, and the protection employed by the ECM through β-mannan and β-glucans that bind with fluconazole and amphotericin B (Flemming et al., 2007; Seneviratne et al., 2008). In addition to β-mannan and β-glucan, eDNA is an important constituent of the ECM and promotes the structural integrity of biofilms (Mitchell et al., 2016). The addition of DNase enzyme improves the susceptibility of mature *C. albicans* biofilms against some antifungal agents (Martins et al., 2010). Furthermore, the presence of polysaccharides or eDNA was reported as a bacterial biofilm mechanism of protection against the diffusion of antibiotics (Al-Fattani and Douglas, 2006; Anderson and O'Toole, 2008; Mulcahy et al., 2008).

Because the ECM has been related to biofilm protection (Nobile et al., 2008), the use of enzymes capable of hydrolyzing polysaccharides and nucleic acids has been investigated, as it represents an alternative way of increasing the susceptibility of the biofilm to antifungal drugs (Nobile et al., 2008). DNase I enzyme can significantly reduce eDNA, soluble matrix proteins, and water-soluble polysaccharides of a fluconazole-resistant *C. albicans* (Panariello et al., 2019). This enzyme acts externally to the cell, reducing biofilm stability and enhancing its susceptibility to photodynamic therapy and antifungals (Liao, 1974; Martins et al., 2012; Tetz and Tetz, 2016; Panariello et al., 2019). The treatment of mature biofilms with DNase I (50 mg/mL) inhibited adhesion, biofilm formation, and reduced the biomass by approximately 30% (Perezous et al., 2005). Incubation of *in vitro* 48 h-old biofilms for 5 min to DNase I reduced eDNA and extracellular polysaccharides in the ECM of fluconazole-susceptible and -resistant *C. albicans* strains (Panariello et al., 2019).

Due to the increase of resistant microorganisms (Kumar et al., 2022), the side effects of antifungals (Campoy and Adrio, 2017), recolonization, and organization into biofilms (Kumar et al., 2022), studies have evaluated alternative strategies to manage fungal infections. In this context, antimicrobial photodynamic therapy (aPDT) is suggested for inactivating microorganisms and treating oral candidiasis (Lambrechts et al., 2005; Konopka and Goslinski, 2007; Donnelly et al., 2008). The photodynamic process requires a photosensitizing agent (PS) combined with light with a wavelength corresponding to the PS absorption band (Donnelly et al., 2008). The interaction of light with PS, in the presence of oxygen, produces reactive species capable of inducing cell inactivation (Machado, 2000). Reactive species have non-specific reactivity with organic molecules and can cause irreversible damage to cellular targets, such as membrane lysis and protein inactivation. Thus, any cellular macromolecule can be considered a target for aPDT (Bonnett and Martínez, 2001; Donnelly et al., 2008).

Photodithazine (PDZ)-aPDT inactivated *Candida* biofilms and treated oral candidiasis (Seneviratne et al., 2008; Martins et al., 2010). A single application of PDZ-aPDT in a murine model decreased the fluconazole-susceptible *C. albicans* (ATCC 90028) viability by 4.36 $\log_{10}$ (Carmello et al., 2015). On the other hand, mice infected by a fluconazole-resistant *C. albicans* strain (ATCC 96901) that received a single session of PDZ-aPDT presented reduced fungal cell viability by 1.96 $\log_{10}$ (Alves et al., 2018). Five consecutive applications of PDZ-aPDT or antifungal nystatin promoted reductions in the fluconazole-susceptible *C. albicans* (ATCC 90028) by 3 and 3.2 $\log s_{10}$, respectively, and yielded the remission of tongue lesions after 24 h of treatment (Carmello et al., 2016). When the animals were inoculated with a fluconazole-resistant strain (ATCC 96901), PDZ-aPDT was as effective as the topical antifungal nystatin in the treatment, reducing viability by around 1.2 $\log_{10}$ (Hidalgo et al., 2019); however, the animals showed white or pseudomembranous patches on the dorsum of the tongues. In animals inoculated with fluconazole-resistant *C. albicans*, the associations of treatments (PDZ-aPDT and nystatin) reduced ~2.3 $\log_{10}$ of fluconazole-resistant *C. albicans* (Hidalgo et al., 2019), and the macroscopic analysis revealed remission of oral lesions ranging ~95% after 24 h (Hidalgo et al., 2019). In general, previous studies (Carmello et al., 2015, 2016; Alves et al., 2018; Hidalgo et al., 2019) demonstrated the efficacy of PDZ-aPDT in treating infections caused by fluconazole-susceptible *C. albicans*. However, fluconazole-resistant *C. albicans* have reduced susceptibility to aPDT, and to find similar outcomes in the treatment of infections with these strains, it is necessary to combine treatments.

DNase treatment might be an adjuvant to anti-biofilm therapies since it reduces most ECM components that can hinder antifungal drug penetration into biofilms without interfering with cell viability (Panariello et al., 2019; Abreu-Pereira et al., 2022). The incubation of fluconazole-susceptible *C. albicans* biofilm with DNase I (5 min) before PDZ-aPDT reduced the counting of viable colonies (CFU) and the quantity of eDNA in the ECM (Panariello et al., 2019). This treatment strategy applied to fluconazole-resistant *C. albicans* biofilm decreased CFU (~1.62 $\log_{10}$), water-soluble polysaccharides (36.3%), and eDNA (72.3%) (Abreu-Pereira et al., 2022). Hence, the effect of photodynamic treatment was potentiated because DNase I disturbed the ECM and allowed the diffusion of PDZ and light through the ECM of fluconazole-susceptible and -resistant *C. albicans* biofilm, increasing treatment efficacy (Abreu-Pereira et al., 2022). Hence, the present study evaluated whether the application of DNase could potentiate the action of PDZ-aPDT treatment in mice infected with fluconazole-susceptible and -resistant *C. albicans*, focusing on fungal viable population recovery and resolution of candidiasis lesions on the mice's tongues.

2 Materials and methods

2.1 Photosensitizer, DNase enzime and LED parameters

Photodithazine® (PDZ) is a chlorin e6 derivative (VETAGRAND, Co, Moscow, Russia), which has an absorption peak of 660 nm. The PDZ was prepared on the day of use from the stock solution (5,000 mg/L) at a concentration of 200 mg/L in natrosol gel (Farmácia Santa Paula, Araraquara, SP, Brazil) and was kept protected from light (Hidalgo et al., 2019). The bovine pancreas DNase I enzyme stock solution (AMPD1, Sigma-Aldrich, St. Louis, MO, USA) was prepared

on the day of use in 0.1 M sodium acetate buffer (pH 5.5) at the concentration of 20 units/mL (Abreu-Pereira et al., 2022).

The red LED light device (LXHLPR09, Luxeon® III Emitter, Lumileds Lighting, San Jose, California, USA) was used with an absorption band of 660 nm, and the light intensity at the end of the device (5 mm in diameter) was 44.6 mW/cm^2. Thus, a light dose of 50J/cm^2 (19 min) was applied to the tongues of animals infected with *C. albicans*.

2.2 Experimental oral candidiasis and treatments performed

The present study was approved by the Animal Ethics Committee of the School of Dentistry of Araraquara, UNESP (Case number: 09/2020). A total of 180 female mice of the Swiss strain (≅ 5 weeks old) were used from the vivarium of the School of Dentistry of Araraquara, UNESP. The animals were allocated in cages, with five animals per cage according to the study groups, and kept in a room with a controlled temperature (23 ± 2°C) with standard chow and water *ad libitum* (Carmello et al., 2016; Hidalgo et al., 2019).

Strains of *C. albicans* ATCC (American Type Culture Collection, Rockville, USA), susceptible to fluconazole (ATCC 90028; CaS) and resistant to fluconazole (ATCC 96901; CaR) were defrosted, reactivated on Agar Sabouraud Dextrose (SDA) medium (37°C, 48 h). Next, colonies were transferred and cultivated in RPMI 1640 (Sigma-Aldrich, St. Louis, MO, USA) buffered to a pH of 7.0 with 3-(N-Morpholino) propanesulfonic acid 4-Morpholinepropanesulfonic acid (MOPS) (Sigma-Aldrich, St. Louis, MO, USA) at 37°C for 16 h. Then, the cells were washed twice with sterile phosphate buffered saline (PBS) (50 mM), resuspended with 3 mL of RPMI 1640, and the cell suspension was standardized spectrophotometrically with an optical density (OD) of 540 nm (1.0 nm ± 0.08, corresponding to 10^7 CFU/mL) (Carmello et al., 2016; Hidalgo et al., 2019).

For the induction of oral candidiasis, the methodology described before (Takakura et al., 2003; Carmello et al., 2016) was used with some modifications. Tetracycline (0.83 mg/mL) was administered in the water available to the animals during the experimental period. The animals were immunosuppressed with subcutaneous injections of prednisolone at a dose of 100 mg/kg of body mass on days 1, 5, 9, and 13. Inoculation with the strains was performed on day 2 of the experiment (Figure 1; Takakura et al., 2003; Carmello et al., 2016; Hidalgo et al., 2019). For this procedure, the animals were sedated with 0.1 mL of chlorpromazine hydrochloride (2 mg/mL), and sterile mini-swabs soaked in the CaS or CaR suspension were scrubbed across the dorsum of the animals' tongues for 30 s.

On day 7, the presence of white patches or pseudomembranous lesions was verified, and the treatments were performed. The animals were anesthetized with an intraperitoneal injection of ketamine [100 mg/kg body weight (National Pharmaceutical Chemistry Union S/A, Embu, SP, Brazil)] and xylazine [10 mg/kg body weight (Veterinary JA Ltda., Sponsor Paulista, SP, Brazil)]. Then, the animals were placed in a supine position on the work table, the tongues were gently taken out of the oral cavity, and 50 µL of PDZ diluted in natrosol gel (200 mg/L) was applied with a pipette (Carmello et al., 2016; Hidalgo et al., 2019). The mice stayed in the dark for 20 min for a pre-incubation time. Then, each dorsum of the tongue was illuminated with LED for 19 min (50 J/cm^2) (P + L+ group). The effect of the isolated application of PDZ (P + L-) and the LED (P-L+ group) was also evaluated. For DNase treatment, the tongue of the mice received 50 µL of DNase (20 units/mL) for 5 min. One group received the combined treatment with the enzyme and PDZ-aPDT (DNase+P + L+ group). After the treatments, neither DNase nor PDZ was removed from the mice' tongue. The untreated control group (P-L- group) received no PDZ, light, or DNase. In addition, two additional negative infection control groups (NIC groups) with healthy animals were evaluated. In one of them, mice were immunosuppressed on days 1, 5, 9, and 13 (NIC+ group); in the other group, animals did not receive immunosuppression (NIC- group). Seven animals were evaluated for each experimental condition, except the group NIC+ ($n = 3$) and NIC- ($n = 3$). The therapies were performed once a day for five consecutive days (from day seven until day 11).

2.3 Fungal viable population

After five consecutive days of treatment (day 11) and 7 days after the end of the treatment (day 18), *C. albicans* cells were recovered from the tongue of mice. For this procedure, the mini-swabs were swabbed on the dorsum of each tongue for 1 min. Then, they were transferred to tubes with 1 mL of saline solution and vortexed for 1 min to detach *C. albicans* cells. Then, serial dilutions were made (10^{-1} a 10^{-3}) and plated in duplicate in SDA culture medium containing 5 µg/mL of chloramphenicol. After 48 h of incubation at 37°C, the viable colonies were counted, and the values of CFU/mL were determined.

2.4 Macroscopic analysis of tongue's lesions

The white patches or pseudomembranous lesions in the tongues of mice were photographed before the beginning of the treatments, 24 h (day 12), and 7 days (day 18) after the last application. All photographs were standardized and obtained with the same digital camera (Sony Cyber-Shot DSCF717; Sony Corporation, Tokyo, Japan), by the same operator and under the same conditions (place, light, angle, and position of the animals), thus aiming to facilitate the reproducibility. The extension area of the lesion on the tongue in each photograph was evaluated using the ImageJ.exe program.[1] The percentage of the extension area of each lesion over the total area of the tongue was calculated using this software (Hidalgo et al., 2019).

2.5 Histopathological analyses and animal sacrifice

Initially, mice were anesthetized with an intraperitoneal injection of ketamine and xylazine. Then, animals' tongues were surgically removed and destinated for histopathological and fluorescence microscopic analyses. After the tongue excision, mice were euthanized by intramuscular injection of a lethal dose of

1 https://imagej.nih.gov/ij/docs/install/windows.html

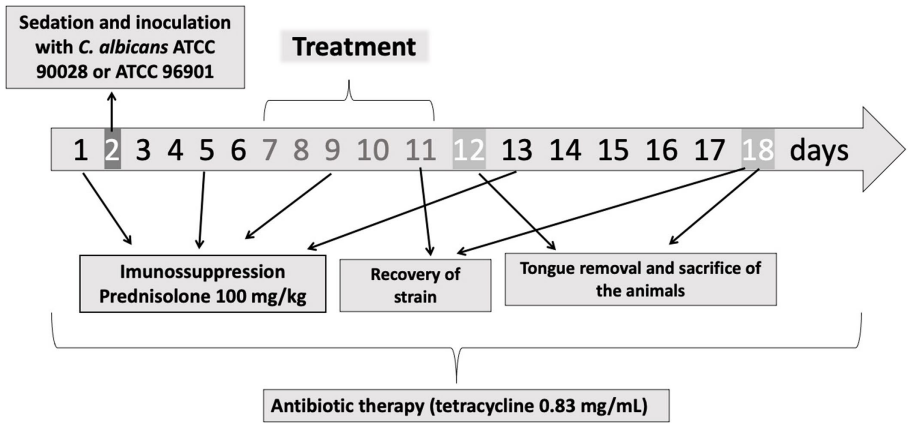

FIGURE 1
Experimental protocol. On the days 1, 5, 9, and 13 the animals were immunosuppressed with subcutaneous injections of prednisolone. On day 2, the animals were inoculated with CaS or CaR. The treatment was performed during 5 days (days 7–11). On days 11 and 18, the fungal load was recovered from the mice's tongue. The tongue removal and euthanasia were performed on days 12 and 18. During the experimental period (18 days), tetracycline hydrochloride was administered in the water system.

TABLE 1 Probes and stains used in the fluorescence microscopic analysis.

Labeling target	Labeling (stain or probe) (excitation/emission nm)	Brand	References
C. albicans	ConcanavalinA (ConA) lectin conjugated with tetramethylrhodamine (488/520 nm)	Molecular Probes (Cat. No. C860)	Lobo et al. (2019) and Falsetta et al. (2014)
Nucleic acids	HOESCHT 33342	ABCAM Staining Staining Dye Solution (Cat. No. ab228551)	Chazotte (2011)
Polysaccharides produced by *C. albicans*	Primary monoclonal antibody to (1 → 4)-β-mannan and galacto-(1 → 4)-β-mannan	Biosupplies (Cat. No. 400-4)	Lobo et al. (2019) and Wartenberg et al. (2014)
Secondary antibody	Goat Anti-Mouse IgG H&L (Alexa Fluor® 594) (561/620 nm)	Abcam (Cat. No. ab175660)	Lobo et al. (2019) and Wartenberg et al. (2014)

ketamine (0.2 mL) and xylazine (0.4 mL) 24 h (day 12) and 7 days (day 18) after the last application of treatment (Carmello et al., 2016; Hidalgo et al., 2019).

The tongues were placed in plastic cassettes for the histopathological and fluorescence microscopic analyses. These cassettes were immersed in 10% paraformaldehyde (pH 7.2) (441.244, Sigma-Aldrich, St Louis, MO, USA). Then, the histological fixation process was made, and the blocks were fixed on wooden supports and placed in a rotating microtome. Sixteen serial histological sections of each block were obtained. These cuts were placed on glass slides and stained with hematoxylin–eosin (HE) stain to evaluate the histological events that occurred in each of the groups through light microscopy [Zeiss microscope LSM 700 (Carl Zeiss, Heidelberg, Germany)] at 100 and 200X magnification. A pathologist performed the histological analysis, and the following aspects were evaluated: the presence/absence of yeast and inflammatory infiltrate, epithelial tissue integrity, and adjacent connective tissue response. The material was classified into scores: 0—the absence of inflammation; 1—the presence of inflammatory infiltrate; 2—moderate inflammation; 3: severe inflammation; and 4: abscess formation (ISO 7405:1997). The evaluation was performed by a single examiner blinded to each experimental group at each evaluated time after treatment.

2.6 Microscopy analysis of fluorescence to determine fungal colonization on tongues

Initially, the samples were deparaffinated and hydrated in water. The antigenic retrieval was performed by heat. The sections were then immersed in 10 mM buffered sodium citrate, pH 6.0, and placed in the microwave twice for 5 min each (El-Habashi et al., 1995). Next, the slides were dried, and the sections were circled with a hydrophobic barrier pen (Sigma Advanced PAP Pen-Z377821) and 20 µL of the primary antibody (1 → 4)-β-mannan and galacto-(1 → 4)-β-mannan (400–4) (Table 1) diluted in 2% bovine serum albumin (BSA) and 0.1% Triton X100 (1:20 dilution) was pipetted on each section (Lobo et al., 2019). The slides were incubated overnight (4°C). After incubation, sections were carefully washed with 0.89% NaCl solution, and a blocking solution (3% BSA) was added, followed by incubation for 15 min (room temperature). Then, the sections were washed again with 0.89% NaCl solution, and the secondary antibody (20 µL) labeled with Alexa Fluor® 594 nm (1:500 dilution in 2% BSA) was added (Table 1), followed by incubation for 2 h (4°C). After the secondary antibody incubation time, the sections were washed with 0.89% NaCl and incubated with 20 µL of concavalin-A lectin conjugated with Alexa Fluor® 488 nm (200 µg/mL) (Table 1) and Hoescht (6 µg/mL) (Table 1) for 30 min. Next, samples were washed with 0.89% NaCl. The

mounting media [Fluoromount ™ Aqueous Mounting Medium (F4680, Sigma-Aldrich, St Louis, MO, USA)] was added, and the slides were ready for image acquisition. Images were acquired using the Leica DM2500 LED microscope (Leica Microsystems, Wetzlar, Germany).

2.7 Statistical analysis

Analyses were performed using the IBM SPSS Statistics for Windows Version 27; IBM Corp., Armonk, NY, USA. Data from each strain was evaluated separately. The normality and homoscedasticity of the data from CFU converted in base-10 logarithms for each strain were assessed using the Shapiro–Wilk and Levene's tests, respectively. The data were normal and heteroscedastic, so they were analyzed by a two-way ANOVA test, considering two treatment evaluation periods (immediate and 7 days after). Games-Howell post-hoc analysis was performed for multiple comparisons ($\alpha = 5\%$). The percentage values of tongue's lesions assumed normality and were homoscedastic for the data evaluated in both periods (24 h and 7 days after the treatments) for CaS and CaR. Thus, they were analyzed by one-way ANOVA, followed by Tukey's post-hoc ($\alpha = 5\%$). Descriptive analyses were performed for the images obtained for the histopathological and fluorescence microscopy evaluations.

3 Results

3.1 Fungal viable population from mice inoculated with CaS and CaR

The results of viability from CaS immediately after the treatments demonstrated that the animals treated with DNase followed by PDZ-aPDT (DNase+P + L+ group) showed the highest $\log_{10}$ reduction value (CFU/mL), compared to the negative control group (P-L-) equivalent to 4.26 $\log_{10}$ (Figure 2) and different from the other groups and the control ($p \leq 0.0001$). The P + L+ group (PDZ-aPDT) showed a reduction of approximately 2.50 $\log_{10}$ compared to the control (P-L- group) (Figure 2). The other groups showed statistically similar values with the control (P-L-) ($p \geq 0.05$) (Figure 2).

The results of CaR showed that DNase+P + L+ group immediately after the treatments was statistically different from the other groups and exhibited the highest $\log_{10}$ reduction value (CFU/mL), compared to the P-L-group ($p \leq 0.0001$), equivalent to 2.89 $\log_{10}$ (Figure 3). The group treated only with PDZ-aPDT (P + L+ group) showed a reduction of 0.34 $\log_{10}$ compared to the P-L- group. The P + L-, P-L+, P + L+, DNase and P-L-groups presented statistically similar effects (Figure 3).

The results of 7 days after the end of the treatments demonstrated that the DNase+P + L+ group exhibited the greatest reduction in the viable colonies of CaS when compared to the negative control group (P-L-) ($p \leq 0.0001$); this reduction was approximately 1.97 $\log_{10}$ (Figure 2). The P + L+ group was similar to DNase+P + L+ group and showed a statistically different value from the other groups, with a reduction of 1.18 $\log_{10}$ compared to the P-L- group ($p \leq 0.0001$). The other experimental groups (P + L-, P-L+, DNase) showed statistically similar effects among themselves and with the negative control (P-L-) ($p \geq 0.05$) (Figure 3).

For CaR after 7 days of the end of the treatments, the DNase+P + L+ group showed the greatest reduction in viable colonies when compared to the P-L- group ($p \leq 0.0001$), with a reduction of approximately 1.27 $\log_{10}$ (Figure 3). The P + L+ group showed a reduction of 0.22 $\log_{10}$ compared to the P-L- group. The other experimental groups (P + L-, P-L+, P + L+, and DNase) showed statistically similar values among themselves and the P-L- group ($p \geq 0.05$) (Figure 3).

3.2 Clinical evaluation from mice inoculated with CaS and CaR

The results after 24 h of treatment (Figure 4) for mice inoculated with the CaS showed that the DNase+P + L+ and P + L+ groups significantly reduced oral lesions by 98.92 and 97.71%, respectively,

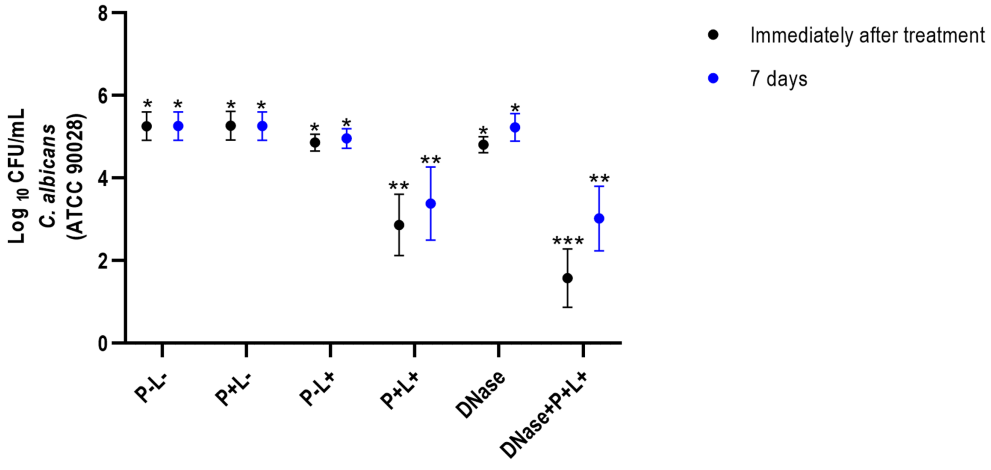

FIGURE 2
Mean values +/− standard deviation of $\log_{10}$ (CFU/mL) for different experimental groups and periods evaluated (immediately and 7 days after treatments) for animals inoculated with CaS. Different number of asterisks denotes statistical difference between the groups.

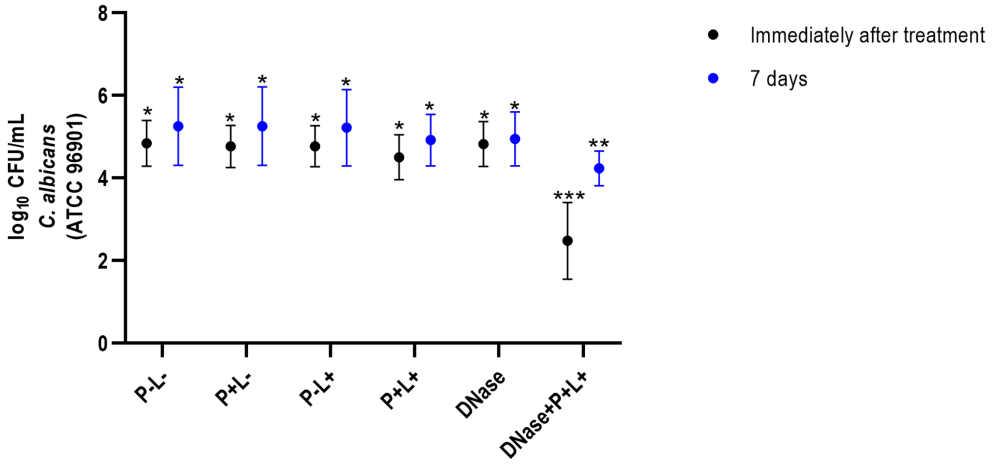

FIGURE 3
Mean values +/− standard deviation of log_{10} (CFU/mL) for different experimental groups and periods evaluated (immediately and 7 days after treatments) for animals inoculated with CaR. Different number of asterisks denotes statistical difference between the groups.

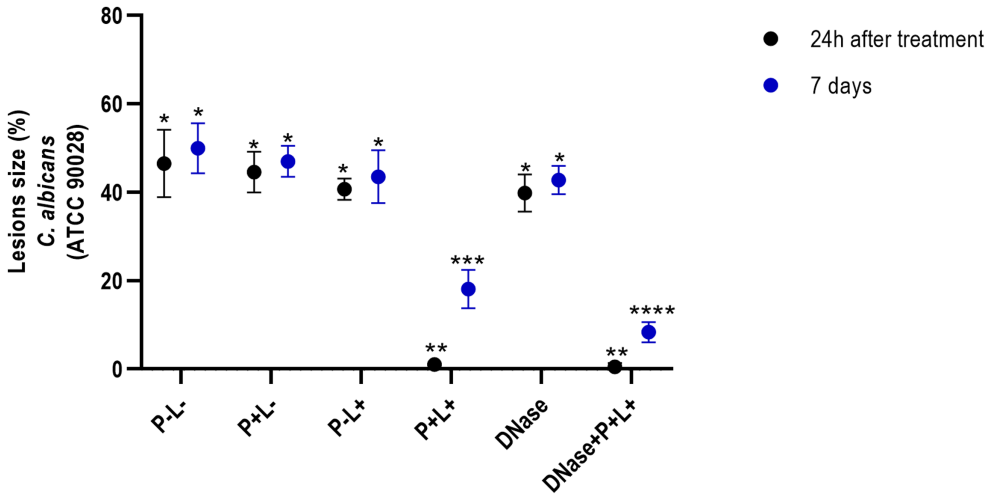

FIGURE 4
Mean values +/− standard deviation of the lesion size (with the size of the patches) in percentages (%) on the tongue's dorsum of the mice inoculated with CaS evaluated 24 h (black circle) and 7 days (blue circle) after the end of the treatments. * denotes statistical difference. Different number of asterisks denotes statistical difference between the groups.

when compared to the P-L- group ($p \leq 0.0001$). The results for 7 days after the treatments showed a reduction in oral lesions of 83.31% for DNase+P + L+ group, compared to the P-L- group ($p \leq 0.0001$). The DNase+P + L+ group was statistically different from P + L+ group that reduced the oral lesions by around 63.81% compared to the P-L- group ($p \leq 0.0001$). The other groups evaluated immediately and after 7 days (Figure 4) showed a statistically similar effect to the P-L- control ($p \geq 0.05$). The images presented in Figure 5 illustrate the presence of white patches or pseudomembranous plaques on the dorsum of the animals' tongues inoculated with CaS for each group 24 h and 7 days after the treatments.

The results obtained for CaR (Figure 6) demonstrated that the DNase+P + L+ and P + L+ groups immediately after the treatments exhibited reductions of oral lesions by 96.07 and 50.41%, respectively, when compared to the P-L- group ($p \leq 0.0001$). Immediately after the treatments, the other groups showed a statistically similar effect to the P-L- group ($p \geq 0.05$). In addition, 7 days after the treatments, the DNase+P + L+ group showed a significant reduction in oral lesions by 75.24% when compared to the P-L- group ($p \leq 0.0001$). The other groups showed statistically similar values to the P-L- control ($p \geq 0.05$) (Figure 6).

The images in Figure 7 illustrate the presence of white patches or pseudomembranous plaques on the dorsum of the tongues 24 h and 7 days after the treatments performed on animals inoculated with CaR (Figure 7).

3.3 Histopathological evaluation

The histopathological evaluation demonstrated that the sections from tongues contaminated with CaS exhibited mild inflammatory infiltrates for groups DNase+P + L+ and P + L+ 24 h after the

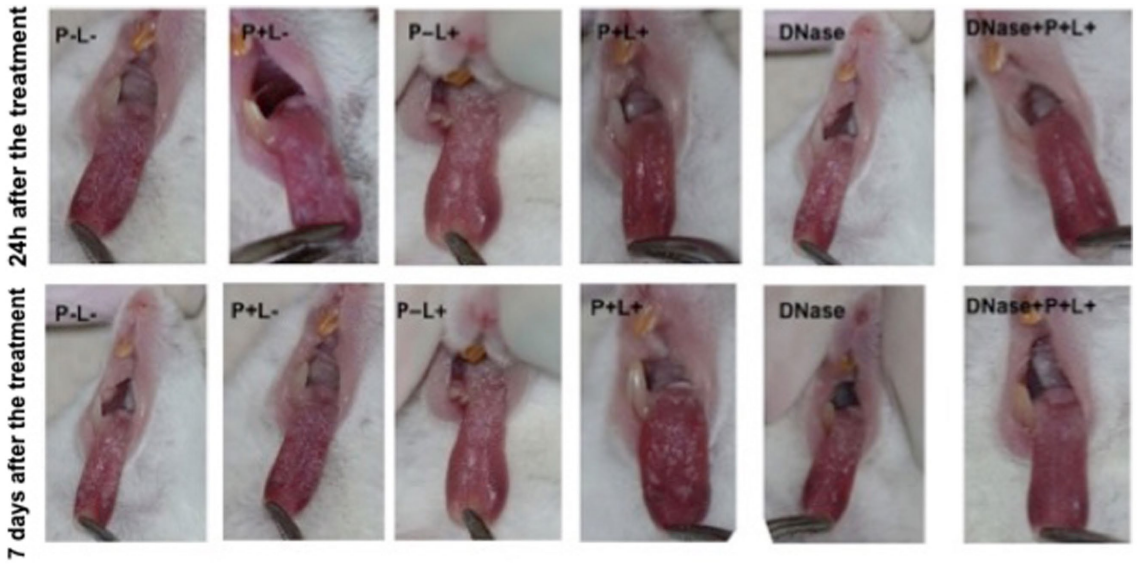

FIGURE 5
Representative images of the white or pseudomembranous patches of mice' tongues inoculated with CaS for the groups P-L-, P + L-, P-L+, and DNase 24 h and 7 days after the end of treatment. Also, representative images of the remission of tongue lesions were observed in the mice submitted to the P + L+ 24 h and DNase+P + L+ 24 h and 7 days after the treatments.

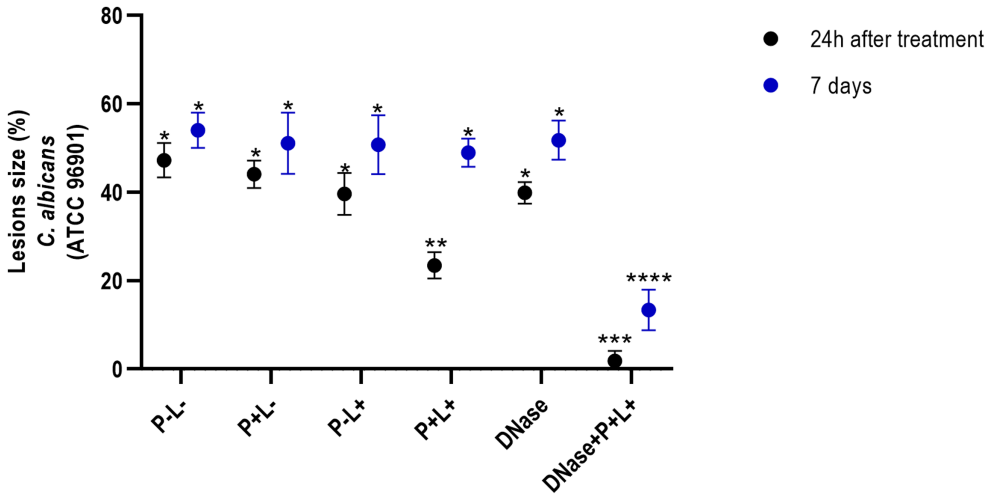

FIGURE 6
Mean values +/– standard deviation of the lesion size (with the size of the patches) in percentages (%) on the tongue's dorsum of the mice inoculated with CaR evaluated 24 h (black circle) and 7 days (blue circle) after the end of the treatment. * denotes statistical difference. Different number of asterisks denotes statistical difference between the groups.

treatment (Figure 8). These groups presented histopathological characteristics similar to those observed in the NIC- and NIC+ groups. The stratified epithelium exhibited normal and healthy features, with lingual papillae covered by a fine keratin layer. The other groups (P-L-, P-L+, P + L- and DNase) presented similar histopathological characteristics with moderate inflammatory infiltration and the presence of numerous hyphae/pseudohyphae on the keratin layer and some hyphae/pseudohyphae invading the epithelial tissue of the tongues (Figure 8). Regarding the histological sections evaluated at 7 days after the treatment for CaS, the morphological characteristics remained relatively unchanged, with the exception of the P-L-, P + L-, P-L+, and DNase groups, which showed moderately degraded muscle tissue (Figure 8).

For the animals inoculated with CaR (Figure 9), the group treated with DNase+P + L+ presented histopathological characteristics similar to those observed in the NIC- and NIC+ groups (Figure 8) after 24 h of the treatments. The stratified epithelium exhibited normal and healthy features, with lingual papillae covered by a fine keratin layer (Figure 9). The group treated with P + L+ showed a greater number of hyphae and pseudohyphae within the keratin epithelial layer. The animals in the P-L-, P + L-, P-L+, and DNase groups presented extensive amounts of *C. albicans* covering the epithelial tissue, and there was a loss of the

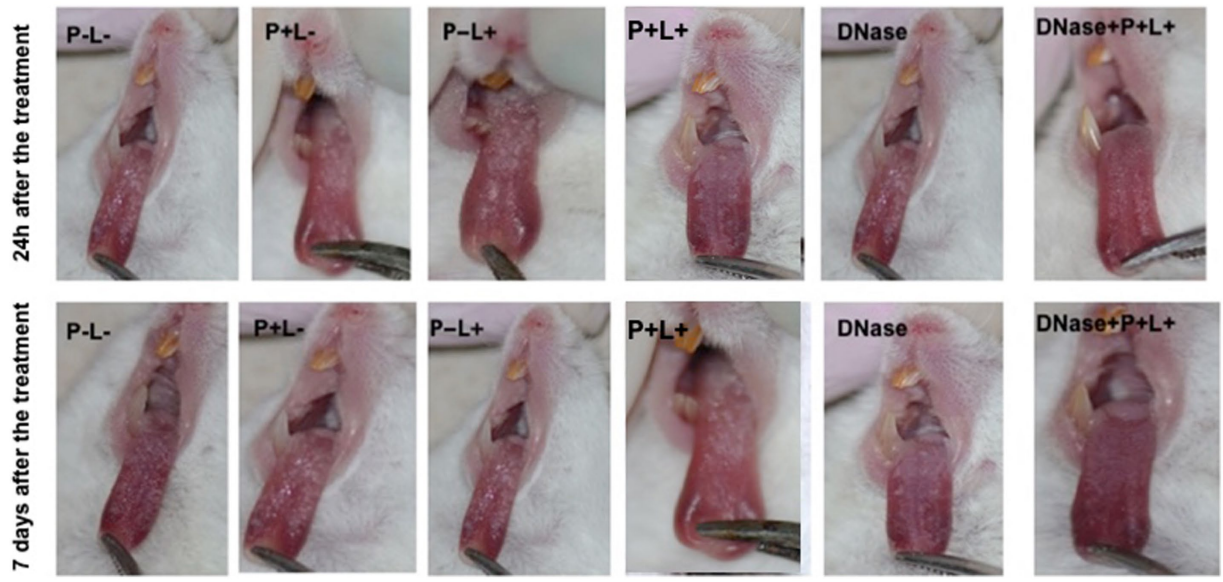

FIGURE 7
Representative images of the white or pseudomembranous patches of mice' tongues inoculated with CaR for the groups P-L-, P + L-, P-L+, P + L+, and DNase 24 h and 7 days after the end of treatment. Also, representative images of the remission of tongue lesions in the mice submitted to the DNase+P + L+ treatment are observed 24 h and 7 days after the treatment.

papillae (Figure 9). This epithelium showed intense inflammation with the existence of mononuclear cells inside the dilated blood vessels caused by the inflammation. The underlying connective tissue was formed by muscle fibers with normal characteristics.

The histological findings 7 days after treatments (Figure 9) for the P-L-, P + L-, P-L+, and DNase groups contaminated with CaR were similar to those observed 24 h after treatments associated with damage in the muscular tissue. In the P + L+ and DNase+P + L+ groups, many hyphae and pseudohyphae were observed in the epithelium keratin layer, but the epithelial tissue remained with normal characteristics (Figure 9).

3.4 Microscopy fluorescence evaluation

The representative images from animals for P-L- group inoculated with CaS and CaR 24 h after the treatment (Figures 10, 11, respectively) showed a thick layer of biofilm (green) surrounded by polysaccharides (1–4 β-mannan and galacto) (red) produced by *C. albicans*. The images of DNase+P + L+ group presented similarity with NIC group once the polysaccharides (red) and fungal cells (green) were not labeled. The P + L+ group showed a small amount of biofilm (green) and polysaccharides (red) (Figures 10, 11).

After 7 days of the treatment for CaS and CaR (Figures 12, 13), the P-L- group was labeled with polysaccharides produced by *C. albicans* (red), with higher intensity of label in fungal cells (green) (Figures 12, 13). The DNase+P + L+ group of animals contaminated with CaS presented a small layer of *C. albicans* biofilm and polysaccharides (red color) (Figure 12). The P + L+ group demonstrated a slight presence of fungal biofilm (green) and polysaccharides (red color) (Figure 12). For CaR, the group DNase+P + L+ presented less biofilm and polysaccharides than the group treated only with PDZ-aPDT (P + L+ group) once there was a thick layer of CaR biofilm (green) surrounded by polysaccharides (red) (Figure 13).

4 Discussion

In vitro studies report the improved efficacy of PDZ-aPDT combined with DNase against *C. albicans* biofilms (Panariello et al., 2019; Abreu-Pereira et al., 2022). Enzymes decrease the integrity of the ECM by hydrolyzing proteins, polysaccharides, and nucleic acids. DNase I reduces biofilm stability, increasing the susceptibility of the biofilm to the action of antifungals and aPDT (Liao, 1974; Martins et al., 2012; Tetz and Tetz, 2016; Panariello et al., 2019; Abreu-Pereira et al., 2022). The current study investigated whether applying DNase I enzyme could potentiate PDZ-aPDT outcomes in mice infected by susceptible- and fluconazole-resistant *C. albicans*. Here, DNase I (20 units/mL) combined with PDZ-aPDT promoted antifungal effects against CaR in the oral lesions of mice with experimental oral candidiasis, and macroscopic analysis showed that 24 h after completion of treatment, the animals presented 96.7% remission of lesions. To our knowledge, no previous published study has investigated *in vivo* the efficacy of DNase I associated with aPDT in treating induced oral candidiasis in mice.

The results from mice inoculated with CaR showed that DNase I prior PDZ-aPDT promoted a reduction in viable colony counts by around 2.89 and 1.27 $\log_{10}$, respectively, immediately and 7 days after the treatments. In addition, the macroscopic oral lesions were reduced by around 96.07 and 75.24% 24 h and 7 days after the treatment, respectively. These results observed here corroborate with a previous study (Hidalgo et al., 2019), that evaluated the combination of PDZ (200 mg/L) mediated aPDT associated with nystatin in the treatment of mice infected with fluconazole-resistant *C. albicans* (ATCC 96901). Using the same methodology for induction of infection in mice, the

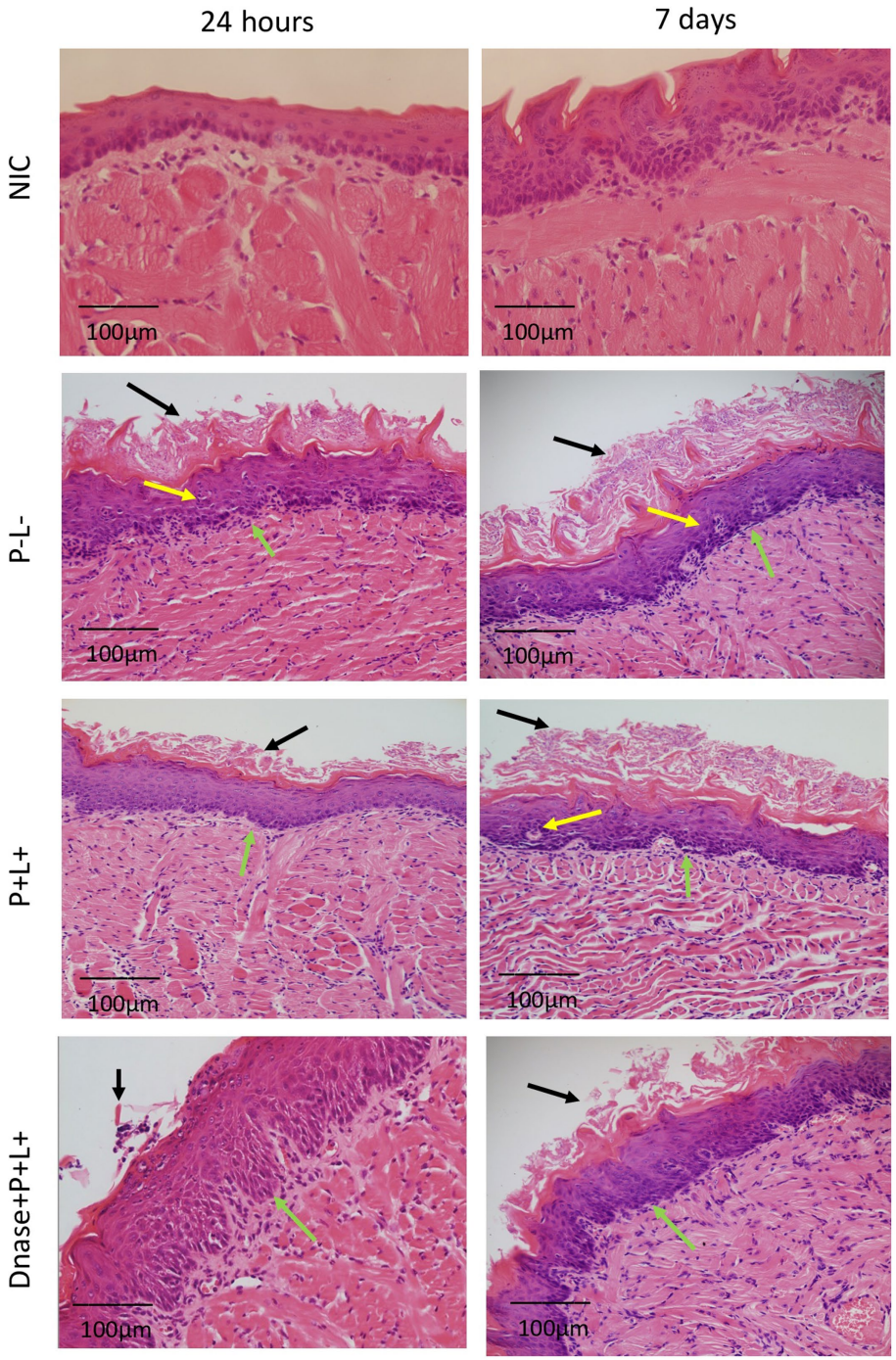

FIGURE 8
Representative images of the histological sections of tongues from mice inoculated with CaS and recovered 24 h and 7 days after the end of treatments. Muscle tissue was stained with hematoxylin–eosin (HE) (40X). Black arrow – keratin layer contaminated with hyphae and pseudohyphae; green arrow – lamina propria and yellow arrow – dilated blood vessels in response to the local inflammatory reaction.

combination of treatments reduced ~2.60 $\log_{10}$ the fungal viability and ~95% the macroscopic oral lesions 24 h after the treatment (Hidalgo et al., 2019). The results obtained after 7 days of the end treatment showed that nystatin combined with PDZ-aPDT promoted a reduction of ~1 $\log_{10}$ in fungal viability and macroscopic reduction in oral lesions by around ~50% (Hidalgo et al., 2019). Here, DNase yielded an outcome more favorable than nystatin in decreasing fungal viability and reducing the rate of lesion recurrence. Using alternative sources can lead to access to novel therapeutic agents with fewer side effects without the risk of antifungal resistance (Sandai et al., 2016; Torabi et al., 2022). DNase may be an adjuvant for biofilm treatments since it degrades eDNA in the extracellular matrix of biofilms (Rajendran et al., 2014; Hamblin and Abrahamse, 2019). Therefore, we suggest that DNase enabled PDZ diffusion in the extracellular matrix of biofilms, potentiating the effects of PDZ-aPDT and promoting the inactivation of biofilms *in vivo*.

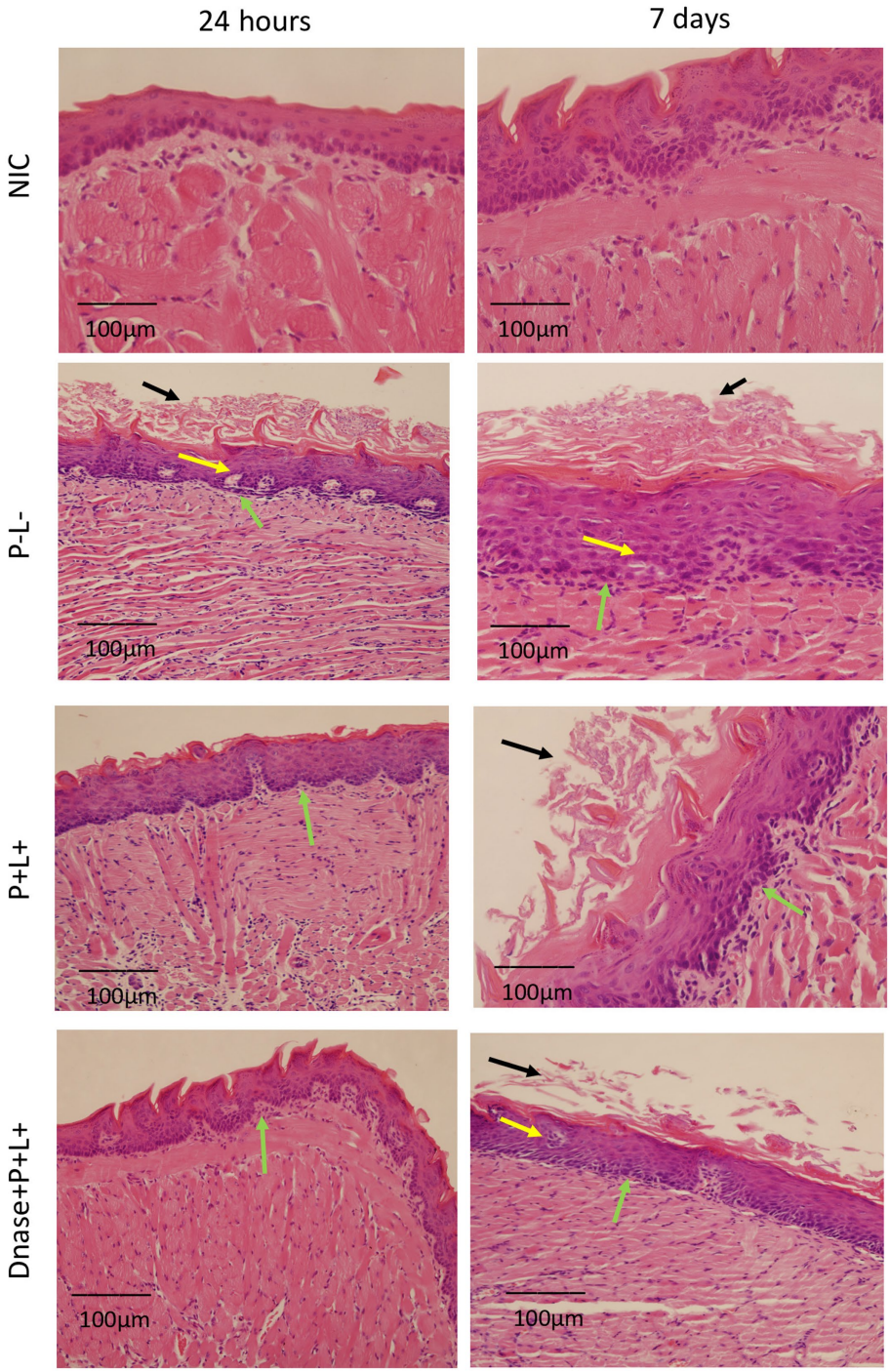

FIGURE 9
Representative images of the histological sections of tongues from mice inoculated with CaR and recovered 24 h and 7 days after the end of treatments. Muscle tissue was stained with hematoxylin–eosin (HE) (40X). Black arrow – keratin layer contaminated with hyphae and pseudohyphae; green arrow – lamina propria and yellow arrow – dilated blood vessels in response to local inflammatory reaction.

The enzyme associated with PDZ-aPDT reduced the fungal viability of CaS by around 4.26 and 1.97 log_{10}, respectively, immediately and 7 days after the treatments. In addition, there was a remission in the oral lesions, around 98.92 and 83.31%, respectively, after 24 h and 7 days. *In vivo* investigation (Carmello et al., 2015) demonstrated that five applications of PDZ-aPDT or antifungal nystatin promoted reductions in the cell viability of *C. albicans* (ATCC 90028) of 3 and 3.22 $logs_{10}$, respectively 24 h after the treatment (Carmello et al., 2016). After 7 days of treatment, a reduction of ~2 log_{10} for PDZ-aPDT and nystatin groups was observed (Carmello et al., 2016). Compared to antifungal, the lack of development of antimicrobial resistance increases further studies using aPDT (Hamblin and Abrahamse, 2019). Thus, our findings revealed that DNase improves aPDT

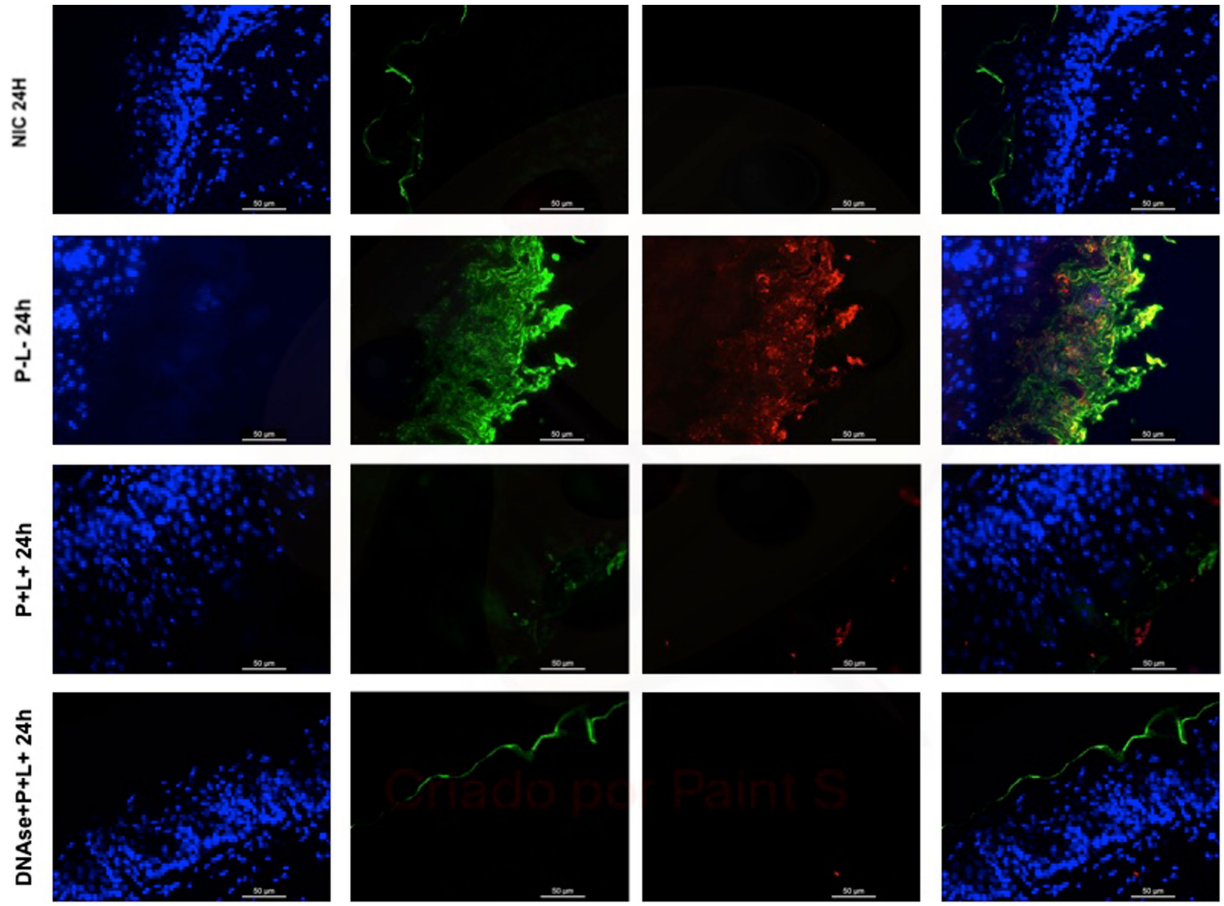

FIGURE 10
Representative fluorescence microscopy images of histological tongues sections recovered 24 h after treatments from the mice inoculated with CaS, labeled with Hoestch (first left column), concanavalin A conjugated with Alexa 488 nm (second column), and with primary antibody (1→4)-β-mannan and galacto-(1→4)-β-mannan (400–4) paired with secondary antibody conjugated with Alexa Fluoride 594 nm (third column). The tongue tissue cells (cell nucleus) were represented by the color blue. Fungal cells and matrix polysaccharides of *C. albicans* were represented by the colors green, and red, respectively. In the last column are the merged images.

outcomes, being a promising alternative for fungal inactivation, including resistant microorganisms.

DNase I (5 min) combined with PDZ-aPDT decreased the fungal viability in ~2.16 $\log_{10}$ and the levels of eDNA in the ECM of biofilms formed by fluconazole-susceptible *C. albicans* (ATCC 90028) (Panariello et al., 2019). When fluconazole-resistant *C. albicans* biofilms were treated with DNase prior to the PDZ-aPDT, there was a decrease of ~1.92 $\log_{10}$ in the fungal viability, water-soluble polysaccharides (36.3%), and eDNA (72.3%) (Abreu-Pereira et al., 2022). Here, the fluorescence microscopy images of histological tongue sections 24 h after treatment demonstrated that DNase I before PDZ-aPDT promoted a reduction in fungal polysaccharides, similar to healthy animals (NIC). After 7 days of the treatment, the presence of polysaccharides was observed only in mice infected by fluconazole-resistant *C. albicans*. Still, the fungal viable count was smaller than that in the PDZ-aPDT group. Thus, DNase treatment reduced the fungal polysaccharides *in vitro* (Panariello et al., 2019; Abreu-Pereira et al., 2022) and in the animal model here. Among the components present in the ECM, eDNA, associated with β-glucans and β-mannans, contributes to the organizational integrity of biofilms and antifungal tolerance of *C. albicans* (Martins et al., 2012; Rajendran et al., 2014; Mitchell et al., 2016). Some reports found an association between eDNA levels and increased microbial resistance to antibiotics (Rice et al., 2007; da Silva et al., 2008). Therefore, disrupting the ECM and reducing eDNA levels of *C. albicans* biofilms are essential to optimize antifungal therapies.

The histological sections of the tongues recovered after the treatment with DNase before PDZ-aPDT for both strains (CaS and CaR) demonstrated histological characteristics similar to those of the NIC group (healthy animals). The tissues presented a reduced amount of hyphae/pseudohyphae/blastopore on the keratin layer, minor inflammation in the subjacent connective tissue, and intact muscle tissue. In a previous study, mice treated with 5 applications of nystatin associated with PDZ-aPDT presented normal histological characteristics, which are outcomes very similar to those observed in the present study (Hidalgo et al., 2019). In addition, the inoculation of mice with fluconazole-resistant *C. albicans* promoted an intense inflammatory response in the subjacent connective tissue (Alves et al., 2018; Hidalgo et al., 2019) and 5 applications of PDZ-aPDT decreased an inflammatory reaction from intense to mild (Hidalgo et al., 2019). Here, the control groups (P-L-, P + L-, P-L+, and DNase) 24 h after the treatment presented a large area of hyphae/pseudohyphaes covering

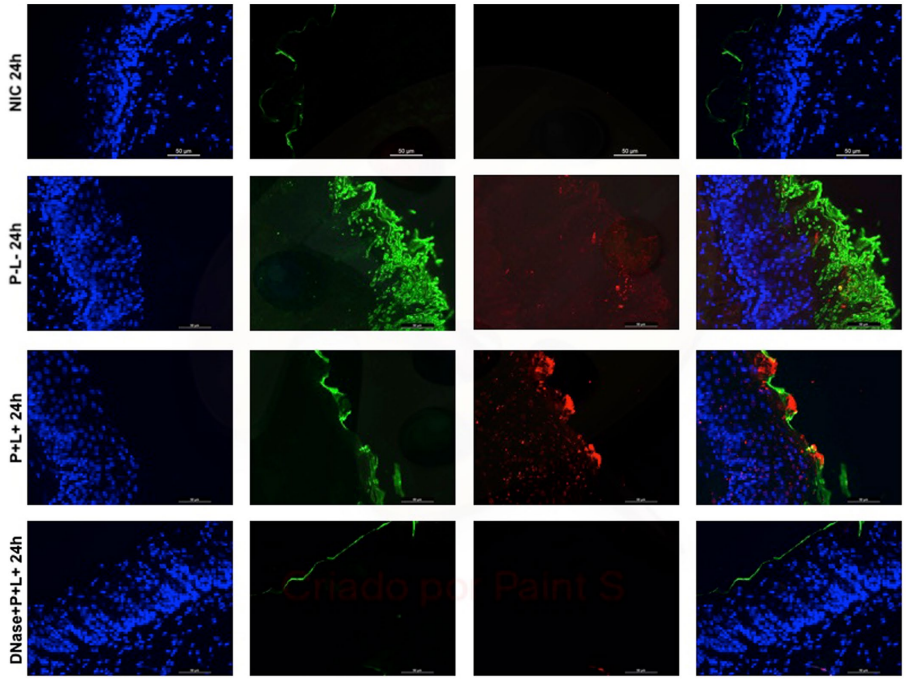

FIGURE 11
Representative fluorescence microscopy images of histological tongues sections recovery 24 h after the treatments from the mice inoculated with CaR, labeled with Hoestch (first left column), concanavalin A conjugated with Alexa 488 nm (second column), and with primary antibody (1 → 4)-β-mannan and galacto-(1 → 4)-β-mannan (400–4) paired with secondary antibody conjugated with Alexa Fluoride 594 nm (third column). The tongue tissue cells (cell nucleus) were represented by the color blue. Fungal cells and matrix polysaccharides of *C. albicans* were represented by the colors green and red, respectively. In the last column are the merged images.

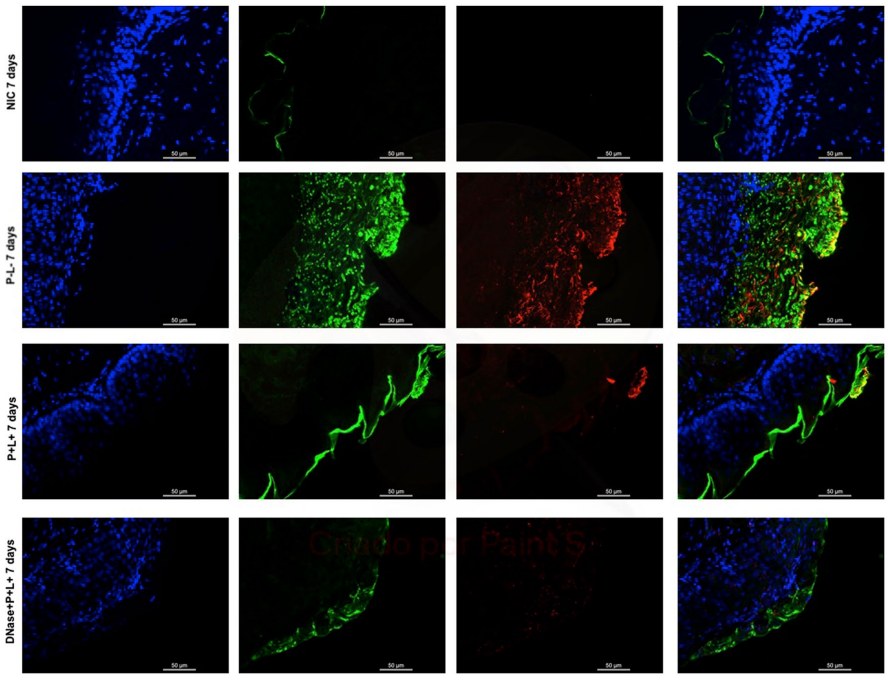

FIGURE 12
Representative fluorescence microscopy images of histological tongues sections recovered 7 days after the end of treatments from the mice inoculated with CaS, labeled with Hoestch (first left column), concanavalin A conjugated with Alexa 488 nm (second column), and with primary antibody (1 → 4)-β-mannan and galacto-(1 → 4)-β-mannan (400–4) paired with secondary antibody conjugated with Alexa Fluoride 594 nm (third column). The tongue tissue cells (cell nucleus) were represented by the color blue. Fungal cells and matrix polysaccharides of *C. albicans* were represented by the colors green and red, respectively. In the last column are the merged images.

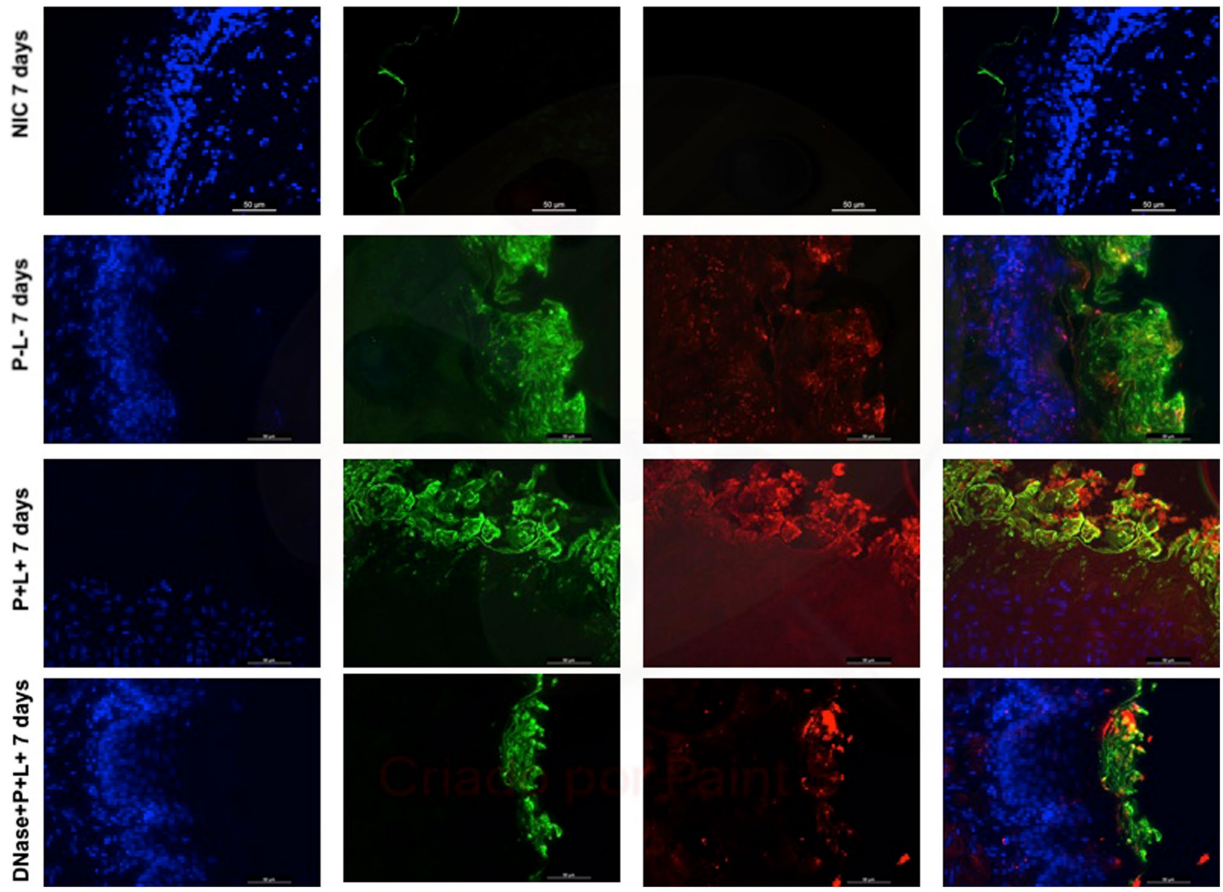

FIGURE 13
Representative fluorescence microscopy images of histological tongues sections recovery 7 days after the end of treatments from the mice inoculated with CaR, labeled with Hoestch (first left column), concanavalin A conjugated with Alexa 488 nm (second column), and with primary antibody (1 → 4)-β-mannan and galacto-(1 → 4)-β-mannan (400–4) paired with secondary antibody conjugated with Alexa Fluoride 594 nm (third column). The tongue tissue cells (cell nucleus) were represented by the color blue. Fungal cells and matrix polysaccharides of *C. albicans* were represented by green and red, respectively. In the last column are the merged images.

the epithelial tissue, which demonstrated acanthosis associated with the papillae destruction.

Moreover, there is an intense inflammation of the epithelium with dilated blood vessels. Seven days after the treatments, the muscle fibers were partially degraded in the superficial region of the tissue in the control groups (P-L-, P + L-, and P-L+ groups). In the sections from animals inoculated with CaR, 7 days after the end of treatment, there were hyphae and pseudohyphae on the keratin layer, suggesting recurrence of the oral infection in the DNase+P + L+ group, but its keratin layer was smaller than that observed for P + L+ group. Furthermore, in the PDZ-aPDT group, there was a return in the oral lesions. Our results demonstrated that DNase before PDZ-aPDT reduces the lesion recurrence rate after 7 days compared to other treatments for fluconazole-resistant *C. albicans*. Therefore, DNase I affected the biofilm composition and hampered the new formation of *C. albicans* biofilm, probably because the complete epithelial restructuring was promoted in the groups treated with DNase+P + L+.

The overall increased occurrences of pathogens resistant to conventional antifungals and the toxicity of drugs have motivated searches for strategies to inactivate fungal species. In addition, the ECM of *C. albicans* biofilms limits the penetration of antimicrobials, antiseptics, and photosensitizers, influencing the efficacy of aPDT and other fungal therapies. In summary, DNase before PDZ-aPDT promoted expressive outcomes by reducing fungal viability and healing the oral lesions in mice. Therefore, this study further demonstrates that DNase is a promising alternative adjuvant for fungal photoinactivation *in vivo* of antifungal-susceptible and -resistant strains.

Data availability statement

The original contributions presented in the study are included in the article/supplementary material, further inquiries can be directed to the corresponding author.

Ethics statement

The animal studies were approved by Animal Ethics Committee of the School of Dentistry of Araraquara, UNESP (Case number: 09/2020). The studies were conducted in accordance with the local legislation and institutional requirements.

Author contributions

CJ: Conceptualization, Data curation, Formal analysis, Funding acquisition, Investigation, Methodology, Validation, Visualization, Writing – original draft, Writing – review & editing. MK: Conceptualization, Validation, Writing – review & editing. PB: Methodology, Writing – review & editing. EM: Writing – review & editing. TS: Methodology, Writing – review & editing. TF: Formal analysis, Methodology, Writing – review & editing. AP: Conceptualization, Data curation, Formal analysis, Funding acquisition, Investigation, Project administration, Resources, Visualization, Writing – original draft, Writing – review & editing.

Funding

The author(s) declare financial support was received for the research, authorship, and/or publication of this article. This work was based on the PhD Thesis of the author CJ. This work was supported by the São Paulo Research Foundation [FAPESP #2013/07276-1 (RIDC) and #2020/09332-0] and scholarship (FAPESP #2019/27634-6 to CJ and #2021/01191-0 to TF). Additional financial support was provided by the National Council for Scientific and Technological Development (CNPq #304787/2020-5) and PROPG-UNESP (# 69/2023-3032).

Conflict of interest

The authors declare that the research was conducted in the absence of any commercial or financial relationships that could be construed as a potential conflict of interest.

Publisher's note

All claims expressed in this article are solely those of the authors and do not necessarily represent those of their affiliated organizations, or those of the publisher, the editors and the reviewers. Any product that may be evaluated in this article, or claim that may be made by its manufacturer, is not guaranteed or endorsed by the publisher.

References

Abreu-Pereira, C. A., Klein, M. I., Lobo, C. I. V., Gorayb Pereira, A. L., Jordão, C. C., and Pavarina, A. C. (2022). DNase enhances photodynamic therapy against fluconazole-resistant *Candida albicans* biofilms. *Oral Dis.* 29, 1855–1867. doi: 10.1111/odi.14149

Akpan, A., and Morgan, R. (2002). Oral candidiasis. *Postgrad. Med. J.* 78, 455–459. doi: 10.1136/pmj.78.922.455

Al-Fattani, M. A., and Douglas, L. J. (2006). Biofilm matrix of *Candida albicans* and *Candida tropicalis*: chemical composition and role in drug resistance. *J. Med. Microbiol.* 55, 999–1008. doi: 10.1099/jmm.0.46569-0

Alves, F., Carmello, J. C., Mima, E. G. O., Costa, C. A. S., Bagnato, V. S., and Pavarina, A. C. (2018). Photodithazine-mediated antimicrobial photodynamic therapy against fluconazole-resistant *Candida albicans in vivo*. *Med. Mycol.* 57, 609–617. doi: 10.1093/mmy/myy083

Anderson, G. G., and O'Toole, G. A. (2008). Innate and induced resistance mechanisms of bacterial biofilms. *Curr. Top. Microbiol. Immunol.* 322, 85–105. doi: 10.1007/978-3-540-75418-3_5

Bonnett, R., and Martínez, G. (2001). Photobleaching of sensitisers used in photodynamic therapy. *Tetrahedron* 57, 9513–9547. doi: 10.1016/S0040-4020(01)00952-8

Campoy, S., and Adrio, J. L. (2017). Antifungals. *Biochem. Pharmacol.* 133, 86–96. doi: 10.1016/j.bcp.2016.11.019

Carmello, J. C., Alves, F., Basso, F. G., de Souza Costa, C. A., Bagnato, V. S., Mima, E. G. O., et al. (2016). Treatment of oral candidiasis using Photodithazine®- mediated photodynamic therapy *in vivo*. *PLoS One* 11:e0156947. doi: 10.1371/journal.pone.0156947

Carmello, J. C., Dovigo, L. N., Mima, E. G., Jorge, J. H., de Souza Costa, C. A., Bagnato, V. S., et al. (2015). *In vivo* evaluation of photodynamic inactivation using Photodithazine® against *Candida albicans*. *Photochem. Photobiol. Sci.* 14, 1319–1328. doi: 10.1039/c4pp00368c

Chazotte, B. (2011). Labeling nuclear DNA with hoechst 33342. *Cold Spring Harb. Protoc.* 2011 doi: 10.1101/pdb.prot5557

da Silva, W. J., Seneviratne, J., Parahitiyawa, N., Rosa, E. A., Samaranayake, L. P., and Del Bel Cury, A. A. (2008). Improvement of XTT assay performance for studies involving *Candida albicans* biofilms. *Braz. Dent. J.* 19, 364–369. doi: 10.1590/S0103-64402008000400014

Donnelly, R. F., McCarron, P. A., and Tunney, M. M. (2008). Antifungal photodynamic therapy. *Microbiol. Res.* 163, 1–12. doi: 10.1016/j.micres.2007.08.001

Eggimman, P., Garbino, J., and Pittet, D. (2003). Epidemiology of *Candida* species infections in critically ill non-imunossupressed patients. *Lancet Infect. Dis.* 3, 685–702. doi: 10.1016/S1473-3099(03)00801-6

El-Habashi, A., El-Morsi, B., Freeman, S. M., El-Didi, M., Aizen, J., and Marrogi, M. D. (1995). Tumor oncogenic expression in malignant effusions as a possible method to enhance cytologic diagnostic sensitivity: an immunocytochemical study of 87 cases. *Pathol. Patterns* 103, 206–214. doi: 10.1093/ajcp/103.2.206

Falsetta, M. L., Klein, M. I., Colonne, P. M., Scott-Anne, K., Gregoire, S., Pai, C. H., et al. (2014). Symbiotic relationship between *Streptococcus mutans* and *Candida albicans* synergizes virulence of plaque bio- films *in vivo*. *Infect. Immun.* 82, 1968–1981. doi: 10.1128/IAI.00087-14

Flemming, H. C., Neu, T. R., and Wozniak, D. J. (2007). The EPS matrix: the "house of biofilm cells". *J. Bacteriol.* 189, 7945–7947. doi: 10.1128/JB.00858-07

Hamblin, M. R., and Abrahamse, H. (2019). Can light-based approaches overcome antimicrobial resistance? *Drug Dev. Res.* 80, 48–67. doi: 10.1002/ddr.21453

Hidalgo, K. J. R., Carmello, J. C., Jordão, C. C., Barbugli, P. A., Costa, C. A. S., Mima, E. G. O., et al. (2019). Antimicrobial photodynamic therapy in combination with nystatin in the treatment of experimental oral candidiasis induced by *Candida albicans* resistant to fluconazole. *Pharmaceuticals* 12:pii: E140. doi: 10.3390/ph12030140

Konopka, K., and Goslinski, T. (2007). Photodynamic therapy in dentistry. *J. Dent. Res.* 86, 694–707. doi: 10.1177/154405910708600803

Kumar, S., Kumar, A., Roudbary, M., Mohammadi, R., Černáková, L., and Rodrigues, C. F. (2022). Overview on the infections related to rare *Candida* species. *Pathogens* 11:963. doi: 10.3390/pathogens11090963

Lambrechts, S. A. G., Aalders, M. C. G., and Van Marle, J. (2005). Mechanistic study of the photodynamic inactivation of *Candida albicans* by cationic porphyrin. *Antimicrob. Agents Chemother.* 49, 2026–2034. doi: 10.1128/AAC.49.5.2026-2034.2005

Liao, T. H. (1974). Bovine pancreatic deoxyribonuclease D. *J. Biol. Chem.* 249, 2354–2356. doi: 10.1016/S0021-9258(19)42737-3

Lobo, C. I. V., Rinaldi, T. B., Christiano, C. M. S., De Sales, L. L., Barbugli, P. A., and Klein, M. I. (2019). Dual-species biofilms of *Streptococcus mutans* and *Candida albicans* exhibit more biomass and are mutually beneficial compared with single-species biofilms. *J. Oral Microbiol.* 11:1581520. doi: 10.1080/20002297.2019.1581520

Machado, A. E. H. (2000). Terapia fotodinâmica: princípios, potencial de aplicação e perspectivas. *Quím Nova* 23, 237–243. doi: 10.1590/S0100-40422000000200015

Martins, M., Henriques, M., Lopez-Ribot, J. L., and Oliveira, R. (2012). Addition of DNase improves the *in vitro* activity of antifungal drugs against *Candida albicans* biofilms. *Mycoses* 55, 80–85. doi: 10.1111/j.1439-0507.2011.02047.x

Martins, M., Uppuluri, P., Thomas, D. P., Cleary, I. A., Henriques, M., Lopez-Ribot, J. L., et al. (2010). Presence of extracellular DNA in the *Candida albicans* biofilm matrix and its contribution to biofilms. *Mycopathologia* 169, 323–331. doi: 10.1007/s11046-009-9264-y

Mitchell, K. F., Zarnowski, R., and Andes, D. R. (2016). Fungal super glue: the biofilm matrix and its composition, assembly, and functions. *PLoS Pathog.* 12:e1005828. doi: 10.1371/journal.ppat.1005828

Mulcahy, H., Charron-Mazenod, L., and Lewenza, S. (2008). Extracellular DNA chelates cations and induces antibiotic resistance in *Pseudomonas aeruginosa* biofilms. *PLoS Pathog.* 4:e1000213. doi: 10.1371/journal.ppat.1000213

Nett, J., Lincoln, L., Marchillo, K., Massey, R., Holoyda, K., Hoff, B., et al. (2007). Putative role of beta-1, 3 glucans in *Candida albicans* biofilm resistance. *Antimicrob. Agents Chemother.* 51, 510–520. doi: 10.1128/AAC.01056-06

Nobile, C. J., Schneider, H. A., Nett, J. E., Sheppard, D. C., Filler, S. G., Andes, D. R., et al. (2008). Complementary adhesin function in *C. albicans* biofilm formation. *Curr. Biol.* 18, 1017–1024. doi: 10.1016/j.cub.2008.06.034

Panariello, B. H. D., Klein, M. I., Alves, F., and Pavarina, A. C. (2019). DNase increases the efficacy of antimicrobial photodynamic therapy on *Candida albicans* biofilms. *Photodiagn. Photodyn. Ther.* 27, 124–131. doi: 10.1016/j.pdpdt.2019.05.038

Perezous, L. F., Flaitz, C. M., Goldschmidt, M. E., and Engelmeier, R. L. (2005). Colonization of *Candida species* in denture wearers with emphasis on HIV infection: a literature review. *J. Prosthet. Dent.* 93, 288–293. doi: 10.1016/j.prosdent.2004.11.015

Rajendran, R., Sherry, L., Lappin, D. F., Nile, C. J., Smith, K., Williams, C., et al. (2014). Extracellular DNA release confers heterogeneity in *Candida albicans* biofilm formation. *BMC Microbiol.* 14:303. doi: 10.1186/s12866-014-0303-6

Rice, K. C., Mann, E. E., Endres, J. L., Weiss, E. C., Cassat, J. E., Smeltzer, M. S., et al. (2007). The cid a murein hydrolase regulator contributes to DNA release and biofilm development in *Staphylococcus aureus*. *Proc. Natl. Acad. Sci. U. S. A.* 104, 8113–8118. doi: 10.1073/pnas.0610226104

Sandai, D., Tabana, Y. M., Ouweini, A. E., and Ayodeji, I. O. (2016). Resistance of *Candida albicans* biofilms to drugs and the host immune system. *Jundishapur J Microbiol.* 9:e37385. doi: 10.5812/jjm.37385

Seneviratne, C. J., Jin, L. J., Samaranayake, Y. H., and Samaranayake, L. P. (2008). Cell density and cell aging as factors modulating antifungal resistance of *Candida albicans* biofilms. *Antimicrob. Agents Chemother.* 52, 3259–3266. doi: 10.1128/AAC.00541-08

Takakura, N., Sato, Y., Ishibashi, H., Oshima, H., Uchida, K., Yamaguchi, H., et al. (2003). A novel murine model of oral candidiasis with local symptoms characteristic of oral thrush. *Microbiol. Immunol.* 47, 321–326. doi: 10.1111/j.1348-0421.2003.tb03403.x

Tetz, V., and Tetz, G. (2016). Effect of deoxyribonuclease I treatment for dementia in end-stage Alzheimer's disease: a case report. *J. Med. Case Rep.* 10:131. doi: 10.1186/s13256-016-0931-6

Torabi, I., Sharififar, F., Izadi, A., and Ayatollahi Mousavi, S. A. (2022). Inhibitory effects of different fractions separated from standardized extract of *Myrtus communis* L. against nystatin-susceptible and nystatin-resistant *Candida albicans* isolated from HIV positive patients. *Heliyon* 8:e09073. doi: 10.1016/j.heliyon.2022.e09073

Wartenberg, A., Linde, J., Martin, R., Schreiner, M., Horn, F., Jacobsen, I. D., et al. (2014). Microevolution of *Candida albicans* in macrophages restores filamentation in a nonfilamentous mutant. *PLoS Genet.* 10:e1004824. doi: 10.1371/journal.pgen.1004824

frontiers | Frontiers in Microbiology

TYPE Original Research
PUBLISHED 02 February 2024
DOI 10.3389/fmicb.2024.1340585

OPEN ACCESS

EDITED BY
Cindy Shuan Ju Teh,
University of Malaya, Malaysia

REVIEWED BY
Laurent Roberto Chiarelli,
University of Pavia, Italy
Alok Kumar Singh,
Johns Hopkins Medicine, United States

*CORRESPONDENCE
Elisabetta Buommino
✉ elisabetta.buommino@unina.it
Margherita Brindisi
✉ margherita.brindisi@unina.it

†These authors share last authorship

RECEIVED 18 November 2023
ACCEPTED 10 January 2024
PUBLISHED 02 February 2024

CITATION
Barone S, Mateu B, Turco L, Pelliccia S, Lembo F, Summa V, Buommino E and Brindisi M (2024) Unveiling the modulation of *Pseudomonas aeruginosa* virulence and biofilm formation by selective histone deacetylase 6 inhibitors.
Front. Microbiol. 15:1340585.
doi: 10.3389/fmicb.2024.1340585

Unveiling the modulation of *Pseudomonas aeruginosa* virulence and biofilm formation by selective histone deacetylase 6 inhibitors

Simona Barone[1], Baptiste Mateu[1], Luigia Turco[1,2], Sveva Pelliccia[1], Francesca Lembo[1], Vincenzo Summa[1], Elisabetta Buommino[1*†] and Margherita Brindisi[1*†]

[1]Department of Pharmacy, University of Naples Federico II, Naples, Italy, [2]Department of Precision Medicine, University of Campania Luigi Vanvitelli, Naples, Italy

Bacterial infections represent a key public health issue due to the occurrence of multidrug-resistant bacteria. Recently, the amount of data supporting the dynamic control of epigenetic pathways by environmental cues has triggered research efforts toward the clarification of their role in microbial infections. Among protein post-translational modifications, reversible acetylation is the most implicated in the feedback to environmental stimuli and in cellular homeostasis. Accordingly, the latest studies identified the histone deacetylase 6 (HDAC6) enzyme as a crucial player in the complex molecular machinery underlying bacterial clearance or killing. A very important milestone for the elucidation of the consequence of HDAC6 activity in bacterial infections is herein described, unveiling for the first time the role of a potent HDAC6 inhibitor in interfering with biofilm formation and modulating virulence factors of *P. aeruginosa*. We demonstrated that compound F2F-2020202 affected the production of some important virulence factors in *P. aeruginosa*, namely pyocyanin and rhamnolipids, clearly impairing its ability to form biofilm. Furthermore, evidence of possible QS involvement is supported by differential regulation of specific genes, namely RhlI, phAz1, and qsrO. The data herein obtained also complement and in part explain our previous results with selective HDAC6 inhibitors able to reduce inflammation and bacterial load in chronic infection models recapitulating the cystic fibrosis (CF) phenotype. This study fosters future in-depth investigation to allow the complete elucidation of the molecular mechanisms underlying HDAC6's role in bacterial infections.

KEYWORDS

antimicrobial resistance, *Pseudomonas aeruginosa*, bacterial biofilm, HDAC6 inhibitors, cystic fibrosis

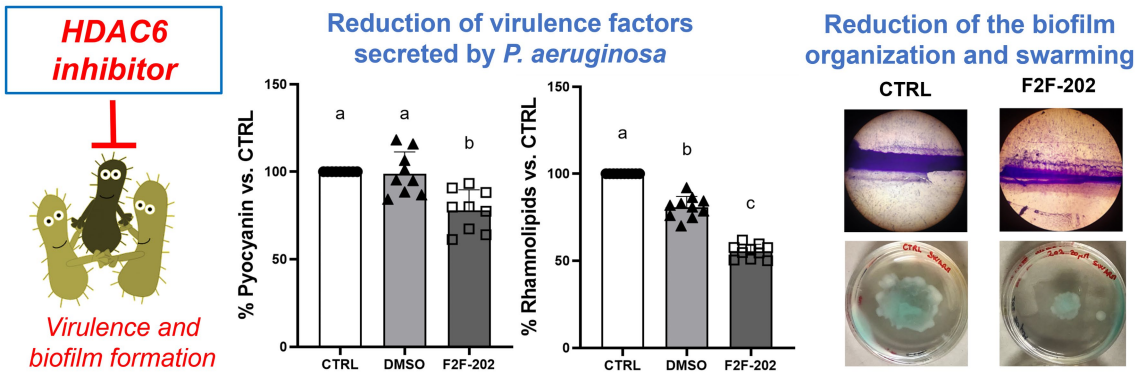

GRAPHICAL ABSTRACT

Introduction

Bacterial infections represent a very serious public health threat due to the emergence of multidrug-resistant bacteria. Common antibiotics are no longer successful against several different microbial species, such as those belonging to the "ESKAPE" pathogens group (Pendleton et al., 2013).

P. aeruginosa and *S. aureus*, including methicillin-resistant *S. aureus* [MRSA], are most frequently isolated from the sputum of patients with cystic fibrosis (CF), a genetic disorder commonly involving polymicrobial infections in the respiratory tract with a different distribution in the course of the disease. Predominant bacterial species that colonize CF lung at the early stages of CF include *S. aureus* and *Haemophilus influenzae*, whereas *P. aeruginosa* and the *Burkholderia cepacia* complex are mainly present in the later stages of the disease (Malhotra et al., 2019).

Several virulence factors generated by *P. aeruginosa* play a major role in chronic respiratory infections, and alginate overproduction may drive *P. aeruginosa* coinfection with *S. aureus*. At the same time, both bacteria display a range of competitive and cooperative interactions (Limoli and Hoffman, 2019). Since *P. aeruginosa* and *S. aureus* are common in CF lung, molecules targeting these pathogens or mechanisms associated with their virulence can be relevant in the treatment of polymicrobial infections in pulmonary disease.

Quorum sensing (QS), a cell density-based intercellular communication network, displays key importance in the control of bacterial resistance and virulence, and biofilm formation during bacterial infections. *P. aeruginosa* uses three main quorum sensing (QS) systems, namely Las, Rhl, and Pqs, controlling the production of virulence factors, including proteases and exoenzymes, allowing the bacteria to trigger the infection process in the host tissue (Garcia-Reyes et al., 2020).

Pyocyanin is a key virulence factor generated and profusely secreted by approximately 95% of *P. aeruginosa* isolates, and it has been demonstrated to be essential for full virulence in animal and human airway infection models (Caldwell et al., 2009; Rada and Leto, 2013). Pyocyanin is a phenazine that can cross biological membranes, allowing *P. aeruginosa* to receive and transport electrons arising from the respiration process and to survive in oxygen-limited environments; in the biofilm, pyocyanin creates a redox potential gradient that enhances iron bioavailability, a key factor for biofilm formation. Molecules able to contrast biofilm formation are of great interest in CF disease. Bacteria embedded in the biofilm are safeguarded against immune system responses, contributing to the establishment of a chronic inflammatory status characterized by mucus hypersecretion and abnormal neutrophil recruitment, major factors contributing to pulmonary manifestations of CF patients (Cohen and Prince, 2012). Finally, several pieces of evidence highlight the detrimental effects of pyocyanin on the host immune function, including dodging of defense mechanisms, modulation of multidrug efflux pump expression in *P. aeruginosa* biofilm, and antibiotic resistance (Raju et al., 2018). Thus, the reduction of pyocyanin production may affect the virulence potential of *P. aeruginosa* during airway infections in CF, and pyocyanin could represent a promising target for developing new therapeutic options against *P. aeruginosa* infection.

Recently, the dynamic regulation of epigenetic players by environmental cues emerged as a key factor in bacterial infections and stimulated increasing research efforts toward the clarification of the role of epigenetic players in the infection process (Grabiec and Potempa, 2018). Among protein post-translational modifications, reversible acetylation is the most implicated in the feedback to environmental stimuli and in cellular homeostasis. In this context, the histone deacetylase (HDAC) class of enzymes has been unveiled as key players in the multifaceted molecular mechanisms underlying bacterial clearance or killing.

The QS signal generated by *P. aeruginosa*, namely 2-AA, triggered the reprogramming of immune cells accompanied by increased HDAC1 expression in human THP-1 monocytes. The process was fully reverted by HDAC1 inhibition, thus clearly demonstrating the involvement of this isoform in endorsing tolerance to *P. aeruginosa* (Bandyopadhaya et al., 2016).

As previously stated, metabolites generated by pathogenic bacteria are also able to influence the host acetylation system. Accordingly, it has been shown that short-chain fatty acids (SCFAs) such as propionic and butyric acids secreted by anaerobic bacteria are able to inhibit class I/II HDACs, thus modulating different pathways of immune response (Correa-Oliveira et al., 2016).

Later on, HDAC6 isoform gained increasing attention, since its key role in infection was shown, with particular reference to the immune response associated with the infection process (Hamon and Cossart, 2008; Bierne et al., 2012). HDAC6 differs from other isoforms due to its exclusive cytoplasmic localization (other isoforms mainly reside in the nucleus), which, of course, implies that its substrates are cytoplasmic proteins such as α-tubulin, HSP90, and cortactin.

Moreover, in contrast to other HDAC isoforms, HDAC6 features two catalytic domains (Brindisi et al., 2020; Barone et al., 2022).

Accordingly, in 2015, it was demonstrated that only the HDAC6-selective inhibitor TubA and not MS-275, which specifically inhibits class I HDACs, enhanced bacterial killing by macrophages (Ariffin et al., 2015). Similar studies also showed that selective HDAC6 inhibition triggered bacterial clearance, reduced the formation of pro-inflammatory cytokines, reestablished the population of innate immune cells in the bone marrow, and enhanced survival in a sepsis mouse model (Li et al., 2015; Zhao et al., 2016).

This evidence, coupled with the data connecting HDAC6 to the modulation of mitochondrial activity and to the triggering of mitochondrial ROS production, supports a key function for HDAC6 in the regulation of bacterial clearance (Chen et al., 2008; Kamemura et al., 2012; Bai et al., 2015), which strongly differentiates HDAC6 isoform from class I HDACs.

In particular, HDAC6 inhibitors can modulate infection by triggering innate immune-mediated bacterial clearance and/or reducing the damage ascribable to the robust inflammation process associated with the infection. Moreover, these data validate the use of HDAC6-selective inhibitors as an innovative therapeutic option for the treatment of airway chronic inflammation.

To further support this evidence, the outcome of *Hdac6* depletion on both the CF inflammatory response and the bacterial load was recently examined in a model of chronic infection using clinical *P. aeruginosa* to recapitulate the CF phenotype. The loss of *Hdac6* led to increased bacterial clearance in CF mice, thus reestablishing responses to bacterial challenge. Moreover, *Hdac6* depletion limited weight loss and modulated neutrophil recruitment, further validating the benefits of HDAC6-selective inhibitors in diseases featuring chronic airway inflammation, such as CF (Rosenjack et al., 2019). We recently confirmed these data through pharmacological inhibition of HDAC6, demonstrating for the first time the efficacy in reducing bacterial load and inflammatory markers in a mouse model of chronic *P. aeruginosa* infection (Brindisi et al., 2022).

While the role of the so-called acetylome enzymes in bacterial infections is being increasingly explored and clarified, still little information is available on their role in the regulation of virulence and QS processes (Grabiec and Potempa, 2018).

We herein unveil for the first time the role of a very potent and selective HDAC6 inhibitor in the modulation of QS and biofilm formation in *P. aeruginosa*. We demonstrated that F2F-2020202 affected the production of important virulence factors in *P. aeruginosa*, namely pyocyanin and rhamnolipids, clearly impairing its ability to form biofilm. Furthermore, evidence of possible QS involvement is supported by differential regulation of specific genes, namely RhlI, phAz1, and qsrO. The implication of such results is discussed.

Materials and methods

Chemicals

F2F-2020202 is a small molecule (chemical formula $C_{36}H_{45}N_5O_6$, MW = 643 g/mol) designed and synthesized at the Department of Pharmacy, University of Naples Federico II. It displays high potency on HDAC6 (IC_{50} = 4.1 nM) and high isoform selectivity over HDAC1, as a representative of nuclear HDAC isoforms (IC_{50} = 2292.0 nM), with a selectivity index (SI) of 422. The molecule is currently subject to a patent application. Antibiotics were purchased from Sigma-Aldrich (Milan, Italy).

Strains

Pseudomonas aeruginosa ATCC 27853 and *P. aeruginosa* PAO1 (ATCC BAA-47-B1) were obtained from the American Type Culture Collection (Rockville, MD). Each tested compound was dissolved in 100 µL DMSO to give a stock solution (40 mM) and diluted in Mueller-Hinton (MH). Upon sequential dilution, the final DMSO concentration in the assays was well below 2% since literature data demonstrate that 2% DMSO in the assay can modulate QS-associated virulence factors in *P. aeruginosa* (Guo et al., 2016).

Bacteria antimicrobial susceptibility testing

The minimal inhibitory concentration (MIC) of all the compounds was determined in Mueller–Hinton medium (MH) by the broth microdilution assay, following the procedure already described (Buommino et al., 2021). The compounds were added to bacterial suspension in each well, yielding a final cell concentration of 1×10^6 CFU/mL and a final compound concentration ranging from 3.25 to 100 µM. Negative control wells were set to contain bacteria in Mueller–Hinton broth plus the amount of vehicle (DMSO) used to dilute each compound. Positive controls included 2 µg/mL of tobramycin (TOB 4.27 µM). All antibiotic concentrations reported are according to breakpoint values reported in the EUCAST v.12.0 (The European Committee on Antimicrobial Susceptibility Testing, 2022). The MIC was defined as the lowest concentration of the drug that caused a total inhibition of microbial growth after 24 h incubation time at 37°C. Medium turbidity was measured by a microtiter plate reader (Thermo Scientific Multiskan GO, Waltham, MA, United States) at 595 nm. All the tests were conducted at least three times using independent cell suspensions.

Motility inhibition assays

Swimming and swarming motilities were performed following a published procedure (Zhou et al., 2018). Briefly, 2 µL of overnight *P. aeruginosa* PAO1 cultures (OD 620 = 0.5) treated with 30 µM compound F2F-2020202 was inoculated at the center of the swimming agar (1% tryptone, 0.5% NaCl, 0.3% agar, pH 7.2) and swarming agar medium (1% tryptone, 0.5% NaCl, 0.5% glucose, 0.5% agar, pH 7.2), respectively. DMSO (0.15%) was used as a negative control. Plates were incubated at 37°C overnight, and migration was then evaluated.

Biofilm inhibition assay

Crystal violet assay

The assay was performed following two procedures, both employing the final crystal violet (CV) staining. First, the assay was conducted in glass test tubes (13×100 mm) as described by Yamamoto et al., with some modifications. Briefly, compound F2F-2020202 was added at a final concentration of 30 µM, at which no growth inhibition was observed, to

a volume of 3 mL of medium containing 10^6 CFU/mL of *P. aeruginosa* PAO1 strain. Control cells were grown in medium broth alone. Negative controls were set to contain bacteria in Mueller–Hinton broth (MH) plus the amount of vehicle (DMSO) used to dilute the compound. After culturing for 24 h at 37°C, the supernatant was gently removed, and the tubes were rinsed with 3 mL of PBS. The biofilm biomass was then measured by staining with 3 mL of 0.1% crystal violet, ensuring that the formed ring pellicle was covered. After 30 min of incubation, the crystal violet was removed, and the biofilm biomass was quantified by adding ethanol (EtOH) 100%. The absorbance was measured at 620 nm using a microtiter plate reader (Thermo Scientific Multiskan GO, Waltham, MA, United States). The percentage of growth inhibition was determined using the following formula: % of biofilm inhibition = ((Control OD – [compound F2F-2020202 or DMSO OD])/Control OD) × 100. [Control represents MH with bacterial inoculum alone]).

P. aeruginosa tends to form a characteristic air–liquid interface biofilm. The second protocol was performed to allow the microscopic visualization of *P. aeruginosa* biofilm on glass surfaces (Kasthuri et al., 2022). Briefly, wells containing 1 mL of MH broth with 15 μM of F2F-2020202 or DMSO were used as treated and control groups, respectively. Then, 10^6 CFU/mL of *P. aeruginosa* PAO1 strain was added to each well. Successively, a 1 cm^2 glass piece was put in the well diagonal to the broth surface and incubated at 37°C for 24 h. After incubation, the slides were carefully taken with forceps, gently washed three times in sterile distilled water, and then stained as above reported. The unabsorbed dyes were removed by washing the slides in sterile distilled water. After air drying at room temperature, the biofilm architecture of control and treated samples was observed at × 400 magnification (Iris Digital System, Twin Helix).

Pyocyanin and rhamnolipid assay

Pyocyanin appears in different colors in media depending on the pH and oxidation status of the culture (Rada and Leto, 2013). To ensure that the 691/600 nm ratio of the untreated bacterial cells was not higher than that of the treated cultures due to a difference in the pH or oxidation status, pyocyanin was first quantified according to Kumar et al. (2014) with some modifications. *P. aeruginosa* PAO1 cultures prepared as above reported (MIC assay) were treated with 30 μM compound F2F-2020202 for 24 h at 37°C. The microbial culture was separately collected from each growth medium and centrifuged at 10,000 rpm for 15 min. The cell-free culture supernatant (CFCS) was extracted with chloroform (5/3, v/v). The organic phase was mixed with 1 mL of hydrochloric acid (0.2 M). After 10 min centrifugation at 4°C, the organic phase was collected. The intensity of the solution color was quantified by measuring its absorbance at the wavelength of 520 nm.

The CFCS was also used for another pyocyanin quantification protocol. The CFCSs of the control and treated groups were collected by centrifugation at 10,000 rpm for 10 min and filtered through a 0.2 μm membrane filter. Pyocyanin concentration was then determined by measuring the absorbance at 691 nm.

For the rhamnolipid assay, *P. aeruginosa strain* PAO1-treated culture was centrifuged (10,000 g for 10 min), the supernatant was collected and acidified to pH 2 (with HCl), and the absorbance was measured at 570 nm.

RNA isolation and real-time PCR

P. aeruginosa was treated with 30 μM of F2F-2020202 for 24 h. Total RNA was isolated using the GenUp Total RNA kit (biotechrabbit, Berlin, Germany) according to the manufacturer's instructions. DNA contamination from the total RNA was removed by incubation with DNase I (RNase-free DNase Set, Qiagen, Hilden, Germany). Measuring the A260/A280 nm ratio assessed the nucleic acid purity. To generate cDNA, total RNA was reverse transcribed using RevertUP II Reverse Transcriptase (biotechrabbit, Berlin, Germany) into cDNA using random hexamer primers (Random hexamer, Roche Diagnostics, Monza, Italy) at 48°C for 60 min according to the manufacturer's instructions. The real-time PCR was carried out using 1 μL of cDNA (5 ng/μl). Expression levels of several quorum sensing genes (see Table 1) were analyzed by quantitative real-time polymerase chain reaction (qRT-PCR) using the CFX96 system (Bio-Rad, Hercules, CA, United States) with the SYBR Green Master Mix kit (Applied Biosystems, Waltham, MA, United States). The thermal cycling parameters were the following: 50°C for 2 min for UDG activation, followed by the activation of the DNA polymerase at 95°C for 2 min, 40 cycles comprising 15 s at 95°C for denaturation, and 1 min at the primer-specific annealing temperature (see Table 1) for annealing and extension. The experiments were carried out in duplicate for each data point, and the ribosomal gene *rpsL* was used as an internal control to normalize all data.

Statistical analysis

Each antimicrobial assay was repeated at least three times. All results of antimicrobial activity are expressed as mean ± standard deviation (S.D.). The results were analyzed using one-way analysis of variance (ANOVA) followed by Tukey's *post-hoc* comparison tests to verify differences between compounds and concentrations ($p < 0.05$).

Results and discussion

Compound F2F-2020202 was first tested for its ability to affect bacterial cell growth on the *P. aeruginosa* PAO-1 strain. As reported in Figure 1, the compound did not induce an evident and significant reduction of cell growth at 30 and 15 μM. Only at 60 μM, a slight reduction of cell growth was observed (growth reduction percentage = 18%).

However, the 30 μM F2F-2020202-treated cells showed a visible reduction in pyocyanin production (yellow staining of the medium) when compared to the control cells (green staining) (Figure 2). The same result was not observed at the 15 μM (data not shown). Consequently, the impact of compound F2F-2020202 on the production of some PAO-1 virulence factors such as pyocyanin and rhamnolipids was further analyzed using biochemical assays.

Biochemical quantification results confirmed the diminished level of pyocyanin (22% decrease) (Figure 3A) and rhamnolipids (44% decrease) (Figure 3B) in 30 μM treated *P. aeruginosa*. DMSO (0.15%), used as a vehicle, did not affect by itself the production of virulence factors.

Pyocyanin is an important *P. aeruginosa* virulence factor capable of directly inducing pulmonary pathophysiology, associated with a decline in lung function, and is essential for the release of extracellular DNA (eDNA), aiding in the formation of biofilm (Das et al., 2013). Additionally, pyocyanin contributes to the dominant colonization of

10.3389/fmicb.2024.1340585

TABLE 1 Primer sequences used for the qRT-PCR and annealing conditions.

Gene	Sequence (5′-3′)		Annealing temperature
LasI	Fw	GGCTGGGACGTTAGTGTCAT	60°C
	Rev	AAAACCTGGGCTTCAGGAGT	
LasR	Fw	CTGTGGATGCTCAAGGACTAC	55°C
	Rev	TCGTAGTCCTGGCTGTCCTT	
RhlI	Fw	AAGGACGTCTTCGCCTACCT	60°C
	Rev	GCAGGCTGGACCAGAATATC	
RhlR	Fw	CATCCGATGCTGATGTCCAACC	55°C
	Rev	ATGATGGCGATTTCCCCGGAAC	
pqsE	Fw	GGATGCCGAATTGGTTTG	53°C
	Rev	GGTCGTAGTGCTTGTGGG	
phzA1	Fw	AACGGTCAGCGGTACAGGGAAAC	60°C
	Rev	ACGAACAGGCTGTGCCGCTGTAAC	
phzA2	Fw	CTGTAACCGTTCGGCCCCCTTCATG	60°C
	Rev	ATGCGAGAGTACCAACGGTTGAAAG	
qsrO	Fw	ATGCTTACGTTTTGGGCTAT	53°C
	Rev	ATGGAAATGGATTCTTTTGAGTT	
rpsL	Fw	GCAACTATCAACCAGCTGGTG	60°C
	Rev	GCTGTGCTCTTGCAGGTTGTG	

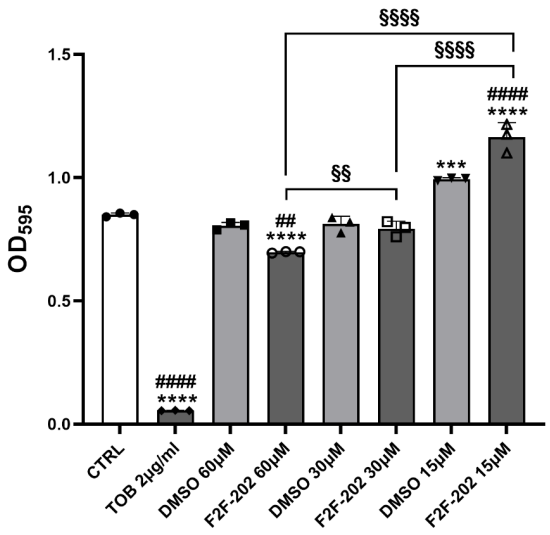

FIGURE 1
MIC determination of compound F2F-2020202 against *P. aeruginosa* PAO-1. The bacterial growth was determined at different concentrations of compound F2F-2020202 (from here onward reported in figures as F2F-202, 60, 30, and 15 µM) after 24 h incubation time at 37°C. CTRL represents the untreated bacteria. DMSO 60 µM and 30 µM (0.3 and 0.15%, respectively) served as the negative controls. TOB represents tobramycin at 2 µg/mL (4.27 µM). Three replicates were performed. The error bars indicate the mean ± standard deviation of the mean. Statistical differences were determined using ANOVA followed by Tukey's test (***$p < 0.001$ and ****$p < 0.0001$ vs. CTRL; ##$p < 0.01$; ####$p < 0.0001$ vs. DMSO; §$p < 0.01$ and §§§§$p < 0.0001$ for significant differences among the compound F2F-2020202 at different concentrations). Tobramycin showed a significant difference with DMSO at every concentration (####$p < 0.0001$).

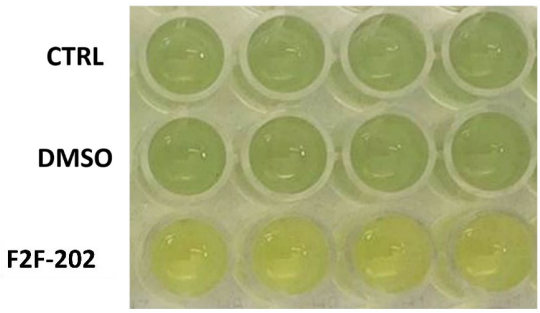

FIGURE 2
Pyocyanin reduction induced by compound F2F-2020202 at 30 µM. CTRL represents the untreated bacteria. DMSO 30 µM (0.15%) served as the negative control. F2F-202 is the abbreviation for F2F-2020202. The yellow staining of 30 µM F2F-2020202-treated cell media reflects a reduction of pyocyanin production when compared to the control and DMSO-treated cells (green staining). The image is representative of nine different experiments.

P. aeruginosa in the CF lung (Carlsson et al., 2011). Considering the important role of pyocyanin in biofilm formation, we analyzed the potential effect of F2F-2020202 on biofilm inhibition at 30 µM. The treatment with F2F-2020202 significantly affects *P. aeruginosa* biofilm formation, as the pellicle in the glass tube was thin and slightly colored (Figure 4A). A crystal violet assay allowed the estimation of biofilm formation by quantifying the crystal violet uptake by the biofilm matrix. As shown in Figure 4B, treatment with F2F-2020202 reduced biofilm formation by 38% compared to untreated and DMSO-treated cells. We used also a second method to allow the microscopic visualization of *P. aeruginosa* biofilm on glass surfaces. In Figure 4C,

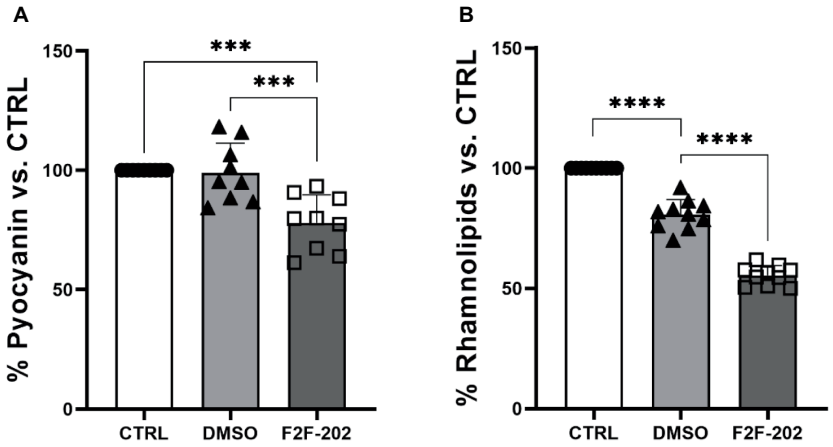

FIGURE 3
Effect of compound F2F-2020202 on virulence factors secreted by *P. aeruginosa* PAO1. CTRL represents the untreated bacteria. DMSO 30 μM (0.15%) served as the negative control. F2F-202 is the abbreviation for F2F-2020202. The levels of pyocyanin **(A)** and rhamnolipids **(B)** at 30 μM concentration were evaluated. Bar errors showed the standard deviations of nine, nine, and ten replicates, respectively. Statistical differences were determined using ANOVA followed by Tukey's test (***$p < 0.001$ and ****$p < 0.0001$).

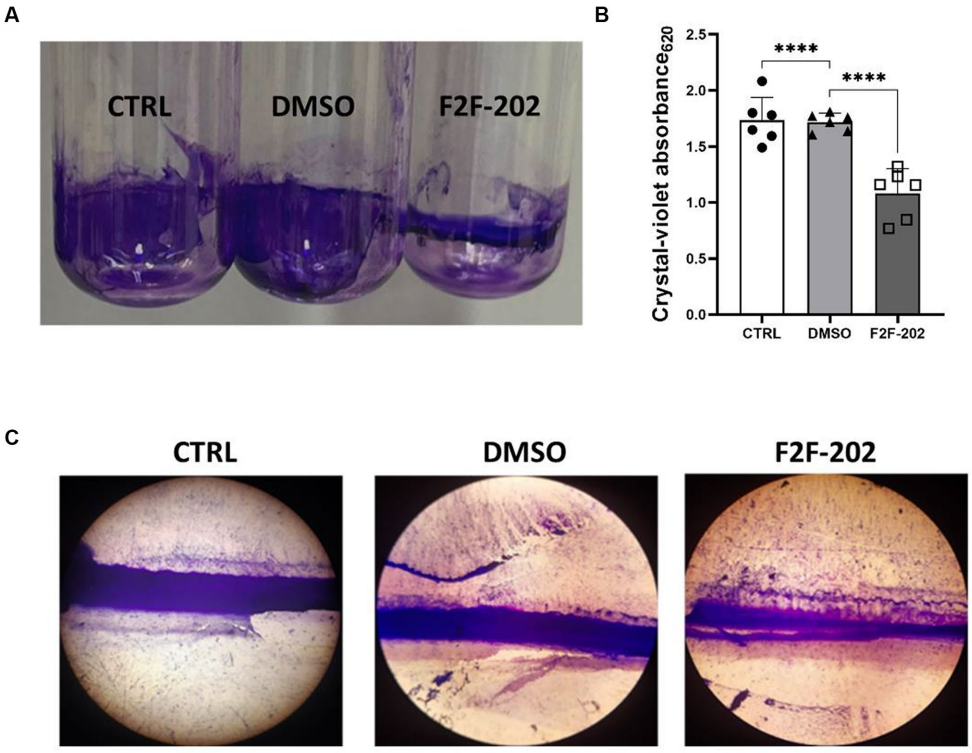

FIGURE 4
Effect of compound F2F-2020202 at 30 μM on biofilm formation. CTRL represents the untreated bacteria. DMSO 30 μM (0.15%) served as the negative control. F2F-202 is the abbreviation for F2F-2020202. **(A)** The biofilm assay in glass tubes at air–liquid interfaces showed a visible reduction of the biomass attached to the glass walls. **(B)** Crystal violet staining. The absorbance values obtained at 620 nm are presented as mean ± standard deviation. Statistical differences were determined using ANOVA followed by Tukey's test (****$p < 0.0001$). **(C)** Representative image of three independent experiments performed on *P. aeruginosa* PAO1 showing the reduction of the biofilm organization and compactness. Images were micrographed using the light microscope.

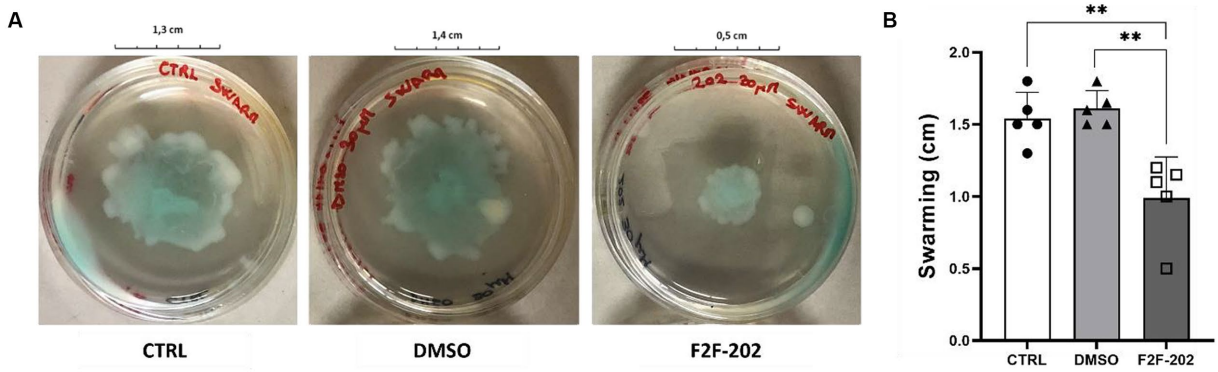

FIGURE 5
(A) The pictures are representative of three independent experiments conducted on *P. aeruginosa* PAO1. CTRL represents the untreated bacteria. DMSO 30 μM (0.15%) served as the negative control. F2F-202 is the abbreviation for F2F-2020202. Compound F2F-2020202 at 30 μM showed a visible reduction in the swarming mobility on plate agar. **(B)** The bar chart shows the effect of compound F2F-2020202 at 30 μM on the swarming motility. Five replicates were done for the statistical comparisons. The measurements are presented as centimeters ± standard deviation. Statistical differences were determined using ANOVA followed by Tukey's test (**$p < 0.01$).

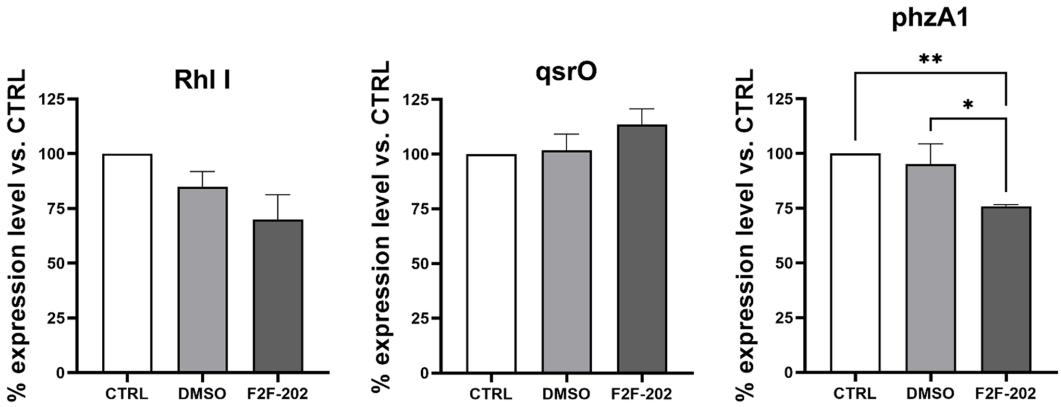

FIGURE 6
Expression levels of rhlI, qsrO, and phzA1 expressed as a percentage of the expression level of these genes in the control group. CTRL represents the untreated bacteria. F2F-202 is the abbreviation for F2F-2020202. DMSO 30 μM (0.15%) served as the negative control. Three replicates were done for the statistical comparisons. Statistical differences were determined using ANOVA followed by Tukey's test (*$p < 0.05$, **$p < 0.01$).

biofilm was allowed to form on a 1cm^2 glass piece. It is evident that F2F-2020202 reduced the thickness of the biofilm, resulting in less organization and compactness compared to DMSO-treated and control cells.

Finally, since motility is a key factor in biofilm development, we analyzed the activity of compound F2F-2020202 on swarming motility, an organized form of surface translocation useful in the early stages of biofilm development (Shrout et al., 2006). Swarming motility was affected by treatments with F2F-2020202 at 30 μM, as shown in Figures 5A,B. This result is in accord with the observed reduced rhamnolipid production, a rhamnose-containing glycolipid surface-active molecule with hemolytic activity, encoded by the QS-controlled Rhl genes. The importance of such results relies on the role played by rhamnolipids in chronic and acute *P. aeruginosa* lung infection. They contribute to atelectasis, inhibit the mucociliary transport and ciliary function of the human respiratory system, are implicated in swarming motility, and finally play a crucial role in biofilm formation (Davey et al., 2003).

To confirm the biochemical results herein reported, we sought to determine using real-time PCR the efficiency of F2F-2020202 to modulate some QS-related genes that are involved in the regulation of the above-mentioned virulence factors. We focused our analysis on Las, Rhl, and Pqs. In summary, LasI and RhlI control the synthesis of their autoinducers (AIs) N-(3-oxododecanoyl)-L-homoserine lactone (3-oxo-C12-HSL) and N-butanoyl-L-homoserine lactone (C4-HSL), respectively, which bind to LasR and RhlR. The chemical signaling pathways are hierarchically organized, with Rhl modulated by Las. The third QS network in *P. aeruginosa* is the *Pseudomonas* quinolone signal (Pqs), which is a non-acylated homoserine lactone (AHL)-mediated QS signaling network employing alkyl-4-quinolones (AQs), among which 2-heptyl-3-hydroxy-1H-quinolin-4-one (PQS) and 2-heptyl-1H-quinolin-4-one (HHQ) as signal chemical effectors. These diversified AIs used by the QS network are strongly interconnected and mutually modulate their activities. Upon binding to LasR, RhlR, or PqsR, these signal molecules activate the expressions of QS-related genes of *P. aeruginosa*, controlling the

production of virulence factors, including proteases and exoenzymes, allowing the bacteria to trigger the infection process in the host tissue (Garcia-Reyes et al., 2020). QS controls the pyocyanin biosynthesis through a cascade of complex steps orchestrated by two enzymes encoded on two homologous operons phzABCDEFG, named phzA1 and phzA2, whose expression can be repressed by the *qsrO* gene product (Mavrodi et al., 2001; Kohler et al., 2014). The regulator gene *qsrO* plays an important role in the QS system since it can downregulate all QS system regulatory and target genes. Finally, AHLs and HHQs also participate in the modulation of inflammation and immune responses in the host (Caldwell et al., 2009). In this context, molecules targeting QS have been suggested to have a beneficial effect by reducing *P. aeruginosa* virulence factors and, thus, its pathogenicity (Rada and Leto, 2013) and boosting the susceptibility to antibiotics of the bacteria embedded in biofilm (Cohen and Prince, 2012). We analyzed the expression levels of genes coding signal molecule catalyzing enzymes (*pqsE, lasI,* and *rhlI*), the expression levels of genes coding for transcriptional activators binding with signal molecules (*lasR* and *rhlR*), and *qsrO* gene expression, which are the main QS genes investigated in *P. aeruginosa*. Surprisingly, despite the relevant reduction of virulence factors described above, we did not observe a strong modulation of the gene expression (Figure 6). Gene expression levels decreased by 30% for rhlI and 24% for phzA1, while qsrO was induced by 18%. On the contrary, lasI, lasR, rhlR, pqsE, and phzA2 were not modulated (data not shown). With these data in hand, we have tried to provide a rational explanation of the experimental results and to link the QS gene expression to the observed biochemical results. Of course, the biochemical results offer an unambiguous picture of the F2F-2020202 effect on the modulation at the molecular level of QS. Accordingly, upon our preliminary investigation of gene expression, the registered reduction in *rhlI* gene expression might lead to reduced C4-HSL production, inducing an absence of regulation of the hierarchically connected QS genes. This could explain the reduction of pyocyanin and rhamnolipid synthesis, both under the control of *rhlI*. Rhamnolipid regulation is also under the control of *pqsE*, which is involved in bacterial response to PQS and pqsR. Unfortunately, we did not observe a *pqsE* gene expression modulation, thus making even more complex the interpretation of the phenotypic results. Worthy of note, the null mutation in PQS leads to reduced biofilm formation and decreased pyocyanin, elastase, PA-IL lectin, and rhamnolipid production (Yan and Wu, 2019).

However, due to the complexity of the QS system in *P. aeruginosa*, from the results obtained in this study, it is difficult to link the QS gene expression to the observed biochemical results. The partial reduction of some QS gene expressions, as well as the lack of modulation of others, suggests that the observed effects are not directly under the control of the *rhl* system but, rather, linked to a more complex interaction among QS regulators.

Conclusion

In this study, we showed for the first time the activity of new selective HDAC6 inhibitors in the attenuation of *P. aeruginosa* virulence. Compound F2F-2020202 reduced the production of pyocyanin and rhamnolipids and affected the ability of *P. aeruginosa* to form biofilm. Our results are strongly relevant since they demonstrate for the first time the effect of such inhibitors on the modulation of virulence factors of *P. aeruginosa*.

The data herein obtained can also in part explain our previous results with selective HDAC6 inhibitors showing the reduced inflammation and bacterial load in chronic infection models recapitulating CF phenotype. The significant reduction in pyocyanin and rhamnolipid production, key players in the pathophysiology of CF, and subsequent biofilm reduction should lead to reduced inflammation and recovered protective immune response. This study fosters future in-depth investigation to allow the complete elucidation of the molecular mechanisms underlying F2F-2020202 activity. In particular, targeted RNA sequencing to profile-specific QS transcripts will be helpful in studying and unveiling genes and pathways regulated by HDAC6 inhibitors.

Data availability statement

The original contributions presented in the study are included in the article/supplementary material, further inquiries can be directed to the corresponding authors.

Author contributions

SB: Investigation, Writing – review & editing, Formal analysis, Data curation. BM: Formal analysis, Investigation, Writing – review & editing. LT: Investigation, Writing – review & editing. SP: Investigation, Methodology, Writing – review & editing. FL: Formal Analysis, Supervision, Writing – review & editing. VS: Resources, Validation, Writing – review & editing. EB: Conceptualization, Supervision, Writing – original draft. MB: Investigation, Writing – review & editing, Conceptualization, Funding acquisition, Supervision, Writing – original draft.

Funding

The authors declare financial support was received for the research, authorship, and/or publication of this article. This research was supported by EU funding within the MUR PNRR Extended Partnership initiative on Emerging Infectious Diseases (Project no. PE00000007, INF-ACT). BM is part of the CRESCENDO Doctoral Program, which has received funding from the European Union's Horizon 2020 Research and Innovation Program under the Marie Skłodowska-Curie Program (MSCA-COFUND-2020) with Grant Agreement No. 101034245. SP and MB acknowledge MUR (Ministero dell'Università e della Ricerca), PON R&I 2014-2020- Asse IV "Istruzione e Ricerca per il recupero-REACT-EU," Azione IV.6 "Contratti di Ricerca su tematiche Green." The MIUR Grant "Dipartimento di Eccellenza 2023–2027" to the Department of Pharmacy of the University of Naples "Federico II" is gratefully acknowledged.

Conflict of interest

The authors declare that the research was conducted in the absence of any commercial or financial relationships that could be construed as a potential conflict of interest.

The author(s) declared that they were an editorial board member of Frontiers, at the time of submission. This had no impact on the peer review process and the final decision.

Publisher's note

References

Ariffin, J. K., Gupta, K. D., Kapetanovic, R., Iyer, A., Reid, R. C., Fairlie, D. P., et al. (2015). Histone deacetylase inhibitors promote mitochondrial reactive oxygen species production and bacterial clearance by human macrophages. *Antimicrob. Agents Chemother.* 60, 1521–1529. doi: 10.1128/AAC.01876-15

Bai, J., Lei, Y., An, G. L., and He, L. (2015). Down-regulation of deacetylase HDAC6 inhibits the melanoma cell line A375.S2 growth through ROS-dependent mitochondrial pathway. *PLoS One* 10:e0121247. doi: 10.1371/journal.pone.0121247

Bandyopadhaya, A., Tsurumi, A., Maura, D., Jeffrey, K. L., and Rahme, L. G. (2016). A quorum-sensing signal promotes host tolerance training through HDAC1-mediated epigenetic reprogramming. *Nat. Microbiol.* 1:16174. doi: 10.1038/nmicrobiol.2016.174

Barone, S., Cassese, E., Alfano, A. I., Brindisi, M., and Summa, V. (2022). Chasing a breath of fresh air in cystic fibrosis (CF): therapeutic potential of selective HDAC6 inhibitors to tackle multiple pathways in CF pathophysiology. *J. Med. Chem.* 65, 3080–3097. doi: 10.1021/acs.jmedchem.1c02067

Bierne, H., Hamon, M., and Cossart, P. (2012). Epigenetics and bacterial infections. *Cold Spring Harb. Perspect. Med.* 2:a010272. doi: 10.1101/cshperspect.a010272

Brindisi, M., Barone, S., Rossi, A., Cassese, E., Del Gaudio, N., Feliz Morel, A. J., et al. (2022). Efficacy of selective histone deacetylase 6 inhibition in mouse models of *Pseudomonas aeruginosa* infection: a new glimpse for reducing inflammation and infection in cystic fibrosis. *Eur. J. Pharmacol.* 936:175349. doi: 10.1016/j.ejphar.2022.175349

Brindisi, M., Saraswati, A. P., Brogi, S., Gemma, S., Butini, S., and Campiani, G. (2020). Old but gold: tracking the new guise of histone deacetylase 6 (HDAC6) enzyme as a biomarker and therapeutic target in rare diseases. *J. Med. Chem.* 63, 23–39. doi: 10.1021/acs.jmedchem.9b00924

Buommino, E., De Marino, S., Sciarretta, M., Piccolo, M., Festa, C., and D'Auria, M. V. (2021). Synergism of a novel 1,2,4-oxadiazole-containing derivative with oxacillin against methicillin-resistant *Staphylococcus aureus*. *Antibiotics (Basel)* 10:1258. doi: 10.3390/antibiotics10101258

Caldwell, C. C., Chen, Y., Goetzmann, H. S., Hao, Y., Borchers, M. T., Hassett, D. J., et al. (2009). *Pseudomonas aeruginosa* exotoxin pyocyanin causes cystic fibrosis airway pathogenesis. *Am. J. Pathol.* 175, 2473–2488. doi: 10.2353/ajpath.2009.090166

Carlsson, M., Shukla, S., Petersson, A. C., Segelmark, M., and Hellmark, T. (2011). *Pseudomonas aeruginosa* in cystic fibrosis: pyocyanin negative strains are associated with BPI-ANCA and progressive lung disease. *J. Cyst. Fibros.* 10, 265–271. doi: 10.1016/j.jcf.2011.03.004

Chen, J., Shi, X., Padmanabhan, R., Wang, Q., Wu, Z., Stevenson, S. C., et al. (2008). Identification of novel modulators of mitochondrial function by a genome-wide RNAi screen in *Drosophila melanogaster*. *Genome Res.* 18, 123–136. doi: 10.1101/gr.6940108

Cohen, T. S., and Prince, A. (2012). Cystic fibrosis: a mucosal immunodeficiency syndrome. *Nat. Med.* 18, 509–519. doi: 10.1038/nm.2715

Correa-Oliveira, R., Fachi, J. L., Vieira, A., Sato, F. T., and Vinolo, M. A. (2016). Regulation of immune cell function by short-chain fatty acids. *Clin. Transl. Immunology* 5:e73. doi: 10.1038/cti.2016.17

Das, T., Kutty, S. K., Kumar, N., and Manefield, M. (2013). Pyocyanin facilitates extracellular DNA binding to *Pseudomonas aeruginosa* influencing cell surface properties and aggregation. *PLoS One* 8:e58299. doi: 10.1371/journal.pone.0058299

Davey, M. E., Caiazza, N. C., and O'Toole, G. A. (2003). Rhamnolipid surfactant production affects biofilm architecture in *Pseudomonas aeruginosa* PAO1. *J. Bacteriol.* 185, 1027–1036. doi: 10.1128/JB.185.3.1027-1036.2003

Garcia-Reyes, S., Soberon-Chavez, G., and Cocotl-Yanez, M. (2020). The third quorum-sensing system of *Pseudomonas aeruginosa*: Pseudomonas quinolone signal and the enigmatic PqsE protein. *J. Med. Microbiol.* 69, 25–34. doi: 10.1099/jmm.0.001116

Grabiec, A. M., and Potempa, J. (2018). Epigenetic regulation in bacterial infections: targeting histone deacetylases. *Crit. Rev. Microbiol.* 44, 336–350. doi: 10.1080/1040841X.2017.1373063

Guo, Q., Wu, Q., Bai, D., Liu, Y., Chen, L., Jin, S., et al. (2016). Potential use of dimethyl sulfoxide in treatment of infections caused by *Pseudomonas aeruginosa*. *Antimicrob. Agents Chemother.* 60, 7159–7169. doi: 10.1128/AAC.01357-16

Hamon, M. A., and Cossart, P. (2008). Histone modifications and chromatin remodeling during bacterial infections. *Cell Host Microbe* 4, 100–109. doi: 10.1016/j.chom.2008.07.009

Kamemura, K., Ogawa, M., Ohkubo, S., Ohtsuka, Y., Shitara, Y., Komiya, T., et al. (2012). Depression of mitochondrial metabolism by downregulation of cytoplasmic deacetylase, HDAC6. *FEBS Lett.* 586, 1379–1383. doi: 10.1016/j.febslet.2012.03.060

Kasthuri, T., Barath, S., Nandhakumar, M., and Karutha Pandian, S. (2022). Proteomic profiling spotlights the molecular targets and the impact of the natural antivirulent umbelliferone on stress response, virulence factors, and the quorum sensing network of *Pseudomonas aeruginosa*. *Front. Cell. Infect. Microbiol.* 12:998540. doi: 10.3389/fcimb.2022.998540

Kohler, T., Ouertatani-Sakouhi, H., Cosson, P., and van Delden, C. (2014). QsrO a novel regulator of quorum-sensing and virulence in *Pseudomonas aeruginosa*. *PLoS One* 9:e87814. doi: 10.1371/journal.pone.0087814

Kumar, N. V., Murthy, P. S., Manjunatha, J. R., and Bettadaiah, B. K. (2014). Synthesis and quorum sensing inhibitory activity of key phenolic compounds of ginger and their derivatives. *Food Chem.* 159, 451–457. doi: 10.1016/j.foodchem.2014.03.039

Li, Y., Zhao, T., Liu, B., Halaweish, I., Mazitschek, R., Duan, X., et al. (2015). Inhibition of histone deacetylase 6 improves long-term survival in a lethal septic model. *J. Trauma Acute Care Surg.* 78, 378–385. doi: 10.1097/TA.0000000000000510

Limoli, D. H., and Hoffman, L. R. (2019). Help, hinder, hide and harm: what can we learn from the interactions between Pseudomonas aeruginosa and *Staphylococcus aureus* during respiratory infections? *Thorax* 74, 684–692. doi: 10.1136/thoraxjnl-2018-212616

Malhotra, S., Hayes, D. Jr., and Wozniak, D. J. (2019). Cystic fibrosis and *Pseudomonas aeruginosa*: the host-microbe Interface. *Clin. Microbiol. Rev.* 32:e00138-18. doi: 10.1128/CMR.00138-18

Mavrodi, D. V., Bonsall, R. F., Delaney, S. M., Soule, M. J., Phillips, G., and Thomashow, L. S. (2001). Functional analysis of genes for biosynthesis of pyocyanin and phenazine-1-carboxamide from *Pseudomonas aeruginosa* PAO1. *J. Bacteriol.* 183, 6454–6465. doi: 10.1128/JB.183.21.6454-6465.2001

Pendleton, J. N., Gorman, S. P., and Gilmore, B. F. (2013). Clinical relevance of the ESKAPE pathogens. *Expert Rev. Anti-Infect. Ther.* 11, 297–308. doi: 10.1586/eri.13.12

Rada, B., and Leto, T. L. (2013). Pyocyanin effects on respiratory epithelium: relevance in *Pseudomonas aeruginosa* airway infections. *Trends Microbiol.* 21, 73–81. doi: 10.1016/j.tim.2012.10.004

Raju, H., Sundararajan, R., and Sharma, R. (2018). The structure of BrlR reveals a potential pyocyanin binding site. *FEBS Lett.* 592, 256–262. doi: 10.1002/1873-3468.12950

Rosenjack, J., Hodges, C. A., Darrah, R. J., and Kelley, T. J. (2019). HDAC6 depletion improves cystic fibrosis mouse airway responses to bacterial challenge. *Sci. Rep.* 9:10282. doi: 10.1038/s41598-019-46555-4

Shrout, J. D., Chopp, D. L., Just, C. L., Hentzer, M., Givskov, M., and Parsek, M. R. (2006). The impact of quorum sensing and swarming motility on *Pseudomonas aeruginosa* biofilm formation is nutritionally conditional. *Mol. Microbiol.* 62, 1264–1277. doi: 10.1111/j.1365-2958.2006.05421.x

The European Committee on Antimicrobial Susceptibility Testing. Breakpoint tables for interpretation of MICs and zone diameters. Version 12.0. (2022). Available at: http://www.eucast.org.

Yan, S., and Wu, G. (2019). Can biofilm be reversed through quorum sensing in *Pseudomonas aeruginosa*? *Front. Microbiol.* 10:1582. doi: 10.3389/fmicb.2019.01582

Zhao, T., Li, Y., Liu, B., Pan, B., Cheng, X., Georgoff, P., et al. (2016). Inhibition of histone deacetylase 6 restores innate immune cells in the bone marrow in a lethal septic model. *J. Trauma Acute Care Surg.* 80, 34–40. doi: 10.1097/TA.0000000000000897

Zhou, J. W., Luo, H. Z., Jiang, H., Jian, T. K., Chen, Z. Q., and Jia, A. Q. (2018). Hordenine: a novel quorum sensing inhibitor and Antibiofilm agent against *Pseudomonas aeruginosa*. *J. Agric. Food Chem.* 66, 1620–1628. doi: 10.1021/acs.jafc.7b05035

frontiers | Frontiers in Microbiology

TYPE Original Research
PUBLISHED 05 March 2024
DOI 10.3389/fmicb.2024.1210313

OPEN ACCESS

EDITED BY
Rustam Aminov,
University of Aberdeen, United Kingdom

REVIEWED BY
Bijit Bhowmik,
Croda Inc, United States
Carlos Henrique Camargo,
Adolfo Lutz Institute, Brazil

*CORRESPONDENCE
Xiaoli Zhang
jmszxl123@163.com

†These authors have contributed equally to this work

RECEIVED 22 April 2023
ACCEPTED 30 January 2024
PUBLISHED 05 March 2024

CITATION
Li X, Zhang J, Wang J, Long W, Liang X, Yang Y, Gong X, Li J, Liu L and Zhang X (2024) Activities of aztreonam in combination with several novel β-lactam-β-lactamase inhibitor combinations against carbapenem-resistant *Klebsiella pneumoniae* strains coproducing KPC and NDM.
Front. Microbiol. 15:1210313.
doi: 10.3389/fmicb.2024.1210313

Activities of aztreonam in combination with several novel β-lactam-β-lactamase inhibitor combinations against carbapenem-resistant *Klebsiella pneumoniae* strains coproducing KPC and NDM

Xinhui Li†, Jisheng Zhang†, Jianmin Wang†, Wenzhang Long, Xushan Liang, Yang Yang, Xue Gong, Jie Li, Longjin Liu and Xiaoli Zhang*

Department of Microbiology, Yongchuan Hospital of Chongqing Medical University, Chongqing, China

Isolates coproducing serine/metallo-carbapenems are a serious emerging public health threat, given their rapid dissemination and the limited number of treatment options. The purposes of this study were to evaluate the *in vitro* antibacterial activity of novel β-lactam-β-lactamase inhibitor combinations (BLBLIs) against carbapenem-resistant *Klebsiella pneumoniae* (CRKP) coproducing metallo-β-lactamase and serine-β-lactamase, and to explore their effects in combination with aztreonam, meropenem, or polymyxin in order to identify the best therapeutic options. Four CRKP isolates coproducing *K. pneumoniae* carbapenemase (KPC) and New Delhi metallo-β-lactamase (NDM) were selected, and a microdilution broth method was used to determine their susceptibility to antibiotics. Time-kill assay was used to detect the bactericidal effects of the combinations of antibiotics. The minimum inhibitory concentration (MIC) values for imipenem and meropenem in three isolates did not decrease after the addition of relebactam or varbobactam, but the addition of avibactam to aztreonam reduced the MIC by more than 64-fold. Time-kill assay demonstrated that imipenem-cilastatin/relebactam (ICR) alone exerted a bacteriostatic effect against three isolates (average reduction: 1.88 $\log_{10}$ CFU/mL) and ICR combined with aztreonam exerted an additive effect. Aztreonam combined with meropenem/varbobactam (MEV) or ceftazidime/avibactam (CZA) showed synergistic effects, while the effect of aztreonam combined with CZA was inferior to that of MEV. Compared with the same concentration of aztreonam plus CZA combination, aztreonam/avibactam had a better bactericidal effect (24 h bacterial count reduction >3 $\log_{10}$CFU/mL). These data indicate that the combination of ATM with several new BLBLIs exerts powerful bactericidal activity, which suggests that these double β-lactam combinations might provide potential alternative treatments for infections caused by pathogens coproducing-serine/metallo-carbapenems.

KEYWORDS

carbapenem-resistant *Klebsiella pneumoniae*, β-lactamase inhibitor, bactericidal effect, time-kill assay, aztreonam

Introduction

The emergence and widespread dissemination of acquired β-lactamase genes have made carbapenem-resistant Enterobacterales (CRE) a formidable challenge in global public health and clinical management (Gandra and Burnham, 2020). Meanwhile, carbapenem-resistant *Klebsiella pneumoniae* (CRKP) causes severe infections in debilitated and immunocompromised patients, leading to extended hospital stays and increased mortality, and has been classified as an "urgent threat" by the US Centers for Disease Control and Prevention (CDC) (Tzouvelekis et al., 2012). Resistance of CRKP to β-lactam antibiotics is usually associated with the production of β-lactamases, including extended-spectrum β-lactamases (ESBLs) and carbapenemases belonging to various molecular classes (Nordmann and Poirel, 2019). To counteract the hydrolytic activity of these enzymes and to restore the antimicrobial activity of some β-lactam antibiotics, combinations of β-lactam with β-lactamase inhibitor (BLI) have been developed; this represented a breakthrough for clinical treatment, and some of these combinations have been approved by the Food and Drug Administration (FDA). The main novel groups are diazobicyclooctanes (DBOs) (avibactam and relebactam) and boronic acid derivatives (vaborbactam) (Yahav et al., 2020). Avibactam has been used in combination with ceftazidime, which provides extensive activity against Enterobacterales and *Pseudomonas aeruginosa* expressing one or multiple β-lactamases (Zhanel et al., 2013; Castanheira et al., 2015). Relebactam, which is closely related to avibactam at the structural level, was developed to enhance the activity of imipenem after displaying compatibility and effectiveness both *in vitro* and in mouse infection models of CRE (Blizzard et al., 2014; Papp-Wallace et al., 2018). A multicenter comparative study found that imipenem-cilastatin/relebactam (ICR) was more effective than imipenem plus polymyxin therapy and was an efficacious and well-tolerated treatment option for carbapenem-resistant infections (Motsch et al., 2020). Vaborbactam was approved for use in combination with meropenem [meropenem/vaborbactam (MEV)] by the FDA in August 2017, showing excellent *in vitro* activity against KPC-producing Enterobacterales (Hackel et al., 2018). Although these combinations are very active against class A β-lactamase-producing Enterobacterales, none of them display activity against metallo-β-lactamase (MBL)-producing isolates.

Aztreonam remains a clinically available agent for metallo-β-lactamase-producing strains due to its ability to evade MBL-mediated hydrolysis, but it can be hydrolyzed by most clinically relevant serine beta-lactamases, such as ESBLs, AmpC, and KPC (Brogden and Heel, 1986). The most troubling isolates are probably those that produce both serinase and MBLs, since most β-lactam antibiotics and BLI inhibitors are ineffective against them. In recent years, more and more studies have sought to use combination therapy treatment against MBL-producing strains, and some of these have indicated that a combination of aztreonam plus CZA displays *in vitro* synergy against MBL-producing Enterobacterales (Marshall et al., 2017; Jayol et al., 2018). It has also been found that the combination of aztreonam plus avibactam is highly active against MBL-producing strains, with the MIC_{90} being 0.5 mg/L in a wide range of CREs (Karlowsky et al., 2017). This raises the question of whether a combination of aztreonam with other β-lactam-β-lactamase inhibitor combinations (BLBLIs) is a potential treatment option against strains coproducing serinase and MBL. In this study, to explore the best potential treatment combination against strains coproducing serine-β-lactamase and MBL, time-kill assay was used to assess and compare the antibacterial effects of several combinations of aztreonam with antibiotics (including CZA, MEV, ICR, AVI, polymyxin, and meropenem).

Materials and methods

Bacterial strains and resistance characteristics

A total of 127 CRKP isolates were collected from patients admitted to Yongchuan Hospital of Chongqing Medical University from 2019 to 2020. Identification at the species level was performed by matrix-assisted laser desorption/ionization–time-of-flight (MALDI-TOF) mass spectrometry (Bruker Daltonik, Bremen, Germany) and by analysis using a VITEK-2 automated microbiology analyzer (bioMérieux, France). A modified carbapenem inactivation method (mCIM) and an EDTA-modified carbapenem inactivation method (eCIM) were used to conduct preliminary screening of the production of carbapemase, as described in the Supplementary materials. The beta-lactamase genes bla_{CTX-M}, bla_{SHV}, bla_{TEM}, bla_{OXA}, bla_{KPC}, and bla_{NDM} were routinely amplified via PCR, and the positive results were sequenced via Sanger sequencing. All primers were obtained from previous studies (Gong et al., 2018; Huang et al., 2021). The patient electronic medical records corresponding to all strains were collected from the hospital information management system and the laboratory information management system of our hospital. Four *K. pneumoniae* clinical isolates that were coproducers of KPC and NDM (CRKP238, CRKP241, CRKP279, and CRKP319) were obtained and utilized for all experiments.

Multilocus sequence typing (MLST)

Multilocus sequence typing (MLST) was performed using seven housekeeping genes of *K. pneumoniae* that were amplified using primers from online databases,[1] and sequence types (STs) were determined using online database tools. The novel allele profiles were sent to klebsiellaMLST@pasteur.fr for confirmation.

Antimicrobial susceptibility testing

The antibiotics tested in this study were tigecycline, polymyxin, meropenem, imipenem, amikacin, levofloxacin, aztreonam, CZA, MEV, ICR, and aztreonam/avibactam. All antibiotic powders were weighed in an electronic balance and prepared in stock antibiotic solutions at all storage concentrations in sterile water (DMSO for aztreonam) and stored at −80°C. The specific dissolution method is shown in Supplementary Table S1. Subsequently, the aliquots were thawed and diluted to the desired concentrations with cation-adjusted Mueller Hinton broth (CAMHB). Antimicrobial susceptibility was evaluated using reference broth microdilution methods, conducted according to Clinical and Laboratory Standards Institute (CLSI)

1 https://bigsdb.pasteur.fr/klebsiella/primers-used/

procedures (document M07). Quality control strains included *Escherichia coli* ATCC 25922, *K. pneumoniae* ATCC 700603, and ATCC BAA-1705, and the minimum inhibitory concentrations (MICs) were interpreted according to CLSI recommendations.

Time-kill experiment

Time-kill studies were performed to analyze the bactericidal activity of the selected antibiotics alone and in combination with BLBLIs at clinically achievable free-drug concentrations. All experiments were performed in duplicate. An overnight culture of isolate was diluted with LB broth and further incubated at 37°C (120 rpm) for 12 h to reach early log-phase growth. The initial bacterial inoculum was adjusted to 10^6CFU/mL in fresh CAMHB broth. Antibiotic concentrations used during time-kill experiments represent mean steady-state concentrations of non-protein-bound drug in humans, as calculated from data in the literature (based on the area under the antibiotic concentration–time curve in serum or plasma over 24 h divided by 24 h [AUC_{0-24}/24 h]). The following antibiotic concentrations were used: aztreonam, 17 mg/L (Tangden et al., 2014); meropenem, 10 mg/L (Benitez-Cano et al., 2020); polymyxin, 2 mg/L (Tsuji et al., 2019); CZA, 33.5/6 mg/L (Das et al., 2020); aztreonam/avibactam, 17/6 mg/L; MEV, 23.2/25.5 mg/L (Wenzler et al., 2015); and ICR, 11.4/7.5 mg/L (Rizk et al., 2018). Viable colony counts were performed by obtaining samples after 0, 2, 4, 8, 12, and 24 h of antibiotic exposure. Synergy was defined as induction of a reduction by ≥2 $\log_{10}$ CFU/mL by the combination compared with the most active agent alone. Bactericidal activity was defined as a ≥ 3 $\log_{10}$ CFU/mL reduction in viable bacterial count at 24 h compared with the initial inoculum. The detection limit of the time-kill assay was 2.17 $\log_{10}$ CFU/mL.

Results

Bacterial strains and patient characteristics

The CZA resistance rate of 127 CRKP isolates collected from 2019 to 2020 was 12.5% (16/127). The resistance and carbapenemase production status of these isolates are shown in Supplementary Table S2; among these, four CZA-resistant isolates contained NDM enzyme and KPC enzyme, nine isolates only produced NDM enzyme, one isolate produced IMP enzyme, and two isolates only produced KPC-2 enzyme. The treatment history of patients with isolates coproducing NDM and KPC was further analyzed. As shown in Figure 1, three strains (CRKP238, CRKP268, and CRKP216) were isolated from patient A, who was admitted to the respiratory critical care unit due to pneumonia. After a period of treatment with meropenem and cefepime, an ST170 isolate (CRKP238) carrying bla_{KPC-2} and bla_{NDM-5} was isolated from sputum. After the patient was transferred to the respiratory intermediate care unit (RICU) and had continued to be treated with meropenem and cefoperazone/sulbactam for a period of time, two ST11 isolates (CRKP268 and CRKP216) that only produced KPC-2 enzyme were isolated in the urine and secretions, respectively. Patient B was admitted to the respiratory critical care department due to chronic obstructive pulmonary disease (COPD). After 7 days of treatment with cefepime, CRKP241 was isolated from the patient; he was then discharged after 5 days of treatment with tigecycline. Patient C, a preterm infant, was treated with meropenem, imipenem, and ceftazidime, after which a multidrug-resistant isolate (CRKP279) was isolated from sputum. After treatment with amikacin cefoperazone/sulbactam, patient C was cured and discharged. Finally, CRKP319 belongs to ST6279, which is a novel ST identified in our study, exhibiting a multidrug resistance phenotype; it was isolated from patient D, with neonatal pneumonia, who was discharged after treatment with ceftazidime and cefoperazone/sulbactam.

Antimicrobial susceptibility testing

As shown in Table 1, the four isolates selected in this study carried bla_{TEM}, bla_{KPC-2}, and bla_{NDM-1} or bla_{NDM-5}, respectively. In addition, CRKP238 also produced $bla_{CTX-M-65}$. Four strains were resistant to meropenem and imipenem; addition of neither 4 mg/L relebactam nor 8 mg/L vaborbactam resulted in a decrease in the MIC values, except in the case of CRKP238. For CRKP238, adding relebactam to imipenem reduced the MIC value by 256-fold, and adding vaborbactam to meropenem reduced the MIC value by more than 128-fold. All strains were highly resistant to CZA (MIC >256 mg/L) and aztreonam (MIC≥32 mg/L). While the addition of 4 mg/L avibactam to aztreonam significantly decreased the MIC by more than 64-fold, MIC values of three of the strains against polymyxin were 2 mg/L, the exception being CRKP241, which was resistant to polymyxin.

Time-kill assay results

The growth and kill trends for four isolates cultured with seven antibiotics at average steady-state serum concentrations are shown in Figure 2; Supplementary Figure S1. Bacterial growth without antibiotics reached 10 to 11 $\log_{10}$ CFU/mL at 24 h for all isolates. Single antibiotics (aztreonam, meropenem, and polymyxin) were not bactericidal against any of the isolates at 24 h. CZA and MEV monotherapy were also not bactericidal against any of the isolates at 24 h. The CZA combination therapies with different antibiotics showed different effects as compared with monotherapy. Neither CZA plus meropenem nor CZA plus polymyxin was bactericidal against CRKP241, CRKP279, or CRKP319. For CRKP238, CZA combined with meropenem or polymyxin achieved more than 3 $\log_{10}$ CFU/mL reduction compared with the initial inoculum (Figure 2; Supplementary Figure S1). Although aztreonam alone was ineffective against all four strains, it had a synergistic effect when combined with CZA. The combination of aztreonam plus CZA produced bactericidal activity at 12 h, which achieved more than 3.78 $\log_{10}$ CFU/mL bacteria reduction, except in the case of strain CRKP241. However, in all isolates, regrowth was observed at 24 h, with an average reduction of 2.30 $\log_{10}$ CFU/mL compared with the initial inoculum.

Similar to CZA monotherapy, the use of MEV alone produced no bactericidal activity against any strains at 24 h. However, the combination of MEV plus aztreonam had a synergistic effect, resulting in more than 3.78 log10 CFU/mL reduction at 24 h. Unlike CZA and MEV monotherapy, ICR alone decreased bacteria relative to the inoculum to varying degrees at 24 h (for CRKP238, 1.8 $\log_{10}$CFU/mL reduction; for CRKP241, approximately 2.12 $\log_{10}$ CFU/mL reduction; for CRKP319, approximately 1.72 $\log_{10}$ CFU/mL reduction). However,

10.3389/fmicb.2024.1210313

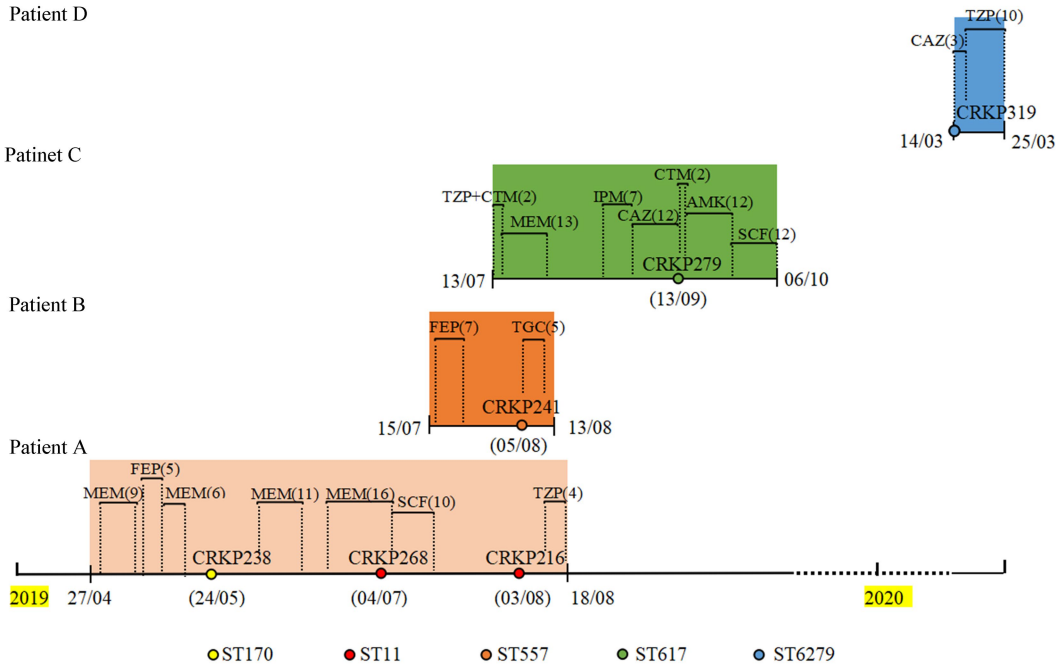

FIGURE 1
Timeline of CRKP infection and treatments during the patients' hospitalizations. CRKP238, CRKP268, CRKP216, CRKP241, CRKP279, and CRKP319 are carbapenem-resistant *Klebsiella pneumoniae* strains. MEM, meropenem; FEP, cefepime; SCF, cefoperazone/sulbactam; TZP, piperacillin/tazobactam; TGC, Tigecycline; CTM, cefotiam; IPM, imipenem; CAZ, ceftazidime; AMK, amikacin.

TABLE 1 The minimum inhibitory concentrations (MICs) of antibiotics and antimicrobial resistance genes (ARGs) of four carbapenem-resistant *Klebsiella pneumoniae* isolates.

Antibiotics	CRKP238	CRKP241	CRKP279	CRKP319
MIC (mg/L)				
Imipenem	64	8	16	16
Meropenem	>128	16	64	32
Amikacin	2	2	2	>128
Levofloxacin	64	4	<0.125	16
Tigecycline	2	32	2	4
Polymyxin	2	4	2	2
Aztreonam	>128	>128	32	>128
ATM/AVI	0.5/4	0.5/4	0.5/4	0.25/4
CZA	>256/4	>256/4	>256/4	>256/4
ICR	0.25/4	8/4	32/4	16/4
MEV	1/8	16/8	>32/8	16/8
ARGs	bla_{KPC-2} bla_{NDM-5} bla_{TEM} $bla_{CTX-M-65}$	bla_{KPC-2} bla_{NDM-1} bla_{TEM} *qnrS*	bla_{KPC-2} bla_{NDM-5} bla_{TEM}	bla_{KPC-2} bla_{NDM-1} bla_{TEM} bla_{SHV} *qnrS*

ATM/AVI, aztreonam/avibactam; CZA, ceftazidime/avibactam; ICR, imipenem-cilastatin/relebactam; MEV, meropenem/vaborbactam.

ICR plus aztreonam produced bactericidal activity against all strains, but this effect was only an additive one. In addition, the combination of aztreonam and avibactam tested in this study was found to exhibit bactericidal activity and reduced the amount of bacteria by more than 3.78 $\log_{10}$ CFU/mL.

Discussion

β-lactam antibiotics are the most widely used and abundant antibiotics in clinical practice. Unfortunately, the abuse of carbapenems has undoubtedly contributed to the emergence and

10.3389/fmicb.2024.1210313

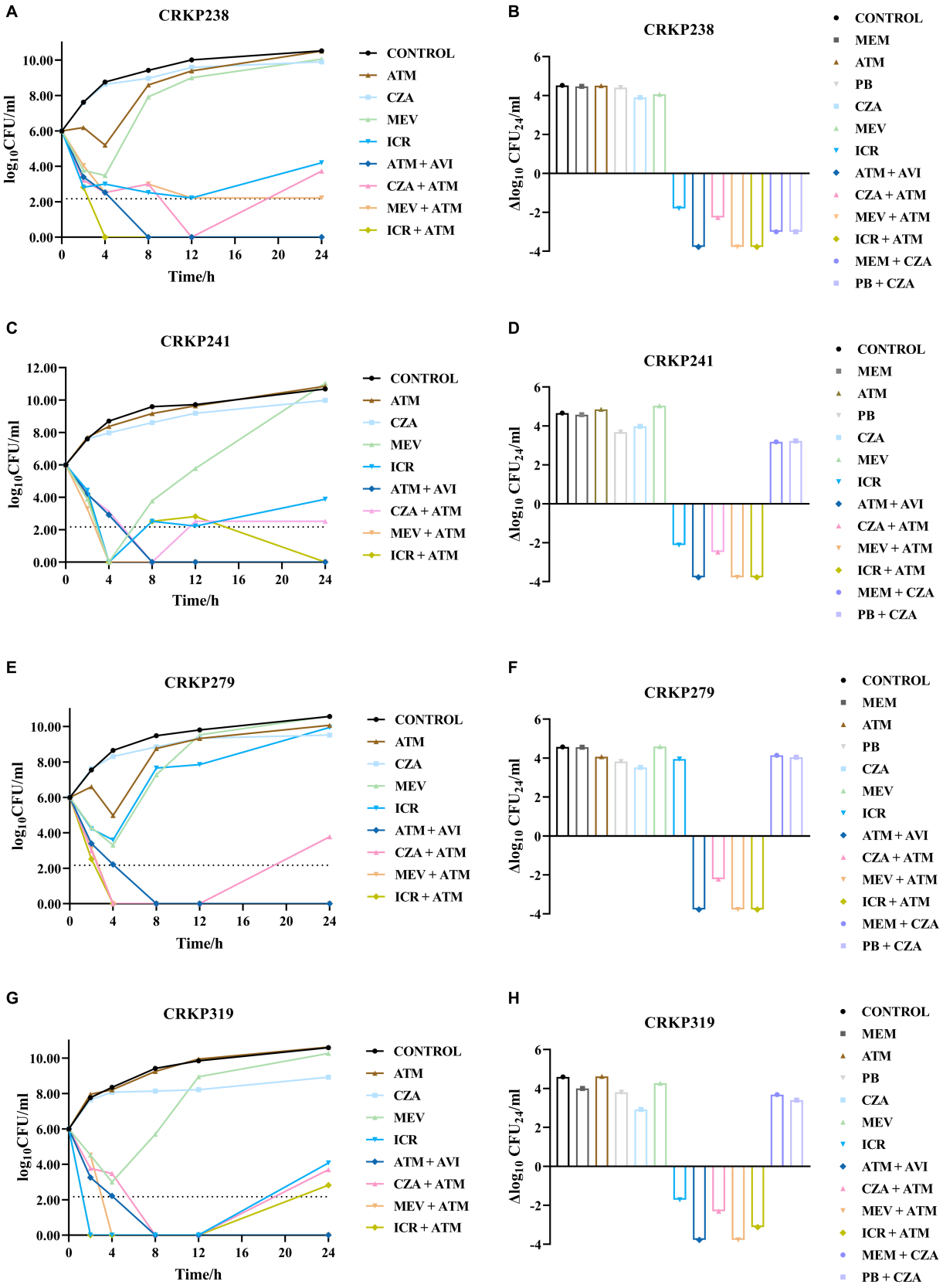

FIGURE 2
Bacterial load (log10 CFU/mL) over the course of 24 h in the four carbapenem-resistant *Klebsiella pneumoniae* isolates coproducing KPC and NDM for each antibiotic combination regimen were shown in **A–H**. LOD (lower limit of detection) = 2.17 log10 CFU/mL. ATM, aztreonam; CZA, ceftazidime/avibactam; MEV, meropenem/vaborbactam; ICR, imipenem-cilastatin/relebactam; AVI, avibactam; MEM, meropenem; PB, polymyxin.

widespread distribution of acquired β-lactamase genes, which have led to an increasing resistance rate. In the case of serine/metallo-enzyme-coproducing pathogens, often referred to as "superbugs," which are capable of hydrolyzing nearly all available β-lactam antibiotics, BLBLI preparations may not be effective in terms of their bactericidal effect, and there is an ongoing quest for new treatment.

It was expected that no bactericidal effect would be observed for CZA and MEV monotherapy, although the MIC values against MEV were lower than the concentrations used in the time-kill assay, except in the case of CRKP279. Published data show that ICR has excellent *in vitro* activity against isolates carrying class A and C β-lactamases (Hirsch et al., 2012) but is not effective in restoring susceptibility to isolates expressing OXA-48 or MBL carbapenemases (Lapuebla et al., 2015). However, recent data from a small sample showed that 42.9% of MBL-producing *K. pneumoniae* isolates (6/14) were susceptible to ICR (Yang et al., 2022). Contrary to expectations, ICR showed bacteriostatic activity against three strains in this study, although the addition of relebactam to imipenem did not reduce the MIC against three of the strains, with CRKP238 being the exception. In a study by Yu et al., ICR displayed bactericidal activity against four MBL-producing isolates at 24 h (Yu et al., 2021); the amount of bacteria in three isolates producing NDM or IMP enzyme decreased by >5 $\log_{10}$ CFU/mL. These observations highlight a need to further evaluate the effectiveness of ICR against MBL-producing isolates.

Aztreonam is a special β-lactam, given its resistance to MBL inhibition, while the presence of KPC can hydrolyze it, so aztreonam alone is not enough to fight against strains coproducing MBL and KPC enzyme. The synergistic effects of aztreonam plus CZA or MEV have been confirmed *in vitro* and *in vivo* (Marshall et al., 2017; Biagi et al., 2019), and a recent observational study indicated that the combination of CZA plus aztreonam offers a therapeutic advantage for patients with bloodstream infections due to MBL-producing Enterobacterales (Falcone et al., 2021). Our results demonstrated that the combinations of aztreonam plus CZA or MEV both had a synergistic effect, whereas MEV combinations had better bactericidal activity at 24 h compared with CZA combinations. In addition, bacterial regrowth was observed in three strains at 24 h, which suggests that clinical killing of bacteria may be possible by increasing the frequency of drug administration. We also found that the bactericidal effect achieved by the combination of aztreonam plus ICR was similar to that of aztreonam plus MEV, which can reduce the amount of bacteria by more than 3.78 $\log_{10}$ CFU/mL.

Avibactam is also currently in development in combination with aztreonam; although avibactam does not inhibit MBLs, this combination restores the activity of aztreonam against MBL-producing pathogens via inhibition of co-expressed serinase. The aztreonam/avibactam combination has demonstrated potent *in vitro* activity against MBL-producing Enterobacterales in several surveillance studies. In the global INFORM surveillance study, the $MIC_{50/90}$ against OXA-48 plus MBL (n = 23) was 0.25/0.5 mg/L, respectively (Kazmierczak et al., 2018). Our *in vitro* susceptibility test (MIC values ≤0.5/4 mg/L) and time-kill assay also showed that aztreonam/avibactam was potent against CRKPs coproducing NDM and KPC.

While the theory behind combining aztreonam with avibactam, CZA, MEV, or ICR is the same, notable differences between these combinations are present in the form of the penicillin-binding protein (PBP) targets of the β-lactams and the β-lactamase affinity of the inhibitors, which may lead to different effects. Aztreonam has high affinity for PBP3, while ceftazidime mainly binds to PBP1a/b and PBP3, disrupting peptidoglycan synthesis in *K. pneumoniae* (Sutaria et al., 2018). In this study, the time-kill assay results demonstrated that aztreonam/avibactam was more effective than aztreonam plus CZA, reducing the amount of bacteria to a greater extent. We speculate that ceftazidime and aztreonam competitively bind to PBP3, while ceftazidime can be hydrolyzed by NDM to counteract its bactericidal effect, resulting in the inferior combined effect of aztreonam plus CZA as compared to aztreonam/avibactam. It has been found that the saturation of one or more PBPs also results in different bacterial dissolution rates, and the saturation of multiple PBP sites leads to higher bacterial dissolution rates (Satta et al., 1995). Meropenem and imipenem bind to PBP2 and PBP4 (Sutaria et al., 2018), and when these are combined with aztreonam, the combination could lead to the saturation of multiple sites, which may explain the better combined effect of MEV or ICR plus aztreonam in this experiment. In view of the different bactericidal effects of these double β-lactam combinations, promising dual-drug and triple-drug combination administration strategies can be rationally designed and optimized in the future based on existing PBP binding sites and β-lactamase mechanisms against multidrug-resistant *K. pneumoniae*, which may be superior to unoptimized, empirical double β-lactam combinations.

Different effects have been observed for the combination of polymyxin plus CZA. Some experiments have found that this combination does not improve the survival rate of *Galleria mellonella* (Borjan et al., 2020), while others have found that the combination of colistin plus CZA has a synergistic bactericidal effect against MBL-producing strains (Montero et al., 2021). In addition, one study tested the efficacy of a double β-lactam strategy against carbapenemase-producing isolates, finding that CZA combined with meropenem or imipenem showed synergy against certain KPC-producing strains (Gaibani et al., 2017). However, our results only detected one strain that showed synergistic effect in time-kill assay. The effects of meropenem or polymyxin combined with CZA need further investigation.

Conclusion

The combination of aztreonam plus avibactam, CZA, MEV, and ICR showed good antibacterial activity. These double β-lactam combinations offer potential solutions for isolates coproducing MBL and KPC. However, the collection in this study was monocentric, and the 24-h static nature of *in vitro* time-kill experiments is a limitation of this study. More isolates are needed to conduct *in vitro* and *in vivo* studies to further determine the appropriate selection of and optimal dosing regimen for novel agents.

Data availability statement

The datasets presented in this study can be found in online repositories. The names of the repository/repositories and accession number(s) can be found in the article/Supplementary material.

Ethics statement

The studies involving humans were approved by the Ethics Committee of Yongchuan Hospital of Chongqing Medical University. The studies were conducted in accordance with the local legislation and institutional requirements. The human samples used in this study were primarily isolated as part of a previous study, for which ethical approval was obtained. Written informed consent for participation was not required from the participants or the participants' legal guardians/next of kin in accordance with the national legislation and institutional requirements.

Author contributions

XZ, XiL, JW, and JZ designed the study. XiL and LL performed the experiments. YY, XG, and JL analyzed and interpreted the data, collected the isolates, and the clinical data. XiL and XZ drafted the manuscript. XZ reviewed the manuscript and provided recommendations. All authors contributed to the article and approved the submitted version.

Funding

This work was supported by the General Projects of Chongqing Natural Science Foundation (cstc2020jcyj-msxm0067); Yongchuan Natural Science Foundation (2021yc-jckx20053); the Talent Introduction project of Yongchuan Hospital of Chongqing Medical University (YJYJ202004 and YJYJ202005); and the Program for Youth Innovation in Future Medicine, Chongqing Medical University (W0113).

Conflict of interest

The authors declare that the research was conducted in the absence of any commercial or financial relationships that could be construed as a potential conflict of interest.

Publisher's note

All claims expressed in this article are solely those of the authors and do not necessarily represent those of their affiliated organizations, or those of the publisher, the editors and the reviewers. Any product that may be evaluated in this article, or claim that may be made by its manufacturer, is not guaranteed or endorsed by the publisher.

Supplementary material

The Supplementary material for this article can be found online at: https://www.frontiersin.org/articles/10.3389/fmicb.2024.1210313/full#supplementary-material

References

Benitez-Cano, A., Luque, S., Sorli, L., Carazo, J., Ramos, I., Campillo, N., et al. (2020). Intrapulmonary concentrations of meropenem administered by continuous infusion in critically ill patients with nosocomial pneumonia: a randomized pharmacokinetic trial. *Crit. Care* 24:55. doi: 10.1186/s13054-020-2763-4

Biagi, M., Wu, T., Lee, M., Patel, S., Butler, D., and Wenzler, E. (2019). Searching for the optimal treatment for Metallo-and serine-β-lactamase producing Enterobacteriaceae: Aztreonam in combination with ceftazidime-avibactam or Meropenem-vaborbactam. *Antimicrob. Agents Chemother.* 63:e01426. doi: 10.1128/AAC.01426-19

Blizzard, T. A., Chen, H., Kim, S., Wu, J., Bodner, R., Gude, C., et al. (2014). Discovery of MK-7655, a β-lactamase inhibitor for combination with Primaxin®. *Bioorg. Med. Chem. Lett.* 24, 780–785. doi: 10.1016/j.bmcl.2013.12.101

Borjan, J., Meyer, K. A., Shields, R. K., and Wenzler, E. (2020). Activity of ceftazidime-avibactam alone and in combination with polymyxin B against carbapenem-resistant *Klebsiella pneumoniae* in a tandem in vitro time-kill/in vivo galleria mellonella survival model analysis. *Int. J. Antimicrob. Agents* 55:105852. doi: 10.1016/j.ijantimicag.2019.11.009

Brogden, R. N., and Heel, R. C. (1986). Aztreonam. A review of its antibacterial activity, pharmacokinetic properties and therapeutic use. *Drugs* 31, 96–130. doi: 10.2165/00003495-198631020-00002

Castanheira, M., Mills, J. C., Costello, S. E., Jones, R. N., and Sader, H. S. (2015). Ceftazidime-avibactam activity tested against Enterobacteriaceae isolates from U.S. hospitals (2011 to 2013) and characterization of β-lactamase-producing strains. *Antimicrob. Agents Chemother.* 59, 3509–3517. doi: 10.1128/AAC.00163-15

Das, S., Zhou, D., Nichols, W. W., Townsend, A., Newell, P., and Li, J. (2020). Selecting the dosage of ceftazidime-avibactam in the perfect storm of nosocomial pneumonia. *Eur. J. Clin. Pharmacol.* 76, 349–361. doi: 10.1007/s00228-019-02804-z

Falcone, M., Daikos, G. L., Tiseo, G., Bassoulis, D., Giordano, C., Galfo, V., et al. (2021). Efficacy of ceftazidime-avibactam plus Aztreonam in patients with bloodstream infections caused by Metallo-β-lactamase-producing Enterobacterales. *Clin. Infect. Dis.* 72, 1871–1878. doi: 10.1093/cid/ciaa586

Gaibani, P., Lewis, R. E., Volpe, S. L., Giannella, M., Campoli, C., Landini, M. P., et al. (2017). In vitro interaction of ceftazidime-avibactam in combination with different antimicrobials against KPC-producing *Klebsiella pneumoniae* clinical isolates. *Int. J. Infect. Dis.* 65, 1–3. doi: 10.1016/j.ijid.2017.09.017

Gandra, S., and Burnham, C. D. (2020). Carbapenem-resistant Enterobacterales in the USA. *Lancet Infect. Dis.* 20, 637–639. doi: 10.1016/S1473-3099(20)30066-9

Gong, X., Zhang, J., Su, S., Fu, Y., Bao, M., Wang, Y., et al. (2018). Molecular characterization and epidemiology of carbapenem non-susceptible Enterobacteriaceae isolated from the eastern region of Heilongjiang Province, China. *BMC Infect. Dis.* 18:417. doi: 10.1186/s12879-018-3294-3

Hackel, M. A., Lomovskaya, O., Dudley, M. N., Karlowsky, J. A., and Sahm, D. F. (2018). In vitro activity of Meropenem-Vaborbactam against clinical isolates of KPC-positive Enterobacteriaceae. *Antimicrob. Agents Chemother.* 62:969. doi: 10.1128/AAC.01904-17

Hirsch, E. B., Ledesma, K. R., Chang, K. T., Schwartz, M. S., Motyl, M. R., and Tam, V. H. (2012). In vitro activity of MK-7655, a novel β-lactamase inhibitor, in combination with imipenem against carbapenem-resistant gram-negative bacteria. *Antimicrob. Agents Chemother.* 56, 3753–3757. doi: 10.1128/AAC.05927-11

Huang, W., Zhang, J., Zeng, L., Yang, C., Yin, L., Wang, J., et al. (2021). Carbapenemase production and epidemiological characteristics of Carbapenem-resistant *Klebsiella pneumoniae* in Western Chongqing, China. *Front. Cell. Infect. Microbiol.* 11:775740. doi: 10.3389/fcimb.2021.775740

Jayol, A., Nordmann, P., Poirel, L., and Dubois, V. (2018). Ceftazidime/avibactam alone or in combination with aztreonam against colistin-resistant and carbapenemase-producing *Klebsiella pneumoniae*. *J. Antimicrob. Chemother.* 73, 542–544. doi: 10.1093/jac/dkx393

Karlowsky, J. A., Kazmierczak, K. M., De Jonge, B. L. M., Hackel, M. A., Sahm, D. F., and Bradford, P. A. (2017). *In Vitro* activity of Aztreonam-avibactam against Enterobacteriaceae and Pseudomonas aeruginosa isolated by clinical laboratories in 40 countries from 2012 to 2015. *Antimicrob Agents Chemother* 61:472. doi: 10.1128/AAC.00472-17

Kazmierczak, K. M., Bradford, P. A., Stone, G. G., De Jonge, B. L. M., and Sahm, D. F. (2018). In VitroActivity of ceftazidime-avibactam and Aztreonam-avibactam against OXA-48-carrying Enterobacteriaceae isolated as part of the international network for optimal resistance monitoring (INFORM) global surveillance program from 2012 to 2015. *Antimicrob. Agents Chemother.* 62:62. doi: 10.1128/AAC.00592-18

Lapuebla, A., Abdallah, M., Olafisoye, O., Cortes, C., Urban, C., Landman, D., et al. (2015). Activity of imipenem with Relebactam against gram-negative Pathogens from new York City. *Antimicrob. Agents Chemother.* 59, 5029–5031. doi: 10.1128/AAC.00830-15

Marshall, S., Hujer, A. M., Rojas, L. J., Papp-Wallace, K. M., Humphries, R. M., Spellberg, B., et al. (2017). Can ceftazidime-avibactam and Aztreonam overcome

β-lactam resistance conferred by Metallo-β-lactamases in Enterobacteriaceae? *Antimicrob. Agents Chemother.* 61:e02243. doi: 10.1128/AAC.02243-16

Montero, M. M., Domene Ochoa, S., López-Causapé, C., Luque, S., Sorlí, L., Campillo, N., et al. (2021). Time-kill evaluation of antibiotic combinations containing ceftazidime-avibactam against extensively drug-resistant Pseudomonas aeruginosa and their potential role against ceftazidime-avibactam-resistant isolates. *Microbiol. Spectr.* 9:e0058521. doi: 10.1128/Spectrum.00585-21

Motsch, J., Murta De Oliveira, C., Stus, V., Köksal, I., Lyulko, O., Boucher, H. W., et al. (2020). RESTORE-IMI 1: a multicenter, randomized, double-blind trial comparing efficacy and safety of imipenem/Relebactam vs Colistin plus imipenem in patients with imipenem-nonsusceptible bacterial infections. *Clin. Infect. Dis.* 70, 1799–1808. doi: 10.1093/cid/ciz530

Nordmann, P., and Poirel, L. (2019). Epidemiology and diagnostics of Carbapenem resistance in gram-negative Bacteria. *Clin. Infect. Dis.* 69, S521–s528. doi: 10.1093/cid/ciz824

Papp-Wallace, K. M., Barnes, M. D., Alsop, J., Taracila, M. A., Bethel, C. R., Becka, S. A., et al. (2018). Relebactam is a potent inhibitor of the KPC-2 β-lactamase and restores imipenem susceptibility in KPC-producing Enterobacteriaceae. *Antimicrob. Agents Chemother.* 62:e00174. doi: 10.1128/AAC.00174-18

Rizk, M. L., Rhee, E. G., Jumes, P. A., Gotfried, M. H., Zhao, T., Mangin, E., et al. (2018). Intrapulmonary pharmacokinetics of Relebactam, a novel β-lactamase inhibitor, dosed in combination with imipenem-Cilastatin in healthy subjects. *Antimicrob. Agents Chemother.* 62:e01411. doi: 10.1128/AAC.01411-17

Satta, G., Cornaglia, G., Mazzariol, A., Golini, G., Valisena, S., and Fontana, R. (1995). Target for bacteriostatic and bactericidal activities of beta-lactam antibiotics against *Escherichia coli* resides in different penicillin-binding proteins. *Antimicrob. Agents Chemother.* 39, 812–818. doi: 10.1128/AAC.39.4.812

Sutaria, D. S., Moya, B., Green, K. B., Kim, T. H., Tao, X., Jiao, Y., et al. (2018). First penicillin-binding protein occupancy patterns of β-lactams and β-lactamase inhibitors in *Klebsiella pneumoniae*. *Antimicrob. Agents Chemother.* 62:e00282. doi: 10.1128/AAC.00282-18

Tangden, T., Hickman, R. A., Forsberg, P., Lagerback, P., Giske, C. G., and Cars, O. (2014). Evaluation of double-and triple-antibiotic combinations for VIM-and NDM-producing *Klebsiella pneumoniae* by in vitro time-kill experiments. *Antimicrob. Agents Chemother.* 58, 1757–1762. doi: 10.1128/AAC.00741-13

Tsuji, B. T., Pogue, J. M., Zavascki, A. P., Paul, M., Daikos, G. L., Forrest, A., et al. (2019). International consensus guidelines for the optimal use of the Polymyxins: endorsed by the American College of Clinical Pharmacy (ACCP), European Society of Clinical Microbiology and Infectious Diseases (ESCMID), Infectious Diseases Society of America (IDSA), International Society for Anti-infective Pharmacology (ISAP), Society of Critical Care Medicine (SCCM), and Society of Infectious Diseases Pharmacists (SIDP). *Pharmacotherapy* 39, 10–39. doi: 10.1002/phar.2209

Tzouvelekis, L. S., Markogiannakis, A., Psichogiou, M., Tassios, P. T., and Daikos, G. L. (2012). Carbapenemases in Klebsiella pneumoniae and other Enterobacteriaceae: an evolving crisis of global dimensions. *Clin. Microbiol. Rev.* 25, 682–707. doi: 10.1128/CMR.05035-11

Wenzler, E., Gotfried, M. H., Loutit, J. S., Durso, S., Griffith, D. C., Dudley, M. N., et al. (2015). Meropenem-RPX7009 concentrations in plasma, epithelial lining fluid, and alveolar macrophages of healthy adult subjects. *Antimicrob. Agents Chemother.* 59, 7232–7239. doi: 10.1128/AAC.01713-15

Yahav, D., Giske, C. G., Grāmatniece, A., Abodakpi, H., Tam, V. H., and Leibovici, L. (2020). New β-lactam-β-lactamase inhibitor combinations. *Clin. Microbiol. Rev.* 34:e00115. doi: 10.1128/CMR.00115-20

Yang, T. Y., Hsieh, Y. J., Kao, L. T., Liu, G. H., Lian, S. H., Wang, L. C., et al. (2022). Activities of imipenem-relebactam combination against carbapenem-nonsusceptible Enterobacteriaceae in Taiwan. *J. Microbiol. Immunol. Infect.* 55, 86–94. doi: 10.1016/j.jmii.2021.02.001

Yu, W., Luo, Q., Shen, P., Chen, Y., Xu, H., Xiao, Y., et al. (2021). New options for bloodstream infections caused by colistin-or ceftazidime/avibactam-resistant *Klebsiella pneumoniae*. *Int. J. Antimicrob. Agents* 58:106458. doi: 10.1016/j.ijantimicag.2021.106458

Zhanel, G. G., Lawson, C. D., Adam, H., Schweizer, F., Zelenitsky, S., Lagacé-Wiens, P. R., et al. (2013). Ceftazidime-avibactam: a novel cephalosporin/β-lactamase inhibitor combination. *Drugs* 73, 159–177. doi: 10.1007/s40265-013-0013-7

Frontiers in Microbiology

Explores the habitable world and the potential of microbial life

The largest and most cited microbiology journal which advances our understanding of the role microbes play in addressing global challenges such as healthcare, food security, and climate change.

Discover the latest Research Topics

See more →

Frontiers

Avenue du Tribunal-Fédéral 34
1005 Lausanne, Switzerland
frontiersin.org

Contact us

+41 (0)21 510 17 00
frontiersin.org/about/contact